MOLECULAR AND PROTEOMIC CHARACTERISATION OF THE ~700 kDa APOPTOSOME

Thesis submitted for the degree of
Doctor of Philosophy
At the University of Leicester

by

Davina Deborah Twiddy
Mechanisms of Apoptosis
MRC Toxicology Unit

September 2005

ProQuest LLC
789 East Eisenhower Parkway
P.O. Box 1346
Ann Arbor, MI 48106-1346

Molecular and proteomic characterisation of the ~700 kDa apoptosome

Davina Twiddy, MRC Toxicology Unit, University of Leicester, Leicester, LE1 9HN

The apoptosome is a caspase-activating complex consisting of Apaf-1, caspase-9 and cytochrome *c*, which is essential for the induction of stress-mediated apoptosis. This complex ranges in size from ~700 kDa to ~1.4 MDa, possibly due to the stable association of modulatory proteins. In the current study I employed two strategies to isolate and characterise the active ~700 kDa apoptosome *in vitro*. Firstly, I used GST-Casp9$^{1-130}$, which binds to the CARD domain of Apaf-1 in a dATP and cytochrome *c*-dependent manner, to affinity-purify an apoptosome containing only Apaf-1$_{XL}$ and cytochrome *c*. This result was confirmed by the second approach, which used an antibody to the caspase-9 to immunoprecipitate of the native apoptosome, which contained Apaf-1 and caspase-9 (p34/p35). However, in the absence of SMAC and Omi, the native apoptosome also contained caspase-3 and XIAP, both of which associated via the catalytic domains of caspase-9. When isolating the apoptosome from apoptotic cells using TAP-tagged caspase-9 variants, I discovered that the location of the TAP-tag can affect the ability of caspase-9 to interact with known binding partners and consequently can influence the induction of cell death. I have also studied the role of the apoptosome in the caspase-3 null cell line, MCF-7, and have demonstrated that an active ~700 kDa apoptosome complex is formed in both dATP-activated cell lysates and in apoptotic MCF-7 cells. Furthermore, the active apoptosome can directly process and activate caspase-7. However, the association between caspase-7 and the apoptosome is only transient as caspase-7 is rapidly sequestered into a ~200-300 kDa complex with XIAP, in the presence of SMAC and Omi. Taken together, the data in this thesis has demonstrated that the native active apoptosome is composed only of Apaf-1 and caspase-9. Furthermore, I have shown that XIAP, SMAC and Omi can modulate the transient associations with the apoptosome.

Acknowledgements

I would like to start by thanking my supervisors: Drs Kelvin Cain and Marion MacFarlane. Their doors have never been closed and I really appreciate their continued advice, discussion and support. Also, thanks to Prof. Gerry Cohen for his invaluable input and knowledge. I would also like to thank David Brown, Dr. Michelle Hughes, Dr. Michael Butterworth and Dr. Nick Harper for their technical advice and useful discussions. A great big thank-you goes to all those involved in badminton, for convincing me to take out my frustration on a shuttlecock; it really helped!

A special thank-you goes to my Mum and Dad for always having faith in me. I would never have come so far without their unwavering support and encouragement, Thank-you. Finally, thanks to my husband Colin, who has been my rock, my friend and at times, my sanity during the past 4 years. I could not have done it if it wasn't for the love and support he has given me, and all those late night drives around Rutland water! Not forgetting Bonsai and Eucey, who are blissfully unaware of the importance of their roles.

Table of Contents

Chapter 1

Chapter 2

Chapter 3

Chapter 4

Table of Figures

Chapter 1

Chapter 2

Chapter 3

Chapter 4

Chapter 5

Chapter 6

Chapter 7

Abbreviations

aa	Amino Acid
Ac-DEVD.AFC	Acetyl-Aspartic acid-Glutamine-Valine-Aspartic acid-7-amino-4-trifluromethylcoumarin
AChE	Acetylcholinesterase
AIF	Apoptosis Inducing Factor
Ala	Alanine
Amp	Ampicillin
Apaf-1	Apoptotic Protease Activating Factor-1
Arg	Arginine
Asn	Asparagine
Asp	Aspartic acid
ATP	Adenosine triphosphate
ATPF	Alanine-Threonine-Proline-Phenylalanine
AVPI	Alanine-Valine-Proline-Isoleucine
AVPS	Alanine-Valine-Proline-Serine
B-CLL	B-cell chronic lymphatic leukeamia
BIR	Baculovirus IAP Repeat
BSA	Bovine Serum Albumin
CARD	Caspase Activation and Recruitment Domain
Caspase	Cysteinyl aspartate-specific protease
Ced	Cell death defective gene (*C. elegans)*
CED	Cell death defective protein (*C. elegans)*
C. elegans	*Caenorhabditis elegans*
CBP	Calmodulin-Binding Protein
CHAPS	3-[3-cholamidopropyl)dimethylammonio]-propanesulphonate
cIAP	Cellular Inhibitor of Apoptosis
CTL	Cytotoxic T-lymphocytes
CO_2	Carbon Dioxide
CT	C terminal
Cys	Cysteine
Da	Dalton
dADP	Deoxyadenosine-diphosphate
DARK	*Drosophila* Apaf-1-related killer
Dapaf	*Drosophila* apoptotic protease-activating factor-1
dATP	Deoxyadenosine 5'-Triphosphate
DD	Death domain
DECAY	*Drosophila* executioner caspase related to Apopain/Yama
DEFCAP	Death effector filament-forming Ced-4-like apoptosis protein
DCP-1	*Drosophila* caspase-1
DED	Death effector domain
DEVDase	Ability to process the flourogenic substrate Aspartic acid-Glutamine-Valine-Aspartic acid-7-amino-4-trifluromethylcoumarin
DIABLO	Direct IAP binding protein with low pI
DIAP	*Drosophila* inhibitor of apoptosis
Dig/Hom	Digitonin/homogenisation
DISC	Death-Inducing Signalling Complex
DMEM	Dulbecco's Modified Eagle's Medium
DMP	Dimethyl Pimelimidate
DMSO	Dimethyl sulfoxide
DNA	Deoxyribonucleic acid
DREDD	Death-related *ced-3/Nedd2*-like gene

DrICE	*Drosophila* interleukin-1β converting enzyme
DRONC	*Drosophila* Nedd-2-like caspase
DTT	Dithiothreitol
ECACC	European Collection of Animal Cell Cultures
ECL	Enhanced Chemiluminescence
EDTA	Diaminoethanetetra-acetic acid
Egl-1	Egg-laying defective-1 gene
Egl-1	Egg-laying defective-1 protein
EGTA	1, 2-Di(2-aminoethoxy)ethane-N,N,N',N'-tetra-acetic acid
ENDO G	Endonuclease G
Etop	Etoposide
FADD	Fas receptor associated death domain
Fr	Fraction
F-T	Flow-Through
F/T	Freeze/Thawed
FBS	Fetal Bovine Serum
FITC	Fluorescein Isothiocyanate
FLIP	FADD-like interleukin-1β converting enzyme-like protease (FLICE/C8)-inhibitory protein
FPLC	Fast Performance Liquid Chromatography
GFP	Green Fluorescent Protein
Glu	Glutamine
GSH	Glutathione
GST	Glutathione-S-Transferase
GST-Casp9$^{1-130}$	GST tagged Caspase-9 aa1-130
GTC	GST and CBP TAP-tag
h	Hour (s)
HCl	Hydrochloric acid
HeLa	Human Cervix Adenocarcinoma Cell Line
HEPES	N-[2-Hydroxyethyl]piperazine-N'-[2-ethanesulphonic acid]
HIS	6-Histadine residue tag
His	Histadine
HRP	Horseradish peroxidase
HSP	Heat Shock Protein
ICAD	Inhibitor of caspase-activated Dnase
ICE	Interleukin-1-converting enzyme
IKK	Inhibitor of KappaB kinase
IPTG	Isopropyl-beta-D-thiogalactopyranoside
kDa	Kilodalton
LC/MS-MS	Liquid chromatography tandem mass spectrometry
Leu	Leucine
LLVY.AMC	Succinyl-Leu Leu-Val-Tyr-7-amino-4-methylcoumarin
Lys	Lysine
MALDI-Tof MS	Matrix-assisted laser desorption/ionisation-time of flight mass spectrometry
MCF-7	Breast epithelial cancer cell line
MCS	Multiple Cloning Site
Met	Methionine
MDa	Megadalton
min	Minute(s)
Mg	Magnesium

NAC	NB domain and CARD protein
NaCl	Sodium Chloride
NaOH	Sodium hydroxide
NK	Natural killer cells
NT	N terminal
OD	Optical density
PAGE	Polyacrylamide gel electrophoresis
PARP	Poly (ADP-ribose) polymerase
PCR	Polymerase Chain Reaction
PBS	Phosphate Buffered Saline
PHAP	Putative HLA-DR-associated protein
Phe	Phenylalanine
PI	Propidium iodide
PS	Phosphatidylserine
PIPES	1, 4-piperazinediethanesulphuric acid
PMSF	Phenylmethylsulpfonyl fluoride
Pro	Proline
ProT	Prothymosin
RING	Really interesting new gene
RIP	Receptor interacting protein
SDS	Sodium dodecyl sulphate
sec	Second(s)
SEM	Standard Error of the Mean
SMAC	Second Mitochondria-derived Activator of Apoptosis
STAT1	Signal transducer and activator of transcription-1
STS	Staurosporine
TAP	Tandem affinity purification
TB	Terrific Broth
tBid	Truncated Bid
TBS	Tris-Buffered Saline
TBS-T	Tris-Buffered Saline + 0.1% (v/v) Tween
TEMED	N,N,N',N'-Tetramethylethylenediamine
THP-1	Human Monocytic Tumour Cell Line
Thr	Threonine
TMRE	Tetramethylrhodamine ethyl ester
TNF	Tumour Necrosis Factor
TRAIL	TNF-related apoptosis-inducing ligand
TRIS	2-Amino-2-(hydroxymethyl)-1,3-propanediol
TWEEN™ 20	Polyoxyethylenesorbitan monolaurate
UV	Ultraviolet
Val	Valine
WB	Western Blot
wt	Wild-type
XIAP	X-chromosome linked Inhibitor of Apoptosis Protein
zVAD.FMK	Benzyloxycarbonyl-Valine-Alanine-Aspartic acid-fluromethylketone

Chapter 1

Introduction

1.0 Introduction

The term 'apoptosis' (Greek meaning 'dropping off') was coined in a seminal paper in 1972, to refer to the process by which cells undergo programmed cell death (Kerr *et al*, 1972). This paper showed that paradoxically, death was essential for life, a novel concept that was widely disregarded for 15 years. Apoptosis plays a physiological role in development, initially with intrauterine apoptosis of the interdigital webs between fingers and toes, and later in the maturation of the immune and nervous systems (Jacobson *et al*, 1997; Nagata, 1997; Oppenheim *et al*, 1991). Apoptosis is also involved in the removal of cells affected by environmental stresses such as ultraviolet (UV) light (Schwarz *et al*, 1995) or those infected with viruses (Kagi *et al*, 1994). Abnormal apoptosis has also been implicated in certain disease states such as cancer, neurodegenerative disease and autoimmunity (Reviewed in Strasser *et al*, 2000), where cell death is either absent or mis-directed.

1.1 Initiation of apoptosis

Apoptosis can be initiated via three pathways; by cellular activation, or by the extrinsic or the intrinsic pathway. Cellular activation of apoptosis is induced by cytotoxic T-lymphocytes and removes transformed or infected cells (Reviewed in Igney & Krammer, 2002). The extrinsic pathway is mediated by activation of a subfamily of cell surface Tumour Necrosis Factor (TNF) receptors, which contain an intracellular death domain (DD). Ligation of these receptors leads to the formation and activation of the death-inducing signalling complex (DISC) (Reviewed in Danial & Korsmeyer, 2004). By contrast, the intrinsic pathway is induced by mitochondrial release of cytochrome *c* and results in the formation of the cell death activation complex, termed the apoptosome (Reviewed in Cain *et al*, 2002; Shi, 2002a). A family of evolutionally conserved cysteine aspartyl-specific proteases (caspases) are activated in apoptosis, which cleave substrates resulting in the biochemical and morphological changes characteristic of apoptosis. Importantly, all the apoptotic machinery is constitutively expressed (Jacobson *et al*, 1996; Weil *et al*, 1996), however apoptosis is prevented in healthy cells by compartmentalisation of key proteins, the expression of inactive precursors, and the presence of cytosolic inhibitors.

1.2 Evolutionary cell death pathways

Studies in the nematode worm *Caenorhabdtitis elegans*, the fruitfly *Drosophila* and the mouse indicate that the molecular machinery involved in the intrinsic induction of apoptosis is evolutionarily conserved.

1.2.1 Cell death in *C.elegans*

Many initial studies on cell death were performed in *Caenorhabdtitis elegans*, the nematode worm. There are 14 genes known to be involved in the 131 somatic cell deaths which occur in *C.elegans* during development. The four genes at the centre of the general apoptotic program are *ced-3, ced-4, ced-9* (Yuan *et al*, 1993; Yuan & Horvitz, 1992; Hengartner & Horvitz, 1994) and *Egl-1* (Conradt & Horvitz, 1998). Genetic analysis has shown *ced-9* to be a negative regulatory gene in apoptosis (Hengartner *et al*, 1992), whereas *ced-3*, *ced-4* and *Egl-1* are pro-apoptotic (Ellis & Horvitz, 1986, Conradt & Horvitz, 1998). Furthermore, *ced-9* acts upstream of *ced-3 and ced-4* (Hengartner *et al*, 1992), but downstream of *Egl-1* (Conradt & Horvitz, 1998).

The hierarchy described above for the genes also exist between their protein products. CED-4 is normally bound to CED-9 forming a membrane-associated complex on the mitochondria (Chinnaiyan *et al*, 1997a; Wu *et al*, 1997), which prevents CED-4 from activating CED-3 (Chinnaiyan *et al*, 1997b; Seshagiri & Miller, 1997). EGL-1 is able to induce cell death by binding to CED-9 and displacing CED-4 (Conradt & Horvitz, 1998). This then allows CED-4 to translocate to the perinuclear membrane (Chen *et al*, 2000a) and oligomerise allowing aggregation of CED-3 precursors, which results in their autoactivation (Yang *et al*, 1998a) and consequently cell death (Figure 1.2.1).

As a result of these studies in *C. elegans*, mammalian homologues of CED-3, CED-4, CED-9 and Egl-1 have been identified. The anti-apoptotic protein Bcl-2 shares sequence homology with CED-9 (Hengartner & Horvitz, 1994), and CED-4 shows homology to a mammalian scaffold protein, Apaf-1 (Zou *et al*, 1997). CED-3 has been identified as a caspase (Yuan *et al*, 1993), possessing a caspase-9-like CARD, but also acting as an effector caspase similar to caspase-3. Furthermore,

the role of Egl-1 resembles that of the BH3-only Bcl-2 family member, Bid (Conradt & Horvitz, 1998).

1.2.2 Cell death in *Drosophila*

Drosophila melanogaster has been used as a vertebrate model genetic system for studying apoptosis, with the core components of the apoptotic machinery, conserved from *C. elegans*. The CED-4 homologue, DARK (also known as Dapaf and HAC-1 (Zhou *et al*, 1999; Rodriguez *et al*, 1999; Kanuka *et al*, 1999) contains an N-terminal CARD domain (CED-3 homologous), a CED-4 homologous region and a C-terminal domain containing WD40 repeat regions. The WD40 repeats are not found in CED-4, but are present in the mammalian CED-4 homologue, Apaf-1 (Zou *et al*, 1997). This domain in Apaf-1 is essential for its regulation by cytochrome *c* (see section 1.5.3). Although the WD40 domain exists in *Drosophila* there are not any clear reports illustrating the importance of cytochrome *c* for the activity of DARK (Varkey *et al*, 1999; Kanuka *et* al1999; Rodriguez *et al*, 1999; Dorstyn *et al*, 2002; Zimmermann *et al*, 2002; Dorstyn *et al*, 2004).

There are seven CED-3 homologues (caspases) in *Drosophila*, which can be divided into initiator (DREDD, DRONC, STRICA) and effector caspases (Dcp-1, DRICE, DECAY, DAMM) (Reviewed in Kumar & Doumanis, 2000). DRONC is the only *Drosophila* caspase to contain an N-terminal CARD domain (Dorstyn *et al*, 1999), via which it associates with DARK in order to become activated (Quinn *et al*, 2000). Active DRONC is then able to process effector caspases such as DRICE (Hawkins *et al*, 2000) resulting in apoptosis (Figure 1.2.1). This mechanism is analogous to caspase-9 activation following binding to Apaf-1 in the mammalian apoptosome (see section 1.5.3).

The activity of caspases in *Drosophila* is regulated by the presence of inhibitors of apoptosis (IAPs); DIAP-1 (Thread) and DIAP-2 (Hay *et al*, 1995). DIAP-1 directly binds to, and suppresses the activity of DRONC (Meier *et al*, 2000; Wilson *et al*, 2002; Muro *et al*, 2002) and the active effector caspases (Kaiser *et al*, 1998; Yan *et al*, 2004; Tenev *et al*, 2005). This inhibition can be overcome by the interaction of Reaper, Hid, Grim, Sickle and Jafrac2 (Reviewed in Salvesen & Duckett, 2002; Tenev *et al*, 2002), which can bind to and sequester DIAP-1. This mechanism of

inhibitor antagonism is mirrored in the mammalian apoptotic program by the ability of SMAC/DIABLO and Omi/HtrA2 to sequester mammalian IAPs (see section 1.6.2.2).

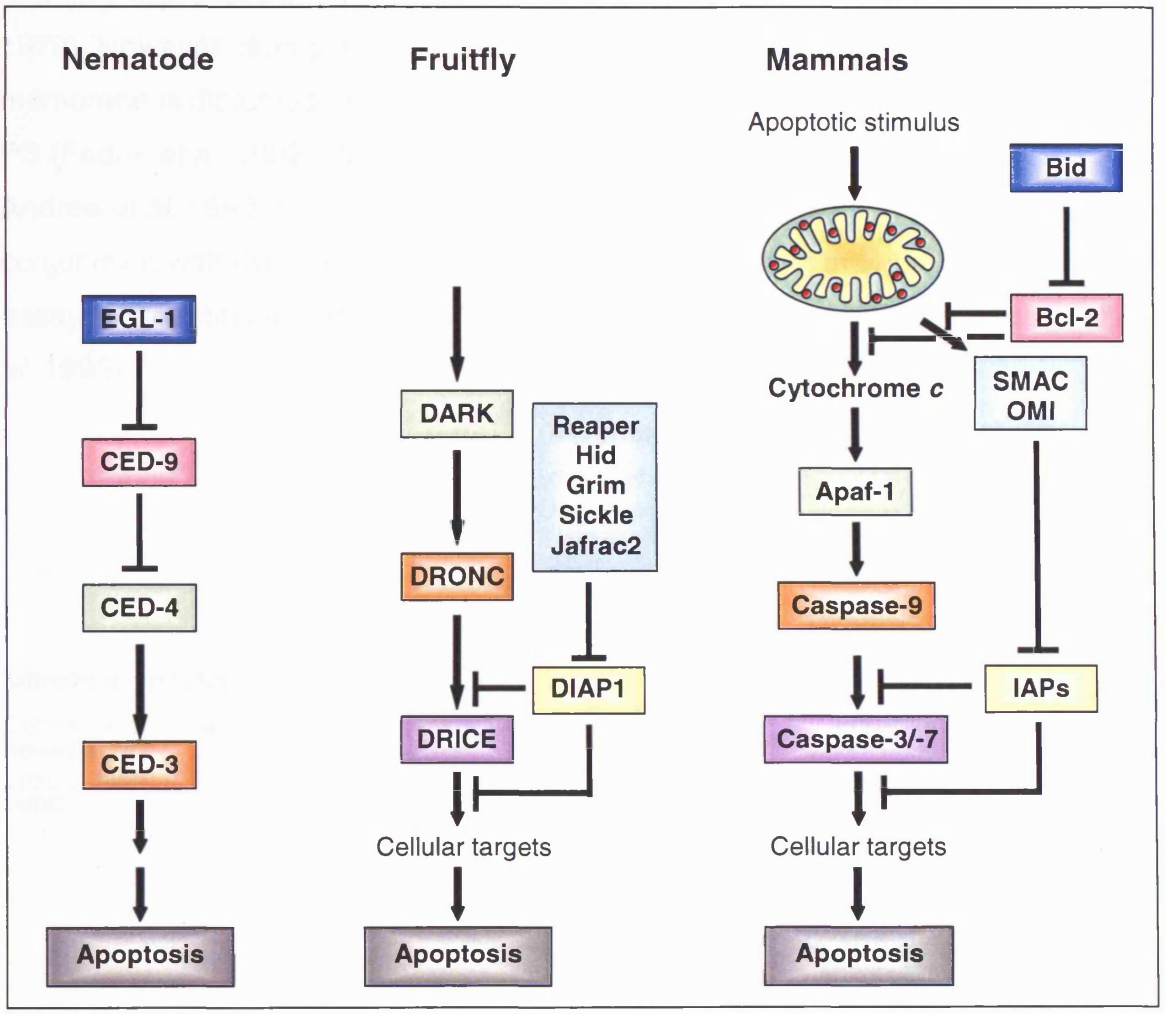

Figure 1.2.1: The evolutionarily conserved intrinsic apoptotic pathway (Adapted from Riedl & Shi, 2004)

1.3 Morphological and biochemical features of apoptosis

After the initial apoptotic signal, caspases are activated and these enzymes are responsible for the biochemical and morphological changes observed in apoptosis (Figure 1.3.1). In contrast to necrosis (during which cells swell and release their contents resulting in an inflammatory response) apoptosis is the controlled dismantling and disposal of unwanted cells. Cellular shrinkage is caused by cleavage of a major component of the plasma membrane-associated cytoskeleton, fodrin, in response to a range of pro-apoptotic stimuli (Martin *et al*, 1995a; 1995b; 1996). Plasma membrane changes due to the caspase-3-dependent cleavage of

gelsolin and actin reorganisation (Kothakota *et al*, 1997) and externalisation of phosphotidylserine (PS) (Fadok *et al*, 1992) also occur during apoptosis. The latter observation has subsequently been exploited to measure apoptosis. PS is normally expressed in the plasma membrane facing the cytosol (Op den Kamp, 1979). However, during apoptosis the phospholipid symmetry of the plasma membrane is disrupted (whilst retaining its integrity), resulting in the exposure of PS (Fadok *et al*, 1992). Annexin V preferentially binds to PS (Tait *et al*, 1989; Andree *et al*, 1990) and when Fluorescently-labelled (i.e. with FITC) and used in conjunction with dye exclusion (Propidium Iodide) to detect membrane integrity, an assay for counting apoptotic cells by flow cytometry was established (Vermes *et al*, 1995).

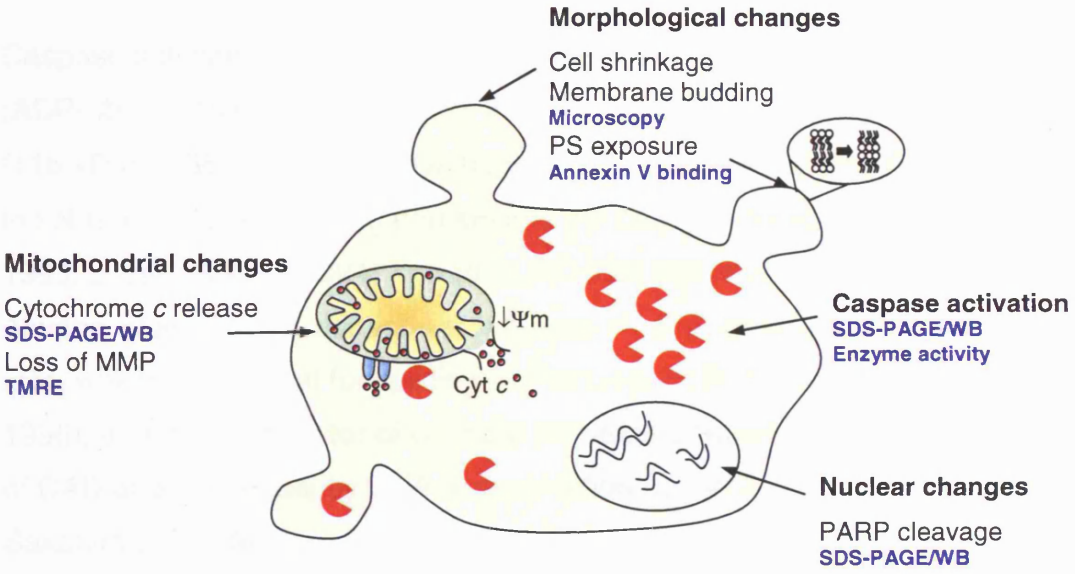

Figure 1.3.1: The morphological and biochemical changes that occur during apoptosis. Including how they were measured in this study (shown in blue bold, WB, Western Blot analysis).

In addition to changes at the plasma membrane during apoptosis, changes are also observed in the mitochondria and the nucleus. The mitochondria are involved in cellular respiration, an essential co-factor in which is cytochrome *c*. During apoptosis, the release of cytochrome *c* from the mitochondria (Liu *et al*, 1996; Yang *et al*, 1997; Kluck *et al*, 1997) can be either caspase-independent or caspase-dependent (Sun *et al*, 1999a; Chen *et al*, 2000b, see later), and induces apoptosis by two mechanisms. Firstly, it dismantles the respiratory chain and thus reduces energy production and secondly, it is critical for apoptosome formation in the intrinsic apoptotic pathway and subsequent caspase activation (see section

1.5.3). The release of cytochrome *c* from the mitochondria into the cytosol can therefore be used as a measurement of cell death induced via activation of the intrinsic pathway. The caspase-dependent release of cytochrome *c* occurs late in apoptosis and is accompanied by the depolarisation of the inner mitochondrial membrane (Heiskanen *et al*, 1999; Chen *et al*, 2000b), which can be measured fluorometrically using the cationic fluorophore TMRE. In healthy cells TMRE accumulates electrophoretically into the mitochondria due to the presence of a negative mitochondrial membrane potential (MMP) (Ehrenberg *et al*, 1988). However apoptotic cells which have lost their MMP, lack the ability to take-up TMRE and hence the fluorophore can be detected as defuse staining in the cytosol by flow cytometry.

Caspase activation also results in the cleavage of the DNA repair enzyme, poly (ADP-ribose) polymerase (PARP). PARP is cleaved from the active form (116 kDa) to 86 kDa and 25 kDa fragments by cleavage at $DEVD^{216}\downarrow G$ between the N-terminal DNA binding domain and the catalytic domain (Kaufmann *et al*, 1993; Lazebnik *et al*, 1994; Tewari *et al*, 1995; Nicholson *et al*, 1995; Fernandes-Alnemri *et al*, 1995). Caspases also cleave other nuclear proteins such as Ul 70 kDa, which is essential for splicing of precursor RNA (Casciola-Rosen *et al*, 1994, 1996), and ICAD (inhibitor of caspase activated DNase), resulting in the activation of CAD and consequently DNA fragmentation (Liu *et al*, 1997; Enari *et al*, 1998; Sakahira *et al*, 1998).

1.4 Caspases

The biochemical and morphological changes observed during apoptosis result from the activation of caspases, the initiators and executioners of cell death.

1.4.1 The caspase family

CED-3 in *C. elegans* shares structural homology to ICE (interleukin-1β (IL-1β) converting enzyme, caspase-1) (Yuan *et al*, 1993), which converts the inactive precursor of IL-1β into the mature active form by proteolytic cleavage (Thornberry *et al*, 1992; Cerretti *et al*, 1992). Following this discovery, 10 human caspases (CED-3 homologues) have since been identified and they share similarities in

amino acid sequence, structure and substrate specificity (Reviewed in Cohen, 1997; Nicholson & Thornberry, 1997; Thornberry & Lazebnik, 1998; Fuentes-Prior & Salvesen, 2004). Seven caspases are implicated in apoptosis (Figure 1.4.1), whereas the remaining three caspases (caspases-1, -4 and -5) are involved in the production of proinflammatory cytokines and contribute to the inflammatory response (Reviewed in Nicholson & Thornberry, 1997; Cohen, 1997).

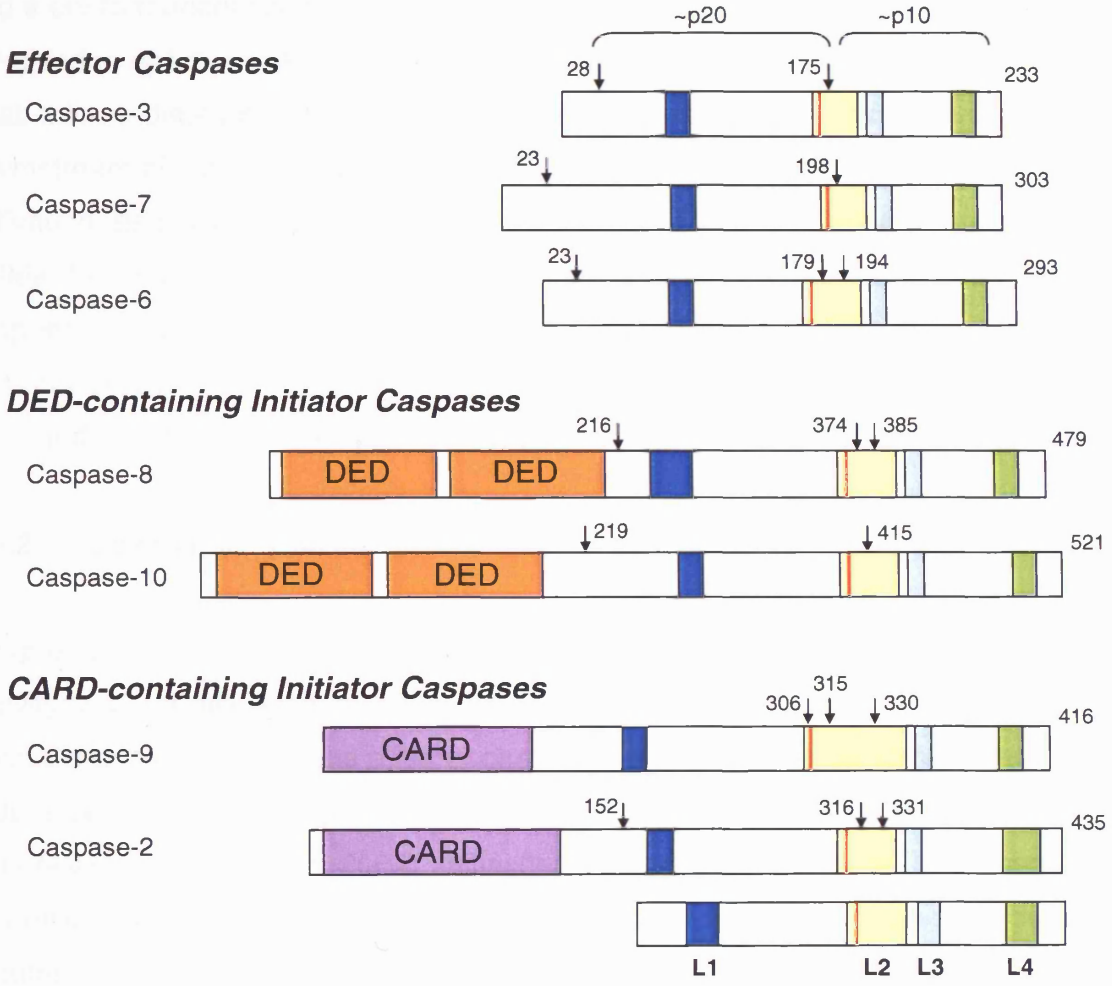

Figure 1.4.1: Structure of caspases involved in apoptosis. The substrate binding grooves are shaped by loops L1-4. (Adapted from Shi, 2002b).

Procaspases consist of three domains: an N-terminal prodomain, followed by a large subunit (~20 kDa) and finally a small subunit (~10 kDa). Caspases that are involved in the initiation of apoptosis ('initiator' caspases) also contain a flexible linker region between the large and small subunit, which allows activation of the caspase in the absence of proteolytic cleavage (Stennicke *et al*, 1999; Bratton *et al*, 2001b) and can also be excised during caspase activation. The nature of the N-

terminal prodomain dictates the role of the caspase. Initiator caspases have long prodomains (>100 amino acids), which contain protein-protein interaction motifs required for their scaffold-mediated activation. In apoptosis these caspases are caspase-8 (-10) and caspase-9, which become activated upon binding via their DED and CARD regions, respectively (described in detail later; Boldin *et al*, 1996; Muzio *et al*, 1996; Li *et al*, 1997). This recruitment to the adapter protein increases the local concentration of these caspases to promote induced-proximity cleavage and a conformational change allowing full activation. In contrast, effector caspases (involved in cell disassembly) have short prodomains (<30 amino acids), which are unable to mediate protein interactions and thus these caspases are activated downstream of initiator caspases solely by proteolytic cleavage. Caspase-8 activation results in the processing of caspases-3, -7 and -9 (Srinivasula *et al*, 1996a; Muzio *et al*, 1997), whereas caspase-9 directly processes and activates caspase-3 and -7 (Srinivasula *et al*, 1998; Li *et al*, 1997). Caspase-6, in contrast, can only be activated by active caspase-3 (Srinivasula *et al*, 1998), and thus is activated as part of the caspase cascade.

1.4.2 Procaspase maturation

Caspases are synthesized as catalytically inactive zymogens with low intrinsic activity. Initiator procaspases exist as monomers (due to their ability to activate upon dimerisation), whereas effector caspase zymogens exist as dimers and require proteolytic cleavage prior to activation (Boatright *et al*, 2003; Reviewed in Fuentes-Prior & Salvesen, 2004). Initial crystal studies of caspase-1 and caspase-3 showed that the processing and self-association of two procaspase zymogens is required to form an active caspase (Wilson *et al*, 1994; Walker *et al*, 1994; Rotonda *et al*, 1996; Mittl *et al*, 1997). Following cleavage at specific Asp-x bonds, the procaspase undergoes a conformational change which allows the formation of a tetrameric complex consisting of a two ~20 kDa and two ~10 kDa subunits (Figure 1.4.2), and in some cases the subsequent removal of the prodomain. In the active caspase tetramer, the two p20/p10 heterodimers align in a head-to-tail configuration with the two adjacent p10 domains surrounded by p20 fragments. This conformation produces two active sites, formed by amino acids from both the p20 and p10 domains, positioned at opposite ends of the molecule. Caspases that contain a linker domain have the flexibility to form the active sites in the absence

of proteolytic cleavage, and exist in their zymogen form as monomers (Boatright *et al*, 2003). However, the unprocessed form has only ~1-10% of the activity of the processed form (Muzio *et al*, 1998; Stennicke *et al*, 1999), and requires association with an adapter protein to significantly enhance this catalytic activity. For example, caspase-9 activity increases by ~2000 fold when bound to the apoptosome (Stennicke *et al*, 1999; Rodriguez & Lazebnik, 1999). In contrast, effector caspases do not possess linker regions and thus require the cleavage between the large and small subunits to allow reorganisation of the heterodimers to form the active site (Reviewed in Fuentes-Prior & Salvesen, 2004).

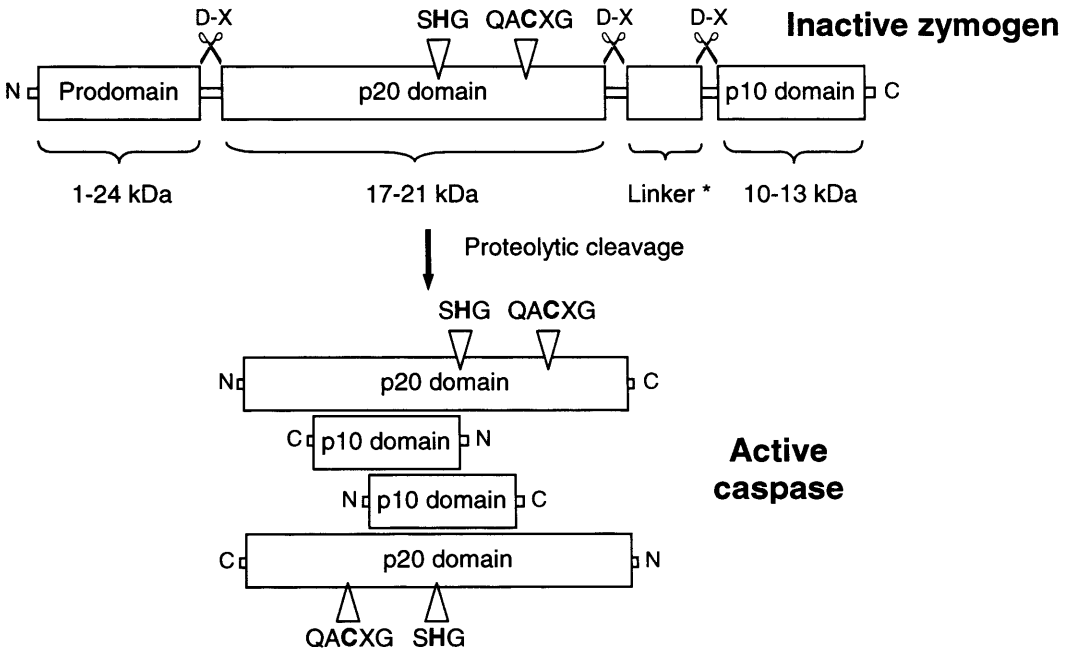

Figure 1.4.2: Schematic of caspase maturation by proteolytic cleavage and rearrangement of subunits (Adapted from Los & Walczak, 2002). Asterisk indicates that the linker region is not present in all caspases. Blue bold depicts catalytic dione.

1.4.3 Caspase recognition and cleavage of substrates

The caspase active site pentapeptide QACXG (where X= R, Q or G) is partially conserved through evolution, with an absolute requirement for a cysteine residue for catalysis, which is always found on the p20 subunit in mammalian caspases. The active site Cys285 is situated close to the His237 (caspase-1 numbering, shown in blue in Figure 1.4.2), where the imidazole side chain enhances the nucleophilic property of the cysteine residue by attracting protons away from it. The cysteine residue then attacks the amide bond of the Aspartic acid in the P1

position in the substrate, forming a covalently bound tetrahedral intermediate, which is stabilised by Glu283 (Wilson *et al*, 1994). The C-terminal region of the substrate is then released, and an acyl-enzyme complex is formed. The oxygen atom of a water molecule then attacks the acyl-enzyme complex and forms another covalently bound tetrahedral intermediate, before electron reorganisation leads to the release of the N-terminal fragment of the substrate, and returns the enzyme to its initial state (Wilson *et al*, 1994).

The side chains of Arg179 (p20) and Arg341 (p10) around the S1 site of the caspase are involved in direct charge-charge interaction with the Aspartic acid of the substrate, and contribute to the selective recognition of Aspartic acid at the P1 position (Wilson *et al*, 1994). The side chains of the amino acids at the P2 and P3 positions (The two residues to the amino side of the P1 Aspartate) are mainly exposed to the cytosol, and confer less stringent requirements at these positions on the substrate, but are involved in the caspase specificity to the substrates. Although Aspartic acid was initially described as conserved at the P1 position (Thornberry *et al*, 1992), caspases have been shown to cleave after a Glutamine residue (Hawkins *et al*, 2000; Srinivasula *et al*, 2001), which is also the preferred amino acid at the P3 position of all caspases (Thornberry *et al*, 1997). Asp-Glu-Val-Asp (DEVD) is the preferred substrate recognition sequence for both caspase-3 and caspase-7 (Thornberry *et al*, 1997), and has been exploited to produce synthetic peptides to measure the 'specific' activity of these caspases (i.e. Ac-DEVD.AMC; Nicholson *et al*, 1995). Furthermore, synthetic competitive inhibitors have also been developed based on the tetrapeptide motif to 'specifically' inhibit individual caspases (i.e. DEVD.CHO) (discussed further in section 1.6.1).

1.5 Activation of caspases and cell death

1.5.1 Cellular activation

Cytotoxic T-lymphocytes (CTLs) and natural killer cells (NK) secrete perforin and cytotoxic granules containing proteolytic enzymes, termed granzymes. Perforin polymerises in the presence of calcium forming channels in the plasma membrane, through which granzymes enter into transformed or virus-containing cells (Kagi *et al*, 1994). Granzyme B is a serine protease which can activate

caspases, via its shared substrate preference for an Aspartic acid residue in the P1 position. Caspases-3, -7, -8 and -9 are activated by Granzyme B, in a manner analogous to apical caspase activation (Yang *et al*, 1998b). Granzyme B can also induce apoptosis by cleaving the proapoptotic Bcl-2 family member, Bid, resulting in the release of cytochrome *c* and consequently the activation of the intrinsic pathway (Heibein *et al*, 2000) (see section 1.5.3).

1.5.2 The extrinsic pathway

Apoptosis initiated by secreted/cell-membrane bound ligands i.e. TNF (Tumour Necrosis Factor), CD95 and TRAIL (TNF-related apoptosis-inducing ligand) results in the activation of the extrinsic (death-receptor mediated) pathway and subsequent activation of caspase-8. However, this induction method of apoptosis sometimes requires amplification via the intrinsic pathway.

1.5.2.1 Death receptor-mediated apoptosis

Death receptors are a subfamily of the TNF receptor superfamily, characterised by the presence of an intracellular death domain (DD). Ligation of the CD95 (Fas) receptor was the first described and is the most studied type of receptor-mediated apoptosis (Itoh *et al*, 1991; Oehm *et al*, 1992). Binding of CD95L causes CD95 homotrimerisation and recruits the adapter molecule FADD (Fas receptor associated death domain) to the intracellular domain of the receptor via a homophilic DD interaction (Boldin *et al*, 1995; Chinnaiyan *et al*, 1995; Figure 1.5.1). FADD also contains an N-terminal death effector domain (DED) via which it recruits caspase-8 to the death receptor complex, forming the death inducing signalling complex (DISC) (Boldin *et al*, 1996; Muzio *et al*, 1996). The aggregation of caspase-8 molecules results in the induced-proximity activation of this apical caspase and initiation of the caspase cascade (Muzio *et al*, 1996; 1998; Boldin *et al*, 1996; Salvesen & Dixit, 1999). Caspase-8 is the apical caspase in receptor-mediated cell death, as shown by the fact that caspase-$8^{-/-}$ fibroblasts are resistant to CD95 and TNF-induced apoptosis, but are able to transmit the TNF pro-survival signal and activate NFκB (Juo *et al*, 1998; Varfolomeev *et al*, 1998).

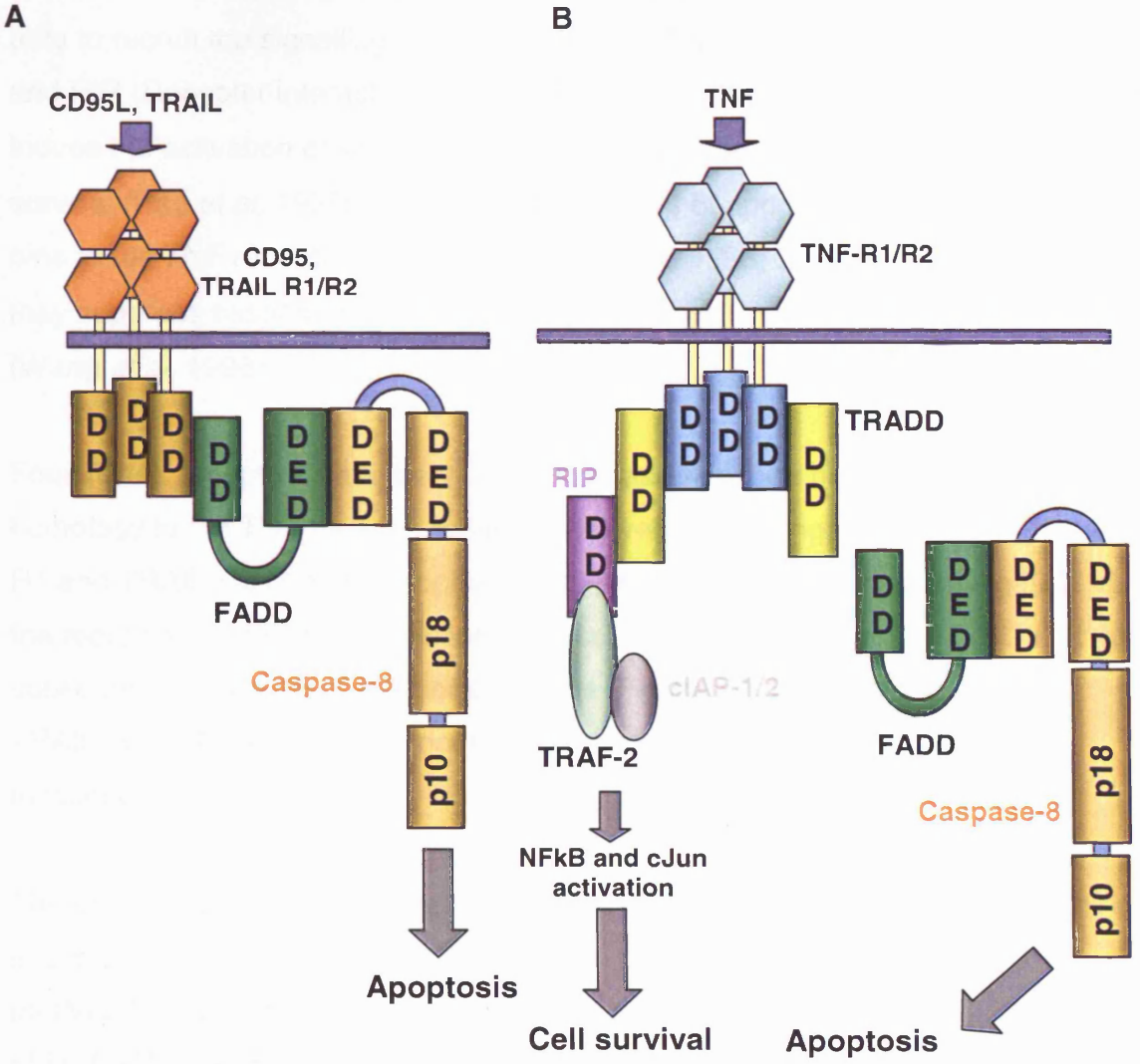

Figure 1.5.1: Caspase activation triggered by cell-surface receptor ligation. A, Signalling through CD95 and TRAIL R1/R2 results in apoptosis. **B**, Ligation of TNF receptors can result either in apoptosis or cell survival and proliferation.

Signalling through TNF receptors can have divergent effects via ligation of alternative TNF receptors; TNF-R1 and TNF-R2, which are structurally similar except for TNF-R2 lacking the intracellular DD domain and therefore is incapable of inducing apoptosis upon ligation. Induction of cell death via ligation of the TNF-R1 receptor is similar to that of CD95, except that the receptor initially recruits TRADD (TNF-receptor associated death domain). This adapter molecule was initially shown to recruit FADD (Hsu *et al*, 1996a), activate caspase-8 and induce apoptosis as described above (Figure 1.5.1B). However, more recent studies have shown that caspase-8 is not activated at the membrane-associated complex in TNF-mediated apoptosis, but rather is processed by associating with FADD in a

cytosolic complex (Harper *et al*, 2003; Michaeu & Tschopp, 2003). TRADD is also able to recruit the signalling molecules TRAF2 (TNF receptor associated factor-2) and RIP (Receptor interacting protein) (Hsu *et al*, 1996a; 1996b, respectively), and induce the activation of kinases in the NFκB and cJun pathways promoting cell survival (Hsu *et al*, 1996b). The cellular inhibitors of apoptosis (cIAP-1/-2) also bind to the TNF receptor via TRAF2 (Rothe *et al*, 1995; Shu *et al*, 1996), where they suppress caspase-8 activation and promote cell survival via NFκB activation (Wang *et al*, 1998).

Four TRAIL receptors have been identified based on their high sequence homology to the TNF receptor family (Reviewed in Spierings *et al*, 2004). TRAIL-R1 and TRAIL-R2 contain cytoplasmic DD and induce apoptosis upon ligation via the recruitment of FADD and the initiator caspase, caspase-8 to the DISC and the subsequent activation of effector caspases (Figure 1.5.1A). Ligation of either TRAIL-R3 or TRAIL-R4 does not result in apoptosis due to an absence of a functional death domain.

The endogenous inhibitor of apoptosis, FLIP (FADD-like interleukin-1β converting enzyme-like protease (FLICE/C8)-inhibitory proteins) regulates the receptor-mediated activation of caspase-8 (Irmler *et al*, 1997; Shu *et al*, 1997). Both forms of FLIP ($FLIP_L$ and $FLIP_S$) share structural homology with procaspase-8 but lack the catalytic site and therefore act as pseudosubstrates for the DISC (Scaffidi *et al*, 1999; Krueger *et al*, 2001). However, this inhibitory effect is only observed with high concentrations of FLIP, as physiological (low) levels of FLIP results in enhanced apoptosis, possibly by forming a dimer with caspase-8 (Chang *et al*, 2002; Micheau *et al*, 2002).

1.5.2.2 Cross-talk between the extrinsic and intrinsic pathway

In some cells (e.g. SKW6.4 and H9), the amount of active caspase-8 formed at the DISC following CD95 ligation is sufficient to elicit apoptosis directly (Type I cells; Scaffidi *et al*, 1998). However, in other cell types (e.g. CEM and Jurkat), the signal from the DISC results in the production of inadequate amounts of active caspase-8 to induce apoptosis alone and therefore requires amplification of the signal via the intrinsic pathway (Scaffidi *et al*, 1998; Figure 1.5.2).

In type II cells, active caspase-8 activates the BH3-only Bcl-2 family member Bid, by proteolytic cleavage (Luo *et al*, 1998; Li *et al*, 1998; Gross *et al*, 1999a). Processing of Bid by caspase-8 results in the formation of the active fragment p15 and minor fragments of p13 and p11 (Gross *et al*, 1999a). The truncated p15 form, tBid, then translocates to the mitochondria where it interrupts the mitochondrial outer membrane and releases cytochrome *c* into the cytosol (Luo *et al*, 1998; Li *et al*, 1998; Gross *et al*, 1999a). Cytosolic cytochrome *c* then contributes to the formation of the apoptosome (see section 1.5.3), by allowing the oligomerisation of Apaf-1 (Liu *et al*, 1996; Adrain *et al*, 1999; Saleh *et al*, 1999). Caspase-9 is then recruited and activated at the apoptosome where it can then process and activate effector caspases resulting in cell death.

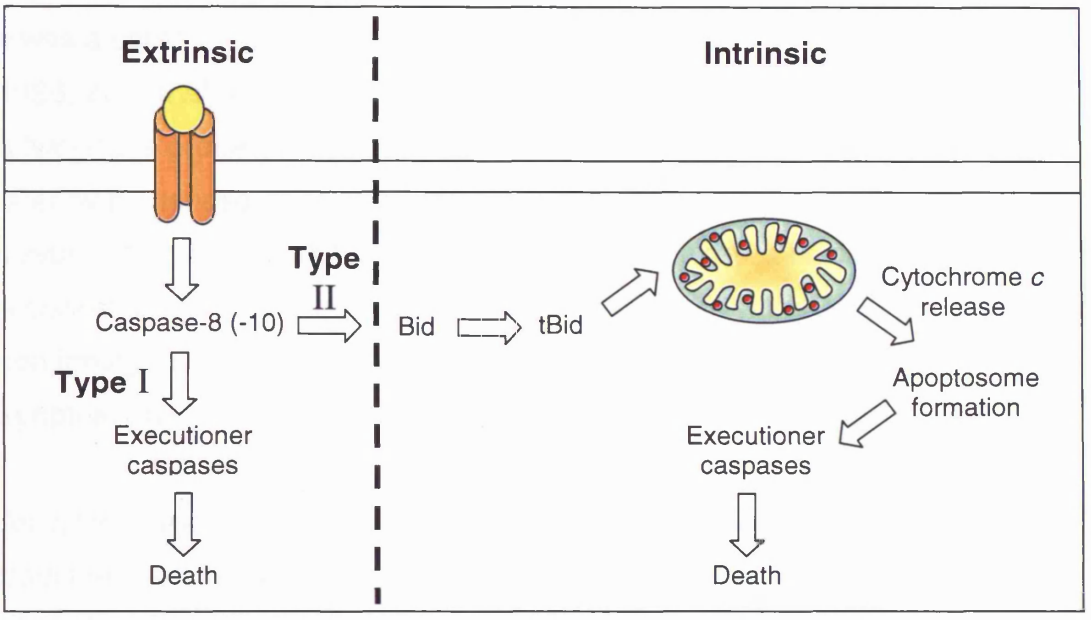

Figure 1.5.2: Cross-talk between the extrinsic and intrinsic apoptotic pathways. (see text for details)

There are three main hypothesises as to how Bid elicits the release of cytochrome *c* (Reviewed in Danial & Korsmeyer, 2004). One theory suggests that Bid induces a conformational change in Bax/ Bak (Bcl-2 family members, see later), which allows their oligomerisation to form multimeric membrane pores. Further to this, the presence of either Bak or Bax is required for the release of cytochrome *c* via tBid (Wei *et al*, 2001). Alternatively, cytochrome *c* is released through a voltage-dependent anion channel-containing pore (Shimizu *et al*, 1999), or by permeabilisation of the outer mitochondrial membrane (Adachi *et al*, 1997; Kluck

et al, 1999). Caspase-3-dependent cleavage of Bid can also occur during intrinsic-mediated apoptosis to amplify the apoptotic signal (Tang *et al*, 2000).

Cytochrome *c* is a member of the electron transport chain in mitochondria, involved in energy production, and is produced in the mitochondrial intermembrane space from two non-apoptogenic precursors, haem and apocytochrome *c* which is taken up by mitochondria (Gonzales & Neuport, 1990). Early studies of CD95-mediated apoptosis in Jurkat cells (type II cells) revealed that mitochondria lost their cytochrome *c* function (Krippner *et al*, 1996) due to release of this proapoptotic protein into the cytosol (Liu *et al*, 1996; Yang *et al*, 1997) and not the inhibited uptake of apocytochrome *c* (Yang *et al*, 1997). The importance of this observation became evident with the discovery that cytochrome *c* was a component of the caspase-activating complex, the apoptosome (Liu *et al*, 1996; Zou *et al*, 1999). The release of cytochrome *c* via the intrinsic pathway is by a two-stage process; with an early release being caspase-independent followed later by a caspase-dependent (tBid-induced) release (Kluck *et al*, 1997; Sun *et al*, 1999a; Chen *et al*, 2000b). Further to this, cytochrome $c^{-/-}$ cells were shown to be resistant to UV irradiation, STS treatment and serum withdrawal (Li *et al*, 2000a), confirming the importance of this mitochondrial protein in the activation of apoptosis via the intrinsic pathway.

As cytochrome *c* can be instrumental in the progression of apoptosis, its release from the mitochondria is strictly regulated. This regulation is provided by members of the Bcl-2 family (CED-9 homologues), which contain up to four conserved homology domains, termed BH1-4 (Reviewed in Gross *et al*, 1999b). This family can be divided into two groups: anti-apoptotic proteins e.g. Bcl-2, Bcl-$_{XL}$; and proapoptotic members which either only lack the BH4 domain e.g. Bax, Bak or only contain the BH3 domain e.g. Bid, Bad. Bcl-2 and Bcl-$_{XL}$ prevent the tBid-induced release of cytochrome *c* and consequently apoptosis induced by STS, Etoposide and UV irradiation, and also in type II cells treated with TNF (Kharbanda *et al*, 1997; Yang *et al*, 1997; Kluck *et al*, 1997; Li *et al*, 1998; Gross *et al*, 1999a). Bcl-2 and Bcl-$_{XL}$ also inhibit the release of SMAC, which is involved in antagonising the endogenous caspase inhibitors (see section 1.6.2.2) (Sun *et al*, 2002). The proapoptotic function of Bid is also regulated via its phosphorylation by casein

kinases, which prevents the proteolytic cleavage to form tBid (Desagher *et al*, 2001).

1.5.3 Cytochrome *c*-mediated cell death (Intrinsic pathway)

The formation of the apoptosome results from exposure to environmental stresses such as DNA damage, heat shock and oxidative stress, or as an amplification pathway in type II cells (described in section 1.5.2.2), and consequently leads to mitochondrial perturbation. Molecular and chromatography techniques have identified three apoptotic protease activating factors (APAFs) essential for stress-mediated apoptosis, termed Apaf-1, Apaf-2 and Apaf-3. Apaf-1 is a mammalian CED-4 homologue (Zou *et al*, 1997), which oligomerises to form an apoptosome in the presence of Apaf-2 (cytochrome *c*) and dATP (Liu *et al*, 1996; Li *et al*, 1997). Apaf-3 (caspase-9) is then processed and activated when bound to oligomerised Apaf-1 via their respective N-terminal CARD domains (Li *et al*, 1997; Qin *et al*, 1999). The active initiator caspase is then able to process effector caspases and elicit the execution phase of apoptosis.

The importance of the apoptosome *in vivo* was shown in Apaf-$1^{-/-}$ mice embryos, where the absence of Apaf-1 results in brain and facial deformities, in addition to persisting interdigital webs (Cecconi *et al*, 1998; Yoshida *et al*, 1998). Apaf-$1^{-/-}$ embryonic fibroblasts are more resistant to apoptosis induced by the intrinsic pathway (i.e. ceramide and staurosporine treatment) but not to CD95-mediated apoptosis (Cecconi *et al*, 1998), demonstrating the specific role of Apaf-1 in the intrinsic apoptotic pathway.

1.5.3.1 The domain structure of Apaf-1 and formation of the apoptosome

Apaf-1 is a ~135 kDa protein with an N-terminal CED-3 homology domain, a CED-4 homology domain and a C-terminal domain with 12-13 WD40 repeats (Zou *et al*, 1997; 1999; Hu *et al*, 1999) (Figure 1.5.3). The N-terminal CED-3 homologous region consists of 97 amino acids, which allows protein interactions via its CARD (Hofmann *et al*, 1997). C-terminal to the CARD domain is a region that shares 48% similarity in amino acid sequence to the *C.elegans* death-promoting protein CED-4 (Zou *et al*, 1997). The two longest stretches of conserved amino acid

sequence correspond to the location of Walker boxes A (p-loop) and B, respectively, which are proposed to be involved in nucleotide binding (Walker *et al*, 1982; Zou *et al*, 1997). Mutations in these nucleotide binding sites abolish both Apaf-1 and CED-4 function, thus highlighting the importance of these regions (Seshagiri & Miller, 1997; Hu *et al*, 1998b). Both the CED-3 and CED-4 homology domains of Apaf-1 have been shown to be critical for the caspase processing activity of the apoptosome, with the CED-3 domain essential for caspase-9 recruitment and the CED-4 domain indispensable for Apaf-1 oligomerisation (Srinivasula *et al*, 1998; Hu *et al*, 1998b).

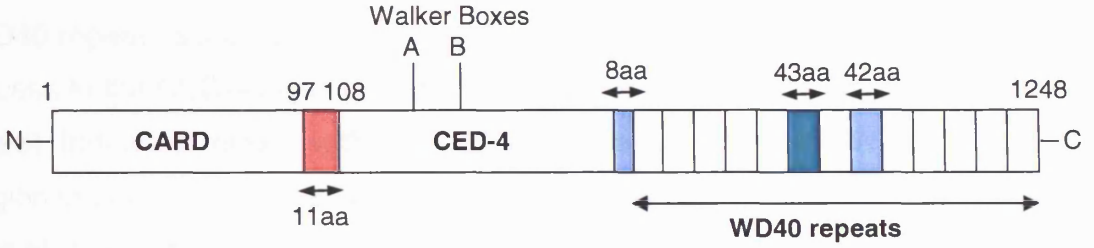

Figure 1.5.3: The domain structure of Apaf-1 (Adapted from Benedict *et al*, 2000).

To date, six isoforms of Apaf-1 have been identified, four of which vary in the presence or absence of a 43 amino acid WD40 repeat and an 11 amino acid region after the CARD domain (Figure 1.5.3). These isoforms are termed Apaf-1S (-43/-11), Apaf-1_{XL} (+43/+11), Apaf-1M (-43/+11) and Apaf-1L (+43/-11) (Zou *et al*, 1997; 1999; Hu *et al*, 1999; Benedict *et al*, 2000). Two shorter variants of Apaf-1 have also been described; Apaf-1-XS and Apaf-1-Alt (Hahn *et al*, 1999; Ogawa *et al*, 2003). Whereas Apaf-1XS only differs from Apaf-1M by the absence of a 42aa region in the WD40 domain and the insertion of 8aa (shown in blue; Hahn *et al*, 1999), Apaf-1-Alt is a C-terminally truncated isoform with only a CARD and partial CED-4 domain (Ogawa *et al*, 2003). Apaf-1_{XL} and Apaf-1LC are the only two forms of Apaf-1 capable of forming a functional apoptosome and supporting caspase activation due to the presence of the additional WD40 domain, which allows binding of cytochrome *c* (Benedict *et al*, 2000).

The N-terminal CARD domain consists of a 6 membered antiparallel α helical bundle (Chou *et al*, 1998), which acts as a docking region to only allow the CARD domain of caspase-9 to bind to Apaf-1, and not other CARD-containing caspases (Pan *et al*, 1998b; Slee *et al*, 1999). Mutagenesis studies of the CARD domain of

caspase-9 have identified Arginine 56 (R56) to be crucial for the binding of Apaf-1 and caspase-9, as mutation to Alanine results in the loss of association (Qin *et al*, 1999). However, caspase-9 is only recruited to the CARD domain of Apaf-1 once Apaf-1 has oligomerised (Saleh *et al*, 1999) an event which occurs via the CED-4 homology region and linker domain (Adrain *et al*, 1999) in the presence of dATP and cytochrome *c* (Li *et al*, 1997; Zou *et al*, 1999; Saleh *et al*, 1999).

Typically WD40 repeats are a set of sequences proposed to mediate protein-protein interactions, and are found in regulatory proteins including the β-subunits of heterotrimeric G-proteins (Neer *et al*, 1994; Wall *et al*, 1995). In Apaf-1 the WD40 repeats act as an internal negative regulator by binding and preventing access to the CED-4 oligomerisation domain (Hu *et al*, 1998b; Srinivasula *et al*, 1998). Indeed, a residue within the CED-4 domain may lock the WD40 repeat region in place, as a mutation at M368L reduces the binding of the WD40 region and allows processing and activation of caspase-9 in the absence of dATP and cytochrome *c* (Hu *et al*, 1999). The inhibition by the WD40 domains can be overcome with the addition of cytochrome *c* (Adrain *et al*, 1999), which allows the exposure of the CED-4 domain and facilitates dATP binding (Jiang & Wang, 2000), resulting in Apaf-1 oligomerisation. The reversal of the inhibition induced by the WD40 domain is only possible in the splice variants of Apaf-1 containing 13 WD40 repeats (Benedict *et al*, 2000), and therefore suggests that cytochrome *c* binds to Apaf-1 via this extra WD40 domain. The oligomerisation of Apaf-1 then allows the recruitment and activation of caspase-9 (Zou *et al*, 1999; Saleh *et al*, 1999), which can be activated by autocatalytically processing by induced close-proximity (Srinivasula *et al*, 1998; Hu *et al*, 1998b; Salvesen & Dixit, 1999) (Figure 1.5.4).

Further evidence for the negative regulatory role of the WD40 repeats is provided by the fact that C-terminally truncated forms of Apaf-1 (Apaf-1-530 and 1-559) are able to oligomerise and recruit/process caspase-9 independently of dATP and cytochrome *c* (Srinivasula *et al*, 1998; Hu *et al*, 1998b). However these forms of Apaf-1 are unable to release mature caspase-9 from the apoptosome and are also unable to recruit and process caspase-3. It is thought that caspase-9 is released from the apoptosome by cleavage of Apaf-1 by caspase-3 in the CED-4 domain, which results in the formation of a 30 kDa fragment (Bratton *et al*, 2001a).

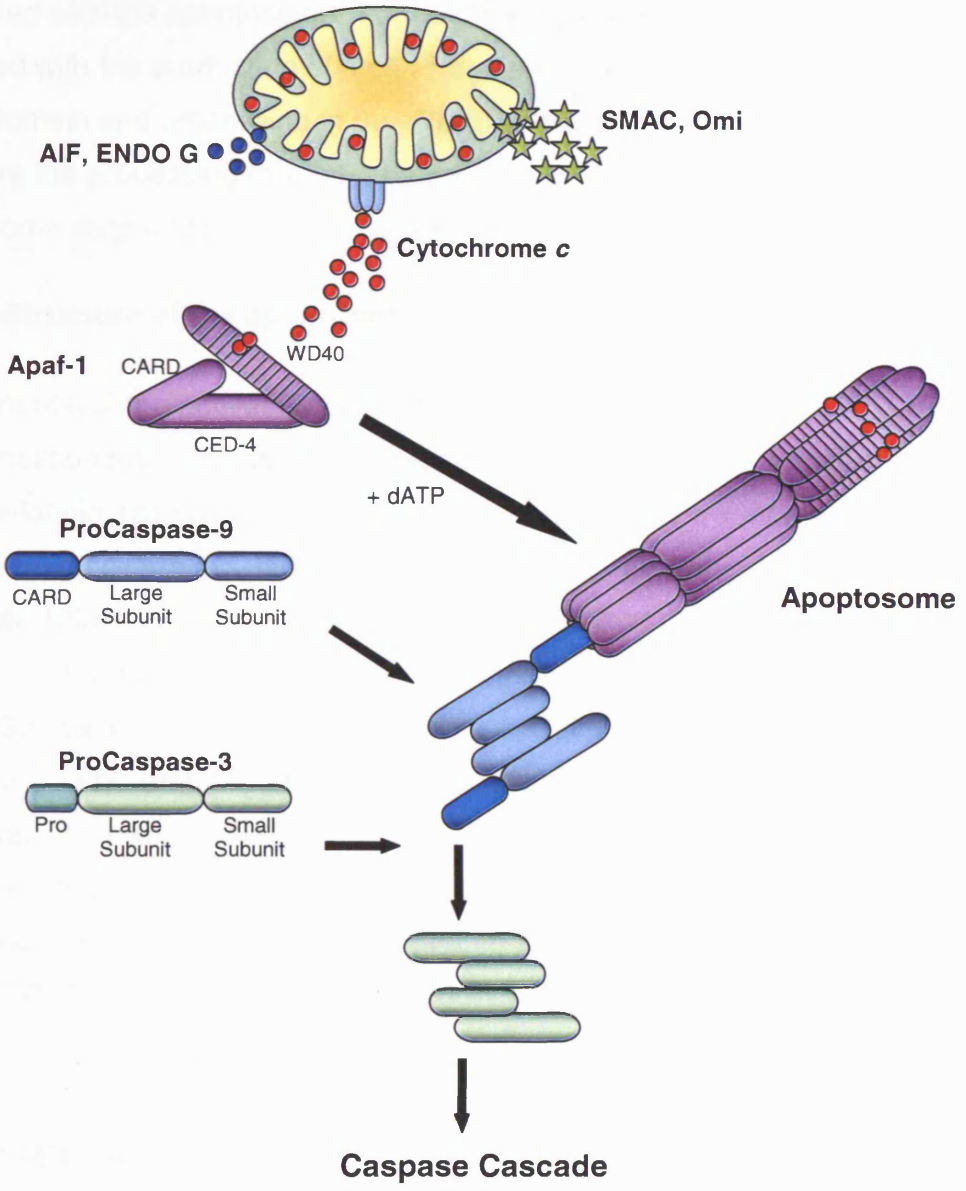

Figure 1.5.4: Schematic of Apoptosome Formation. Access to the CARD domain of Apaf-1 in resting cells is usually blocked by the interaction between the CED-4 domain and the WD40 repeats (Srinivasula *et al*, 1998; Hu *et al*, 1998b). However, following an apoptotic insult, cytochrome c is released from the mitochondria (Liu *et al*, 1996) where is can bind to the WD40 repeats of Apaf-1 and promote binding of dATP/ATP (Hu *et al*, 1999; Adrain *et al*, 1999; Jiang & Wang, 2000). The binding of these co-factors causes a conformational change in Apaf-1 to expose the CED-4 domain and allow oligomerisation (Hu *et al*, 1999; Zou *et al*, 1999). The oligomerised Apaf-1 complex (the apoptosome) can then recruit and bind caspase-9 via CARD:CARD interactions (Qin *et al*, 1999; Zou *et al*, 1999; Saleh *et al*, 1999). Caspase-9 can then recruit and activate caspase-3 and initiate the execution phase of apoptosis.

Therefore in the absence of effector caspase activation, caspase-9 remains associated with the apoptosome. Further cleavage of Apaf-1 has also been described with the production of a p84 fragment, resulting from cleavage in the CARD domain and processing in the WD40 domains (Lauber *et al*, 2001). Therefore the processing of Apaf-1 by active effector caspases could result in apoptosome degradation and the release of associating proteins.

1.5.3.2 Structure of the apoptosome

The formation of the active mammalian apoptosome requires Apaf-1 oligomerisation and recruitment of caspase-9. Apaf-1 is usually found in the monomeric/ dimeric form, eluting from gel filtration columns with a molecular weight ranging between ~130 and ~300 kDa (Zou *et al*, 1999; Saleh *et al*, 1999; Cain *et al*, 1999). In recombinant studies Apaf-1 and caspase-9 form a complex between ~1 MDa and ~1.4 MDa when activated with dATP and cytochrome *c* (Zou *et al*, 1999; Saleh *et al*, 1999; Acehan *et al*, 2002). However, in cellular lysates from THP-1 cells, dATP activation induces oligomerisation of Apaf-1 into two complexes of ~700 kDa and ~1.4 MDa (Cain *et al*, 1999; 2000), of which only the ~700 kDa complex has caspase-3 processing activity (Cain *et al*, 2000). Furthermore, the predominant form of the apoptosome detected in apoptotic cells is the ~700 kDa complex (Cain *et al*, 2000; Freathy *et al*, 2000; Almond *et al*, 2001).

In the ~1 MDa recombinant apoptosome visualised by cryoelectromicroscopy, the CARD domains and part of the CED-4 homology region of seven Apaf-1 molecules form the central hub of the apoptosome (Figure 1.5.5A), to which procaspase-9 binds to form a dome-like structure (Figure 1.5.5B; Acehan *et al*, 2002). Radiating from the hub are the arms, which contain part of the CED-4 homology domain and the linker region to the WD40 repeats. The latter form two β propeller-like structures in a Y-shaped structure; to which either one or two molecules of cytochrome *c* bind to cause the conformational changes in Apaf-1 necessary for oligomerisation (Purring-Koch & McLendon, 2000).

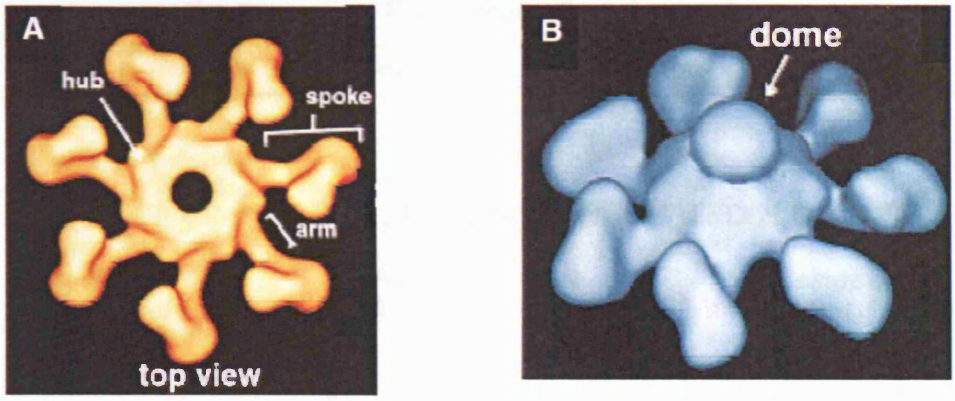

Figure 1.5.5: 3-Dimensional structure of the apoptosome. (Acehan *et al*, 2002).

1.5.3.3 Activation of caspase-9 at the apoptosome

Caspase-9 (also termed ICE-LAP6 (Duan *et al*, 1996b) and Mch6 (Srinivasula *et al*, 1996b)) is an initiator caspase activated either at the apoptosome or by Granzyme B (Zou *et al*, 1999; Saleh *et al*, 1999; Duan *et al*, 1996b). Autocatalytic processing at Asp315 is induced by the close-proximity of caspase-9 molecules as a result of binding to the apoptosome, and induces the formation of the p35/p12 enzyme (Li *et al*, 1997; Srinivasula *et al*, 1998). Caspase-9 is also cleaved at Asp330 by caspase-3, resulting in the formation of a p37/p10 or p35/p10 caspase conformation, which increases the enzymatic activity compared with the p35/p12 form of caspase-9 (Srinivasula *et al*, 1998; Slee *et al*, 1999; Zou *et al*, 2003) (Figure 1.5.6). Although dimerisation of caspase-9 is sufficient to induce activation (Srinivasula *et al*, 1998), the activity of this caspase is significantly enhanced upon the binding to Apaf-1, forming an active holoenzyme with ~2000 fold more activity than the unprocessed zymogen (Rodriguez & Lazebnik, 1999; Stennicke *et al*, 1999).

Caspase-9 normally resides in a monomeric zymogen form (Boatright *et al*, 2003) but at high concentrations caspase-9 is dimeric and has two different active sites (Renatus *et al*, 2001). One of the sites is competent at processing substrates, while the other has disrupted catalytic activity (Renatus *et al*, 2001). Binding to Apaf-1 allows allosteric changes to occur in caspase-9 permitting the correct conformation of the active site (Rodriguez & Lazebnik, 1999) and consequently intramolecular autocatalytic cleavage of caspase-9 occurs (Zou *et al*, 1999).

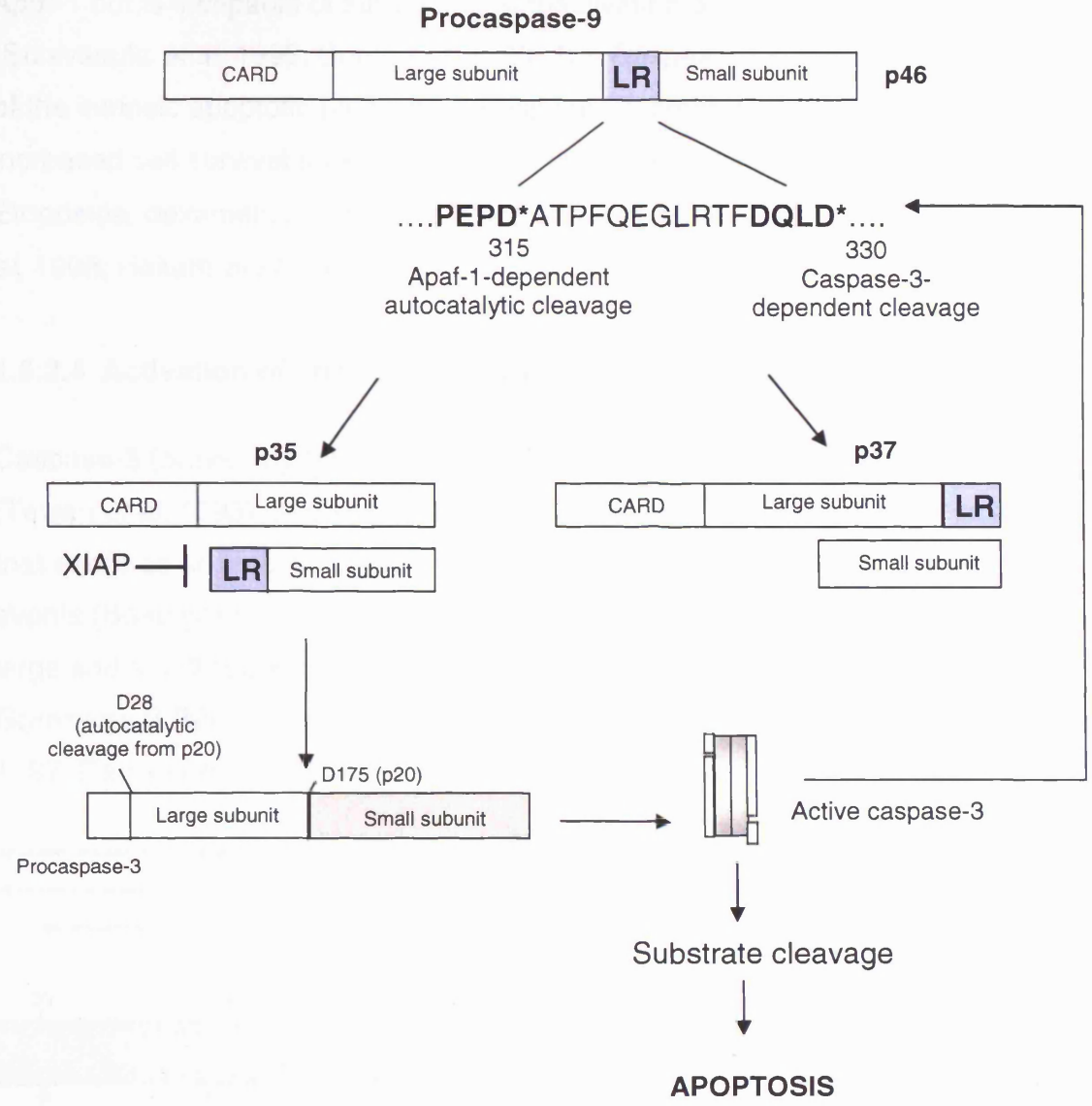

Figure 1.5.6: Processing of Caspase-9 (Adapted from Cain *et al*, 2002). The autoprocessing of caspase-9 occurs at Asp315, and exposes a tetrapeptide recognised by XIAP, which can then reduce its ability to process effector caspases (Srinivasula *et al*, 1998; 2001) (discussed later). Cleavage of caspase-9 by caspase-3 at Asp330 however, removes the recognition motif and prevents inhibition by XIAP (Srinivasula *et al*, 2001), providing an amplification mechanism. LR, linker region.

Caspase-9 needs to be present in the apoptosome for caspase-3 recruitment and subsequent activation (Bratton *et al*, 2001b). However, caspase-9 does not need to be processed itself to have caspase processing ability (Stennicke *et al*, 1999). The noncleavable caspase-9 mutant (D315/330A) still processes caspase-3 independent of caspase-9 processing, but the processed caspase-3 is not released from the apoptosome (Stennicke *et al*, 1999; Bratton *et al*, 2001b). In contrast, the C287A catalytically inactive mutant caspase-9 can also bind to

Apaf-1 but is incapable of supporting autoactivation or effector caspase activation (Srinivasula *et al*, 1998; Bratton *et al*, 2001b). Caspase-9 is crucial for the initiation of the intrinsic apoptotic pathway as caspase-$9^{-/-}$ embryonic thymocytes show increased cell survival (due to abrogated caspase-3 activation) after treatment with Etoposide, dexamethasone and γ-irradiation, but not to CD95 treatment (Kuida *et al*, 1998; Hakem *et al*, 1998).

1.5.3.4 Activation of effector caspases by the apoptosome

Caspase-3 (previously termed CCP32 (Fernandes-Alnemri *et al*, 1994), Yama (Tewari *et al*, 1995), and apopain (Nicholson *et al*, 1995)) is an effector caspase that exists as an inactive dimer prior to activation by two sequential proteolytic events (Boatright *et al*, 2003; Figure 1.5.7). The first cleavage occurs between the large and small subunits, at Asp175, and is performed by initiator caspases or Granzyme B (Nicholson *et al*, 1995; Fernandes-Alnemri *et al*, 1996; Han *et al*, 1997; Darmon *et al*, 1995).

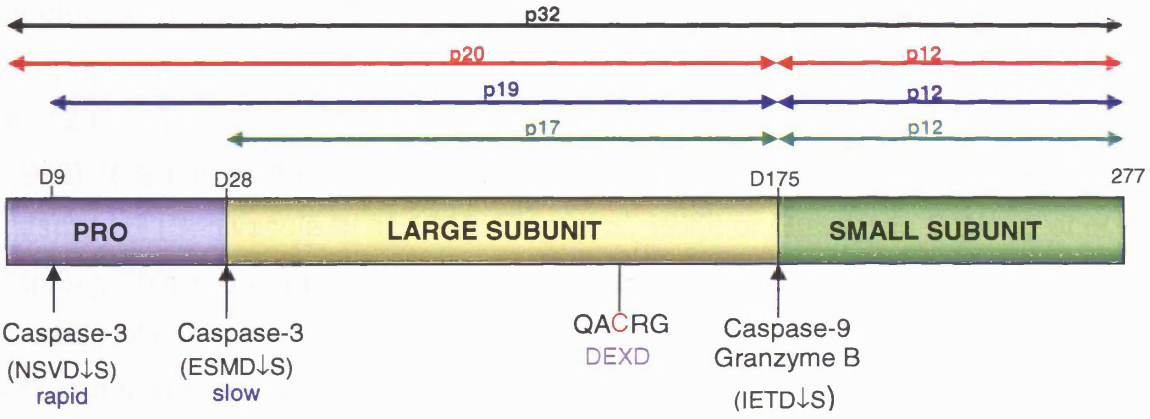

Figure 1.5.7: Schematic of the domain structure caspase-3 (Adapted from Fernandes-Alnemri *et al*, 1996).

Unlike apical caspases, effector caspases have no residual activity and are incapable of autoproteolytic cleavage in the proform, presumably through the absence of a linker region, which doesn't allow the peptide chain enough flexibility to form the catalytic site in the absence of proteolytic cleavage between the large and small subunits (Riedl *et al*, 2001b; Boatright *et al*, 2003). When caspase-3 has been cleaved to the p20/p12 form, caspase-3 can then autocatalytically remove the prodomain by rapid proteolysis at Asp9 (to form the p19 subunit) (Fernandes-Alnemri *et al*, 1996; Han *et al*, 1997), followed by a slow cleavage at Asp28, which

forms the p17 form of caspase-3. There appears to be no difference in substrate processing ability between the p17 and p19 forms of caspase-3 (Stennicke *et al*, 1998).

The preferred substrate recognition motif for caspase-3 is DEXD↓A (Thornberry *et al*, 1997), a motif that is found in a number of key cellular enzymes. These proteins include DNA repair enzymes (PARP, U1-70kD, ICAD), cytoskeletal proteins (actin and gelsolin), inhibitors of apoptosis (XIAP and Bcl-2) proapoptotic proteins (Bid, caspase-8 and caspase-9) and downstream caspases (caspase-6 and caspase-7). Interestingly, of the above-mentioned substrates only PARP (Germain *et al*, 1999) and ICAD (Houde *et al*, 2004) are cleaved by caspase-7, despite possessing the same substrate preference motif as caspase-3 (Thornberry *et al*, 1997).

Procaspase-7 (Mch3/CMH-1/ICE-LAP3 Fernandes-Alnemri *et al*, 1995; Lippke *et al*, 1996; Duan *et al*, 1996a) exists as a 35 kDa zymogen and shows the highest homology to caspase-3 (52% identity, Lippke *et al*, 1996). Caspase-7 is activated in apoptosis induced by a range of stimuli including CD95, TNF and p53 (Duan *et al*, 1996a; Chandler *et al*, 1997), and following dATP activation *in vitro* (Slee *et al*, 1999). It is initially cleaved between the large and small subunits at Asp198 by caspase-9 (Srinivasula *et al*, 1998; Slee *et al*, 1999) or Granzyme B (Yang *et al*, 1998b). This allows the caspase to rearrange the subunits to form the active site in a p22/p12 conformation (Figure 1.5.8). The N-terminal peptide is then removed by either autocatalytic processing or by caspase-3 at Asp23 (Fernandes-Alnemri *et al*, 1996; Duan *et al*, 1996a; MacFarlane *et al*, 1997), producing a p19/p12 fully active enzyme. The prodomain can also be removed by active caspase-3 prior to cleavage of caspase-7 in the linker domain (Yang *et al*, 1998b). This cleavage increases the avidity for caspase-9 cleavage and subsequent activation of caspase-7 (Denault & Salvesen, 2003). When expressing recombinant caspase-7 in bacteria, an alternative start site at Met45 results in the formation of a 30 kDa form of the caspase, which can be further processed to form an active p18/p12 conformation (Fernandes-Alnemri *et al*, 1996).

Although caspase-7 shares the same substrate recognition motif as caspase-3 (Thornberry *et al*, 1997) it does not share the same substrates, and therefore

cannot completely compensate for the absence of caspase-3. However, the breast cancer cell line MCF-7, which lacks the expression of caspase-3 (due to a 47-base pair deletion in the *CASP3* gene (Janicke *et al*, 1998)) still undergoes apoptosis induced by a range of apoptotic stimuli, albeit with a different morphology (Tang *et al*, 2000; MacFarlane *et al*, 2000; Liang *et al*, 2001).

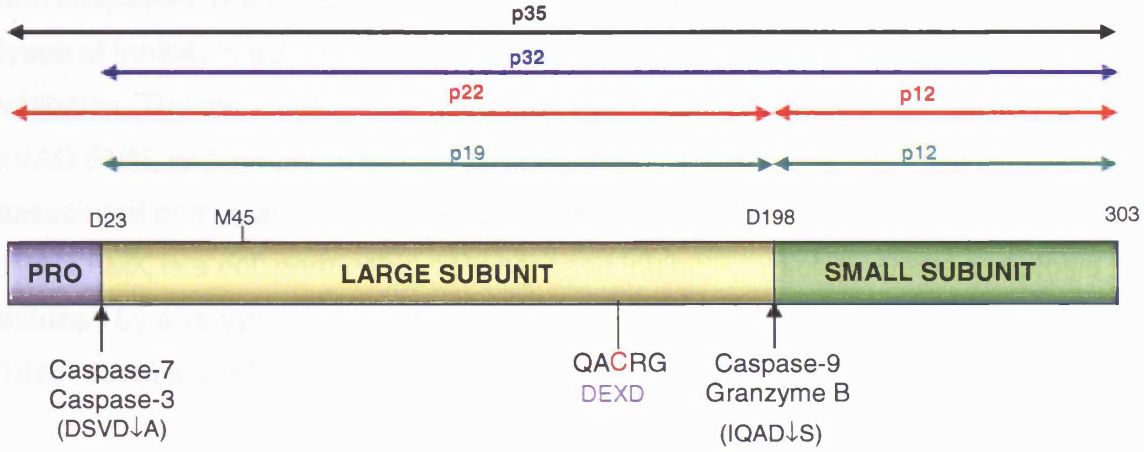

Figure 1.5.8: Schematic of the domain structure of caspase-7. The cleavage sites and the alternative translation start site (M45) are shown (Adapted from Fernandes-Alnemri *et al*, 1996).

The differential subcellular fractionation following processing of caspase-7 has highlighted an interesting difference between caspase-7 and caspase-3. Although procaspase-7 is located in the cytosol (Duan *et al*, 1996a), the p19 active form is found in the mitochondrial/microsomal fractions (Chandler *et al*, 1998), compared with active caspase-3, which is situated in the cytosol. In addition, the pI of caspase-7 has also been shown to change from 5.5 to 8.0 upon caspase activation (Denault & Salvesen, 2003), in contrast to caspase-3, which therefore suggests that caspase-7 could dismantle the cell by interacting and cleaving a different set of proteins (compared to caspase-3) because of its unique charge and subcellular distribution.

1.6 Modulators of caspases and the apoptosome

Once activated, effector caspases embark on dismantling the cell in preparation for phagocytosis. However, caspase activity is regulated by a number of endogenous proteins, and can also be inhibited by a range of pharmacological inhibitors as experimental tools.

1.6.1 Pharmacological inhibitors

'Specific' caspase inhibitors have been developed based on their preferred tetrapeptide substrate recognition sequence. For example, Ac-DEVD.CHO was designed to mimic the cleavage site in PARP and 'specifically' inhibit caspase-3 and caspase-7 (Fernandes-Alnemri *et al*, 1995; Nicholson *et al*, 1995). These types of inhibitors act as pseudosubstrates and inhibit the caspase by competitive inhibition. The most commonly used caspase inhibitors are DEVD.CHO and zVAD.FMK, which bind reversibly or irreversibly, respectively, as a result of the associated chemical group (reviewed in Ekert *et al*, 1999). O-methylated zVAD.FMK is a cell permeable poly-caspase inhibitor, which prevents apoptosis induced by a range of stimuli (Chow *et al*, 1995; Fearnhead *et al*, 1995; Zhu *et al*, 1995; Jacobson *et al*, 1996; Slee *et al*, 1996).

1.6.2 Endogenous modulators of caspase activity

The endogenous regulation of caspase activity is under the control of the inhibitors of apoptosis (IAPs) and their antagonists (SMAC and Omi). Their opposing effects on caspase activity determine the fate of the cell.

1.6.2.1 Inhibitors of apoptosis (IAPs)

The activity of active caspases produced either by the apoptosome or at the DISC is inhibited by a group of proteins termed IAPs. The mammalian IAP family consists of XIAP, cIAP-1, cIAP-2, Survivin, Livin, NAIP and BRUCE, with two homologues present in *Drosophila*, DIAP-1 and DIAP-2 (Reviewed in Verhagen *et al*, 2001). The members of this family are characterised by the presence of evolutionary conserved ~70 amino acid zinc-finger motifs, termed BIR (Baculovirus IAP repeat) domains (Uren *et al*, 1998; Figure 1.6.1), which are essential for caspase inhibition (Deveraux *et al*, 1997; Roy *et al*, 1997; Takahashi *et al*, 1998). In addition, XIAP, cIAP-1 and cIAP-2 and the *Drosophila* homologues contain C-terminal RING domains (Uren *et al*, 1996), which increases the potency of the IAP by acting as an E3 ligase which ubiquitinates proteins, thus targeting them for degradation (Roy *et al*, 1997; Suzuki *et al*, 2001b).

The most potent caspase inhibitor is XIAP, the X chromosome-linked IAP, with a K_i value of 0.2-0.8 nM, compared to 1-20 nM for other IAPs (Deveraux & Reed, 1999). IAPs can inhibit initiator (caspase-9) and effector caspases (caspase-3 and -7) via different BIR domains (Deveraux *et al*, 1997; Roy *et al*, 1997; Deveraux *et al*, 1999; Sun *et al*, 2000), but only when the caspase is in an active conformation (Deveraux *et al*, 1997; Roy *et al*, 1997; Ekert *et al*, 2001; Srinivasula *et al*, 2001). The latter proviso is also true in *Drosophila*, with DIAP-1 unable to interact with the zymogen of drICE (Kaiser *et al*, 1998). The BIR3 domain is essential for the inhibition of caspase-9, whereas the BIR1/BIR2 linker region and the BIR2 domain inhibit caspases-3 and -7 (Takahashi *et al*, 1998; Deveraux *et al*, 1999; Sun *et al*, 1999b; Srinivasula *et al*, 2001).

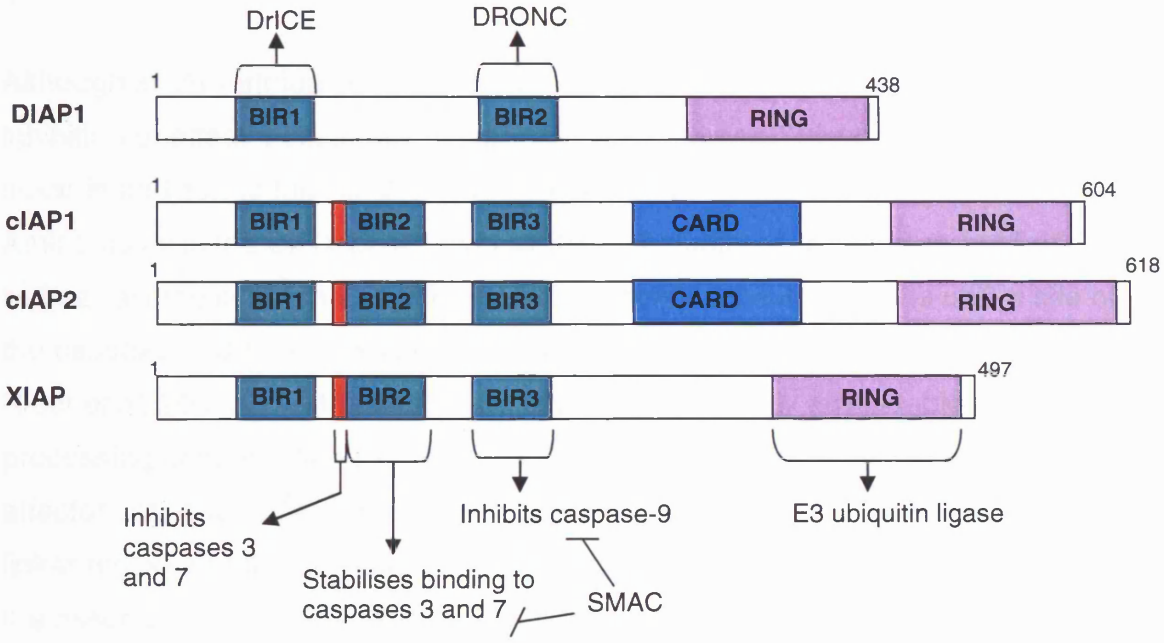

Figure 1.6.1: Schematic of the domain structure of the IAPs (Adapted from Holcik & Korneluk, 2001 and Riedl & Shi, 2004).

The BIR3 domain of XIAP binds to processed (p35) caspase-9 via the last four amino acids at the N-terminal of the p12 caspase subunit Ala-Thr-Pro-Phe (ATPF) revealed following autocatalytic cleavage (Asp315) termed the IAP binding motif (IBM) (Srinivasula *et al*, 2001). The inhibition of caspase-9 by XIAP can be overcome if caspase-3 is active as caspase-3 cleaves procaspase-9 at $DQLD^{330}\downarrow A$ to form the active p37/p10 conformation, or following autocatalytic cleavage to form the p35/p10 active caspase (Srinivasula *et al*, 1998). This results in the IBM not being exposed (p37/p10) or instead is removed (p35/p10)

abrogating the inhibition of caspase-9 by XIAP (Srinivasula *et al*, 2001; Bratton *et al*, 2002). The p2 subunit produced is then additionally thought to act as a decoy peptide and sequester XIAP (Holcik & Korneluk, 2001). This provides a feed-forward mechanism, amplifying the apoptosis signal by preventing IAP inhibition of caspase-9 (Figure 1.5.6). However, *in vitro* studies have shown that the enhanced activity seen in the p35/p10 caspase-9 (compared with p35/p12) is due to an increase in caspase-processing ability of caspase-9 and not due to the removal of XIAP (Zou *et al*, 2003). Cleavage of the N-terminus of the p12 fragment of caspase-9 by caspase-3 reveals an AISS motif that can still bind to XIAP (Zou *et al*, 2003). However, as this study was performed with mutant constructs this prevented the production of the p2 fragment containing the ATPF motif, and was therefore unable to act as a decoy peptide and sequester XIAP.

Although initially attributed to the BIR2 domain alone (Takahashi *et al*, 1998), the inhibition of effector caspases (caspase-3 and caspase-7) involves the BIR1-BIR2 linker in addition to the BIR2 domain (Deveraux *et al*, 1999; Sun *et al*, 1999b). Amino acids in the BIR1-BIR2 linker of XIAP (including Asp148; Sun *et al*, 1999b) lie in a reverse conformation (compared to peptide inhibitors) in the active site of the caspase and prevent substrate access (Chai *et al*, 2001; Huang *et al*, 2001; Riedl *et al*, 2001a). As the active site of a caspase is only assessable following processing/conformational change, this accounts for why XIAP only binds to active effector caspases (Deveraux *et al*, 1997). Following interaction between the BIR linker region and the caspase active site, the BIR2 domain of XIAP then stabilises the association (Sun *et al*, 1999b; Huang *et al*, 2001; Riedl *et al*, 2001a). Takahashi and colleagues initially described this stabilising mechanism as the ability of the BIR2 domain of XIAP to bind to the N-terminus of the large subunit of caspase-7, but not to caspase-3 (Suzuki *et al*, 2001a). This interaction was independent of an accessible active site (as zVAD.FMK did not disturb the association) but required exposure of Ala24. The BIR2 domain has also been shown to stabilise the linker interaction by binding to residues on the N-terminus of the small subunit of the effector caspases (Riedl *et al*, 2001a; Scott *et al*, 2005). Following cleavage at Asp175 (caspase-3) a SGVD motif is revealed on the p10 subunit, which can interact with the BIR2 domain of XIAP (Riedl *et al*, 2001a). Cleavage of caspase-7, initially at Asp198 and subsequently at Asp206 (predominantly by caspase-8) reveals an ANPR sequence, again recognised by

XIAP (Scott *et al*, 2005). These studies provide evidence for the role in IBM recognition for the inhibition of caspase-9 and the effector caspases.

Recent work by Meier and co-workers has also suggested a role for an IBM in effector caspase inhibition by IAPs (Tenev *et al*, 2005). The data suggests that cIAP-1 binds to active caspase-7 in a non-competitive manner, similar to that initially suggested for the BIR2 domain of XIAP (Suzuki *et al*, 2001a; Tenev *et al*, 2005). After removal of the prodomain from caspase-7, an IBM of Ala-Lys-Pro is revealed via which cIAP-1 (but not cIAP-2 or XIAP) can bind, and is independent of an accessible active site (Tenev *et al*, 2005). This mechanism is similar to that proposed for the regulation of the effector caspase, drICE, by DIAP-1 in *Drosophilia*, although in contrast, DIAP1 also required the presence of an accessible active site on drICE (Tenev *et al*, 2005).

1.6.2.2 Inhibitor antagonists: SMAC/Diablo and Omi/HtrA2

In *Drosophila* IAPs are regulated by direct binding of proteins such as Reaper, Hid and Grim (Reviewed in Salvesen & Duckett, 2002). These proapoptotic proteins bind via their N-terminal domain to the BIR domains of the IAP, disrupting their binding to caspases. Subsequently, mammalian homologues of Reaper, Hid and Grim were identified; SMAC/DIABLO (Du *et al*, 2000; Verhagen *et al*, 2000) and HtrA2/Omi (Suzuki *et al*, 2001c; Hegde *et al*, 2002; Martins *et al*, 2002; Verhagen *et al*, 2002).

SMAC (Second mitochondria-derived activator of caspases) is synthesized as a precursor protein, containing a mitochondrial targeting sequence of 55 amino acids at the N-terminus, which is removed upon entry to the mitochondria (Chai *et al*, 2000; Du *et al*, 2000). This results in the AVPI motif being exposed, which is essential for its ability to bind to the BIR3 domain of XIAP (Liu *et al*, 2000; Wu *et al*, 2000; Ekert *et al*, 2001; Srinivasula *et al*, 2001). This IBM is reminiscent of the ATPF motif exposed by caspase-9 processing (Srinivasula *et al*, 2001), and similar to the N-terminal sequence of the *Drosophila* homologues Reaper, Hid and Grim (Figure 1.6.2). Mature SMAC is released from the mitochondria following cellular insult (Du *et al*, 2000; Verhagen *et al*, 2000) and is thought to be a caspase-catalysed event that occurs downstream of cytochrome *c* release (Adrain *et al*,

2001). This provides a feedback mechanism to ensure the caspases activated at the apoptosome are not sequestered by the IAPs. The IBM of SMAC is essential for its ability to displace caspase-9 from XIAP, by binding across the BIR3 domain (Srinivasula *et al*, 2001; Liu *et al*, 2000). In contrast, SMAC displaces XIAP from effector caspases by binding to the BIR2 domain of XIAP, in a mutually exclusive complex via both N-peptide and protein-protein interactions (Chai *et al*, 2000; Liu *et al*, 2000; Srinivasula *et al*, 2000; Wu *et al*, 2000; Chai *et al*, 2001; Riedl *et al*, 2001a).

Smac/DIABLO	**A**	**V**	**P**	**I**	A	Q	K	S
HtrA2/Omi	**A**	**V**	**P**	**S**	F	S	G	E
Reaper	**A**	**V**	**A**	**F**	Y	I	P	D
Grim	**A**	**I**	**A**	**Y**	F	L	P	D
Hid	**A**	**V**	**P**	**F**	Y	L	P	E
hCasp-9	**A**	**T**	**P**	**F**	Q	E	G	L
mCasp-9	**A**	**V**	**P**	**Y**	Q	E	G	P

Figure 1.6.2: Structural similarities between IAP binding motifs on target proteins (Adapted from Salvesen & Duckett, 2002).

HtrA2/Omi was identified as a binding partner of XIAP concurrently by four independent groups (Suzuki *et al*, 2001c; Hegde *et al*, 2002; Martins *et al*, 2002; Verhagen *et al*, 2002). Like SMAC, Omi is synthesised as a precursor (~50 kDa), which is processed at the N-terminus to produce the active form (36 kDa) after mitochondrial transport (Suzuki *et al*, 2001c). The N-terminus of the mature Omi (AVPS) then resembles the IBM of caspase-9, SMAC and the *Drosophila* homologues (Figure 1.6.2; Suzuki *et al*, 2001c), and is released from the mitochondria into the cytosol during apoptosis (Suzuki *et al*, 2001c). Interestingly, over-expression of Omi was shown to induce apoptosis, and RNAi of Omi reduced spontaneous apoptosis to a greater extent than the RNAi of SMAC (Martins *et al*, 2002), therefore suggesting that Omi has an alternative proapoptotic mechanism. Indeed, Omi is a serine protease and its activity is regulated by the C-terminal PDZ domains (Li *et al*, 2002). In apoptotic cells, Omi cleaves XIAP, cIAP-1, cIAP-2, livin and DIAP-1 (*Drosophila* homologue), although it is most effective against cIAP-1 (Yang *et al*, 2003). The IBM of Omi is essential for binding to, and cleavage of the IAPs, but is not required for the processing of other Omi substrates (i.e. β-casein, Yang *et al*, 2003).

1.7 Proposed modulators of the formation and activity of the apoptosome

Since the discovery of the apoptosome many groups have investigated interactions with its components and the complex itself to identify possible regulators. A number of proteins have been proposed to modulate the formation and/or the activity of the apoptosome, with some conflicting results.

1.7.1 Modulation of cytochrome *c* release and binding to Apaf-1

As CED-9 directly binds to CED-4 preventing it from activating CED-3 in *C.elegans* (Chinnaiyan *et al*, 1997a; Seshagiri & Miller, 1997), it was hypothesised that the mammalian Bcl-2 family members could function by the same mechanism. Indeed initial work using over-expression of Apaf-1 and the Bcl-2 family suggested an association between Apaf-1 and Bcl-2 (Fang *et al*, 1998) and Apaf-1 and Bcl_{XL} (Hu *et al*, 1998a; Pan *et al*, 1998a). However, these associations could not be confirmed when using endogenous protein levels and monoclonal antibodies to Apaf-1 (Moriishi *et al*, 1999) or co-localisation experiments (Hausmann *et al*, 2000). Nevertheless, Bcl-2 and $Bcl\text{-}_{XL}$ regulate the release of cytochrome *c* from the mitochondria and therefore indirectly modulate the formation of the apoptosome (as described previously; Figure 1.7.1). The heat shock proteins Hsp72 and Hsp27 also regulate apoptosome formation by interacting at this stage. Hsp72 inhibits cytochrome *c* release (Steel *et al*, 2004), whereas Hsp27 can bind to and sequester cytochrome *c* following its release from the mitochondria (Garrido *et al*, 1999; Bruey *et al*, 2000; Figure 1.7.1). In addition, the binding of cytochrome *c* to the WD40 domains of Apaf-1 is thought to depend upon the presence of acetylcholinesterase (AChE) (Park *et al*, 2004). The observation that AChE is expressed in tissues devoid of cholinergic responses and is upregulated in apoptotic cells could therefore provide another layer of apoptosome regulation (Small *et al*, 1996; Zhang *et al*, 2002).

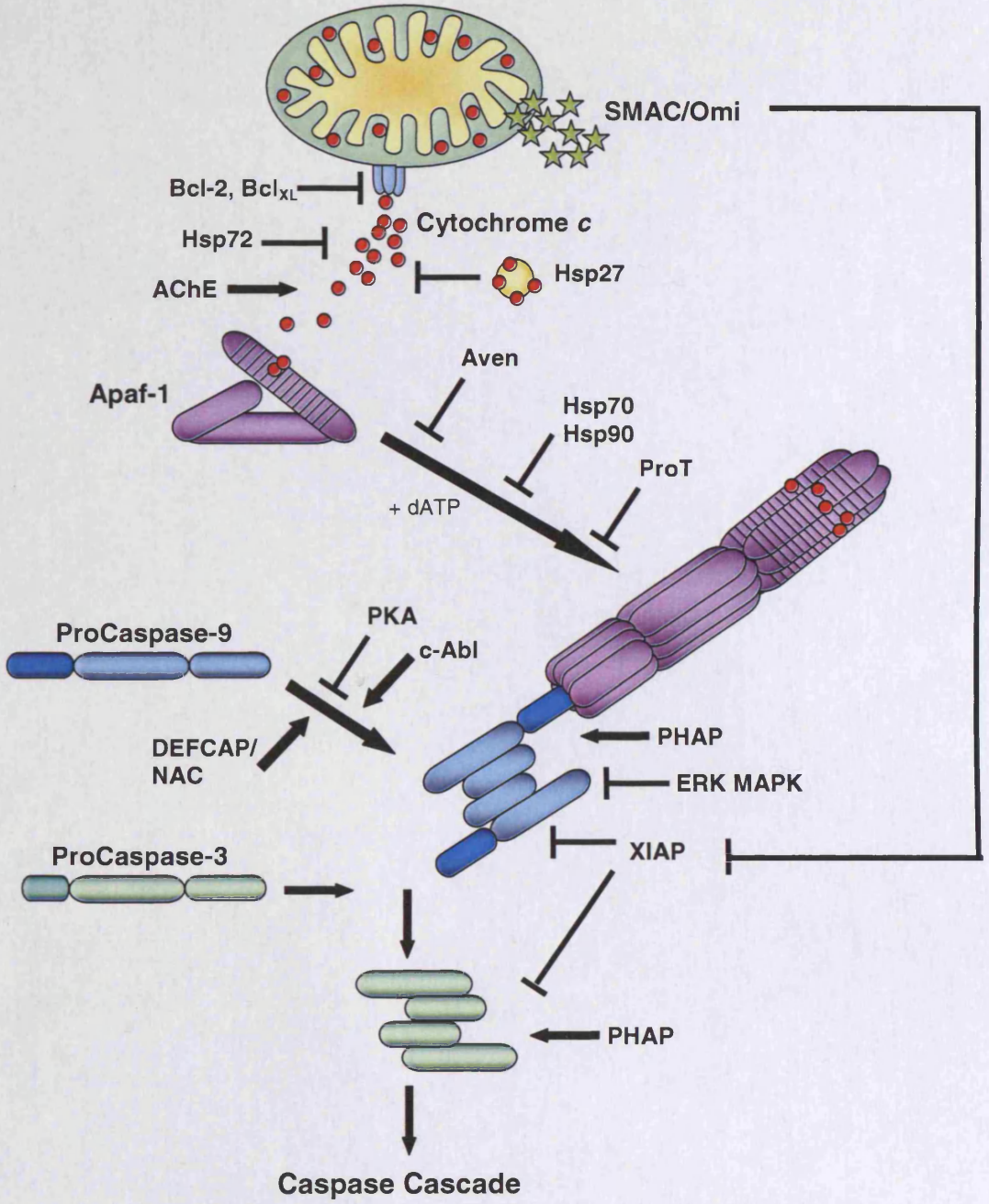

Figure 1.7.1: Proposed modulators of apoptosome formation and activity. The formation of the apoptosome is regulated by the release of cytochrome *c* and the ability of Apaf-1 to oligomerise. The subsequent recruitment and activation of the apical caspase, caspase-9, can then be modulated to affect the activity of the apoptosome. Finally, inhibition of caspase-9 and recruited effector caspases can also regulate the caspase-activating activity of this apoptotic complex.

1.7.2 Regulation of Apaf-1 oligomerisation

Hsp70 was initially shown to act downsteam of cytochrome *c* release but upstream of caspase-3 activation (Li *et al*, 2000b) and was then shown bind to Apaf-1 (via the CARD domain) after heat shock treatment, preventing Apaf-1 oligomerisation (Saleh *et al*, 2000; Beere *et al*, 2000). However, Steel and colleagues have subsequently dismissed this observation, as the high salt concentration found in the Hsp70 preparation was found to be responsible for the inhibitory effect of Hsp70 on apoptosome activity (Steel *et al*, 2004; Cain *et al*, 2001). Hsp90 inhibits apoptosome formation by directly binding to monomeric Apaf-1, thus preventing oligomerisation (Pandey *et al*, 2000). This method of inhibition is overcome in the presence of high concentrations of cytochrome *c* (Pandey *et al*, 2000), similar to the inhibitory effect of potassium chloride (Cain *et al*, 2001).

Aven, a Bcl-$_{XL}$-interacting protein, is also able to associate independently with Apaf-1, by preventing oligomerisation and consequently cell death (Chau *et al*, 2000). However, the prosurvival role of Aven is only evident in the presence of cell cytosols and therefore it is likely that its role is via another mediator (Chau *et al*, 2000). Another proposed modulator of apoptosome formation is ProT (prothymosin-α), which inhibits the formation of the apoptosome, by a mechanism that is antagonised by PETCM (Jiang *et al*, 2003). RNAi and immunodepletion studies confirmed the inhibitory role of ProT in apoptosome formation (Jiang *et al*, 2003); however, no direct association between Apaf-1 and ProT was presented. Furthermore, like Aven, the inhibitory effect of ProT was only observed in the presence of cell cytosol, and therefore their influence on apoptosome activity is probably due to the presence of other cytosolic proteins.

1.7.3 Modulation of caspase-9 recruitment and caspase activation at the apoptosome

Caspase-9 recruitment to the ~700 kDa apoptosome is enhanced by DEFCAP/ NAC (Hlaing *et al*, 2001; Chu *et al*, 2001), which is structurally similar to Apaf-1. NAC associates with Apaf-1 (but not caspase-9) in a cytochrome c-dependent manner to form a >1 MDa inactive apoptosome complex (Chu *et al*, 2001). This association prevents caspase-9 recruitment to the inactive complex, and therefore

forces caspase-9 to be recruited the active ~700 kDa apoptosome complex. In contrast, caspase-9 recruitment is inhibited by the cyclic AMP regulated Protein kinase A (PKA), which phosphorylates caspase-9 rendering it incapable of being recruited to the apoptosome (Martin *et al*, 2005). However, the phosphorylation of caspase-9 is not the only mechanism by which PKA can inhibit caspase-9 activation (Martin *et al*, 2005).

Apoptosome-mediated caspase-9 activation was thought to be facilitated by PHAP1 (Putative HLA-DR-associated protein-1) in the presence of cytosolic factors (Jiang *et al*, 2003). However, the direct association between PHAP and the apoptosome was not presented in the above report, and was not confirmed in the subsequent analysis of the *in vitro* Jurkat apoptosome (Hill *et al*, 2004). Nevertheless, PHAP was noted to enhance the activity of active caspase-3, and therefore was suggested as cofactor for caspase-3 activity (Hill *et al*, 2004).

Caspase-9 activation can be prevented by its phosphorylation at Thr125 by ERK MAPK (Allan *et al*, 2003). This modification precludes the appropriate conformational change required for caspase-9 activation, but not its recruitment to the apoptosome (Allan *et al*, 2003). Yet, phosphorylation by the tyrosine kinase, c-Abl, at Tyr153 actually potentiates caspase-9 processing to the p35 form, and consequently enhances apoptosis in response to DNA-damage (Raina *et al*, 2005). Taken together, these data show an important regulatory mechanism provided by caspase phosphorylation. Caspase activity in the apoptosome can also be regulated by XIAP (Bratton *et al*, 2001b; 2002; Hill *et al*, 2004). By its ability to bind to autocatalytically processed caspase-9, XIAP is recruited to the apoptosome, where it can simultaneously interact with processed caspase-3 and prevent the release of this effector caspase from the apoptosome (Bratton *et al*, 2002). These interactions stabilise the complex and inhibit the caspase processing activity of the apoptosome (Bratton *et al*, 2002; Hill *et al*, 2004).

1.8 Aims

Previous studies in the laboratory have focused on purifying the apoptosome, formed *in vitro*, by conventional chromatographic techniques, resulting in a partially purified apoptosome. The main aim of this project was therefore to employ affinity-purification procedures (using single and tandem-affinity tags) to purify the apoptosome and identify its components by proteomic analysis. This would be performed in dATP-activated cell lysates and in cells treated with an apoptotic chemical stimulus. This would allow a comparison to be drawn between the constituents of the apoptosome when formed under the different conditions.

In addition, with the majority of the studies investigating the apoptosome in the presence of caspase-3, the role of the apoptosome in caspase-3-deficient cells would also be characterised. The aims of this work were therefore to identify an apoptosome formed in apoptotic MCF-7 cells and in dATP-activated cellular lysates, and also to determine whether caspase-7 is directly activated by the apoptosome, in a manner analogous to caspase-3.

Chapter 2

Materials and Methods

All chemicals used were of the highest quality and were from Sigma-Aldrich unless otherwise stated.

2.1 THP-1 cell culture

Human monocytic tumour cells (THP-1), obtained from the European collection of animal cell cultures (ECACC, Porton Down, UK), were cultured in RPMI 1640 medium (Invitrogen) supplemented with 10% (v/v) heat-inactivated fetal bovine serum (FBS), 2 mM glutamax (L-glutathione) and 1% (v/v) MEM non-essential amino acids, in 5% CO_2 at 37 °C. Cells were seeded at 3 x 10^5/ml and passaged every 3 to 4 days.

2.2 Preparation of THP-1 cell lysate

a) Freeze-thaw

Essentially as described previously (MacFarlane *et al*, 1997). The cells were pelleted at 200 x g, 4 °C for 5 min using a Beckman centrifuge and resuspended in ice-cold phosphate buffered saline (PBS). This was repeated and the cells were resuspended in supplemented PIPES buffer (50 mM PIPES/KOH pH 6.5, 2 mM EDTA (Fisher Scientific), 0.1% (w/v) CHAPS, 5 mM DTT, 1 protease inhibitor tablet-EDTA (Roche)/10 ml and 2 mM PMSF) at 166 µl/10^8 cells. The cells were freeze-thawed three times (liquid nitrogen/37 °C) and centrifuged at 20,000 x g, at 4 °C for 30 min in a Sigma bench-top centrifuge. The supernatant was removed and centrifuged at 100,000 x g for 45 min at 4 °C in a Beckman Optima TLX Ultracentrifuge. The protein concentration of the S-100 cytosol (lysate) was then measured by Bradford Assay (see section 2.18).

b) Digitonin/homogenisation

As described previously (Twiddy *et al*, 2004). Briefly, cells were pelleted and washed in PBS as above. The cell pellet was then resuspended in MSH buffer (210 mM Mannitol, 7 mM sucrose, 5 mM HEPES, 1 mM EGTA, pH 7.4 with the addition of protease inhibitor tablet-EDTA/10 ml and 1 mg/10 ml Pefabloc (Roche)) with 0.05% Digitonin (10 ml/ 1 x 10^9 cells) and incubated on ice for 7 min. The concentration of Digitonin was then diluted to 0.01% with MSH buffer and the cells were passed through an 18 µm ball-bearing homogeniser for 5 strokes. The cell lysate was then centrifuged at 100,000 x g to produce a cell free lysate. The S-100 lysate was buffer exchanged with MSH to remove any remaining Digitonin and

concentrated using 10,000 MWCO Vivaspin tubes (Viva Science). The protein concentration of the resulting lysate was then determined by Bradford assay (section 2.18) and stored in aliquots at -80 °C.

2.3 Jurkat cell culture

Human T-cells (Jurkat, E6.1), obtained from the ECACC (Porton Down, UK), were cultured in RPMI 1640 medium supplemented with 10% (v/v) heat-inactivated FCS, 2 mM glutamax and 1% (v/v) MEM non-essential amino acids, in 5% CO_2 at 37 °C. Cells were seeded at 3 x 10^5/ml and passaged every 3 to 4 days.

2.4 Preparation of Jurkat cell lysate

S-100 lysate lysate was produced by freeze/thawing as described for THP-1 cell lysate (section 2.2a)

2.5 Preparation of B-CLL cell lysate

A patient with Chronic Lymphoid Leukaemia (CLL) underwent plasmaphoresis, and a blood sample was obtained with patient consent and local ethical committee approval. B-CLL cells were separated from the blood with Ficoll (Undertaken by R. Snowden). The purified B-cells were then washed twice in ice cold PBS and resuspended in the lysis buffer mentioned above (83 µl/10^8 cells). The cells then underwent freeze/thaw cell lysis in the same manner as described for THP-1 cells (section 2.2a).

2.6 MCF-7 cell culture

Human breast carcinoma cells (MCF-7) lack caspase-3 due to a 47 base-pair deletion in the *CASP3* gene (Jänicke *et al*, 1998), which allows investigation of caspase-7 as the main effector caspase. These cells were a kind gift from M. Jaattela (Denmark) and grown in RPMI media supplemented with 10% (v/v) heat-inactivated FCS and 2 mM glutamax. MCF-7 cells stably expressing caspase-3 (MCF-7/CASP3) and those containing the empty vector (MCF-7/pcDNA3) were obtained from A. Porter (Singapore) and grown in media as above with geneticin (G418, Invitrogen) at 400 µg/ml. Cells were seeded at 4 x 10^5/ml, cultured in an environment of 5% CO_2, 37 °C and passaged every 3 to 4 days.

2.7 Preparation of MCF-7 cell lysate

a) Freeze thaw

As described for THP-1 cell lysate (Section 2.2a).

b) Digitonin/homogenisation

Essentially as described in section 2.2b, except cells were harvested using trypsin/EDTA (Invitrogen) and resuspended in media before being pelleted and washed twice in PBS as above. The cell pellet was then resuspended in MSH buffer with 0.05% Digitonin (7 ml/1.5 x 10^8 cells) and incubated on ice for 7 min. The cells were then homogenised and the S-100 cell lysate produced as described in section 2.2b.

2.8 Induction of apoptosis in MCF-7 cells with Staurosporine

MCF-7 cells were seeded at 2 x 10^5 cells/75cm^2 flask, 18 h prior to treatment. The cells were then treated with either anhydrous DMSO (vehicle control) or Staurosporine (1 µM) for 3-24 h. To establish the extent of caspase involvement, the poly-caspase inhibitor zVAD.FMK (Enzyme Systems) was incubated where indicated with the cells, 1 h prior to exposure with the apoptosis-inducing agent.

2.9 HeLa cell culture

Human cervix adenocarcinoma (HeLa) cells were obtained from ECACC and grown in DMEM media (high glucose, without pyruvate, Invitrogen) supplemented with 10% (v/v) heat-inactivated FCS. Cells were seeded at 4 x 10^5/ml and cultured in 5% CO_2, at 37 °C. For transfections, 6 well plates (NUNC) were seeded with 8 x 10^4 cells/well in 3 ml media and transfected 24 h later. In some experiments, medium flasks (T75, Falcon) and large flasks (T150, Falcon) were seeded with 6.25 x 10^5 cells and 1.25 x 10^6 cells for 24 h, respectively.

2.10 HeLa cell transfections with GTC-tagged caspases

For 6 well plates, 1 µl FuGENE (Roche) and 1 µg dsDNA were incubated for 45 min in 100 µl optimem + glutamax (Invitrogen). If GFP was to be co-transfected, then 0.25 µg GFP plasmid and 0.75 µg GTC/GTC-Caspase were used. The transfection mix was then added to each well in addition to penicillin/streptomycin (Invitrogen) (20 µl/1ml medium). After 18 h transfection, either Etoposide (100-200 µM final concentration) or anhydrous DMSO (vehicle control) was added to

the cells. The extent of cell death was determined either by cell detachment from the plate of transfected cells (green GFP-transfected cells only) or by assessment of phosphatidylserine (PS) exposure by Annexin V binding (section 2.11). Where indicated, the poly-caspase inhibitor, zVAD.FMK, was added 1 h prior to Etoposide or DMSO treatment when required, to give a final concentration of 50-100 µM.

Samples for Western blotting were produced by pooling the trypsinised cells and their medium, followed by centrifugation at 200 x g for 3 min. The cells were resuspended in medium and allowed to recover for 20 min at 37 °C, 5% CO_2. They were then harvested by centrifugation, washed twice in PBS, and finally resuspended in 25 µl/well lysis buffer. The lysate was then freeze-thawed three times (liquid nitrogen/37 °C) before protein concentration was determined (see section 2.18) and storage at -80 °C

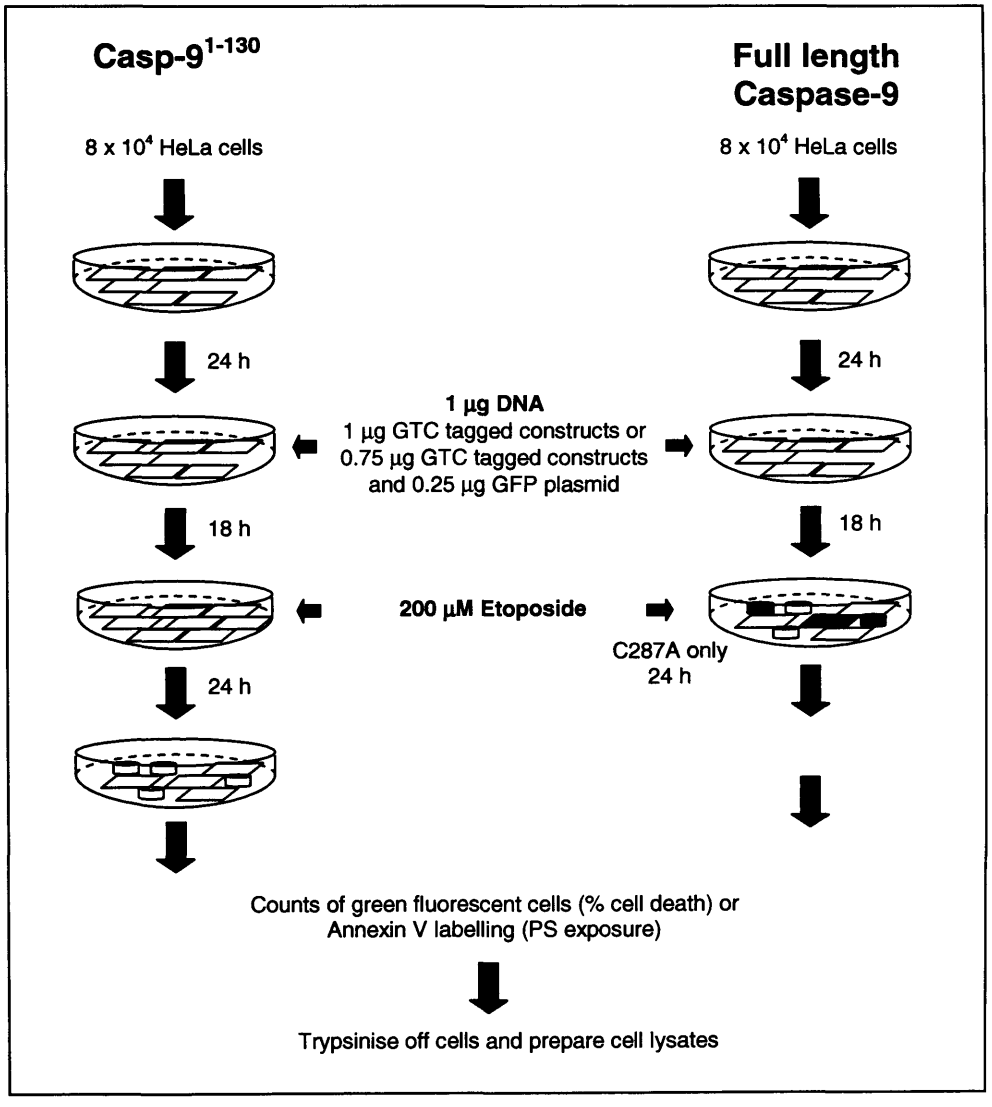

Figure 2.10.1: Schematic of HeLa cell transfections.

2.11 Measurement of Cell Death

In normal, non-apoptotic cells, phosphatidylserine (PS) is localised to the inner leaflet of the plasma membrane. During the early stages of apoptosis this asymmetry is dismantled and PS is exposed on the outer surface to provide an engulfment signal (Fadok *et al*, 1998). Annexin V is a protein that preferentially binds to PS, and therefore the fluorescently-tagged Annexin V (FITC-Annexin V) can measure the extent of apoptosis in a given population (Vermes *et al*, 1995). This is used in conjunction with dye exclusion (i.e. Propidium iodide (PI) to establish membrane integrity) to distinguish between apoptotic and necrotic cells (apoptosic cells are Annexin V positive, but PI negative). Approximately 1 x 10^5 cells were harvested using trypsin/EDTA as described above, to measure apoptosis by this method. The cell pellet was then resuspended in fresh media and the cells allowed to recover for 20 min at 37 °C (in 5% CO_2). A sample of this was then transferred to a FACS tube (Becton Dickinson) and centrifuged at 200 x g in a benchtop centrifuge. The media was then aspirated off and the pellet resuspended in 1 ml Annexin buffer (Bender MedSystems), and incubated with 2 µl Annexin V-FITC labelled antibody (Bender MedSystems) for 10 min at room temperature following gentle vortexing. Propidium Iodide (50 µg/ml PBS) was added (10 µl) and the tube gently vortexed before being transferred to ice and cell death was measured on a FACS Calibur flow cytometry machine (Beckton Dickinson).

When GFP was used to indicate which cells had been transfected, Annexin V-FITC labelling could not be used to measure apoptosis, due to the fluorescence emitted by GFP. Therefore cell counts were performed on >300 GFP-expressing cells/sample and cell death was determined by microscopy as cell rounding and detachment from the plate surface (Srinivasula *et al*, 2000). This method of measuring cell death was always used in conjunction with other measures of apoptosis, such as cytochrome *c* release and caspase activation.

In MCF-7 cells, in the absence of caspase-3, PS is not efficiently exposed onto the outer leaflet of the cell membrane, therefore preventing the accurate measurement of apoptosis by Annexin V binding. Consequently, a loss of mitochondrial membrane potential ($\Delta\psi m$) was used as a measure of apoptosis in these cells.

MCF-7 cells were harvested using trypsin/EDTA (3 wells/sample), resuspended in 600 µl warm culture medium and allowed to recover for 15 min at 37 °C, 5% CO_2. An aliquot was taken (100 µl) and incubated with 900 µl of fresh warm medium and 0.5 µl 100 µM TMRE (Molecular Probes) for 10 min at 37 °C. FACS analysis then took place immediately, to identify the percentage of cells which had lost the ability to retain the TMRE dye (apoptotic cells).

2.12 Cytochrome *c* release

In normal cells, cytochrome *c* is confined to the intermembrane space of the mitochondria. However, during stress-mediated apoptosis, cytochrome *c* is released from the mitochondria and can then be detected in the cytosol (Liu *et al*, 1996). By comparing the levels of cytochrome *c* in the cytosol and mitochondrial pellet a conclusion can be made on the induction pathway initiated and extent of apoptosis induced.

For a 6 well plate, the media and floating cells were collected and stored on ice. The adherent cells were washed in 1 ml PBS and combined with the collected medium. Trypsin/EDTA was then added to each well (0.5 ml) and incubated at 37 °C for 2-3 min. The cells were tapped off the plate and 1 ml of fresh medium added to stop the reaction. The cells were then pooled and centrifuged at 200 x g for 3 min. The cell pellet was washed in ice cold PBS and centrifuged again before being resuspended in 100 µl of lysis buffer (250 mM sucrose, 20 mM HEPES; pH 7.4, 5 mM Magnesium Chloride, 10 mM Potassium Chloride, 1 mM EDTA, 1 mM EGTA and protease inhibitor cocktail-EDTA (Roche) containing 0.025-0.05% Digitonin for 7-10 min on ice (exact conditions were cell type dependent). The cells were centrifuged at 13,000 rpm (bench top centrifuge) for 3 min at 4 °C and the supernatant (cytosol) was collected. The pellet was washed in 100 µl lysis buffer (without Digitonin) and centrifuged as above before resuspension in 100 µl lysis buffer and storage at -80 °C. The membrane fraction was sonicated for 4 cycles (5 sec on and 5 sec off) on ice, before protein concentration determination (section 2.18) and Western blotting analysis (section 2.27).

2.13 Production and purification of recombinant caspases

BL21 (DE3) cells were transformed with a pET-21b plasmid containing the gene for the appropriate His-tagged caspase (procaspase-3, -7 and caspase-9), and grown at 37 °C in terrific broth (TB), 1% glucose and the selective antibiotic, ampicillin (100 μg/ml, Melford laboratories). When the culture density reached an OD_{600} of 0.6, IPTG (Melford laboratories) was added (1 mM) and the bacteria were then incubated at 30 °C for either 15 min (procaspase-3, -7) or 3 h (caspase-9). The bacteria were then pelleted and lysed by 8 cycles of sonication on ice (15 sec on, 45 sec off) in lysis buffer (20 mM HEPES, 100 mM NaCl, 10 mM imidazole, 1 protease inhibitor tablet-EDTA (Roche)/10 ml, pH 8.0). The His-tagged protein was then purified by incubation with Nickel-coated Sepharose beads (QIAgen) for 2 h at 4 °C. The beads were then washed (20 mM HEPES, 500 mM NaCl, 20 mM imidazole, pH 8.0) and eluted (20 mM HEPES, 5% (w/v) sucrose, 0.1% (w/v) CHAPS, 250 mM imidazole, pH 8.0). The concentration of the recombinant caspases (stored in 10% glycerol) was then determined by Bradford assay (section 2.18), and the purity examined by Coomassie staining of an SDS-PAGE gel.

2.14 Production and Purification of GST-Casp9$^{1-130}$

Transformed BL21 (DE3) cells, containing the pGEX4TK2 plasmid with an insert coding for the fusion protein of *Schistosoma japonicum* glutathione-S-transferase (GST) and the CARD region of caspase-9 (aa1-130) (kindly donated by S. Martin, Trinity College, Dublin, Figure 2.14.1A-C), were grown at 37 °C in TB broth containing 100 μg/ml ampicillin for selection. When the OD_{600} reached 0.6, 0.1 mM IPTG was added and the bacteria were then incubated at 22 °C for 3 h. The bacteria were then pelleted and lysed by 5 cycles of sonication (10 sec on, 5 sec off, 3 times) in PBS containing 'complete' protease inhibitors (Roche) on ice. The sonicate was then centrifuged at 15,000 rpm for 15 min at 4 °C and the supernatant incubated with Glutathione (GSH)-coated Sepharose beads (Amersham) for 30 min at 4 °C. The beads were washed twice in cold PBS and the GST-Casp9$^{1-130}$ was eluted with 20 mM GSH. A Bradford assay was then used to determine the protein concentration of the GST-Casp9$^{1-130}$ fusion protein (section 2.18) and the purity examined by SDS-PAGE/Coomassie blue staining as

shown in Figure 2.14.1D. The recombinant GST-Casp9$^{1-130}$ was stored at -80 °C in 10% glycerol.

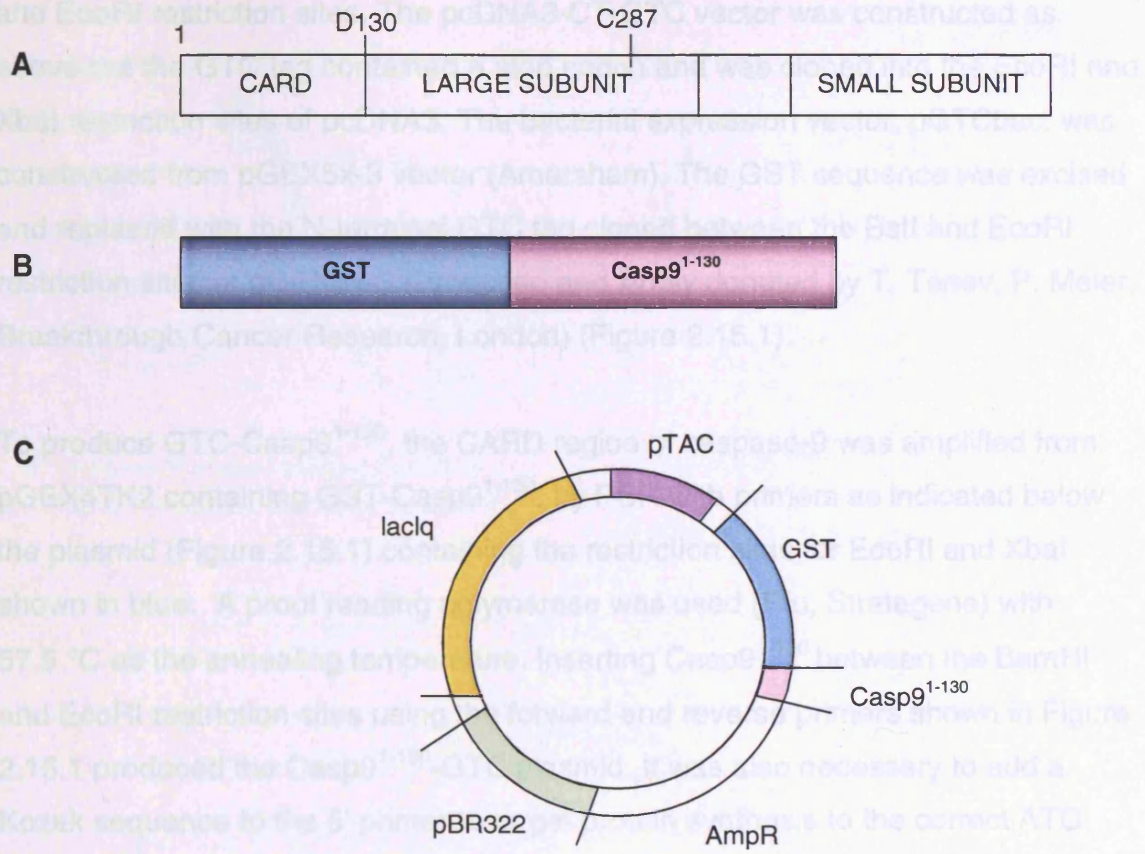

Figure 2.14.1: The production of recombinant GST-Casp9$^{1-130}$. Schematic of caspase-9 (**A**). Schematic of fusion protein GST-Casp9$^{1-130}$ (**B**). Schematic of the plasmid used to transform bacteria to express recombinant protein (**C**). Purification of recombinant GST-Casp9$^{1-130}$ using GSH-Sepharose beads (**D**).

2.15 Production of the GTC-Casp9$^{1-130}$ constructs

The mammalian expression vector pcDNA3-NT-GTC was constructed from pcDNA3 (Invitrogen) by cloning the N-terminal GTC tag (GST-CBP) into HindIII and EcoRI restriction sites. The pcDNA3-CT-GTC vector was constructed as above but the GTC tag contained a stop codon and was cloned into the EcoRI and XbaI restriction sites of pcDNA3. The bacterial expression vector, pGTCbac, was constructed from pGEX5x-3 vector (Amersham). The GST sequence was excised and replaced with the N-terminal GTC tag cloned between the BstI and EcoRI restriction sites of pGEX5x-3 (Produced and kindly donated by T. Tenev, P. Meier, Breakthrough Cancer Research, London) (Figure 2.15.1).

To produce GTC-Casp9$^{1-130}$, the CARD region of caspase-9 was amplified from pGEX4TK2 containing GST-Casp9$^{1-130}$, by PCR with primers as indicated below the plasmid (Figure 2.15.1) containing the restriction sites for EcoRI and XbaI shown in blue. A proof reading polymerase was used (Pfu, Stratagene) with 57.5 °C as the annealing temperature. Inserting Casp9$^{1-130}$ between the BamHI and EcoRI restriction sites using the forward and reverse primers shown in Figure 2.15.1 produced the Casp9$^{1-130}$-GTC plasmid. It was also necessary to add a Kozak sequence to the 5' primer to target protein synthesis to the correct ATG codon (shown in red, Figure 2.15.1)

Casp9$^{1-130}$ was inserted into the bacterial expression vector using the primers shown in Figure 2.15.1, containing restriction digestion sites for EcoRI and NotI (Invitrogen), respectively.

Following amplification of the vectors and insert DNA, restriction digests were performed using the above mentioned enzymes (Invitrogen) for 4 h, except XbaI and NotI which were incubated for 20 h. The restriction digests were then run on a 1% agarose (Invitrogen) gel, and the digests were excised and purified using a gel extraction kit (QIAgen) as per manufacturers instructions. The insert and empty vector were then ligated at a number of different ratios (1:1, 1:3, 1:6) at 16 °C overnight using a T4 DNA ligase (Invitrogen). The resulting ligations (plasmid DNA) were transformed into DH5α cells and a PCR screen was performed after overnight culture, to identify positive clones.

A

i) pcDNA3-NT GTC

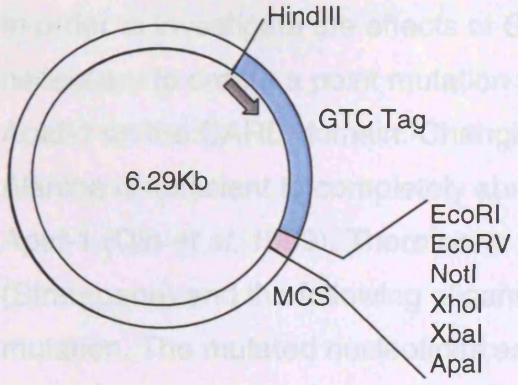

5'- CCG**GAATTC**ATGGACGAAGCGGATCGG-3'

3'- CTAG**TCTAGA**TCAGTCCACTGGTCTGGGTG- 5'.

ii) pcDNA3-CT GTC

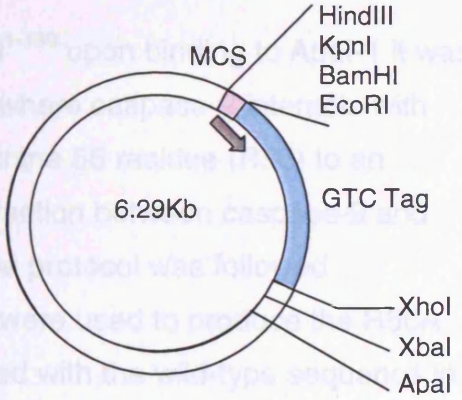

5'- CGC**GGATCC**GCCGCCATGGACGAAGCG-

GATCGGCGGC-3'

3'- CCG**GAATTC**GTCCACTGGTCTGGGTGTTTCCG-5'

B

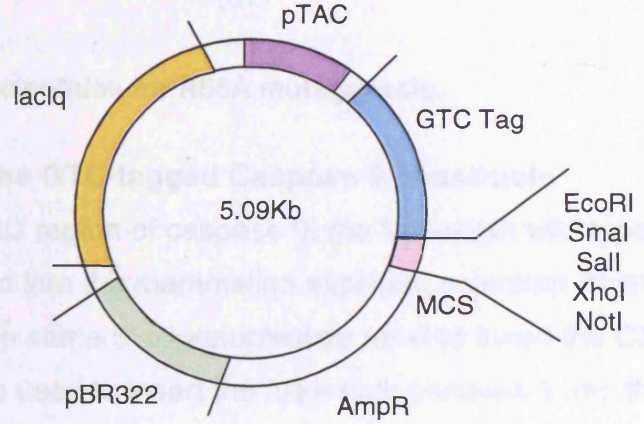

5'- CCG**GAATTC**ATGGACGAAGCGGATCGGCGGC- 3'

3'- ATAGTTTA**GCGGCCGC**TCAGTCCACTGGTCTGGGTGTTTCCG- 5'

Figure 2.15.1: The structure of the GTC vectors and the primers used to insert Casp9$^{1-130}$ DNA. Mammalian expression vectors (**A**), and bacterial expression vector (**B**). Primer restriction sites are shown in blue bold and the inserted Kozac sequence in shown in red bold. MCS, multiple cloning site.

The DNA from selected clones was extracted from the miniprep cultures and sequenced using the appropriate sequencing primers and Big Dye solution, to confirm that the exact DNA sequence was inserted at the correct site.

In order to investigate the effects of GTC-Casp9$^{1-130}$ upon binding to Apaf-1 it was necessary to create a point mutation at the site where caspase-9 interacts with Apaf-1 on the CARD domain. Changing the Arginine 56 residue (R56) to an Alanine is sufficient to completely abrogate interaction between caspase-9 and Apaf-1 (Qin *et al*, 1999). Therefore a Quikchange protocol was followed (Stratagene) and the following oligonucleotides were used to produce the R56A mutation. The mutated nucleotides are underlined with the wild-type sequence in blue underneath.

5'- CGG GAT CAG GCC GCG CAG CTG ATC- 3'
(AG)

3'- GAT CAG CTG CGC GGC CTG ATC CCG- 5'
(CT)

Figure 2.15.2: Oligonucleotides for R56A mutagenesis.

2.16 Production of the GTC-tagged Caspase-9 constructs

In addition to the CARD region of caspase-9, the full-length wild type caspase-9 DNA was also inserted into the mammalian expression vectors (both N- and C-terminally tagged). The same 5' oligonucleotide used to insert the CARD domain of caspase-9 was also used to insert the full-length caspase-9 into the pcDNA3-CT-GTC vector. However, a new 3' oligonucleotide was required to incorporate the full-length caspase-9 and to include an EcoRI restriction site (Figure 2.16.1, shown in blue bold).

3'- CCG **GAA TTC** TGA TGT TTT AAA GAA AAG TTT TTT CCG G- 5'

Figure 2.16.1: 3' oligonucleotide for insertion of full-length caspase-9 into pcDNA3-CT-GTC vector.

To insert the full-length caspase-9 into pcDNA3-NT-GTC new 5' and 3' oligonucleotides were required and are shown below with restriction sites for EcoRI and XbaI respectively (Figure 2.16.2, shown in blue bold).

5'- CCG **GAA TTC** ATG GAC GAA GCG GAT CGG CGG- 3'

3'- ACG **TCT AGA** TTA TGA TGT TTT AAA GAA AAG TTT TTT CC- 5'

Figure 2.16.2: Oligonucleotides for insertion of full-length caspase-9 into pcDNA3-NT-GTC vector.

In addition to the R56A mutation (described in section 2.15), a mutation was also made in the full-length caspase-9 constructs, to abrogate cleavage of caspase-9 by caspase-3. Aspartic acid (D) 330 was changed to Alanine (A) to produce the D330A mutant in the same way as the R56A, but using the oligonucleotides below.

5'- CC TTC GAC CAG CTG GCC GCC ATA TCT AG- 3'
(A)

3'- CT AGA TAT GGC GGC CAG CTG GTC GAA GG-5'
(T)

Figure 2.16.3: Mutagenesis oligonucleotides to create D330A mutant.

In order to characterise the effects of transfecting the potentially active full-length caspase-9 construct, a catalytically inactive mutant (C287A) was created. This was only produced in the C-terminally tagged wild-type and R56A Caspase-9 construct. The mutation was again produced by site-directed mutagenesis with the oligonucleotides shown below.

5'- C ATC CAG GCC GCT GGT GGG GAG CAG- 3'
(TG)

3'- CTG CTC CCC ACC AGC GGC CTG GAT G-5'
(CA)

Figure 2.16.4: Mutagenesis oligonucleotides to create the C287A mutation.

A schematic depicting the structure of all the constructs produced is shown in Figure 2.16.5, illustrating the relative position of the TAP tag and any mutations. Furthermore, the DNA sequence of all the constructs created was confirmed by sequencing, from both the 3' and the 5' end of the target gene. The correct in-frame alignment, mutations (if present) and appropriate restriction sites were confirmed to be correct for all the constructs produced.

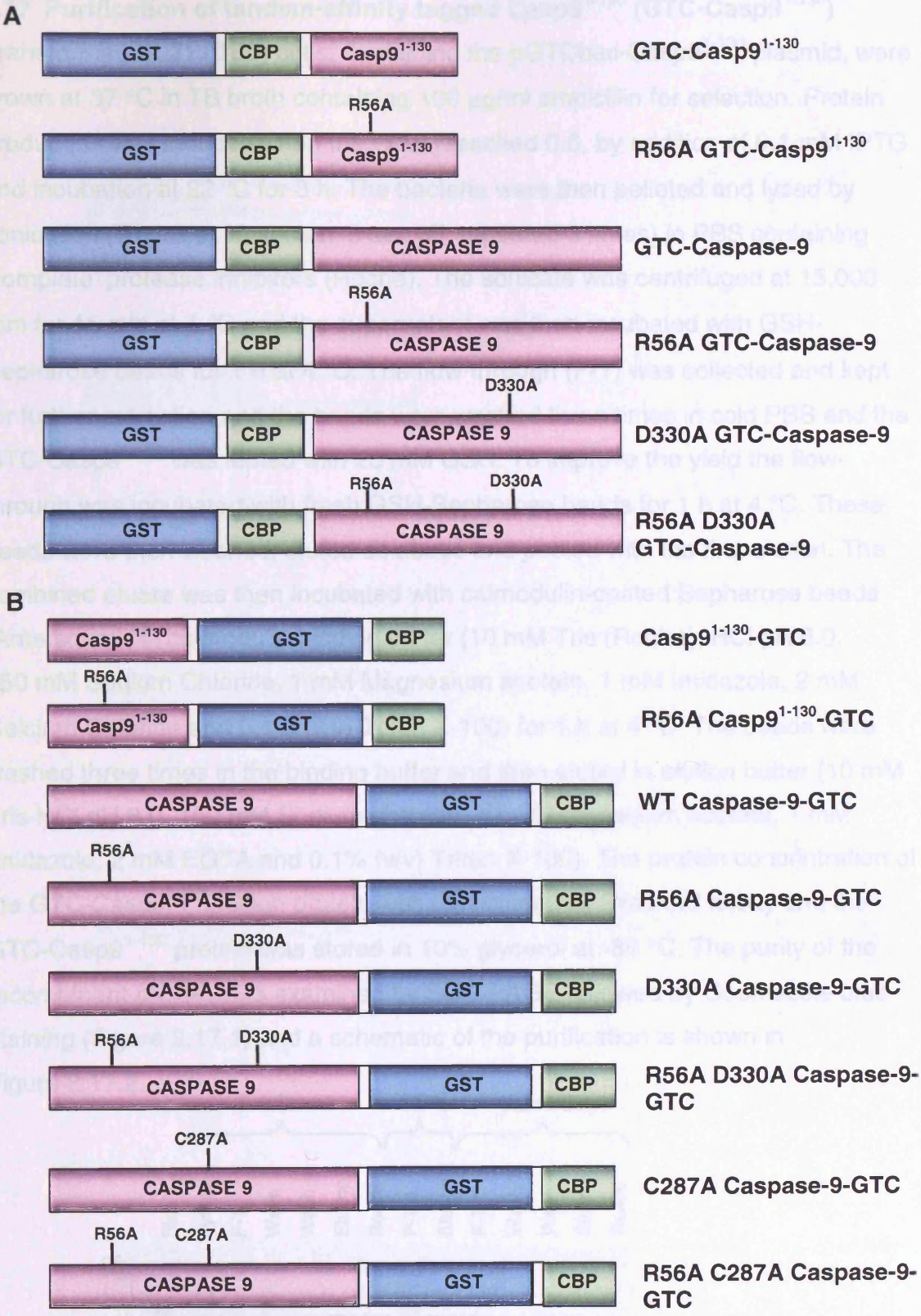

Figure 2.16.5: Schematics of the mammalian GTC constructs produced. Amino terminal-tagged caspase-9 (**A**) C-terminal tagged caspase-9 (**B**).

2.17 Purification of tandem-affinity tagged Casp9$^{1-130}$ (GTC-Casp9$^{1-130}$)

Transformed BL21 (DE3) cells, containing the pGTCbac-Casp9$^{1-130}$ plasmid, were grown at 37 °C in TB broth containing 100 µg/ml ampicillin for selection. Protein production was induced when the OD_{600} reached 0.6, by addition of 0.1 mM IPTG and incubation at 22 °C for 3 h. The bacteria were then pelleted and lysed by sonication (5 cycles, 10 sec on, 5 sec off, repeated 3 times) in PBS containing 'complete' protease inhibitors (Roche). The sonicate was centrifuged at 15,000 rpm for 15 min at 4 °C and the supernatant was then incubated with GSH-Sepharose beads for 1 h at 4 °C. The flow-through (F-T) was collected and kept for further extraction and the beads were washed three times in cold PBS and the GTC-Casp9$^{1-130}$ was eluted with 20 mM GSH. To improve the yield the flow-through was incubated with fresh GSH-Sepharose beads for 1 h at 4 °C. These beads were then washed, eluted as above and pooled with the first elution. The combined eluate was then incubated with calmodulin-coated Sepharose beads (Amersham), in calmodulin binding buffer (10 mM Tris (Roche), HCl pH 8.0, 150 mM Sodium Chloride, 1 mM Magnesium acetate, 1 mM Imidazole, 2 mM Calcium Chloride and 0.1% (v/v) Triton X-100) for 1 h at 4 °C. The beads were washed three times in the binding buffer and then eluted in elution buffer (10 mM Tris-HCl pH 8.0, 150 mM Sodium chloride, 1 mM Magnesium acetate, 1 mM Imidazole, 2 mM EGTA and 0.1% (v/v) Triton X-100). The protein concentration of the GTC-Casp9$^{1-130}$ fusion protein was determined by Bradford assay and the GTC-Casp9$^{1-130}$ protein was stored in 10% glycerol at -80 °C. The purity of the recombinant protein was examined by SDS-PAGE followed by Coomassie blue staining (Figure 2.17.1) and a schematic of the purification is shown in Figure 2.17.2.

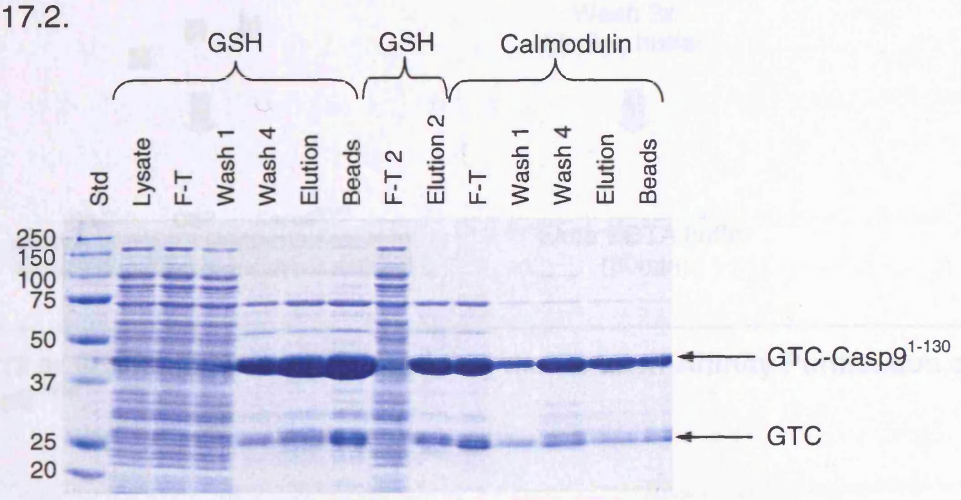

Figure 2.17.1: Tandem-Affinity Purification (TAP) of recombinant GTC-Casp9$^{1-130}$.

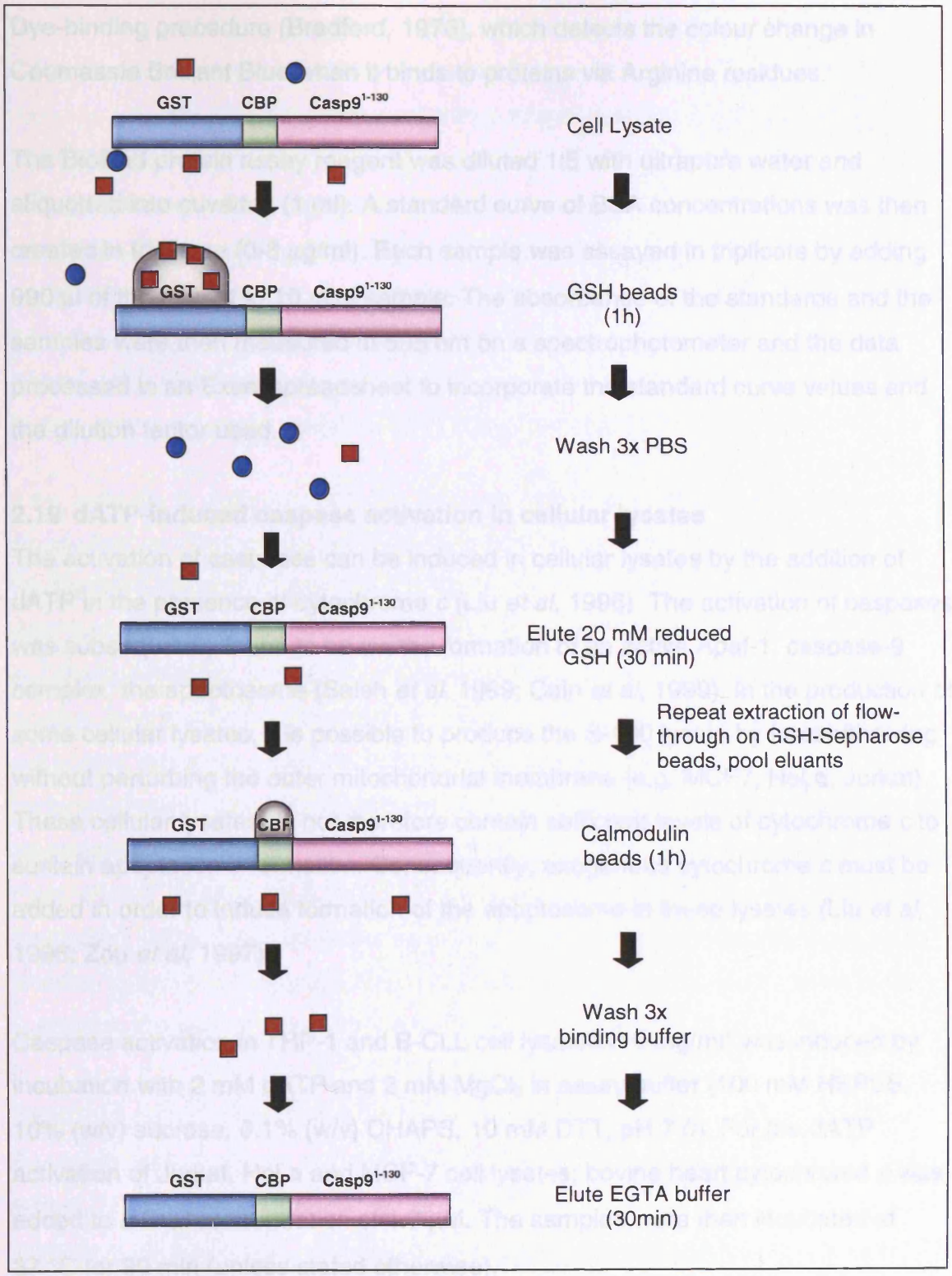

Figure 2.17.2: Schematic flow-chart depicting the Tandem-Affinity Purification of GTC-Casp9$^{1-130}$.

2.18 Protein Concentration

The BioRad method of determining protein concentration is based on the Bradford Dye-binding procedure (Bradford, 1976), which detects the colour change in Coomassie Brilliant Blue when it binds to proteins via Arginine residues.

The BioRad protein assay reagent was diluted 1:5 with ultrapure water and aliquotted into cuvettes (1 ml). A standard curve of BSA concentrations was then created in triplicate (0-8 µg/ml). Each sample was assayed in triplicate by adding 990 µl of the diluent to 10 µl of sample. The absorbance of the standards and the samples were then measured at 595 nm on a spectrophotometer and the data processed in an Excel spreadsheet to incorporate the standard curve values and the dilution factor used.

2.19 dATP-induced caspase activation in cellular lysates

The activation of caspases can be induced in cellular lysates by the addition of dATP in the presence of cytochrome *c* (Liu *et al*, 1996). The activation of caspases was subsequently found to be via the formation of an active Apaf-1: caspase-9 complex, the apoptosome (Saleh *et al*, 1999; Cain *et al*, 1999). In the production of some cellular lysates, it is possible to produce the S-100 lysate by freeze/thawing without perturbing the outer mitochondrial membrane (e.g. MCF7, HeLa, Jurkat). These cellular lysates do not therefore contain sufficient levels of cytochrome *c* to sustain apoptosome formation. Consequently, exogenous cytochrome *c* must be added in order to induce formation of the apoptosome in these lysates (Liu *et al*, 1996; Zou *et al*, 1997).

Caspase activation in THP-1 and B-CLL cell lysates (10 mg/ml) was induced by incubation with 2 mM dATP and 2 mM $MgCl_2$ in assay buffer (100 mM HEPES, 10% (w/v) sucrose, 0.1% (w/v) CHAPS, 10 mM DTT, pH 7.0). For the dATP activation of Jurkat, HeLa and MCF-7 cell lysates; bovine heart cytochrome *c* was added to a final concentration of 1.7 µM. The samples were then incubated at 37 °C for 30 min (unless stated otherwise).

For inhibition studies, GST-Casp9$^{1-130}$ (usual concentration 2 µM) was added as required prior to incubation. The caspase processing ability of the lysate was then

assessed by its ability to cleave Ac-DEVD.AFC (Enzyme Systems) to give a fluorescent readout (Section 2.20)

2.20 Fluorimetric assay of caspase activity

The optimal substrate cleavage recognition site of caspase-3 and caspase-7 is DEXD↓A (Nicholson *et al*, 1995; Thornberry *et al*, 1994)). This has been exploited in the production of fluorogenic substrates to measure the activity of these caspases. DEVD.AFC has a 7-amino-4-trifluoromethylcoumarin (AFC), which can be released following enzymatic cleavage after the DxxD motif. The AFC can then be excited at 400 nm and emits at 505 nm, which can be detected by a Wallac Victor^2 1420 Multilabel counter. It can therefore be concluded that 1 mole of AFC is equivalent to 1 mole Ac-DEVD.AFC being hydrolysed.

Two methods to determine effector caspase activity *in vitro* were employed, depending on whether the samples were from whole cell lysates or from fractionated cell lysates (section 2.23-2.25). In the activated whole lysates, free effector caspases are present which can activate and process the fluorescent substrate. However, in both Superose-6 and Sephacryl 300 gel-filtration, 50 mM sodium chloride (Fisher Scientific) is present in the eluting buffer and removes caspase-3 associated with the apoptosome, which is then eluted in lower molecular weight fractions (Bratton *et al*, 2001a). Therefore in order to quantify the caspase processing activity of the apoptosome, each fraction was incubated with recombinant procaspase-3 (200 nM, see later). The active apoptosomes (with caspase-9 present) will therefore be able to process the procaspase-3 and hence activate the effector caspase. Active caspase-3 can then cleave the fluorogenic substrate, the rate of which can be determined on a Wallac fluorimeter.

DEVDase activity of lysates (10 µl) or column fractions (50 µl) was measured fluorimetrically ($\lambda_{ex}/\lambda_{em}$ = 400-505 nm) at 37 °C in 96 well plates in 200 µl of assay buffer containing 20 µM Ac-DEVD.AFC. The plates were assayed for 10 cycles and cleavage rates were determined by linear regression and expressed as pmol/min. Although caspase-3 and caspase-7 can both process Ac-DEVD.AFC, caspase-7 has a higher Km and lower k_{cat} for this substrate compared with caspase-3 (MacFarlane *et al*, 1997; Garcia-Calvo *et al*, 1999; Denault & Salvesen, 2003). Therefore, 100 µM Ac-DEVD.AFC was used to measure caspase-7 activity

in some experiments using MCF-7 cell lysates. Furthermore, the activity of caspase-7 could not be detected in whole MCF7 cell lysates and therefore procaspase-3 (200 nM) was added to the lysate (10 µl) and assay buffer (to 50 µl) and incubated for 1 h at 37 °C. The apoptosome activity was measured by adding 20 µM Ac-DEVD.AFC to measure the activity of the resulting processed caspase-3.

The chymotrypsin-like activity of the 20S proteosome (LLVYase) can be measured fluormetrically using a 7-amino-4methylcoumarin (AMC)-labelled LLVY motif (Ac-LLVY.AMC (Enzyme Systems). This degradation complex has approximately the same molecular weight as the apoptosome and therefore was used to predict where the apoptosome was eluting from the sucrose density gradients (Cain *et al*, 1999). Each fraction (50 µl) was incubated with 150 µl of 40 µM LLVY.AMC and using the excitation frequency of 380 nm and emission of 460 nm the processing ability of the proteosome was calculated.

2.21 Glutathione (GSH) Pull Down Experiments

Cell lysates (10 mg/ml, 100 µl) were activated with dATP/cytochrome *c* in the presence of 2 µM GST/GST-Casp9$^{1-130}$ for 30 min at 37 °C. The samples were then diluted 1:1 in assay buffer to aid circulation during the extraction process. GSH-coated Sepharose beads (100 µl of a 50% slurry) were then added to each sample and incubated at 4 °C for 1 h on a daisy wheel. The beads were then centrifuged at 200 x g for 3 min, and washed three times in PBS before being eluted in 20 mM GSH.

2.22 Caspase-9, caspase-7 and XIAP immunoprecipitations (IPs) using cross-linked beads.

The cross-linking of antibodies to magnetic protein-coated beads prevents the dissociation of the antibody heavy chain from the bead, which interferes with Western blotting proteins of similar molecular weight (e.g. XIAP). A mouse monoclonal antibody to caspase-9 (R&D #MAB8301), a rabbit polyclonal antibody to active caspase-7 (Cell Signalling #9491) and a mouse monoclonal antibody to XIAP (Transduction Labs #H62120, clone 48) were used in the immunoprecipitation studies. The antibodies were immobilised onto Dyna-beads

(Protein G for caspase-9 and XIAP, and Protein A for caspase-7, Dynal). Using an eppendorf magnet, the holding buffer from 100 µl of beads was removed, and the beads washed three times in PBS/0.05% Tween (500 µl) and resuspended in 100 µl. The required antibody (6.25 µl/100 µl beads) was then incubated with the beads for 1 h at 4 °C on a roller. The magnet was then used to remove the supernatant. The beads were then washed twice in 1 ml 0.2 M triethanolamine, pH 8.2 and resuspended in 1 ml 20 mM DMP in 0.2 M triethanolamine, pH 8.2. This reaction was then allowed to proceed for 30 min at room temperature on a roller. The supernatant was then removed and 50 mM Tris, pH 7.5 (1 ml) was incubated with the beads for 15 min on the roller. The supernatant was removed and the beads were washed three times in PBS/0.5% Tween, before being resuspended in 100 µl. The beads were then stored overnight at 4 °C.

For immunoprecipitations, 20 µl beads were added to 100 µl lysate (caspase-9, 40 µl/100 µl lysate for caspase-7) and incubated overnight at 4 °C on a roller. The supernatant was removed and kept before the beads were washed three times in PBS/0.05% Tween. The bound proteins were eluted with the addition of 50 µl 2x SDS sample buffer/20 µl beads (caspase-9) or /40 µl beads (caspase-7) and incubated at 99 °C for 5 min, which removed the antibody (and any bound proteins) from the beads. The beads were then separated from the elution using the magnet.

2.23 Superose-6 gel filtration

The use of gel filtration chromatography allows separation of proteins/protein complexes based on their molecular weight, and can therefore highlight differences in protein complex formation following dATP activation of lysates or induction of apoptosis (Cain *et al*, 2000; Almond *et al*, 2001). Lysates (200 µl, incorporating 50 mM NaCl) were fractionated by size exclusion chromatography on a Superose-6 FPLC column. The column was equilibrated and eluted at 4 °C with 50 mM NaCl, 20 mM HEPES/NaOH, 5% (w/v) sucrose, 0.1% (w/v) CHAPS and 5 mM DTT, pH 7.0) at 0.4 ml/min with 0.5 ml fractions collected and a UV trace (260 nm) which detected protein was produced. At the end of the run, a sample of each fraction was added to 10 x SDS sample buffer (to create a 1 x

solution) to be run on SDS-PAGE to examine the protein elution profiles. The DEVDase activity of each fraction was also assessed (see section 2.20).

2.24 Sephacryl S300 gel-filtration

To isolate larger quantities of the caspase-7-containing complex, size-exclusion chromatography was employed with a HiPrep 16/60 Sephacryl high-resolution column (Amersham) (Cain *et al*, 1999). The column was equilibrated with the Superose-6 column buffer (section 2.23) and the separations were carried out at 4 °C. Lysates (5-10 mg of protein) were applied to and eluted from the column with a flow rate of 0.4 ml/min, and 2 ml fractions were collected and assayed for DEVDase activity (100 μM Ac-DEVD.AFC). Appropriate fractions were concentrated in Vivaspin concentration tubes (10,000 MWCO) and immunoprecipitated with anti-caspase-7 or anti-XIAP antibodies (section 2.22).

2.25 Sucrose density gradients

In order to separate high molecular weight complexes in large quantities in order to identify proteins by mass spectrometry, it was necessary to use sucrose density gradients. By loading the sample onto the gradient and centrifuging, proteins and protein complexes migrate to fractions where the buoyancy created by the sucrose is equivalent to their molecular weight. Large proteins/ protein complexes migrate to the higher percentage sucrose solution (Cain *et al*, 1999). The gradients were established using 40% and 10% (w/v) sucrose in a buffering solution (0.1% (w/v) CHAPS, 20 mM HEPES, 5 mM DTT, pH 7.0). The resulting gradients run from 35%-10% sucrose, and the linearity of the gradient was verified by refractometry. The control/dATP activated cell lysates (15 mg/ml) were carefully added to the top of the gradient which was subsequently centrifuged at 25,000 rpm for 17 h at 4 °C. Fractions (2 ml) were then collected from the bottom of the gradient and were tested for DEVDase/LLVYase activity, to locate the apoptosome and 'free' effector caspases (as described in section 2.20). An aliquot of each fraction was added to SDS sample buffer and stored for SDS-PAGE and Western blot analysis.

2.26 SDS PAGE Electrophoresis

To detect the presence of known/unknown protein in a given sample, SDS-PAGE was carried out to separate the proteins based on their molecular weight, so that

Western blot analysis or protein staining could be employed. The BioRad mini SDS-PAGE kits (Protean III) were primarily used with separation on 7, 10, 12, 13 or 15% SDS-polyacrylamide gels. The proteins were then either transferred onto nitrocellulose membranes (Hybond C Extra) for detection by immunoblotting (as previously described in MacFarlane *et al*, 1997), or stained to detect unknown proteins. The protein stains used in this study included Coomassie-blue, Silver and SYPRO-Ruby (sections 2.28-2.30). Larger gels were required when resolving large volumes of sample with complex composition (Hoefer Scientific).

2.27 Western blotting

As described in MacFarlane *et al*, 1997, with all primary and secondary antibodies incubated for 1 h at room temperature unless stated otherwise.

Primary Antibodies

Antibody	**Host**	**Source**	**Concentration**
Apaf-1	Mouse	R&D	1/1000
Caspase-2	Rabbit	Santa Cruz	1/1000, 1/500
Caspase-3	Rabbit	Merck, gift from D. Nicholson	1/10,000
Caspase-7	Rabbit	In house xmsR151	1/1000
Caspase-8	Rabbit	In house xmsR355	1/2000
Caspase-9	Mouse	MBL	1/1000
Cytochrome *c*	Mouse	Pharmingen	1/2000
GST	Goat	Amersham	1/8000 or 1/1000
SMAC	Rabbit	In house xmsR853	1/2000
Omi	Rabbit	In house xmsR898	1/2000
XIAP	Mouse	Transduction Labs	1/2000
cIAP-1	Rabbit	R & D	1/1000 o/n
cIAP-2	Rabbit	R & D	1/1000 o/n

Secondary Antibodies conjugated to HRP

Antibody	Host	Source	Concentration
Anti-goat	Rabbit	Dako	1/2000
Anti-mouse	Goat	Sigma	1/2000
Anti-rabbit	Goat	Dako	1/2000

2.28 Coomassie Blue staining

Following electrophoresis, the gel was placed in Coomassie Blue stain (0.25% Coomassie brilliant blue, 45% methanol (Fisher Scientific), 10% acetic acid (Fisher Scientific)) for 1 h and destained until clear in 10% (v/v) acetic acid, 40% (v/v) methanol.

2.29 Silver Staining

The gel was first fixed for 30 min in 10% acetic acid, 40% ethanol and then washed for 3 x 5 min in ultrapure water. The gel was then incubated in a sensitisation buffer (30% ethanol (Fisher Scientific), 12.64 mM sodium thiosulphate, 500 mM sodium acetate, 0.125% (w/v) glutaraldehyde (Fisher Scientific)) for 30 min. The gel was then washed (as above) and incubated in the silver reagent (0.25% (w/v) Silver nitrate, 0.0148% (w/v) formaldehyde (Amersham Biosciences)) for 20 min. The gel was washed 2 x 1 min in ultrapure water and then developed for 2-5 min (236 mM sodium carbonate, 0.074% (w/v) formaldehyde), whilst stirred vigorously. The reaction was then stopped for 10 min in 39 mM EDTA. Finally the gel was then washed 3 x 5 min and then preserved in 4% (v/v) glycerol, 30% (v/v) ethanol.

2.30 SYPRO-Ruby Staining

The gel was fixed for 30 min in 10% (v/v) acetic acid, 40% (v/v) ethanol, washed twice in ultrapure water and then SYPRO-Ruby stain (Molecular Probes) was added. The gel was then protected from the light and incubated with the stain for at least 4 h. The gel was then destained in 10% (v/v) methanol, 6% (v/v) acetic acid.

2.31 Mass spectrometry

Gel plugs (0.8 mm) of bands of interest were excised from the acrylamide gel using an automated spot picker (ProPic, Perkin Elmer, Elmer Life Sciences, Cambs, UK). If a larger percentage of the band was required for protein identification then a 'Montage' approach was used, where the band was excised manually. The plugs/montage were then digested in an automated digestion robot (ProGEST, Perkin Elmer) which reduced the proteins in 10 mM DTT, followed by alkylation with 100 mM iodoacetamide and finally proteins were digested with Promega modified sequencing-grade porcine trypsin.

Peptides produced were then extracted with 21 µl 0.1% formic acid and 5 µl desalted with C18 zip tips (Millipore, Watford, UK). Desalted peptide extracts (0.5 µl) were amalgamated with 0.5 µl α-cyano-4-hydroxycinammic acid in 1% TFA, 50% acetonitrile and were 'spotted' onto MALDI target plates using an automated spotting robot (ProMS, Perkin Elmer).

Peptide analysis was performed on a MALDI-Tof mass spectrometer (M@LDI-R, Microsmass, Manchester, UK) with a mass range of 900-3000 Da. The data was analysed either automatically (ProteinLynx) or manually (MASCOT software) with protein identities determined by submission to SWISS-PROT and TrEMBL databases.

Performed by Rebekah Jukes-Jones and Dr Robert Boyd.

Chapter 3

Affinity purification and characterisation of the ~700 kDa apoptosome from THP-1 cell lysates.

3.1 Introduction

There are two primary caspase activation pathways (extrinsic and intrinsic) with the initial activation event involving ligation of death receptors or the perturbation of the mitochondria, respectively. The intrinsic pathway requires the formation of the apoptosome, a large caspase-activation complex (Reviewed in Cain *et al*, 2002; Shi, 2002a), the core components of which are evolutionarily conserved from *C.elegans* to mammals. Apoptosome formation can be induced in cellular lysates and consists of three central components, originally termed apoptotic protease-activating factors (Apaf 1-3) (Liu *et al*, 1996). Apaf-1 is a mammalian CED-4 homologue (Zou *et al*, 1997), which oligomerises in the presence of Apaf-2 (cytochrome *c*; Liu *et al*, 1996) and dATP to form the apoptosome (Zou *et al*, 1999; Saleh *et al*, 1999). The oligomerisation of Apaf-1 exposes the CARD domain, to which Apaf-3 (caspase-9; Li *et al*, 1997) is recruited via its equivalent CARD domain and is then activated by autocatalytic processing (Srinivasula *et al*, 1998).

Apaf-1, cytochrome *c* and dATP induce the formation of apoptosomes of varying sizes depending on the cell type and conditions used. In THP-1 cell lysates, Apaf-1 oligomerises into ~700 kDa and ~1.4 MDa complexes (Cain *et al*, 2000) whereas in HeLa cell lysates the apoptosome size ranges between ~1.3 MDa and ~1 MDa when activated with dATP (Zou *et al*, 1999; Jiang *et al*, 2003). In addition, the ~700 kDa form of the apoptosome predominates in apoptotic rat heptoma and human B-CLL cells (Freathy *et al*, 2000; Almond *et al*, 2001). This variation in size could be explained by the presence of a variety of modulators binding to the apoptosome and thus potentially influencing the formation/activity of the complex.

Thus, the overall aim of this project was to purify the ~700 kDa apoptosome from cell lysates using an affinity technique and to establish whether there were any other interacting proteins. Previously, in this laboratory, classical biochemical strategies had been used to isolate the ~700 kDa apoptosome complex. However, this also led to the co-purification of other complexes of similar size, i.e. the IKK complex (Langlais, 2002). An affinity purification approach was therefore necessary to specifically purify the ~700 kDa apoptosome complex to homogeneity. In this respect, previous studies in our laboratory using anti-Apaf-1 antibodies to isolate the apoptosome were unsuccessful, as they were not

conformation-specific. A more promising approach was to target the apoptosome via its interaction with caspase-9, as caspase-9 can only bind to oligomerised Apaf-1 within the apoptosome (Zou *et al*, 1999; Saleh *et al*, 1999). Furthermore, the CARD:CARD interaction between Apaf-1 and caspase-9 is of high affinity, and thus it is likely to withstand complex purification procedures. Therefore two approaches using this strategy could be employed; firstly, an affinity tagged form of recombinant caspase-9 and secondly, an antibody to caspase-9.

Fortunately, I was provided with a construct encoding a GST-tagged CARD domain (amino acids 1-130) of caspase-9 (GST-Casp9$^{1-130}$) by C. Adrain and S. Martin, Trinity College, Dublin. This fusion protein should bind to Apaf-1 but not induce the subsequent activation of caspases (due to the absence of the large and small catalytic subunits). As there have been reports of apoptosome degradation by active effector caspases (Bratton *et al*, 2001a; Lauber *et al*, 2001), the prevention of caspase activation by use of a CARD-only variant could result in preservation of the apoptosome and any interacting proteins. Furthermore, WD40 repeats are putative binding domains found in many regulatory proteins (Neer *et al*, 1994; Wall *et al*, 1995; Sondek *et al*, 1996) and therefore the WD40 domains of Apaf-1 could mediate protein interactions with the apoptosome. Thus by using GST-Casp9$^{1-130}$, any proteins that bind to the WD40 domains of Apaf-1 could be assessed without apoptosome degradation. Initial work involved the production and purification of recombinant GST-Casp9$^{1-130}$ and the assessment of whether binding of Apaf-1 to GST-Casp9$^{1-130}$ was dependent on certain factors i.e. dATP, cytochrome *c*. Subsequent to this, it was necessary to prove that the GST-Casp9$^{1-130}$ was incorporated into the ~700 kDa apoptosome. This would then allow an affinity purification of the ~700 kDa apoptosome which could subsequently be subjected to proteomic analysis.

In addition to this approach, an antibody to caspase-9 was used to isolate the ~700 kDa apoptosome complex in its native form. This should allow the identification of proteins that interact with the large and small subunits of caspase-9, in addition to proteins interacting with Apaf-1. It was therefore hoped that a combination of these two techniques would allow a definitive characterisation of the proteomic composition of the ~700 kDa apoptosome complex. From these studies, it was concluded that the native and GST-Casp9$^{1-130}$-inhibited

apoptosomes only consist of Apaf-1, caspase-9 and cytochrome *c*. In addition, we have shown that the levels of SMAC and Omi in the lysate modulate the presence of XIAP and caspase-3 in the native apoptosome.

3.2 Results

3.2.1 GST-Casp9$^{1-130}$ inhibits dATP-dependent caspase activation in THP-1 cell lysates.

The first approach used to isolate the apoptosome was based on the observation that the prodomain of caspase-9 (amino acids 1-130) could bind tightly to Apaf-1, via CARD:CARD interactions (Qin *et al*, 1999). Therefore, if affinity-tagged, the prodomain of caspase-9 should be able to isolate the apoptosome from lysates activated with dATP. Consequently, the CARD domain of caspase-9 was inserted C-terminally to GST in a bacterial expression vector and recombinant GST-Casp9$^{1-130}$ was produced (See Materials and Methods for expression details; Figure 3.2.1A).

Initial experiments were designed to characterise the effects of GST-Casp9$^{1-130}$ on the dATP activation of caspase-3 in THP-1 cell lysates. Treatment of cell lysates with dATP and cytochrome *c* stimulates caspase-3 (DEVDase) activity, which can be measured fluorometrically using Ac-DEVD.AFC. As shown in Figure 3.2.1B, GST-Casp9$^{1-130}$ acted as a dominant negative inhibitor of dATP-activated effector caspase activation when incubated with THP-1 cell lysates, with an IC_{50} ~0.8 μM. This is in accordance with previous studies, which have shown that the CARD domain alone can inhibit caspase activation (Qin *et al*, 1999) and that the catalytically inactive mutant caspase-9 (C287A) can also prevent activation of the caspase cascade (Bratton *et al*, 2001b). Furthermore, the endogenous dominant inhibitor of caspase-9, caspase-9b, which lacks the large catalytic subunit, has been shown to act as an inhibitor of apoptosis (Seol & Billiar, 1999; Srinivasula *et al*, 1999).

When purifying recombinant GST-Casp9$^{1-130}$, some free GST also co-eluted (Materials and Methods, Figure 2.14.1D), therefore it was necessary to evaluate whether GST was affecting the DEVDase activity of the lysate. THP-1 cell lysates were dATP-activated in the presence of either GST or GST-Casp9$^{1-130}$ (2 μM) and the resulting caspase processing profiles were studied (Figure 3.2.1C). The dATP activation alone revealed that caspases-3, -9 and -2 were processed and an

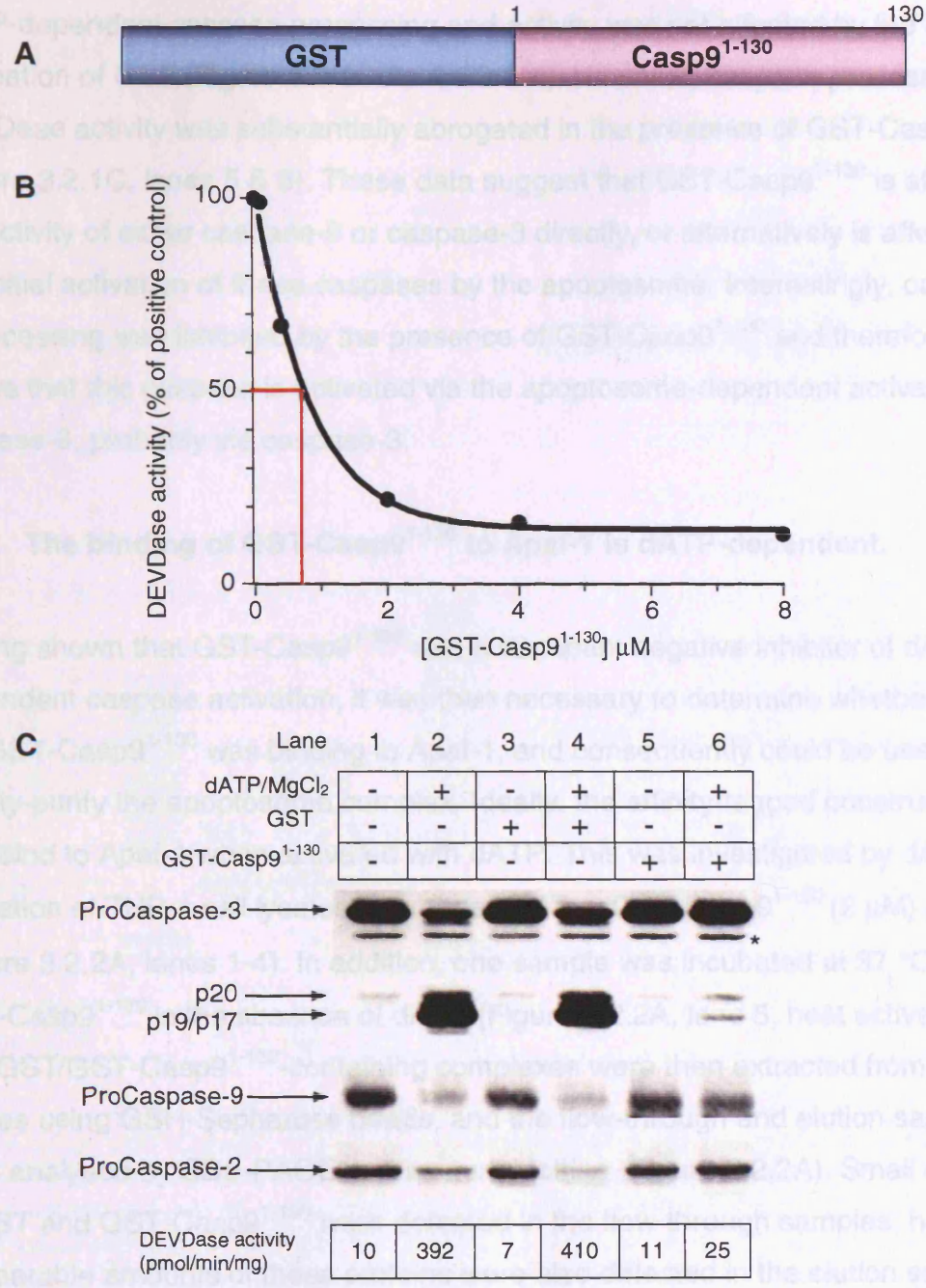

Figure 3.2.1: GST-Casp9$^{1-130}$ acts as a dominant negative inhibitor of dATP activation in THP-1 cell lysates. Schematic representation of the fusion protein GST-Casp9$^{1-130}$ (**A**). THP-1 lysate (10 mg/ml) was activated with 2 mM dATP in the presence of increasing concentrations of GST-Casp9$^{1-130}$. Caspase activation was measured using Ac-DEVD.AFC as a substrate (as described in Materials and Methods) and expressed as a percentage of dATP activated control. (**B**). THP-1 lysates (10 mg/ml) were activated with 2 mM dATP (lanes 1 & 2) for 30 min at 37 °C in the presence of either 2 μM GST (lanes 3 & 4) or 2 μM GST-Casp9$^{1-130}$ (lanes 5 & 6). Total cell lysates (20 μg/lane) were separated by SDS-PAGE and immunoblotted for caspase-3, caspase-9 and caspase-2. A 10 μl aliquot of each sample was assayed for DEVDase activity (expressed in pmol/min/mg) (**C**). The asterisk indicates a non-specific band detected by the caspase-3 Western blotting antibody.

increase in DEVDase activity was observed (Figure 3.2.1C, lanes 1 & 2). This dATP-dependent caspase processing and activity was not affected by the co-incubation of GST (Figure 3.2.1C, lanes 3 & 4). However, caspase processing and DEVDase activity was substantially abrogated in the presence of GST-Casp9$^{1-130}$ (Figure 3.2.1C, lanes 5 & 6). These data suggest that GST-Casp9$^{1-130}$ is affecting the activity of either caspase-9 or caspase-3 directly, or alternatively is affecting the initial activation of these caspases by the apoptosome. Interestingly, caspase-2 processing was inhibited by the presence of GST-Casp9$^{1-130}$ and therefore shows that this caspase is activated via the apoptosome-dependent activation of caspase-9, probably via caspase-3.

3.2.2 The binding of GST-Casp9$^{1-130}$ to Apaf-1 is dATP-dependent.

Having shown that GST-Casp9$^{1-130}$ was a dominant negative inhibitor of dATP-dependent caspase activation, it was then necessary to determine whether or not the GST-Casp9$^{1-130}$ was binding to Apaf-1, and consequently could be used to affinity-purify the apoptosome complex. Ideally, the affinity-tagged construct would only bind to Apaf-1 when activated with dATP. This was investigated by dATP-activation of THP-1 cell lysates with either GST or GST-Casp9$^{1-130}$ (2 μM) present (Figure 3.2.2A, lanes 1-4). In addition, one sample was incubated at 37 °C with GST-Casp9$^{1-130}$ in the absence of dATP (Figure 3.2.2A, lane 5, heat activation). The GST/GST-Casp9$^{1-130}$-containing complexes were then extracted from the lysates using GSH-Sepharose beads, and the flow-through and elution samples were analysed by SDS-PAGE and immunoblotting (Figure 3.2.2A). Small amounts of GST and GST-Casp9$^{1-130}$ were detected in the flow-through samples, however comparable amounts of these proteins were also detected in the elution samples (Figure 3.2.2A). GST alone did not bind to Apaf-1 under any condition tested (Figure 3.2.2A, lanes 6 & 7), whereas GST-Casp9$^{1-130}$ only bound to Apaf-1 when the lysates were dATP-activated (Figure 3.2.2A, lane 8 & 9). Heat activation of the lysates in the absence of dATP did not induce Apaf-1 and GST-Casp9$^{1-130}$ binding (Figure 3.2.2A, lane 10). Thus, GST-Casp9$^{1-130}$ only binds to Apaf-1 under conditions that promote the formation of the apoptosome.

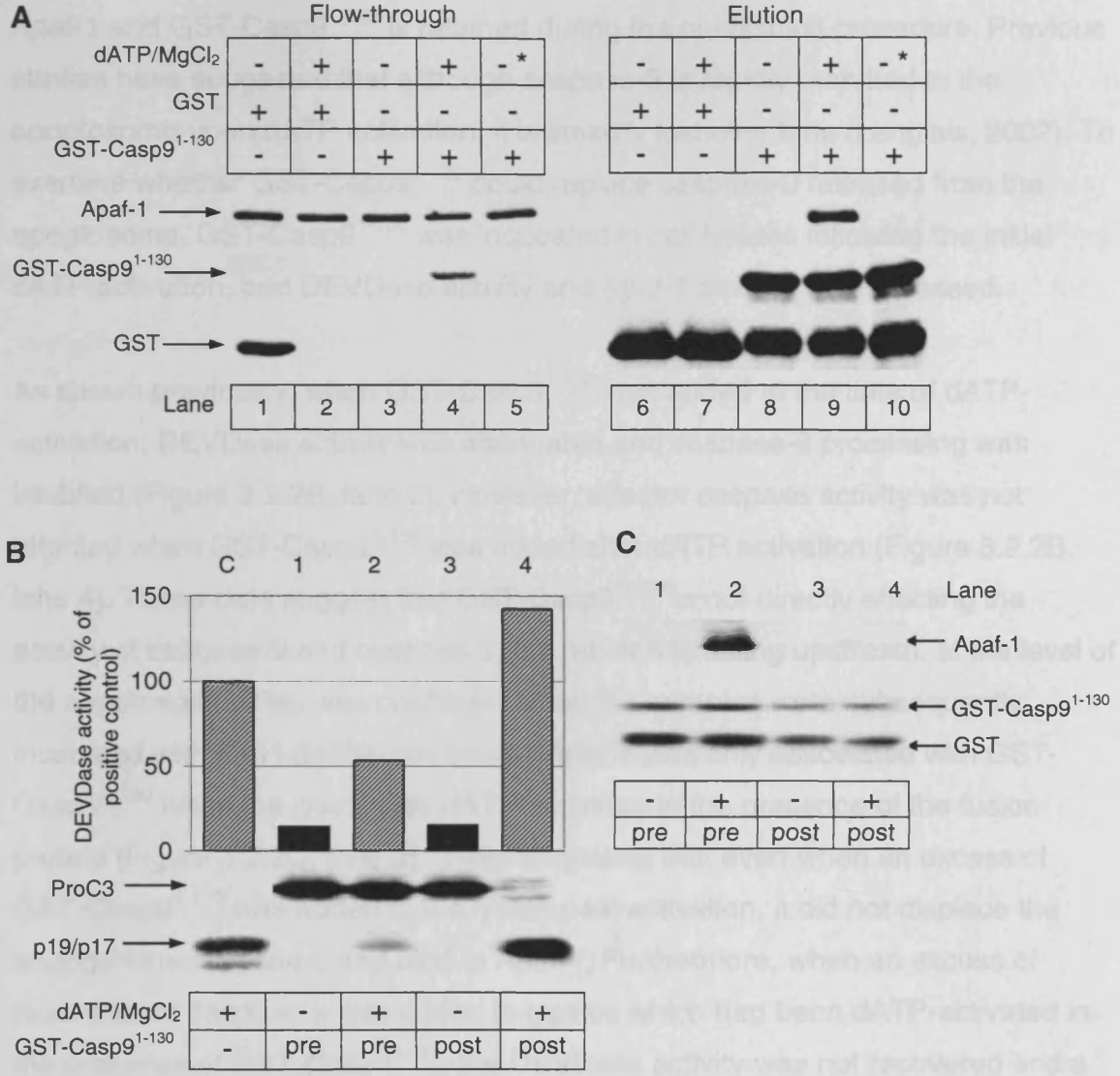

Figure 3.2.2: GST-Casp9$^{1-130}$ directly associates with Apaf-1 in dATP activated lysate only in the presence of dATP and when added at the time of activation.
THP-1 lysates (10 mg/ml) were either activated with 2 mM dATP for 30 min at 37 °C in the presence of either 2 μM GST (lanes 1 & 2) or 2 μM GST-Casp9$^{1-130}$ (lanes 3 & 4) or incubated at 37 °C in the absence of dATP (lane 5). The lysates were then incubated with GSH-Sepharose beads (100 μl) for 1 h at 4 °C. Following centrifugation, the flow-through was collected and the beads washed thoroughly in cold PBS before elution in 20 mM glutathione (50 μl). The flow-through (20 μg/lane) and elution samples were subsequently mixed with SDS sample buffer, separated by SDS-PAGE and immunoblotted for Apaf-1 and GST (**A**). THP-1 lysate (10 mg/ml) was either co-incubated (pre) with 2 μM GST-CASP9$^{1-130}$ with and without 2 mM dATP for 30 min at 37 °C (lanes 1 & 2) or incubated with and without dATP for 30 min before incubating (post) for a further 30 min with GST-Casp9$^{1-130}$ (lanes 3 & 4). The DEVDase activity was then assayed using an aliquot (10 μl) of the incubation, and total cell lysate (20 μg/lane) was separated by SDS-PAGE and immunoblotted for caspase-3 (**B**). The samples were then incubated with GSH beads (as described above) and the elution samples were immunoblotted with anti-Apaf-1 and anti-GST antibodies (**C**).

It is important for the successful affinity purification that any association between Apaf-1 and GST-Casp9$^{1-130}$ is retained during the purification procedure. Previous studies have suggested that although caspase-9 is rapidly recruited to the apoptosome upon dATP activation, it is steadily lost over time (Langlais, 2002). To examine whether GST-Casp9$^{1-130}$ could replace caspase-9 released from the apoptosome, GST-Casp9$^{1-130}$ was incubated in cell lysates following the initial dATP activation, and DEVDase activity and Apaf-1 binding was assessed.

As shown previously, when GST-Casp9$^{1-130}$ was added at the time of dATP-activation, DEVDase activity was attenuated and caspase-3 processing was inhibited (Figure 3.2.2B, lane 2). However, effector caspase activity was not affected when GST-Casp9$^{1-130}$ was added after dATP activation (Figure 3.2.2B, lane 4). These data suggest that GST-Casp9$^{1-130}$ is not directly affecting the activity of caspase-9 and caspase-3, but rather it is acting upstream, at the level of the apoptosome. This was confirmed when the samples were subsequently incubated with GSH-Sepharose beads; Apaf-1 was only associated with GST-Casp9$^{1-130}$ when the lysate was dATP-activated in the presence of the fusion protein (Figure 3.2.2C, lane 2). It was surprising that even when an excess of GST-Casp9$^{1-130}$ was added to the lysate post-activation, it did not displace the endogenous caspase-9 and bind to Apaf-1. Furthermore, when an excess of recombinant caspase-9 was added to lysates which had been dATP-activated in the presence of GST-Casp9$^{1-130}$, the DEVDase activity was not recovered and a decrease in Apaf-1 binding was not observed (data not shown). These observations suggest that when caspase-9 or GST-Casp9$^{1-130}$ binds to the apoptosome it cannot be replaced. This is a key element for the successful purification of the apoptosome, as the interaction between GST-Casp9$^{1-130}$ and Apaf-1 appears to be very stable.

3.2.3 The ability of GST-Casp9$^{1-130}$ to bind to Apaf-1 requires both dATP and cytochrome *c*.

Having determined that dATP was essential for binding of GST-Casp9$^{1-130}$ to Apaf-1, it was logical to presume that this was an apoptosome-related phenomenon. Apaf-1 oligomerisation normally requires both dATP and cytochrome *c* and therefore it was necessary to investigate the role of cytochrome *c* in permitting the

association between GST-Casp9$^{1-130}$ and Apaf-1. However, the THP-1 cell lysates prepared by freeze/thawing invariably contain cytochrome *c* due to the mitochondrial damage caused by the cell breakage method. Thus making it impossible to investigate whether cytochrome *c* is essential for the binding of Apaf-1 to GST-Casp9$^{1-130}$ in these lysates. Therefore a method of cell lysate production was developed which used a milder form of cell membrane disruption. Initially, the cell membrane was permeabilised with Digitonin (0.05%) and then the cells were passed through a ball-bearing homogeniser. The intact mitochondria were removed from the cytosol with a 20,000 x g centrifugation step, and S-100 lysates prepared by centrifugation at 100,000 x g for 1 h (Dig/Hom). Compared to the freeze/thawed cell lysates (Figure 3.2.3A, lane 1), the lysate produced by the Dig/Hom method did not contain detectable levels of cytochrome *c* (Figure 3.2.3A, lane 2) and can therefore be used when reduced levels of cytochrome *c* or other mitochondrial proteins are required in the cell lysate. The pellet resulting from the 20,000 x g centrifugation contained the majority of the cytochrome *c* (Figure 3.2.3A, lane 3) and therefore presumably contains the intact mitochondria.

To further assess the effect of the removal of intact mitochondria and hence cytochrome *c* from the cell lysates, the DEVDase activity of the Dig/Hom cell lysates following dATP-activation was examined in the presence and absence of cytochrome *c* (Figure 3.2.3B). In the absence of cytochrome *c* the lysate contained only basal levels of DEVDase activity, even with dATP present. However, when exogenous cytochrome *c* was incubated during the activation, the DEVDase activity was significantly increased (Figure 3.2.3B). These data showed that cytochrome *c* is required for apoptosome formation and caspase activation in these cellular lysates.

The Dig/Hom cell lysates were then used to investigate whether the binding of GST-Casp9$^{1-130}$ to Apaf-1 was cytochrome *c*-dependent. THP-1 Dig/Hom lysates were activated with dATP and/or cytochrome *c* in the presence of GST (Figure 3.2.3C, lanes 1 - 3) or GST-Casp9$^{1-130}$ (lanes 4 - 6). The lysates were incubated with GSH-Sepharose beads and the flow-through and elutions were analysed by SDS-PAGE and immunoblotting. As shown previously, GST was unable to bind to Apaf-1 in any of the conditions tested (Figure 3.2.3C, lanes 7-9) and GST-Casp9$^{1-130}$ did not bind to Apaf-1 in the absence of dATP (lane 10). However, in the

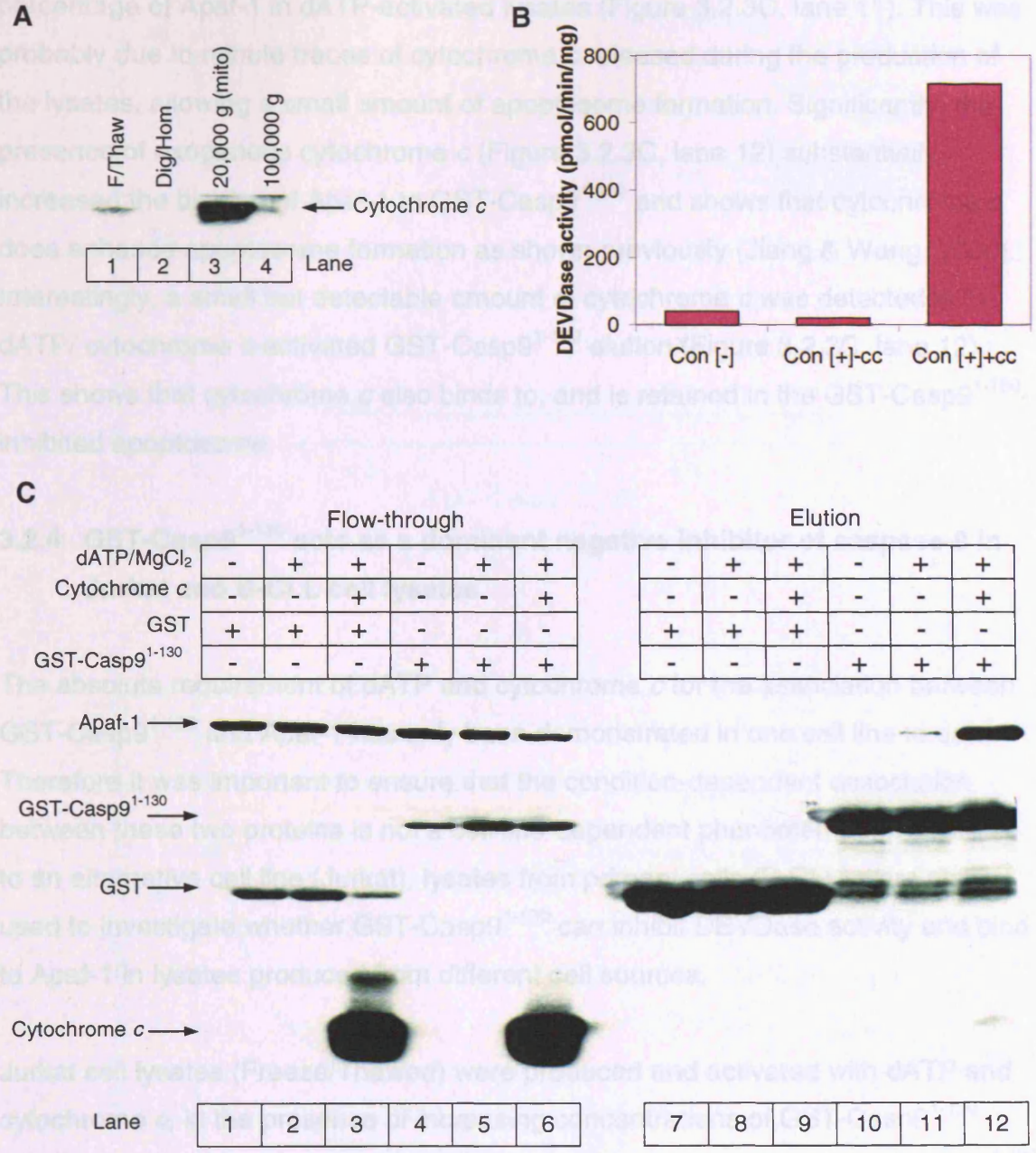

Figure 3.2.3: GST-Casp9$^{1-130}$ only binds to Apaf-1 in the presence of cytochrome *c* and dATP. A comparison of cytochrome *c* content in Freeze/thawed (F/T) and Dig/Hom cell lysate at the centrifugational stages of their preparation. The membrane pellets were sonicated and 20 µg protein/lane of lysate and membrane were analysed by SDS-PAGE and immunoblotting (**A**). Dig/Hom THP-1 lysate (10 mg/ml) was activated with 2 mM dATP and 1.7 µM Cytochrome *c* and incubated for 30 min at 37 °C. An aliquot was then assayed for DEVDase activity (expressed in pmol/min/mg, **B**). Dig/Hom THP-1 lysate (10 mg/ml) was activated with 2 mM dATP and 1.7 µM cytochrome *c* for 30 min at 37 °C in the presence of 2 µM GST (lanes 1-3), or 2 µM GST-Casp9$^{1-130}$ (lanes 4-6). The lysates were then incubated with GSH beads and eluted as described in Figure 3.2. The flow-through and elution samples were mixed with SDS sample buffer and separated by SDS-PAGE and immunoblotted for Apaf-1, GST and cytochrome *c* (**C**).

absence of cytochrome *c*, GST-Casp9$^{1-130}$ was able to capture a very small percentage of Apaf-1 in dATP-activated lysates (Figure 3.2.3C, lane 11). This was probably due to minute traces of cytochrome *c* released during the production of the lysates, allowing a small amount of apoptosome formation. Significantly, the presence of exogenous cytochrome *c* (Figure 3.2.3C, lane 12) substantially increased the binding of Apaf-1 to GST-Casp9$^{1-130}$ and shows that cytochrome *c* does enhance apoptosome formation as shown previously (Jiang & Wang, 2000). Interestingly, a small but detectable amount of cytochrome *c* was detected in the dATP/ cytochrome *c*-activated GST-Casp9$^{1-130}$ elution (Figure 3.2.3C, lane 12). This shows that cytochrome *c* also binds to, and is retained in the GST-Casp9$^{1-130}$-inhibited apoptosome.

3.2.4 GST-Casp9$^{1-130}$ acts as a dominant negative inhibitor of caspase-9 in Jurkat and B-CLL cell lysates.

The absolute requirement of dATP and cytochrome *c* for the association between GST-Casp9$^{1-130}$ and Apaf-1 has only been demonstrated in one cell line to date. Therefore it was important to ensure that the condition-dependent association between these two proteins is not a cell line-dependent phenomenon. In addition to an alternative cell line (Jurkat), lysates from primary cells (B-CLL) were also used to investigate whether GST-Casp9$^{1-130}$ can inhibit DEVDase activity and bind to Apaf-1 in lysates produced from different cell sources.

Jurkat cell lysates (Freeze/Thawed) were produced and activated with dATP and cytochrome *c*, in the presence of increasing concentrations of GST-Casp9$^{1-130}$ (Figure 3.2.4A). Interestingly, this cell line was more susceptible to GST-Casp9$^{1-130}$ inhibition than THP-1 cells, possibly due to a lower abundance of Apaf-1 or the absence of an inhibitory protein in these cells, thus allowing Apaf-1 and caspase-9 to associate more readily. As shown for THP-1 cell lysates, GST-Casp9$^{1-130}$ was only able to bind to Apaf-1 with dATP and cytochrome *c* activation (Figure 3.2.4A, inset).

Freeze/thawed B-CLL cell lysates were produced from a CLL patient blood sample (see Materials and Methods for details) to investigate the effect of GST-Casp9$^{1-130}$ in primary cell lysates. These lysates were incubated with increasing

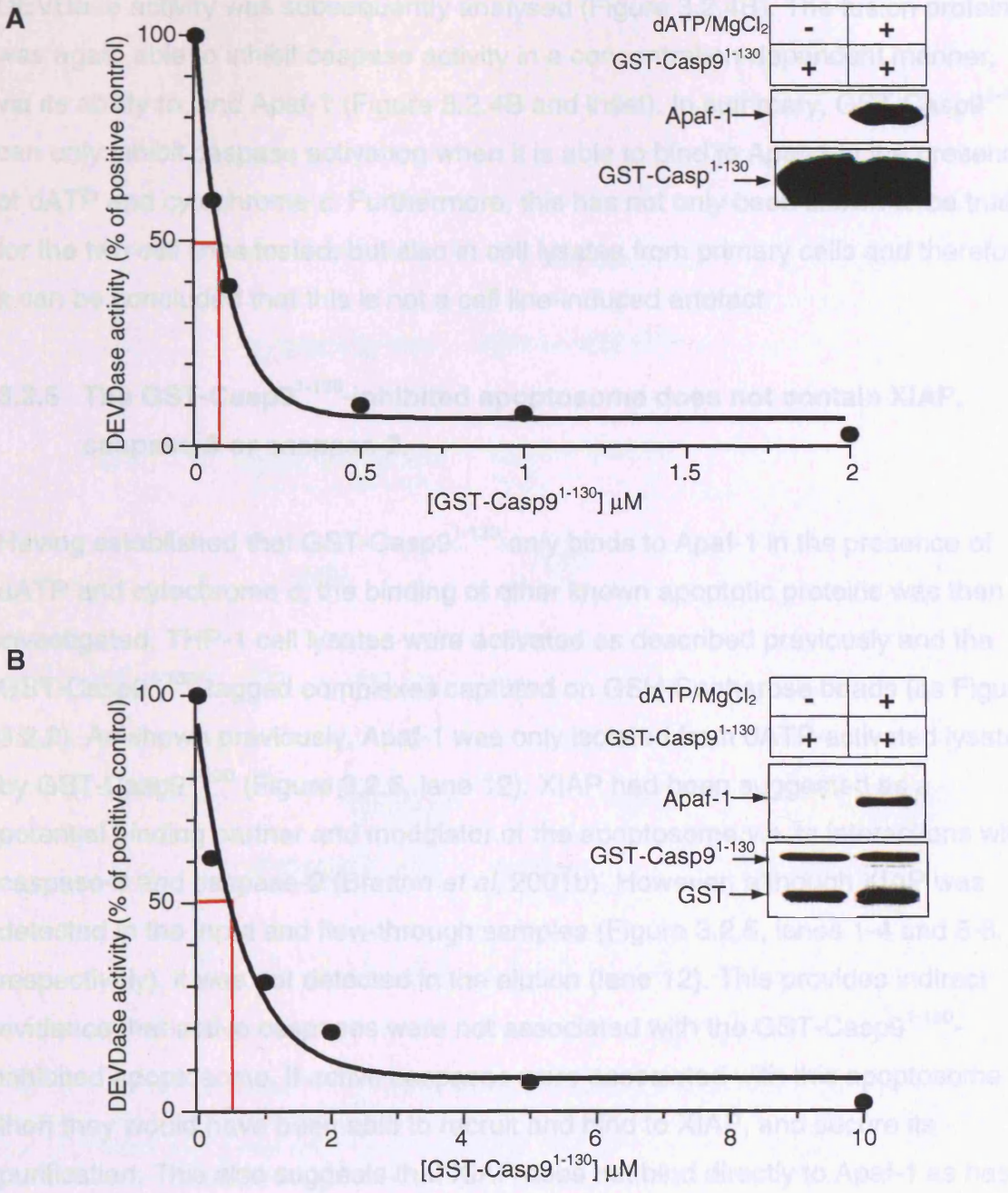

Figure 3.2.4: GST-Casp9$^{1-130}$ acts as a dominant negative inhibitor in Jurkat and B-CLL cell lysates. Jurkat cell lysate (10 mg/ml) was activated with 2 mM dATP and 1.7 µM cytochrome *c* in the presence of increasing concentrations of GST-Casp9$^{1-130}$ for 30 min at 37 °C. An aliquot (10 µl) was then taken and the DEVDase activity assessed. The sample activated with 2 µM GST-Casp9$^{1-130}$ present was then incubated with GSH-Sepharose beads for 1 h at 4 °C. The beads were then washed and eluted and the elution sample was combined with SDS sample buffer and separated by SDS-PAGE and immunoblotted for Apaf-1 and GST (**A**, main and inset). B cell lymphoma (B-CLL) cell lysate (10 mg/ml) was activated with dATP as described previously and the DEVDase activity and association with Apaf-1 was carried out as above (**B**, main and inset).

concentrations of GST-Casp9$^{1-130}$ in the presence of dATP activation and the DEVDase activity was subsequently analysed (Figure 3.2.4B). The fusion protein was again able to inhibit caspase activity in a concentration-dependent manner, via its ability to bind Apaf-1 (Figure 3.2.4B and inset). In summary, GST-Casp9$^{1-130}$ can only inhibit caspase activation when it is able to bind to Apaf-1 in the presence of dATP and cytochrome *c*. Furthermore, this has not only been shown to be true for the two cell lines tested, but also in cell lysates from primary cells and therefore it can be concluded that this is not a cell line-induced artefact.

3.2.5 The GST-Casp9$^{1-130}$-inhibited apoptosome does not contain XIAP, caspase-3 or caspase-2.

Having established that GST-Casp9$^{1-130}$ only binds to Apaf-1 in the presence of dATP and cytochrome *c*, the binding of other known apoptotic proteins was then investigated. THP-1 cell lysates were activated as described previously and the GST-Casp9$^{1-130}$-tagged complexes captured on GSH-Sepharose beads (as Figure 3.2.2). As shown previously, Apaf-1 was only isolated from dATP-activated lysates by GST-Casp9$^{1-130}$ (Figure 3.2.5, lane 12). XIAP had been suggested as a potential binding partner and modulator of the apoptosome via its interactions with caspase-3 and caspase-9 (Bratton *et al*, 2001b). However, although XIAP was detected in the input and flow-through samples (Figure 3.2.5, lanes 1-4 and 5-8, respectively), it was not detected in the elution (lane 12). This provides indirect evidence that active caspases were not associated with the GST-Casp9$^{1-130}$-inhibited apoptosome. If active caspases were associated with this apoptosome then they would have been able to recruit and bind to XIAP, and secure its purification. This also suggests that XIAP does not bind directly to Apaf-1 as has previously been suggested (Bratton *et al*, 2001b). The presence of GST-Casp9$^{1-130}$ again abrogated the dATP-dependent processing of the downstream caspases, caspase-3 and caspase-2 (Figure 3.2.5, lanes 3 & 4). In addition, the GST-Casp9$^{1-130}$-inhibited apoptosome did not contain caspase-3, which would confirm the reason for the absence of XIAP. The absence of caspase-3 in the apoptosome is presumably because GST-Casp9$^{1-130}$ does not possess the large catalytic subunit of caspase-9 to which caspase-3 would associate. Furthermore, caspase-2 was not detected in the GST-Casp9$^{1-130}$-inhibited apoptosome (Figure 3.2.5, lane 12)

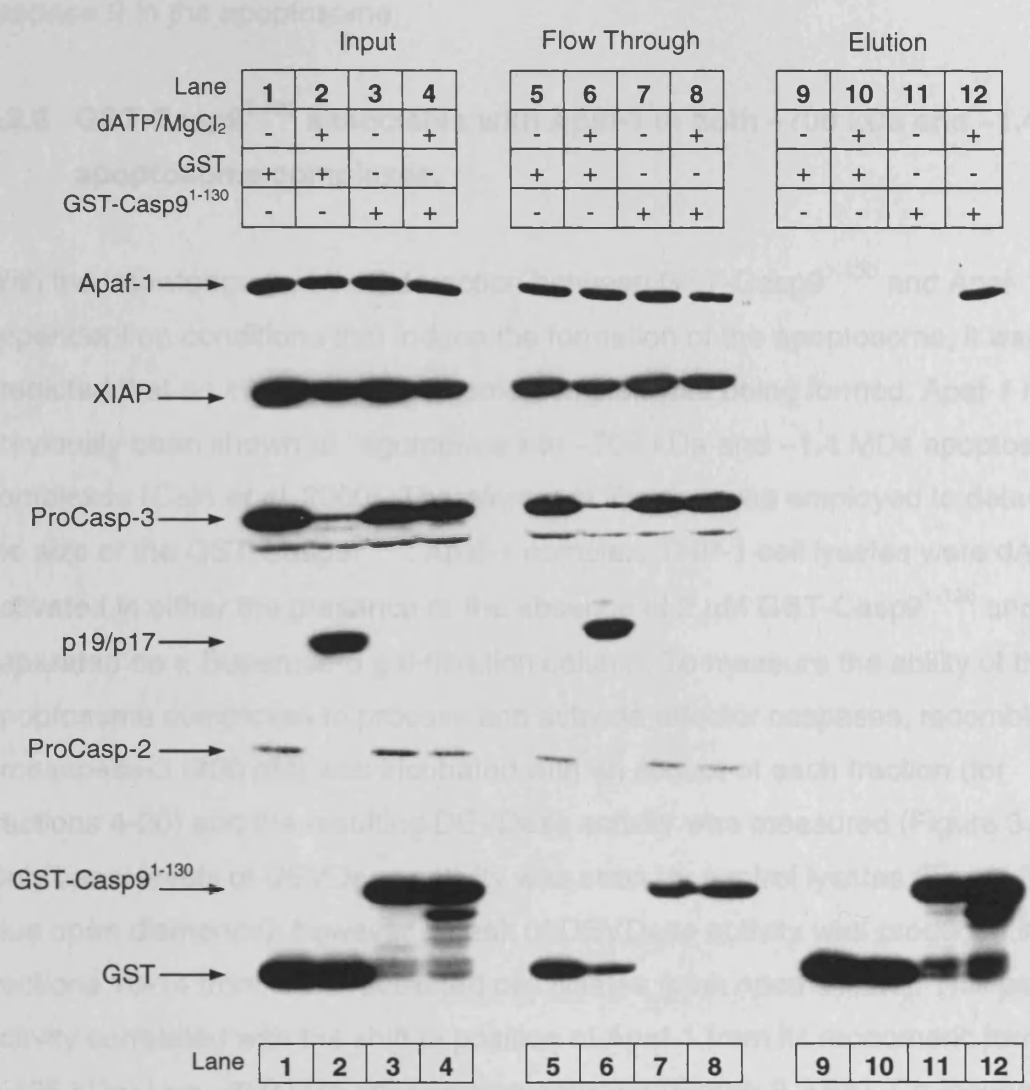

Figure 3.2.5: GST-Casp9$^{1-130}$ binding to Apaf-1 is dATP dependent and does not result in the recruitment of XIAP, caspase-3 or caspase-2. THP-1 lysate (10 mg/ml) was activated with 2 mM dATP and 2 μM GST (lanes 1 & 2) or 2 μM GST-Casp9$^{1-130}$ (lanes 3 & 4) as described previously. The lysates were then incubated with GSH-Sepharose beads (100 μl) for 1 h at 4 °C and the beads harvested by centrifugation. The flow through was collected and the beads washed in cold PBS before being eluted with 20 mM glutathione (50 μl). The lysates (input), flow though and eluates were analysed by SDS-PAGE/Western blotting for Apaf-1, XIAP, caspase-3, caspase-2 and GST (as described previously).

and therefore also does not directly associate with Apaf-1 or the CARD domain of caspase-9 in the apoptosome.

3.2.6 GST-Casp9$^{1-130}$ associates with Apaf-1 in both ~700 kDa and ~1.4 MDa apoptosome complexes.

With the knowledge that the interaction between GST-Casp9$^{1-130}$ and Apaf-1 was dependent on conditions that induce the formation of the apoptosome, it was predicted that an inhibited apoptosome complex was being formed. Apaf-1 has previously been shown to oligomerise into ~700 kDa and ~1.4 MDa apoptosome complexes (Cain *et al*, 2000). Therefore, gel filtration was employed to determine the size of the GST-Casp9$^{1-130}$: Apaf-1 complex. THP-1 cell lysates were dATP-activated in either the presence or the absence of 2 μM GST-Casp9$^{1-130}$ and separated on a Superose-6 gel-filtration column. To measure the ability of the apoptosome complexes to process and activate effector caspases, recombinant procaspase-3 (200 nM) was incubated with an aliquot of each fraction (for fractions 4-20) and the resulting DEVDase activity was measured (Figure 3.2.6A). Only basal levels of DEVDase activity was seen for control lysates (Figure 3.2.6A, blue open diamonds), however a peak of DEVDase activity was produced in fractions 10-14 from dATP-activated cell lysates (pink open circles). This peak of activity correlated with the shift in position of Apaf-1 from its monomeric form (~135 kDa) to a ~700 kDa apoptosome complex (Figure 3.2.6B). Co-incubation of GST-Casp9$^{1-130}$ in dATP-activated lysates resulted in an abrogation of the DEVDase activity in these fractions (Figure 3.2.6, pink closed circles) despite the same shift in the Apaf-1 elution profile being observed (Figure 3.2.6B). Furthermore, GST-Casp9$^{1-130}$ was seen to elute predominately in fractions 18-23 in control activated lysates, however in the presence of dATP a significant shift of GST-Casp9$^{1-130}$ was detected to fractions 5-7 (~1.4 MDa) and to a lesser extent to fractions 10-14 (~700 kDa) (Figure 3.2.6B). These data suggest that Apaf-1 and GST-Casp9$^{1-130}$ are associating in a higher molecular weight complex.

The fractions corresponding to the ~1.4 MDa and ~700 kDa apoptosome complexes were then pooled, concentrated and purified with GSH-Sepharose beads. Each step of the purification was analysed for Apaf-1 and GST-Casp9$^{1-130}$ by SDS-PAGE and immunoblotting (Figure 3.2.7). The resulting purifications

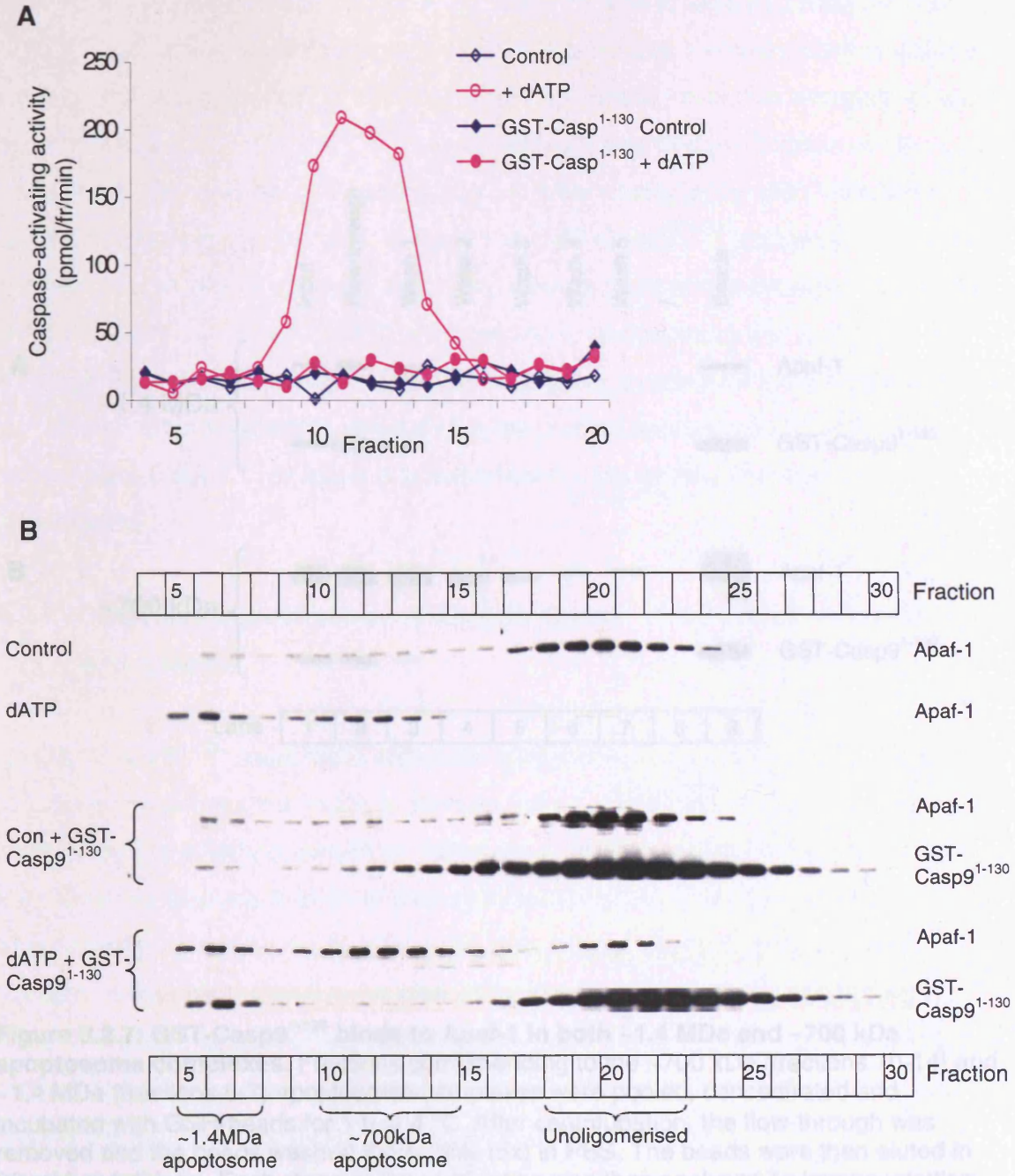

Figure 3.2.6: GST-Casp9$^{1-130}$ associates with Apaf-1 in the ~700 kDa and ~1.4 MDa apoptosome complexes. THP-1 lysates (15 mg/ml) were activated with 2 mM dATP for 1 h at 37 °C plus or minus 2 μM GST-Casp9$^{1-130}$. The lysates were then separated by Superose-6 gel filtration chromatography. Fractions were then assayed for their ability to activate procaspase-3 (**A**) as described in Materials and Methods, and analysed by SDS-PAGE/Western blotting for Apaf-1 and GST-Casp9$^{1-130}$ (**B**).

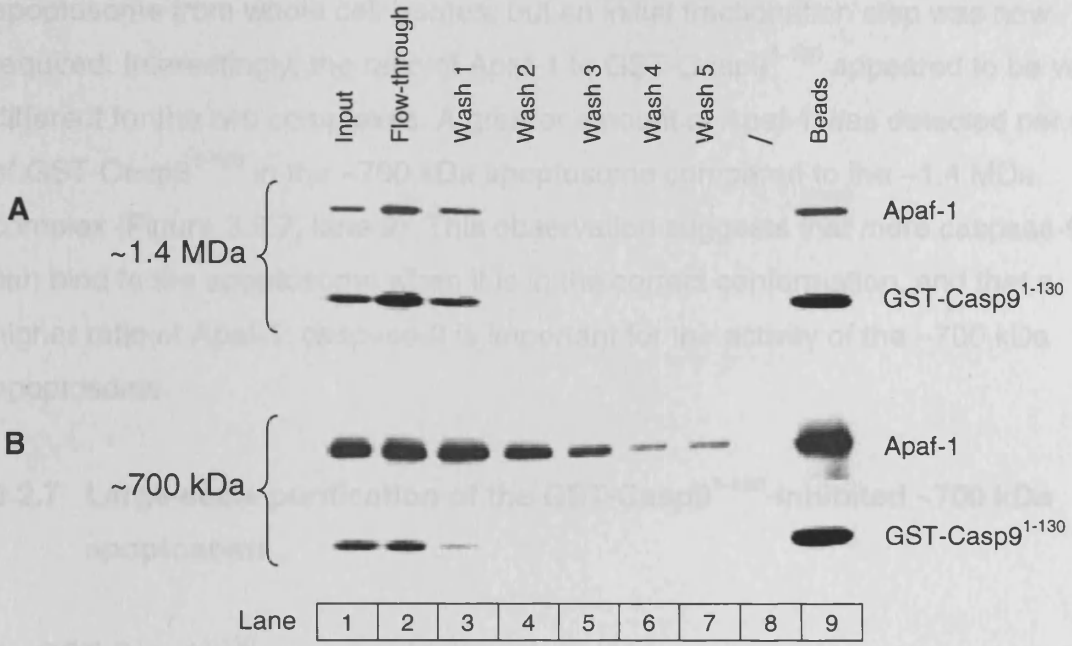

Figure 3.2.7: GST-Casp9$^{1-130}$ binds to Apaf-1 in both ~1.4 MDa and ~700 kDa apoptosome complexes. Fractions corresponding to the ~700 kDa (fractions 10-14) and ~1.4 MDa (fractions 5-7) apoptosome complexes were pooled, concentrated and incubated with GSH-beads for 1 h at 4 °C. After centrifugation, the flow-through was removed and the beads washed thoroughly (5x) in PBS. The beads were then eluted in 20 mM glutathione. Each stage of the purification was then analysed by immunoblotting for Apaf-1 and GST-Casp9$^{1-130}$ (**A** and **B**).

revealed that GST-Casp9$^{1-130}$ was capable of capturing both the ~1.4 MDa and the ~700 kDa apoptosome complexes (Figure 3.2.7A and B, lane 9). However, the ~700 kDa apoptosome complex is the only form of Apaf-1 oligomerisation able to sustain caspase activation (Cain *et al*, 2000) and ideally only this complex would have contained GST-Casp9$^{1-130}$. This would have enabled purification of the apoptosome from whole cell lysates, but an initial fractionation step was now required. Interestingly, the ratio of Apaf-1 to GST-Casp9$^{1-130}$ appeared to be very different for the two complexes. A greater amount of Apaf-1 was detected per mol of GST-Casp9$^{1-130}$ in the ~700 kDa apoptosome compared to the ~1.4 MDa complex (Figure 3.2.7, lane 9). This observation suggests that more caspase-9 can bind to the apoptosome when it is in the correct conformation, and that a higher ratio of Apaf-1: caspase-9 is important for the activity of the ~700 kDa apoptosome.

3.2.7 Large-scale purification of the GST-Casp9$^{1-130}$-inhibited ~700 kDa apoptosome.

As GST-Casp9$^{1-130}$ associated with both apoptosome complexes it was necessary to initially fractionate the lysate to remove the ~1.4 MDa apoptosome before performing the affinity purification. However, in order to obtain sufficient material for proteomic analysis it was necessary to scale-up the GSH-bead capture experiments. As only 3 mg of lysate could be separated by Superose-6 gel-filtration, it was clear that this needed to be increased by a factor of ten to get within the range of MALDI MS identification. I therefore decided to use a method of protein complex separation which employed a sucrose-density gradient to initially isolate the ~700 kDa apoptosome complex (Cain *et al*, 1999).

THP-1 cell lysates (15 mg/ml) were dATP-activated in the presence or absence of GST-Casp9$^{1-130}$ for 1 h. The lysates were then layered onto a continuous 10-35% sucrose gradient, the linearity of which was determined by refractometry (Figure 3.2.8A) and centrifuged at 25,000 rpm for 17 h. Under these conditions the ~700 kDa apoptosome is known to co-elute with the 20 S proteasome which has chymotrypsin-like (LLVYase) activity (Cain *et al*, 1999). Therefore, a fluorescent measure of LLVYase activity was used to screen the fractions to identify the location of the ~700 kDa apoptosome complex (data not shown). The fractions

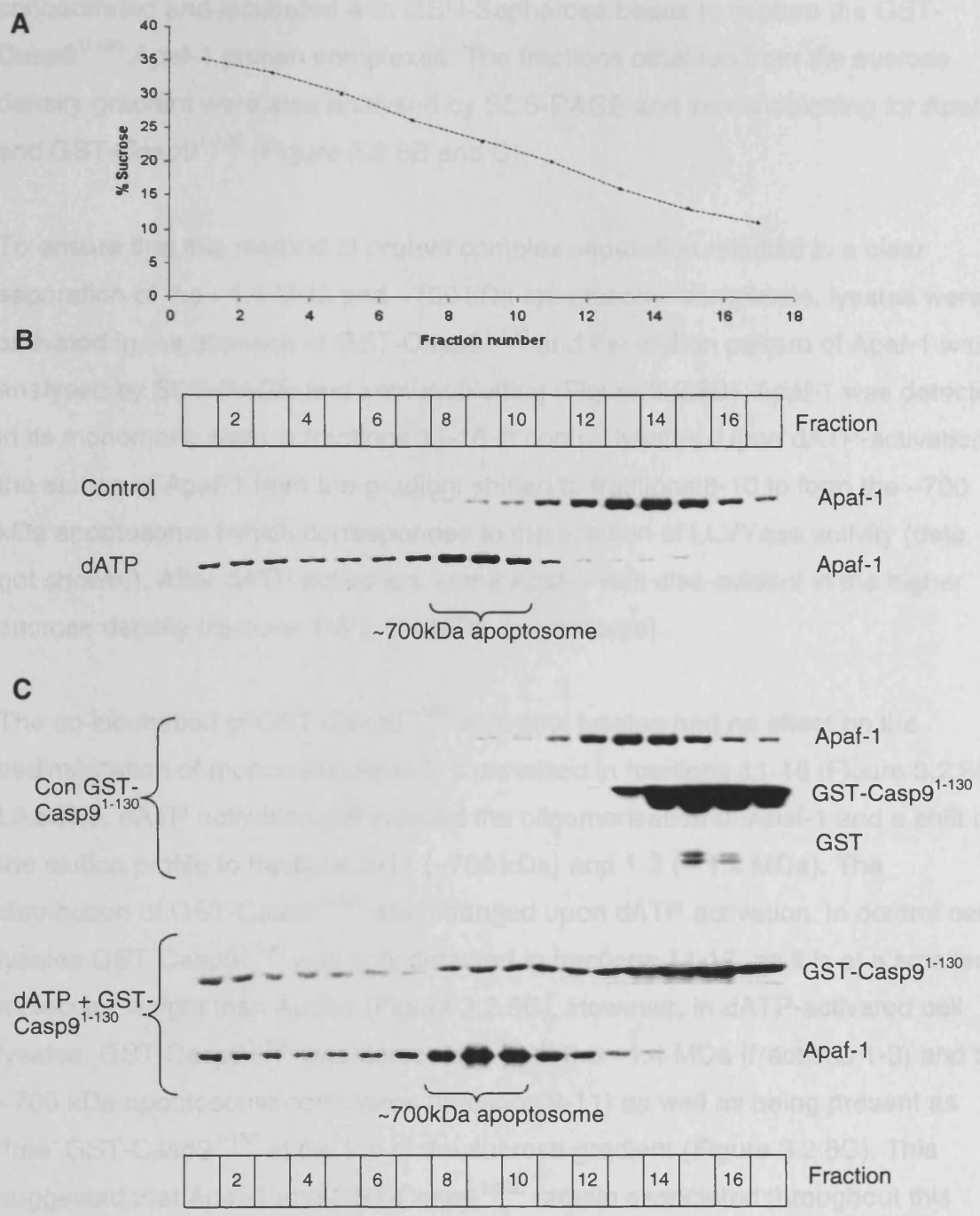

Figure 3.2.8: Apaf-1 and GST-Casp9$^{1-130}$ co-elute from a sucrose density gradient in dATP activated THP-1 cell lysates. Continuous sucrose density gradients were prepared and the linearity of the gradient was measured by refractometry following centrifugation (**A**). THP-1 lysates (15 mg/ml) were activated with 2 mM dATP in the absence or presence of 2 µM GST-Casp9$^{1-130}$ (**B** and **C**, respectively) for 1 h at 37 °C. Lysates were layered onto a 10-35% sucrose gradient and centrifuged at 25,000 rpm for 17 h. The fractionated gradients were analysed for LLVYase activity (data not shown) and immunoblotted for Apaf-1 and GST-Casp9$^{1-130}$.

corresponding to the ~700 kDa apoptosome complex were then pooled, concentrated and incubated with GSH-Sepharose beads to capture the GST-Casp9$^{1-130}$:Apaf-1 protein complexes. The fractions obtained from the sucrose density gradient were also analysed by SDS-PAGE and immunoblotting for Apaf-1 and GST-Casp9$^{1-130}$ (Figure 3.2.8B and C).

To ensure that this method of protein complex separation resulted in a clear separation of the ~1.4 MDa and ~700 kDa apoptosome complexes, lysates were activated in the absence of GST-Casp9$^{1-130}$ and the elution pattern of Apaf-1 was analysed by SDS-PAGE and immunoblotting (Figure 3.2.8B). Apaf-1 was detected in its monomeric state in fractions 11-16 in control lysates. Upon dATP-activation, the elution of Apaf-1 from the gradient shifted to fractions 8-10 to form the ~700 kDa apoptosome (which corresponded to the position of LLVYase activity (data not shown)). After dATP activation, some Apaf-1 was also evident in the higher sucrose density fractions 1-3 (~1.4 MDa apoptosome).

The co-incubation of GST-Casp9$^{1-130}$ in control lysates had no effect on the sedimentation of monomeric Apaf-1; it remained in fractions 11-16 (Figure 3.2.8C). Likewise, dATP activation still induced the oligomerisation of Apaf-1 and a shift in the elution profile to fractions 8-11 (~700 kDa) and 1-3 (~ 1.4 MDa). The distribution of GST-Casp9$^{1-130}$ also changed upon dATP activation. In control cell lysates GST-Casp9$^{1-130}$ was only detected in fractions 11-17, as it is of a smaller molecular weight than Apaf-1 (Figure 3.2.8C). However, in dATP-activated cell lysates, GST-Casp9$^{1-130}$ was detected in both the ~1.4 MDa (fractions 1-3) and the ~700 kDa apoptosome complexes (fractions 9-11) as well as being present as 'free' GST-Casp9$^{1-130}$ at the top of the sucrose gradient (Figure 3.2.8C). This suggested that Apaf-1 and GST-Casp9$^{1-130}$ remain associated throughout this initial purification stage.

In order to prevent contamination of the ~700 kDa apoptosome sample with other GST-Casp9$^{1-130}$-containing complexes, only fractions 8-10 were pooled and concentrated before capturing the apoptosome on GSH-Sepharose beads. The beads were subsequently washed thoroughly and eluted in SDS sample buffer prior to SDS-PAGE and immunoblotting analysis (Figure 3.2.9A). In control lysates a small amount of Apaf-1 was detected in the concentrated fractions, however this

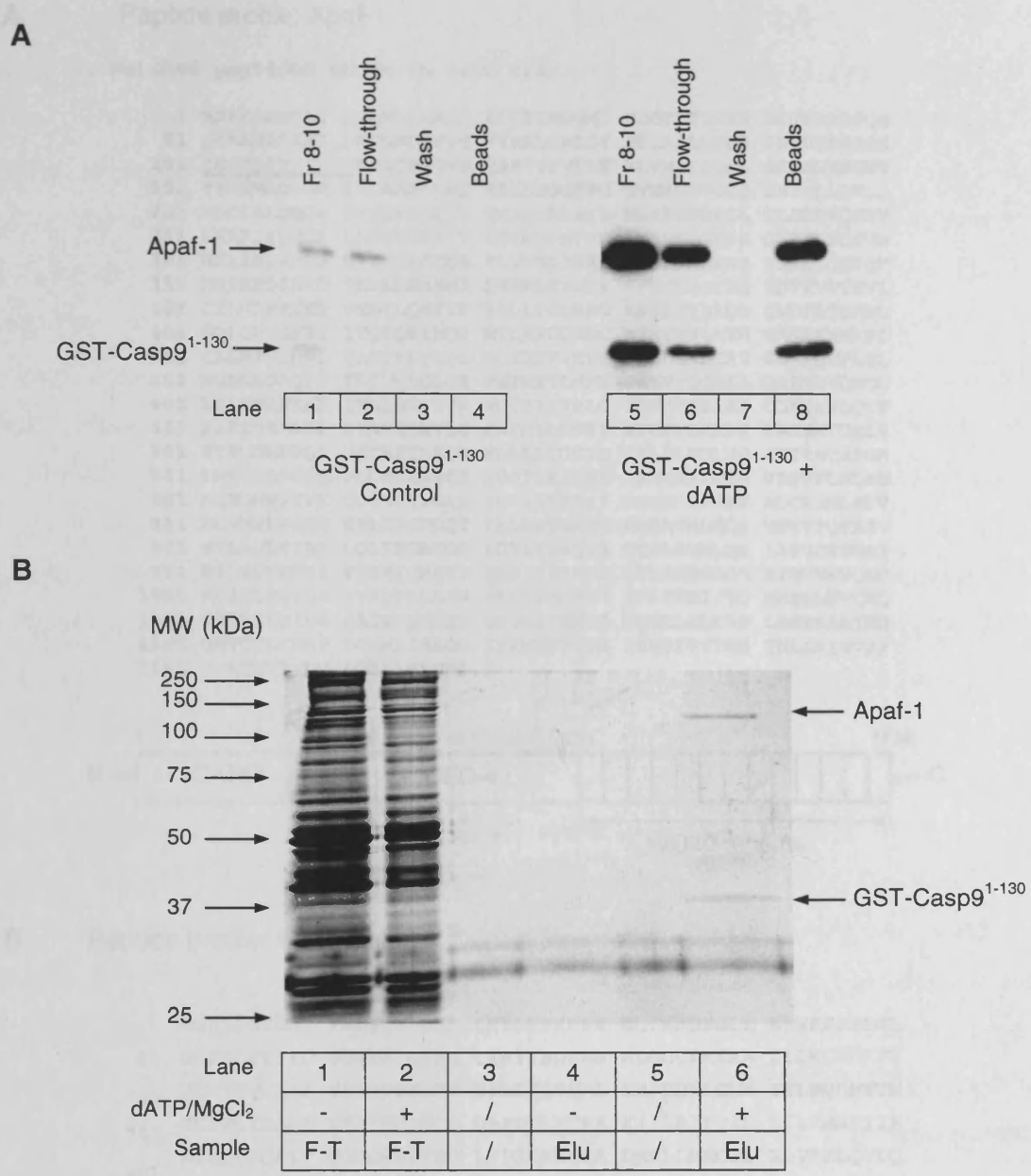

Figure 3.2.9: Only GST-Casp9$^{1-130}$ and Apaf-1 can be detected in the purified GST-Casp91-130-inhibited ~700 kDa apoptosome. Fractions from the sucrose density gradients which correspond to the ~700 kDa apoptosome (fractions 8-10, see Figure 3.2.8) were pooled, concentrated and incubated with GSH-Sepharose beads for 1 h at 4 °C. After centrifugation the flow-through was removed and the beads washed in cold PBS (4x). The beads were then resuspended in 2x SDS loading buffer, heated at 50 °C for 30 min and centrifuged to pellet the beads. The input, flow-through, final wash and eluate were then analysed by SDS-PAGE/Western blotting for Apaf-1 and GST-Casp9$^{1-130}$ (**A**). The flow-through and elution samples were also separated by SDS-PAGE prior to silver staining to detect any other possible binding proteins (**B**).

A Peptide profile: Apaf-1

Matched peptides shown in **Bold Red**

```
   1 MDAKARNCLL QHREALEKDI KTSYIMDHMI SDGFLTISEE EKVRNEPTQQ
  51 QRAAMLIKMI LKKDNDSYVS FYNALLHEGY KDLAALLHDG IPVVSSSSGK
 101 DSVSGITSYV RTVLCEGGVP QRPVVFVTRK KLVNAIQQKL SKLKGEPGWV
 151 TIHGMAGCGK SVLAAEAVRD HSLLEGCFPG GVHWVSVGKQ DKSGLLMKLQ
 201 NLCTRLDQDE SFSQRLPLNI EEAKDRLRIL MLRKHPRSLL ILDDVWDSWV
 251 LKAFDSQCQI LLTTRDKSVT DSVMGPKYVV PVESSLGKEK GLEILSLFVN
 301 MKKADLPEQA HSIIKECKGS PLVVSLIGAL LRDFPNRWEY YLKQLQNKQF
 351 KRIRKSSSYD YEALDEAMSI SVEMLREDIK DYYTDLSILQ KDVKVPTKVL
 401 CILWDMETEE VEDILQEFVN KSLLFCDRNG KSFRYYLHDL QVDFLTEKNC
 451 SQLQDLHKKI ITQFQRYHQP HTLSPDQEDC MYWYNFLAYH MASAKMHKEL
 501 CALMFSLDWI KAKTELVGPA HLIHEFVEYR HILDEKDCAV SENFQEFLSL
 551 NGHLLGRQPF PNIVQLGLCE PETSETLGFE SKKVYQQAKL QAKQEVDNGM
 601 LYLEWINKKN ITNLSRLVVR PHTDAVYHAC FSEDGQRIAS CGADKTLQVF
 651 KAETGEKLLE IKAHEDEVLC CAFSTDDRFI ATCSVDKKVK IWNSMTGELV
 701 HTYDEHSEQV NCCHFTNSSH HLLLATGSSD CFLKLWDLNQ KECRNTMFGH
 751 TNSVNHCRFS PDDKLLASCS ADGTLKLWDA TSANERKSIN VKQFFLNLED
 801 PQEDMEVIVK CCSWSADGAR IMVAAKNKIF LWNTDSRSKV ADCRGHLSWV
 851 HGVMFSPDGS SFLTSSDDQT IRLWETKKVC KNSAVMLKQE VDVVFQENEV
 901 MVLAVDHIRR LQLINGRTGQ IDYLTEAQVS CCCLSPHLQY IAFGDENGAI
 951 EILELVNNRI FQSRFQHKKT VWRIQFTADE KTLISSSDDA EIQVWNWQLD
1001 KCIFLRGHQE TVKDFRLLKN PRLLSWSFDG TVKVWNIITG NKEKDFVCHQ
1051 GTVLSCDISH DATKFSSTSA DKTAKIWNVS NGELLHLCAP LSEEGAATHG
1101 GWVTDLCFSP DGKMLISAGG YIKWWNVVTG ESSQTFYTNG TNLKKIHVSP
1151 DFKTYVTVDN LGILYILQTL E
```

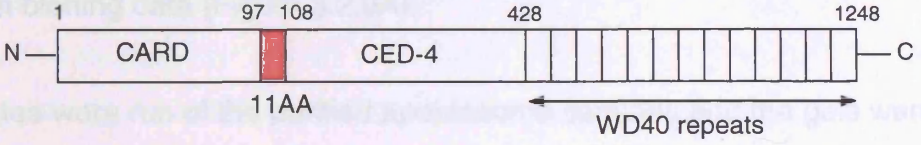

B Peptide profile: GST-Casp9$^{1-130}$

```
   1 MSPILGYWKI KGLVQPTRLL LEYLEEKYEE HLYERDEGDK WRNKKFELGL
  51 EFPNLPYYID GDVKLTQSMA IIRYIADKHN MLGGCPKERA EISMLEGAVL
 101 DIRYGVSRIA YSKDFETLKV DFLSKLPEML KMFEDRLCHK TYLNGDHVTH
 151 PDFMLYDALD VVLYMDPMCL DAFPKLVCFK KRIEAIPQID KYLKSSKYIA
 201 WPLQGWQATF GGGDHPPKSD LVPRGSMDEA DRRLLRRCRL RLVEELQVDQ
 251 LWDALLSSEL FRPHMIEDIQ RAGSGSRRDQ ARQLIIDLET RGSQALPLFI
 301 SCLEDTGQDM LASFLRTNRQ AAKLSKPTLE NLTPVVLRPE IRKPEVLRPE
 351 TPRPVD
```

Figure 3.2.10: MALDI-TOF identification of Apaf-1$_{XL}$ and GST-Casp9$^{1-130}$ in the GST-Casp9$^{1-130}$-tagged ~700 kDa apoptosome. Gel plugs were excised from the SYPRO Ruby stained gels corresponding to the silver-stained bands (Figure 3.2.9) and trypsin digested. MALDI-Tof analysis was then carried out and the peptide masses entered into MASCOT. Matched peptides are shown in red, with Apaf-1$_{XL}$ matching 24 mass values with predicted peptides, giving 29% coverage of the sequence (**A**). The sequence of GST-Casp9$^{1-130}$ and the digested peptide masses were entered into MASCOT and matched 3 out the potential 5 peptides in the CARD domain of the protein, with 16% coverage (**B**). In addition, a repeat of this experiment resulted in the identification of GST from the peptide sequence data (data not shown).

was not detected in the bead eluate (Figure 3.2.9A, lanes 1-4). In contrast, the concentrated fractions from the dATP-activated lysate contained considerable quantities of Apaf-1 and GST-Casp9$^{1-130}$ (Figure 3.2.9A, lane 5). Significantly, both Apaf-1 and GST-Casp9$^{1-130}$ eluted from the GSH-Sepharose beads, which suggests that they are associated (Figure 3.2.9A, lane 8). The purified apoptosome samples were further analysed by SDS-PAGE followed by silver staining to identify the presence of any unknown proteins (Figure 3.2.9B). The large number of bands that were present in the flow-through indicates that there were a large number of proteins still present in the fractions after the initial sucrose fractionation step (Figure 3.2.9B, lanes 1 & 2). In the bead eluate from the control lysate, two bands were detected between 25-30 kDa (Figure 3.2.9B, lane 4), which also appeared in the blank lanes (3 & 5) and hence were considered to be non-specific contaminants. In addition to these two bands, two more predominant bands were detected. The bands correspond to proteins of ~130 kDa and ~37 kDa, and were predicted to be Apaf-1 and GST-Casp9$^{1-130}$ due to the previous Western blotting data (Figure 3.2.9A).

Duplicates were run of the purified apoptosome samples and the gels were stained with SYPRO-Ruby to enable mass spectrometry analysis. The two previously detected bands were excised and their protein sequence mapped (Figure 3.2.10). The band at ~130 kDa was revealed to be Apaf-1 (Mowse score of 91, 29% coverage). In fact, the Apaf-1$_{XL}$ splice form was detected as confirmed by the presence of the 11 amino acid insert between the CARD and CED4 domains (underlined in Figure 3.2.10A) detected by mass spectrometry. The band predicted to be GST-Casp9$^{1-130}$ was not categorically proven to be the fusion protein. However, peptides extracted from this band did match 3 out of the 5 possible peptides produced by trypsin-digest of the CARD domain, and 2 peptides matched in the GST domain (Figure 3.2.10B). Furthermore, a repeat of this experiment did give a positive identification for *Schistosoma japonicum* GST, the type of GST only used for affinity-tagging bait proteins (data not shown).

3.2.8 In SMAC/Omi-reduced cell lysates, the native apoptosome additionally recruits XIAP and caspase-3.

Having concluded that the GST-Casp9$^{1-130}$-inhibited apoptosome only contains Apaf-1 and GST-Casp9$^{1-130}$, the capture of the native apoptosome via an antibody to caspase-9 was then investigated. This would not only allow confirmation that no other proteins are directly associating with Apaf-1 or the CARD domain of caspase-9, but could also allow the identification of other proteins binding to the apoptosome via the large and small subunits of caspase-9.

Initial experiments (performed by D.G. Brown) showed that the antibody was only able to capture Apaf-1 via its interaction with caspase-9, in the presence of dATP and cytochrome *c* (data not shown, Twiddy *et al*, 2004). This approach also confirmed that in freeze/thawed cell lysates the ~700 kDa apoptosome only contains Apaf-1 and caspase-9 (p35, p34) (data not shown, Twiddy *et al*, 2004). This experiment mimics what is thought to occur in the formation of an apoptosome in an apoptotic cell, following the release of pro-apoptotic proteins from the mitochondria into the cytosol (Salvesen & Duckett, 2002).

Previous studies have suggested that XIAP can bind to and modulate the apoptosome via its interactions with caspase-9 and caspase-3 (Bratton *et al*, 2001b). However with the sequestering nature of SMAC and Omi, it was predicted that XIAP would not be present in an apoptosome from freeze/thawed cell lysates. Therefore the Dig/Hom method of cell disruption was again employed, where the integrity of the mitochondria is preserved and thus cytochrome *c*, SMAC and Omi are removed from the lysate (Figure 3.2.12A).

The time and dATP/cytochrome *c*-dependent capture of the native apoptosome under reduced SMAC and Omi conditions, revealed that in addition to Apaf-1 and caspase-9, XIAP and caspase-3 were also associated with the complex (Figure 3.2.11). As XIAP could not be sequestered by the pro-apoptotic molecules, SMAC and Omi, it was free to bind to and modulate the activity of the apoptosome, with a reduced level of DEVDase activity detected in dATP-activated cell lysates (data not shown, Twiddy *et al*, 2004). Cytochrome *c* was also detected briefly in the apoptosome; presumably because it is only required for inducing the initial

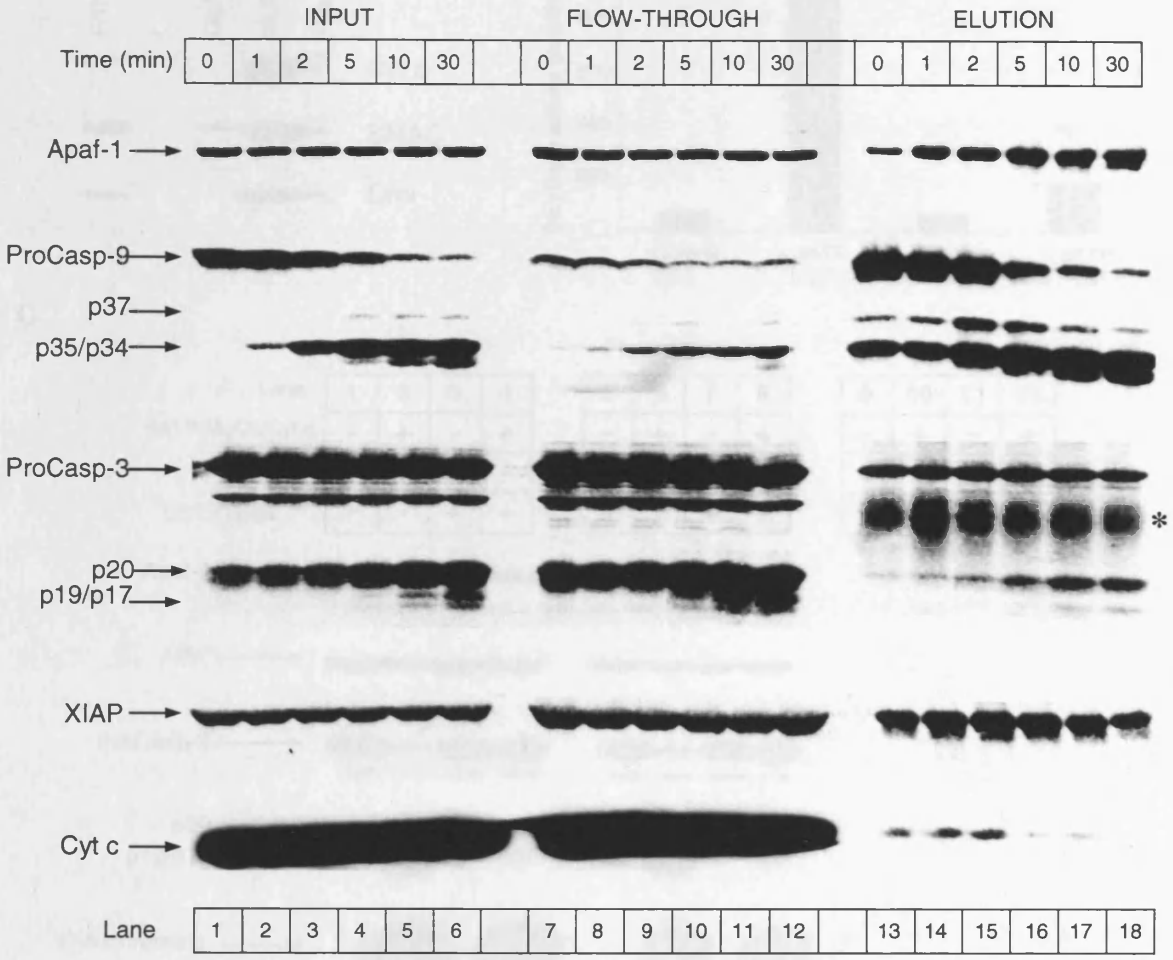

Figure 3.2.11: In THP-1 cell lysates with reduced SMAC and Omi/HtrA2, XIAP and caspase-3 are recruited to the apoptosome, in addition to Apaf-1, caspase-9 and cytochrome *c*. THP-1 Dig/Hom cell lysates (10 mg/ml) were activated in the presence of dATP and cytochrome *c* for the allotted time periods. The zero time point included dATP and cytochrome *c* but was immediately put on ice. The sample was then treated with 200 μM zVAD.FMK and a sample taken (input), before incubation at 4 °C overnight with anti-caspase-9 antibody cross-linked to protein G Dyna-beads. The beads were then removed from the supernatant (flow-through), washed thoroughly and eluted in SDS-sample buffer (elution). The input, flow-through and elution samples were separated by SDS-PAGE electrophoresis and immunoblotted for Apaf-1, caspase-9, caspase-3, XIAP and cytochrome *c*. The asterisk marks the IgG1 light chain which is carried over into the elution. The heavy chain remains covalently bound to the beads due to the cross-linking procedure. (Performed by D. G. Brown, published in Twiddy *et al*, 2004).

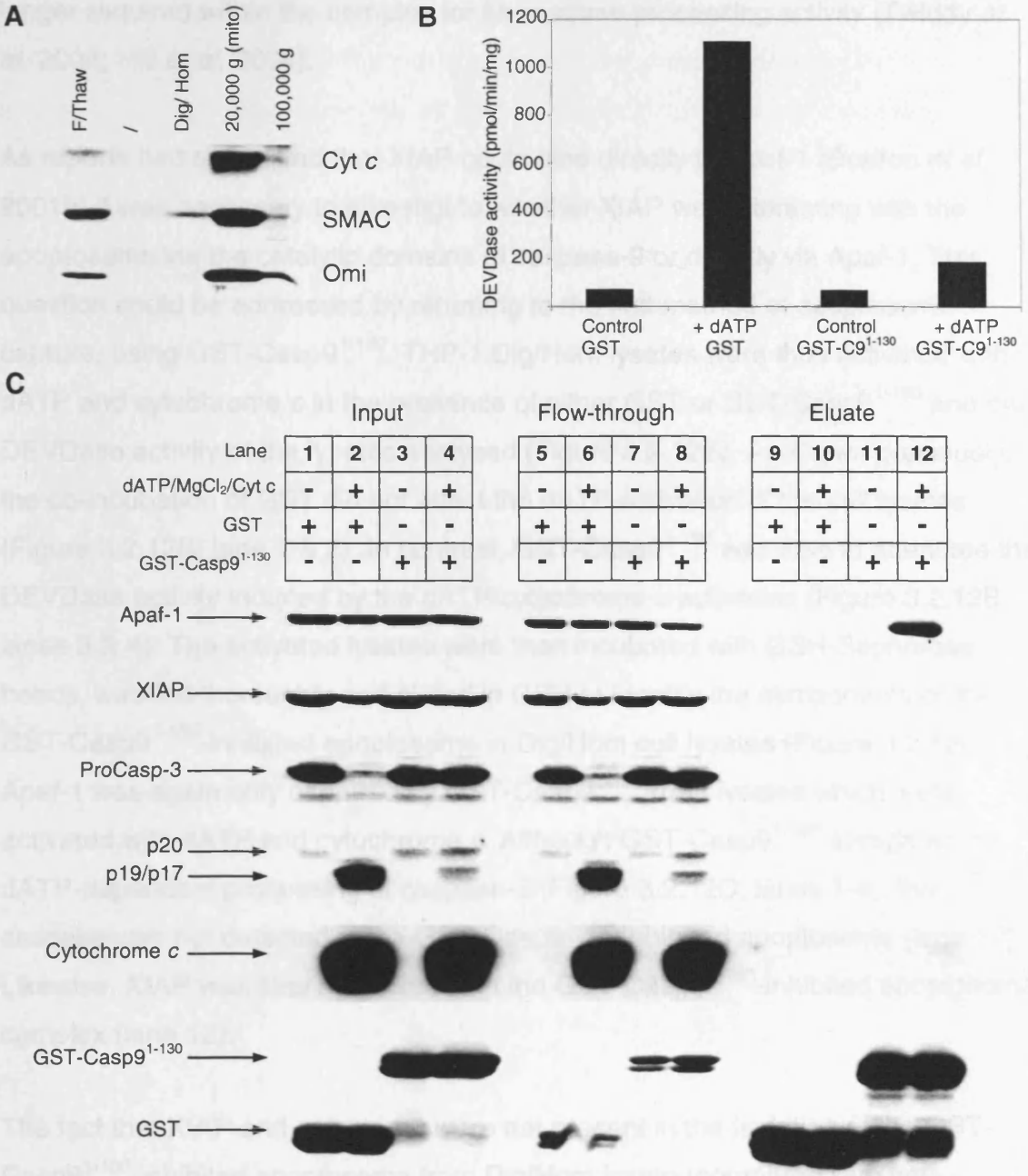

Figure 3.2.12: In SMAC/Omi reduced cell lysate, the GST-Casp9$^{1-130}$-inhibited apoptosome only contains Apaf-1, GST-Casp9$^{1-130}$ and cytochrome *c*. A comparison of the cytochrome *c*, SMAC and Omi content between Freeze-Thawed (F/Thaw) and Dig/Hom cell lysate at the centrifugational stages of their preparation. The membrane pellets were sonicated and 20 µg protein/lane loaded of lysate and membrane (**A**). THP-1 Dig/Hom lysate (10 mg/ml) was activated with 2 mM dATP and 1.7 µM cytochrome *c* in the presence of 2 µM GST or 2 µM GST-Casp9$^{1-130}$ and incubated for 30 min at 37 °C. an aliquot (10 µl) was then assayed for DEVDase activity (expressed in pmol/min/mg, **B**). The remaining sample was then incubated with GSH-Sepharose beads for 1 h at 4 °C. The beads were then washed and eluted as described previously. The input (20 µg), flow-through and elution samples were then mixed with SDS sample buffer and analysed by SDS-PAGE/Western blotting for Apaf-1, XIAP, caspase-3, cytochrome *c* and GST-Casp9$^{1-130}$ (**C**).

conformational change in Apaf-1 which allows caspase-9 to bind, and then is no longer required within the complex for its caspase-processing activity (Twiddy *et al*, 2004; Hill *et al*, 2004).

As reports had suggested that XIAP could bind directly to Apaf-1 (Bratton *et al*, 2001b) it was necessary to investigate whether XIAP was interacting with the apoptosome via the catalytic domains of caspase-9 or directly via Apaf-1. This question could be addressed by returning to the first method of apoptosome capture, using GST-Casp9$^{1-130}$. THP-1 Dig/Hom lysates were thus activated with dATP and cytochrome *c* in the presence of either GST or GST-Casp9$^{1-130}$ and the DEVDase activity of the lysates analysed (Figure 3.2.12B). As shown previously, the co-incubation of GST did not affect the dATP-activation of the cell lysates (Figure 3.2.12B, lane 1 & 2). In contrast, GST-Casp9$^{1-130}$ was able to attenuate the DEVDase activity induced by the dATP/cytochrome *c*-activation (Figure 3.2.12B, lanes 3 & 4). The activated lysates were then incubated with GSH-Sepharose beads, washed thoroughly and eluted in GSH to identify the components of the GST-Casp9$^{1-130}$-inhibited apoptosome in Dig/Hom cell lysates (Figure 3.2.12C). Apaf-1 was again only captured by GST-Casp9$^{1-130}$ from lysates which were activated with dATP and cytochrome *c*. Although GST-Casp9$^{1-130}$ abrogated the dATP-dependent processing of caspase-3 (Figure 3.2.12C, lanes 1-4), this caspase was not detected in the GST-Casp9$^{1-130}$-inhibited apoptosome (lane 12). Likewise, XIAP was also not eluted with the GST-Casp9$^{1-130}$-inhibited apoptosome complex (lane 12).

The fact that XIAP and caspase-3 were not present in the isolation of the GST-Casp9$^{1-130}$-inhibited apoptosome from Dig/Hom lysate (compared with anti-caspase-9 immunoprecipitation) confirms that a full-length caspase-9 molecule needs to be present in order for XIAP to bind to the apoptosome. Subsequently, caspase-3 can be recruited to the apoptosome via caspase-9 and its association with this complex is stabilised by XIAP. This inhibitor of apoptosis has the ability to bind to both caspase-9 and caspase-3 simultaneously through interactions with the BIR3 and BIR1/2 domains of XIAP, respectively (Reviewed in Fesik & Shi, 2001). The sequestering nature of the pro-apoptotic proteins, SMAC and Omi, is responsible for the presence or absence of XIAP in the apoptosome (Figure 3.2.13). In apoptotic cells, SMAC and Omi are released from the mitochondria and

can sequester XIAP; therefore in their presence XIAP can have only a minor role in apoptosome modulation. However, if cytochrome *c* is inappropriately released, XIAP can prevent the activation and activity of caspases at the level of the apoptosome. This regulation has also been demonstrated by the restoration of activity following the addition of recombinant SMAC to the XIAP-modulated apoptosome (Twiddy *et al*, 2004).

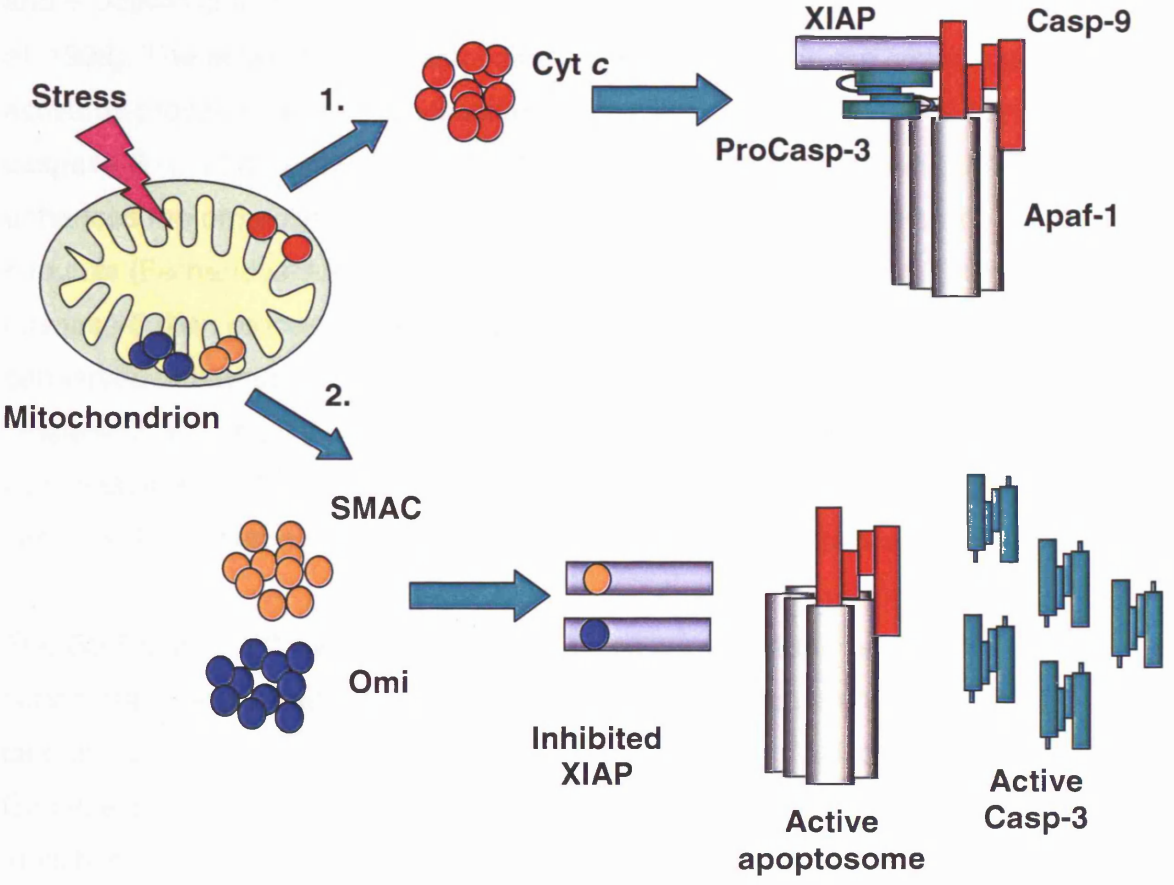

Figure 3.2.13: Schematic of factors which may determine the presence or absence of caspase-3 and XIAP in the apoptosome. With the initial release of cytochrome c from the mitochondria, Apaf-1 is able to oligomerise and recruit caspase-9 to the apoptosome. In the absence of SMAC and Omi/HtrA2, XIAP can bind to caspase-9 (via the BIR3 domain) and to caspase-3 (via the linker and BIR2 domain), thus stabilising the interaction between caspase-3 and the apoptosome (1). With the subsequent release of SMAC and Omi, XIAP is sequestered, allowing caspase-3 to be processed and released from the apoptosome (2).

3.3 Discussion

In a viable cell, Apaf-1 oligomerisation is usually prevented by the inhibitory conformation of the WD40 repeats (Adrain *et al*, 1999). Following its release from the mitochondria in apoptotic cells, cytochrome *c* binds to the WD40 repeats of Apaf-1 thereby altering their conformation (Adrain *et al*, 1999) and allowing oligomerisation of Apaf-1 to form an apoptosome (Saleh *et al*, 1999; Cain *et al*, 1999). Subsequently, caspase 9 binds to Apaf-1 via CARD:CARD interactions, and is activated and autocatalytic cleaved at Asp315 (Li *et al*, 1997; Srinivasula *et al*, 1998). The active apoptosome complex (Apaf-1/cytochrome *c*/caspase-9) activates procaspase-3 by processing at Asp175 to form the p20/p10 form of caspase-3 (Li *et al*, 1997; Slee *et al*, 1999). Autocatalytic processing then enhances the proteolytic activity of caspase-3, producing the p19 and p17 subunits (Fernandes-Alnemri *et al*, 1996; Han *et al*, 1997; Slee *et al*, 1999). Active caspase-3 then processes critical cellular substrates, via recognition of the conserved substrate sequence motif, DEVD (Thornberry *et al*, 1997). In addition, caspase-3 can amplify caspase activation by processing caspase-9 at Asp330 (Srinivasula *et al*, 1998), which produces the p37/p10 conformation, a form of caspase-9 that can no longer be inhibited by XIAP (Srinivasula *et al*, 2001).

The GST-Casp9$^{1-130}$ fusion protein used in the current study produced a concentration-dependent and a dATP/cytochrome *c*-dependent inhibition of the caspase-processing ability of the apoptosome complex. This demonstrated that GST-Casp9$^{1-130}$ is acting as a dominant negative inhibitor by competitively inhibiting caspase-9 binding to the apoptosome. This is in accordance with previous studies using a recombinant CARD domain of caspase-9 (Qin *et al*, 1999), and an endogenous caspase-9 inhibitor that lacks the large catalytic subunit of caspase-9 (caspase-9b, Seol & Billiar, 1999; Srinivasula *et al*, 1999). In addition, these data show that GST-Casp9$^{1-130}$ requires the same conformational change in Apaf-1 to permit binding of the CARD domains as endogenous caspase-9. These data support the theory that the CARD domain of Apaf-1 is not normally exposed, but that in the presence of dATP and cytochrome *c*, Apaf-1 then adopts a more open conformation and binds to GST-Casp9$^{1-130}$ (or endogenous caspase-9) via CARD:CARD interactions (Zou *et al*, 1999; Li *et al*, 1997). GST-Casp9$^{1-130}$ inhibited the processing of endogenous caspase-9 as

detected by the preservation of procaspase-9 (Figure 3.2.1). However, the presence/absence of processed caspase-9 subunits could not be detected due to the cross-reactivity of the Western blotting antibody. However, effector caspase activation (caspase-7 (data not shown) and caspase-3) was significantly attenuated in lysates with GST-Casp9$^{1-130}$. Furthermore, caspase-2 processing was inhibited, confirming that the cleavage of caspase-2 is dependent on the presence of Apaf-1, caspase-9, dATP and cytochrome *c*, and is in agreement with previous work (O'Reilly e*t al* 2002; Read *et al*, 2002).

Interestingly, GST-Casp9$^{1-130}$ only bound to Apaf-1 and inhibited caspase activation when incubated with the lysate at or before the time of dATP-activation, and was ineffective if added after dATP-activation. This questioned whether caspase-9 is released from the apoptosome after processing (Zou *et al*, 1999; Cain *et al*, 1999). Furthermore, addition of excess exogenous caspase-9 did not displace GST-Casp9$^{1-130}$ from the apoptosome once it had formed (data not shown), and importantly the reverse was also true. A possible reason for this could be that once Apaf-1 has oligomerised into the apoptosome complex upon dATP activation and recruited and activated caspase-9, this apical caspase is then lost from the apoptosome, as demonstrated previously in our laboratory (Langlais, 2002). This is in accordance with data showing that procaspase-9 is recruited to the apoptosome and is subsequently released following autocatalytic cleavage (Zou *et al*, 1999; Saleh *et al*, 1999; Cain *et al*, 1999). Alternatively, the release of caspase-9 from the apoptosome could be mediated by cleavage of Apaf-1 by active caspase-3 (Bratton *et al*, 2001a). The incubation of GST-Casp9$^{1-130}$ during dATP-activation of cell lysates prevented the activation of effector caspases (due to the absence of the catalytic subunits), therefore Apaf-1 could not be cleaved and GST-Casp9$^{1-130}$ remained associated with the apoptosome.

Cytochrome *c* was detected in both the native and the GST-Casp9$^{1-130}$-inhibited apoptosome, following exogenous addition. However, cytochrome *c* was rapidly expelled from the native apoptosome, so that by 30 min there was no detectable cytochrome *c* present. This is in agreement with the work of Martin and colleagues, where cytochrome *c* was not detected in the native apoptosome isolated from Jurkat cell lysates (Hill *et al*, 2004), but is in contrast to the recombinant apoptosome, where cytochrome *c* is still reported to be associated

with the complex (Zou *et al*, 1999). However, the recombinant apoptosome characterised by Zou *et al*, was performed in the absence of caspase-9 and caspase-3. The transient association between cytochrome *c* and the native apoptosome could therefore be due to the presence of active caspases in the dATP-activated cell lysates. It is known that Apaf-1 is cleaved by effector caspases during apoptosis and that the resulting p84 fragment lacks the amino terminal 19 amino acids and regions of the WD40 domain (Lauber *et al*, 2001). It is therefore possible that this cleavage of Apaf-1 releases cytochrome *c* from the apoptosome. In accordance, the presence of cytochrome *c* in the GST-Casp9$^{1-130}$-inhibited apoptosome could therefore result from the fact that there are no active caspases to induce apoptosome cleavage and cytochrome *c* release. As the association between cytochrome *c* and the apoptosome appears to be only transient, it suggests that cytochrome *c* is only required to induce a conformational change in Apaf-1 to allow its correct oligomerisation, but is not essential for the activity of the apoptosome. Indeed, studies have shown that the subsequent re-addition of cytochrome *c* to the apoptosome does not enhance its caspase-activating activity (Saleh *et al*, 1999; Hill *et al*, 2004).

The ~700 kDa GST-Casp9$^{1-130}$-inhibited apoptosome only consisted of Apaf-1 and cytochrome *c*, which was in agreement with the composition of the native apoptosome isolated by immunoprecipitation with an anti-caspase-9 antibody. In contrast, when the native apoptosome was purified from lysates with reduced SMAC and Omi concentrations, caspase-3 and XIAP were also present. The presence of the p35 cleavage fragment of caspase-9 allowed XIAP to bind to the apoptosome (via the ATPF motif of caspase-9, Srinivasula *et al*, 2001) and also allowed XIAP to bind to caspase-3, and stabilise its interaction with the apoptosome (Bratton *et al*, 2001b; Hill *et al*, 2004). As these additional proteins were only seen when isolating the apoptosome using an antibody to caspase-9 (and not GST-Casp9$^{1-130}$), it can be concluded that these proteins were interacting via the large and small subunits of caspase-9. The absence of XIAP in the GST-Casp9$^{1-130}$-inhibited apoptosome also indirectly shows that active caspases were not present in this complex, as they would have been expected to recruit and bind to XIAP if they had been present. Previous work (Bratton *et al*, 2001b) has demonstrated that GST-XIAP can bind directly to Apaf-1 in a caspase-9-depleted lysate. However, it is possible that the immunodepletion of caspase-9 was not

complete in that study, and therefore any residual caspase-9 was still able to mediate the observed interaction between Apaf-1 and XIAP. In this current study it appears that either caspase-9 or caspase-3 are essential for XIAP binding, as the absence of these caspases in the eluted fractions corresponded with the absence of XIAP. However, one would predict that in an apoptotic cell, XIAP would not remain associated with the apoptosome after the release of the pro-apoptotic mitochondrial proteins SMAC and Omi (Figure 3.2.13).

In this study we used two distinct affinity approaches to purify the apoptosome and both strategies concluded that there are no other binding partners to the apoptosome other than Apaf-1, caspase-9 and cytochrome *c* (caspase-3 and XIAP were only present under conditions of low SMAC and Omi). Despite previous reports that proteins such as heat shock proteins (Beere *et al*, 2000; Saleh *et al*, 2000; Pandey *et al*, 2000), Bcl-2 family members (Pan *et al*, 1998a; Fang *et al*, 1998), PHAP and ProT (Jiang *et al*, 2003) interact with the apoptosome, none of these proteins were present in the native apoptosome isolated from THP-1 cell lysates (Twiddy *et al*, 2004) or from Jurkat cell lysates (Hill *et al*, 2004). Possible reasons for this discrepancy could be the use of over-expression of key proteins in the original studies, as opposed to the specific targeting of oligomerised Apaf-1 (the apoptosome) in the two recent reports. It was therefore concluded that although other proteins may be required for the formation of the apoptosome, no other proteins remain bound to the apoptosome and affect the caspase-activating activity of the apoptosome once it has been formed.

The fusion protein GST-Casp9$^{1-130}$ provides an invaluable tool in dissecting the cell death pathways. In addition to being used in this study to isolate apoptosome binding partners, it has subsequently been used to investigate the apoptosome in Bcr-Abl cells (Deming *et al*, 2004). The interaction between GST-Casp9$^{1-130}$ and Apaf-1 was significantly attenuated in Bcr-Abl cells compared with control cells and suggests a possible mechanism for the resistance of Bcr-Abl to cell death. Not only can GST-Casp9$^{1-130}$ be used to investigate the apoptosome, but it can also significantly inhibit the intrinsic pathway after mitochondrial perturbation (unlike Bcl-2 over-expression, which can only inhibit mitochondrial perturbation directly). GST-Casp9$^{1-130}$ can therefore be used to assess the role of other pro-apoptotic proteins in the absence of apoptosome-mediated effector caspase activation.

Chapter 4

Casp9$^{1-130}$-GTC Acts As A Dominant Negative Inhibitor In Apoptotic Cells

4.1 Introduction

The previous chapter demonstrated that the truncated caspase-9 fusion protein, GST-Casp9$^{1-130}$, acts as a dominant negative inhibitor, preventing apoptosome activity in THP-1, Jurkat and B-CLL cell lysates (Chapter 3). GST-Casp9$^{1-130}$ binds to Apaf-1 via CARD: CARD interactions, in a cytochrome *c* and dATP-dependent manner. This interaction prevents endogenous caspase-9 from binding to the apoptosome and cleaving downstream caspases. Having used this truncated and tagged protein to affinity-purify the apoptosome in cellular lysates it was concluded that only Apaf-1$_{XL}$ and GST-Casp9$^{1-130}$ were present in the GST-Casp9$^{1-130}$-inhibited apoptosome. Immunoprecipitation studies using an antibody to caspase-9 to isolate the native apoptosome confirmed this result (Twiddy *et al*, 2004). However, the apoptosome had a different composition when it was isolated from cell lysates with reduced levels of SMAC and Omi (prepared by Digitonin permeabilisation and homogenisation). In addition to Apaf-1 and caspase-9, the immunoprecipitated apoptosome then also contained XIAP, caspase-3 and cytochrome *c* (Chapter 3, Twiddy *et al*, 2004). Significantly, when GST-Casp9$^{1-130}$ was incubated in these lysates at the time of dATP activation, the affinity-purified apoptosome only contained Apaf-1, GST-Casp9$^{1-130}$ and cytochrome *c* (Chapter 3). Taken together, these results demonstrated that caspase-3 and XIAP were binding to the apoptosome complex via the large and small subunits of endogenous caspase-9 and were only present in the apoptosome in the absence of proapoptotic molecules such as SMAC and Omi. This observation was also subsequently independently confirmed in immunoprecipitation experiments of the apoptosome in Jurkat cell lysates (Hill *et al*, 2004).

The *in vitro* system of apoptosome formation used in the previous chapter only utilized the S-100 fraction obtained from viable cells. Therefore it was possible that the apoptosome formed in apoptotic cells could contain other proteins that are released from intracellular compartments or organelles during apoptosis. This possibility was addressed in this chapter, where the main aim was to generate affinity-tagged caspase-9 constructs that could be successfully transfected into cells. The transfected cells could then be exposed to an apoptotic stimulus to induce the formation of an apoptosome, which could then contain affinity-tagged

proteins. This would then allow the purification and characterisation of the apoptosome from apoptotic cells.

In such studies it is important to consider the type of affinity tag to be used, and one of the difficulties with GST-tagged protein purification is the binding of endogenous glutathione-based proteins to the glutathione (GSH)-Sepharose beads. These non-specific interactions can be minimised by using tandem-affinity purification (TAP) (Rigaut *et al*, 1999), a technique which had previously been used to show that Omi binds to XIAP-TAP in transfected HEK 293 cells (Martins *et al*, 2002). The TAP tag used in my work contained GST and the calmodulin binding peptide (CBP) (produced by T. Tenev, Breakthrough Breast Cancer Research, London). This tag allows initial purification with GSH-Sepharose beads (as used in Chapter 3), followed by a second purification using Sepharose-beads coated with calmodulin. This tandem-affinity purification should remove any non-specific interactions and purify the TAP-tagged protein/protein complex to homogeneity.

This chapter describes the studies performed with tandem-affinity tagged constructs containing the CARD domain (aa 1-130) of caspase-9 (Casp9$^{1-130}$). The truncated form of caspase-9 was chosen as it would not prevent the formation of the apoptosome, but it would stop apoptosome degradation by abrogating caspase activation, and consequently inhibiting cell death. It was hoped that this would produce affinity-tagged apoptosome complexes in apoptotic cells, which could then be purified and characterised. The results show that these constructs can be successfully transfected and expressed in HeLa cells. Furthermore, as predicted, Casp9$^{1-130}$ can inhibit apoptosis mediated via the intrinsic pathway, by binding to the apoptosome. This binding is a specific interaction, like endogenous caspase-9, as a point mutation in the CARD domain (R56A) abrogated the anti-apoptotic effects of the construct.

4.2 Results

4.2.1 Characterisation of apoptosome-dependent cell-death in HeLa cells.

In order to investigate the possibility of using the caspase-9 constructs to affinity-purify the apoptosome in apoptotic cells, it was necessary to characterise the intrinsic apoptotic pathway in HeLa cells, which were chosen for the transfection experiments. Etoposide is known to induce apoptosis via the intrinsic pathway and apoptosome formation (Cain *et al*, 1999), and thus was selected as the apoptotic stimulus for this study. HeLa cells were used as they are easily transfected, and contain all the apoptotic factors required to form an active apoptosome, as shown originally by Wang and colleagues (Liu *et al*, 1996; Li *et al*, 1997; Zou *et al*, 1997).

Apoptosis induced by Etoposide (100 μM or 200 μM) in HeLa cells was measured by PS exposure (Annexin V binding) and PARP cleavage. Etoposide induced apoptosis in a concentration and time-dependent manner, with 42% cell death observed after 24 h treatment with 200 μM Etoposide (Figure 4.2.1A & B). The poly-caspase inhibitor zVAD.FMK inhibited Etoposide-induced apoptosis (Figure 4.2.1A & B), indicating that the cell death observed was caspase-dependent. The caspase-dependent nature of Etoposide-induced apoptosis was confirmed by Western blot analysis of PARP (Figure 4.2.1C). This nuclear protein is known to be cleaved from the 116 kDa intact enzyme to a 86 kDa fragment by active effector caspases during apoptosis (Kaufmann *et al*, 1993; Tewari *et al*, 1995). Etoposide induced a time- and concentration-dependent cleavage of PARP (Figure 4.2.1C), which was inhibited in the presence of zVAD.FMK (data not shown). Although neither the PS exposure nor PARP cleavage was complete, in subsequent experiments HeLa cells were not exposed to Etoposide for more than 24 h.

These results showed that Etoposide was inducing apoptosis, probably in a caspase-dependent manner. To verify this, HeLa cells were treated with Etoposide for 24 h and cell lysates were extracted by Digitonin permeabilisation (see Materials and Methods for details). The lysates were then assayed for caspase-3 activity using Ac-DEVD.AFC (Figure 4.2.2A). The treatment of HeLa cells with Etoposide induced caspase-3/-7 (DEVDase) activity in a

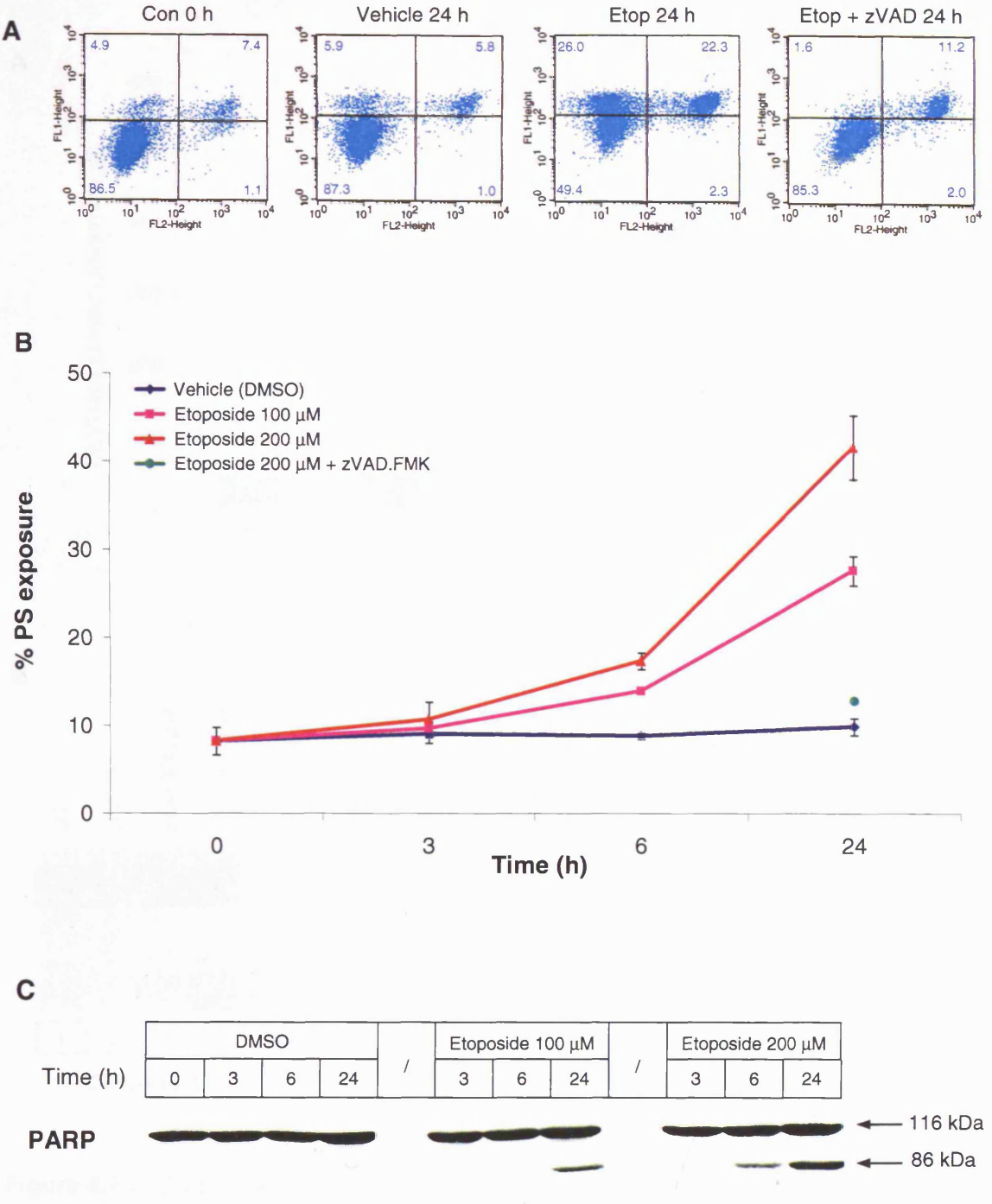

Figure 4.2.1: Etoposide induces apoptosis, which is inhibited by zVAD.FMK. HeLa cells were seeded at 8 x 10^4 cells/well in duplicate 18 h before treatment with vehicle alone (DMSO) or Etoposide (100 µM, 200 µM). Pre-treatment of cells with zVAD.FMK (100 µM, 1 h) prior to Etoposide treatment (200 µM) was performed for a designated sample (n=1). At each time point the cells from the duplicate samples were harvested, pooled and rested in fresh medium. The sample was then divided into two, half the cells were used to analyse PS exposure (as described in Materials and Methods, **A & B**) with data expressed as mean ± SEM (n=3). The remaining cells were washed in cold PBS, snap-frozen on dry ice and resuspended in SDS sample buffer for analysis of PARP cleavage by immunoblotting (**C**).

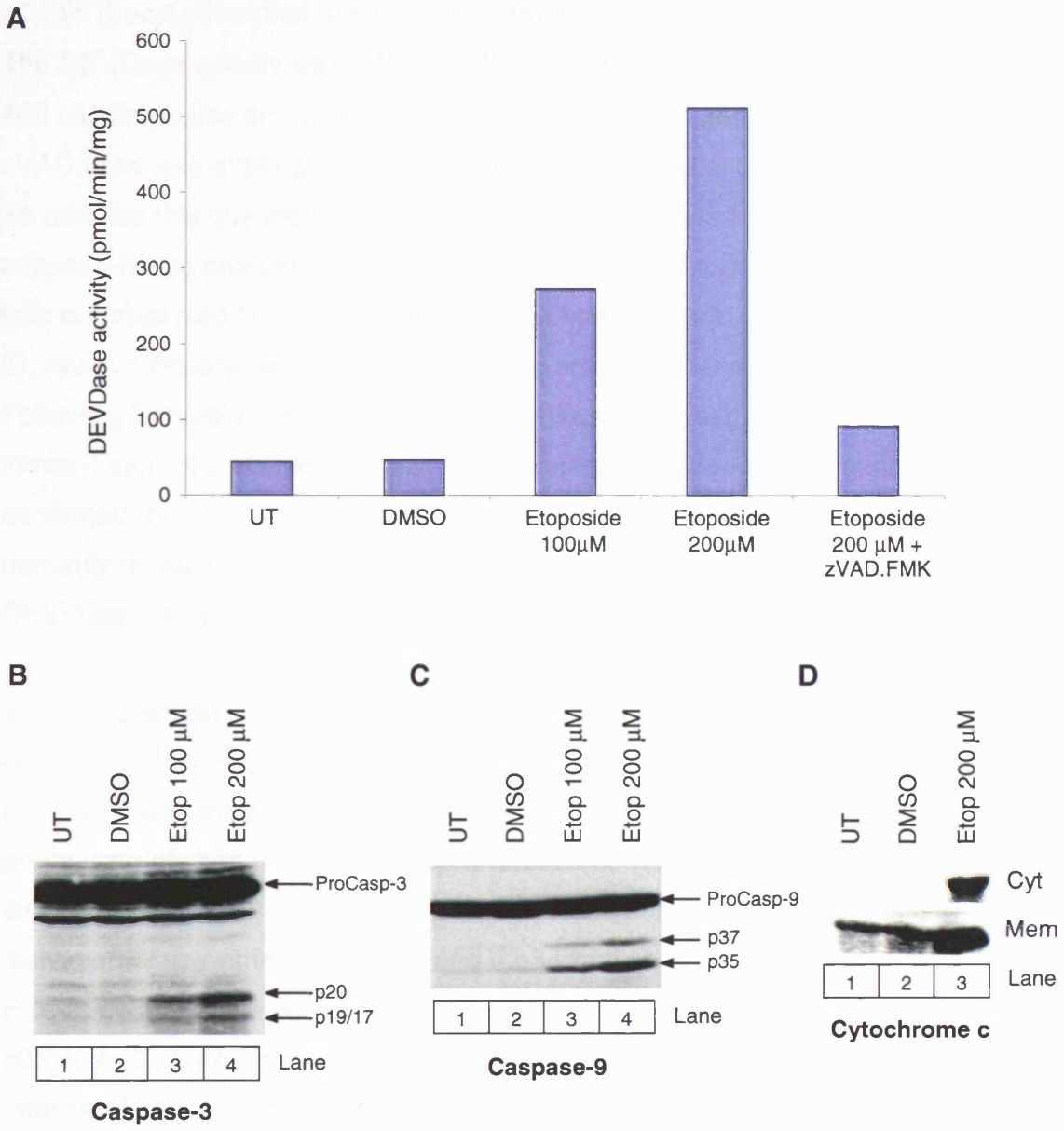

Figure 4.2.2: Etoposide induces caspase-3 activity/processing and induces apoptosis via the intrinsic pathway. HeLa cells were seeded at 6.25 x 10^5 cells/T75 flask for 18 h prior to treatment with DMSO alone, Etoposide (100 μM, 200 μM) or Etoposide (200 μM) in the presence of 100 μM zVAD.FMK (1 h pre-treatment) for 24 h, or left untreated (UT). The cells were then harvested, rested in fresh medium and analysed for PS exposure (data not shown) and DEVDase activity (**A**). Cell lysates were produced by freeze/thawing and centrifugation at 10,000 x g. The DEVDase assay was performed on 100 μg protein/sample. A whole cell pellet sample was taken prior to cell lysis for western blot analysis of caspase processing by immunoblotting for caspase-3 and caspase-9 (**B** & **C**, respectively). In addition, a sample of cells were treated with Digitonin (0.05%, 7 min) on ice, and centrifuged at 13,000 rpm to separate cytosol (Cyt) and membrane fractions (Mem) in order to detect cytochrome *c* release. Proteins (15 μg/lane) were separated by SDS-PAGE and immunoblotted for cytochrome *c* (**D**).

concentration-dependent manner (Figure 4.2.2A) and with 200 μM Etoposide was 10-fold greater than that observed in untreated and vehicle (DMSO) treated cells. The DEVDase activity was attenuated by 80% in lysates from cells treated with 200 μM Etoposide and zVAD.FMK (Figure 4.2.2A). These data suggested that zVAD.FMK was either preventing the activity or the initial processing of caspase-3. To address this question, Western blot analysis was used to assess whether caspase-3 was processed in Etoposide-induced apoptosis. Caspase-3 processing was not observed in the untreated or DMSO-treated cells (Figure 4.2.2B, lanes 1 & 2), which correlates with the low DEVDase activity observed in Figure 4.2.2A. Following Etoposide treatment, caspase-3 was processed to the p20 and p19/17 forms (Figure 4.2.2B, lanes 3 & 4), in a concentration-dependent manner. This confirmed the presence of the active effector caspase, caspase-3, that was primarily responsible for the observed exposure of PS, PARP cleavage and the DEVDase activity.

To assess whether Etoposide would be a suitable drug for investigating the effects of Casp9$^{1-130}$ *in vivo*, it was first necessary to confirm that Etoposide-induced cell death included the activation of caspase-9 as an apical caspase. Although the processing of caspase-9 is not required for its activation (Stennicke *et al*, 1999; Bratton *et al*, 2001b), the detection of processed caspase-9 would indicate activation of the intrinsic pathway and the formation of an active apoptosome. Etoposide induced a concentration-dependent processing of procaspase-9 to the p35 and p37 forms (Figure 4.2.2C, lanes 3 & 4), with no processing of caspase-9 detected in the controls (lanes 1 & 2). These observations suggest that Etoposide induces apoptosis via the activation of caspase-9 as an apical caspase, and that caspase-3 is subsequently activated. The active effector caspase is then able to cleave specific substrates i.e. PARP, and further enhance apoptosis by cleaving caspase-9 to the p37 form (Srinivasula *et al*, 2001).

Another of the characteristic features resulting from the activation of the intrinsic-pathway is the release of cytochrome *c* from the mitochondria, a prerequisite for apoptosome formation (Liu *et al*, 1996). To further establish that Etoposide was indeed inducing cell death via this pathway, the protein levels of cytochrome *c* in the cytosol were investigated by Western blotting. Etoposide treatment resulted in

the release of cytochrome *c* from the mitochondria into the cytosol (Figure 4.2.2D, lane 3), which was not observed under control conditions (lanes 1 & 2). Taken together with the data above, this provides strong evidence that Etoposide treatment is indeed inducing apoptosis via the intrinsic pathway and is a suitable stimulus to investigate the effects of the affinity-tagged Casp9$^{1-130}$ constructs.

4.2.2 Etoposide induces apoptosis via formation of the apoptosome

Having established that Etoposide was inducing apoptosis via the activation of caspase-9, it was logical to presume that an apoptosome was being formed. However, it was still vital to establish this experimentally prior to using TAP-tagged Casp9$^{1-130}$ to isolate the apoptosome from apoptotic cells. To confirm that Etoposide induced the formation of an apoptosome, gel filtration experiments were performed which allows the detection of the active ~700 kDa apoptosome (Cain *et al*, 2000). Following 24 h of Etoposide treatment (200 μM), cells were harvested and the cell lysates extracted by freeze/thawing, and 10,000 g centrifugation. Equal quantities of lysate (0.550 mg) were then loaded onto a Superose-6 gel filtration column, and the eluted fractions analysed by Western blotting. In DMSO-treated control cells, Apaf-1 eluted as a monomer (~130 kDa) in fractions 19-21 (Figure 4.2.3A, upper panel). In addition, caspase-9 and caspase-3 processing was not detected in these lysates (fractions 21-23 and 21-24, respectively, Figure 4.2.3A, centre and lower panel).

Following Etoposide treatment, Apaf-1 was still predominantly detected in fractions 19-21 as seen for the DMSO-control (Figure 4.2.3B, upper panel). However, caspase-9 was processed to the p35 form, with some still remaining as the inactive zymogen (Figure 4.2.3B, centre panel, fractions 21-23). This processing of caspase-9 is indicative of autocatalytic cleavage within the apoptosome, confirming that an active apoptosome had been formed, despite neither Apaf-1 nor caspase-9 being detected in the ~700 kDa apoptosome fractions (11-14). Further evidence for apoptosome activity was provided by the detection of caspase-3 processing to the p20 fragment (Figure 4.2.3B, lower panel), produced by active caspase-9 (Li *et al*, 1997; Slee *et al*, 1999). The subsequent processing of caspase-3 to the p19/p17 forms is then an autocatalytic processing event

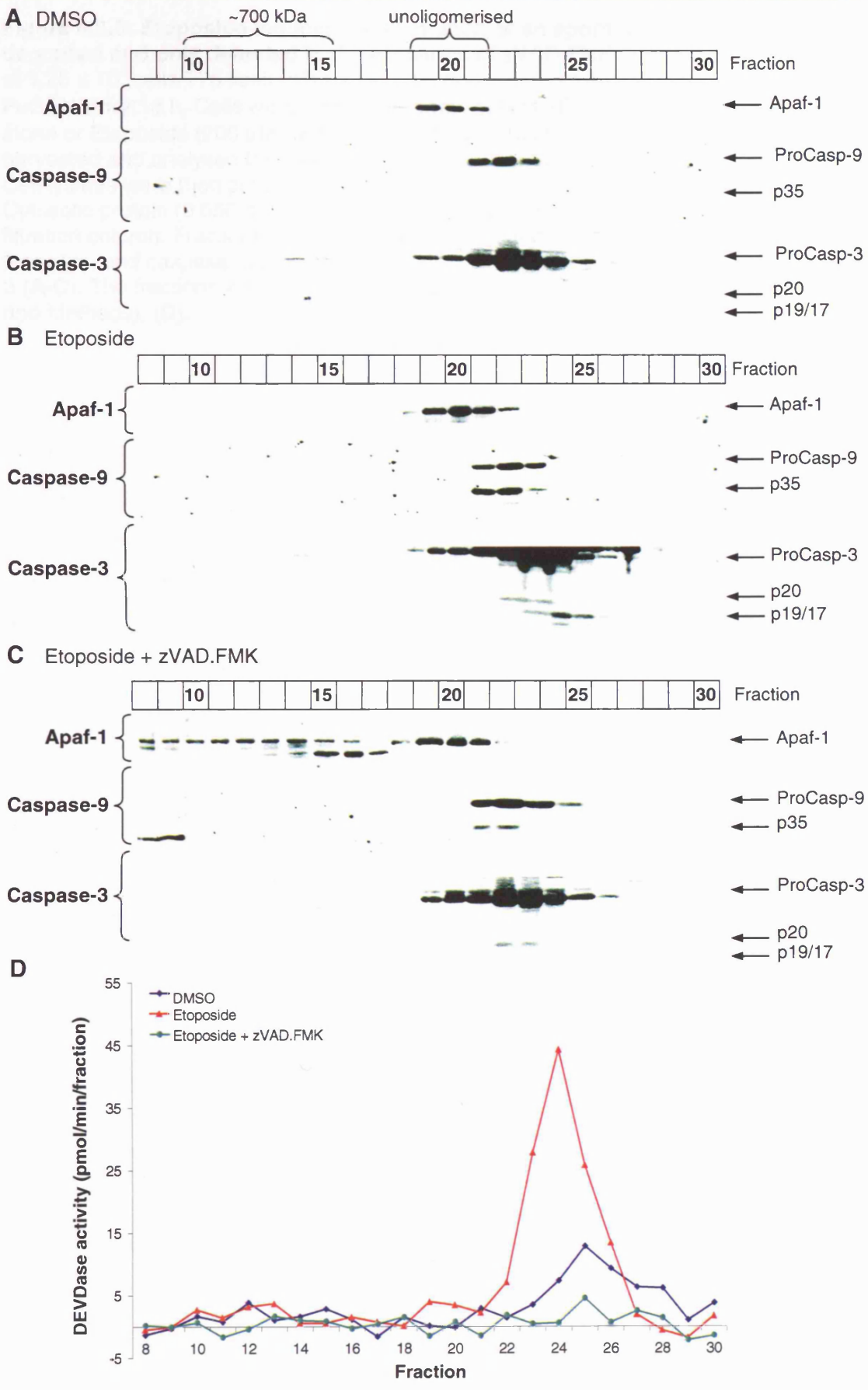

Figure 4.2.3: Etoposide induces the formation of an apoptosome, which is rapidly degraded and only detected in the presence of zVAD.FMK.

Figure 4.2.3: Etoposide induces the formation of an apoptosome, which is rapidly degraded and only detected in the presence of zVAD.FMK. HeLa cells were seeded at 1.25 x 10^5 cells/T75 flask (x3) for 24 h, followed by mock transfection (optimem and FuGENE) for 18 h. Cells were then treated with vehicle (DMSO), Etoposide (200 μM) alone or Etoposide (200 μM) with a 1 h pre-treatment of zVAD.FMK (100 μM). Cells were harvested and analysed for PS exposure (data not shown) to ensure sufficient apoptosis. Cell lysates were then produced by freeze/thawing and centrifugation at 10,000 x g. Cytosolic protein (0.550 mg) for each sample was loaded onto the Superose-6 gel filtration column. Fractions were collected (0.5 ml), and samples analysed for apoptosome formation and caspase processing by immunoblotting for Apaf-1, caspase-9 and caspase-3 (**A-C**). The fractions were also tested for DEVDase activity (as described in Materials and Methods), (**D**).

(Fernandes-Alnemri *et al*, 1996; Han *et al*, 1997). A possible reason for not detecting the presence of the ~700 kDa apoptosome, despite evidence of the consequent apoptosome-specific caspase processing, is that active caspase-3 can degrade the apoptosome (Bratton *et al*, 2001a; Lauber *et al*, 2001). As a result of proteolytic degradation, the ~700 kDa apoptosome is more difficult to detect in apoptotic cells.

To slow down the degradation of the apoptosome and hence increase the probability of observing the ~700 kDa apoptosome in Etoposide-treated cells, zVAD.FMK was added to the incubation medium 1 h prior to Etoposide treatment (Figure 4.2.3C). Gel-filtration then revealed that Apaf-1 eluted in fractions 11-14, where the ~700 kDa apoptosome is known to elute from this column (Cain *et al*, 2000) (Figure 4.2.3C, upper panel), with some still remaining as free Apaf-1 (fractions 19-21). More procaspase-9 was detected in fractions 21-23 in the presence of zVAD.FMK, compared with Etoposide alone, with reduced processing to the p35 form (Figure 4.2.3C, centre panel). Furthermore, the autocatalytic processing of caspase-3 to the active p19/p17 forms was completely inhibited by zVAD.FMK, although small amounts of the p20 fragment (due to processing by active caspase-9) were still detected (Figure 4.2.3C, lower panel).

The caspase-3 activity of these column fractions was also measured and a substantial increase in the DEVDase activity was observed with Etoposide treatment over vehicle-controls in the fractions containing active caspase-3 (fractions 23-25) (Figure 4.2.3D, red and blue lines, respectively). The DEVDase activity of caspase-3 was attenuated in the presence of zVAD.FMK (Figure 4.2.3D, green line) in accordance with previous studies (Sun *et al*, 1999a).

These observations suggest that active caspases prevent the detection of the ~700 kDa apoptosome in apoptotic cell lysates, presumably by degrading the apoptosome (Bratton *et al*, 2001a; Lauber *et al*, 2001). By inhibiting caspase activation (using zVAD.FMK) it was possible to prevent apoptosome degradation and consequently the ~700 kDa apoptosome was observed. Therefore, if as predicted, Casp9$^{1-130}$ acts as a dominant negative inhibitor of caspase activation in transfected cells treated with Etoposide, this should potentially enable purification of an intact ~700 kDa apoptosome using an affinity-tagged Casp9$^{1-130}$.

4.2.3 GTC-Casp9$^{1-130}$ does not inhibit Etoposide-induced apoptosis and does not bind to Apaf-1.

Previous investigations have shown that GST-Casp9$^{1-130}$ can inhibit apoptosome activity *in vitro* (Chapter 3), and that the native endogenous dominant negative form of caspase-9 (Caspase-9b) can inhibit apoptosis in MCF-7 cells (Srinivasula *et al*, 1999; Seol & Billiar, 1999)). It was therefore hypothesised that TAP-tagged Casp9$^{1-130}$ would also act as a dominant negative inhibitor and prevent Etoposide-induced apoptosis. Two TAP-tag variants of Casp9$^{1-130}$ were generated; one with the TAP-tag at the N-terminus (GTC-Casp9$^{1-130}$), the other at the C-terminus (Casp9$^{1-130}$-GTC). The N-terminal tagged variant was initially examined as it shared sequence homology to the construct used in the *in vitro* studies (as described in Chapter 3).

Initially, the transient transfection conditions were optimised to give adequate transfection efficiency (~40%) with low spontaneous apoptosis and minimal caspase-3 processing (due to the toxicity of the transfection reagent) (data not shown). All transfections using GTC-Casp9$^{1-130}$ were performed on cells seeded at 1.25 x 10^5 cells/T75 flask in triplicate, in order to obtain sufficient protein for successful affinity purification and immunoblotting.

HeLa cells were transfected with either GTC vector or GTC-Casp9$^{1-130}$ for 18 h prior to treatment with vehicle alone or Etoposide (200 μM) for 24 h. Apoptosis was then determined by PS exposure/ Annexin V binding (Figure 4.2.4 A). Interestingly, GTC-Casp9$^{1-130}$ was unable to inhibit Etoposide-induced apoptosis (Figure 4.2.4A, red bars), with levels of apoptosis equivalent to that observed for the vector control (~76%).

In order to establish whether the inability of GTC-Casp9$^{1-130}$ to inhibit apoptosis arose from an abrogated interaction with Apaf-1, affinity purification of the GTC-Casp9$^{1-130}$ was performed in cell lysates from transfected cells. HeLa cells were transfected and treated as above, with the cell lysates produced by freeze/thawing lysis of the cells followed by a 10,000 x g centrifugational step. The cell lysates from treated cells were then incubated with GSH-Sepharose beads and any bound

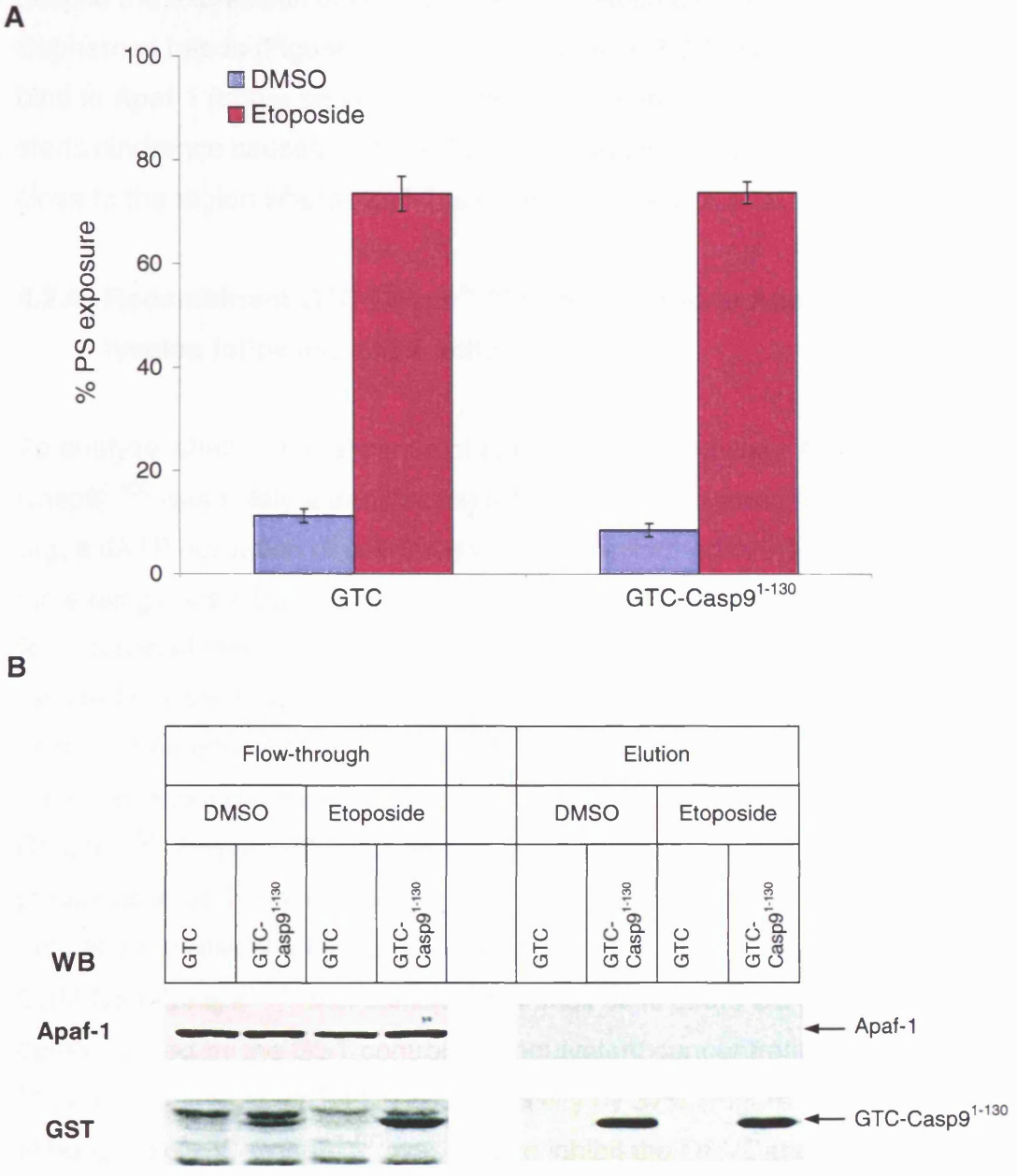

Figure 4.2.4: GTC-Casp9$^{1-130}$ is unable to inhibit Etoposide-induced apoptosis due to its inability to bind to Apaf-1. HeLa cells were transfected with FuGENE/GTC or GTC-Casp9$^{1-130}$ for 18 h prior to treatment with DMSO or Etoposide (200 μM). Cells were harvested after 24 h PS exposure measured by Annexin V binding (**A**). Data expressed as mean ± SEM, n=3. Cell lysates were then produced by freeze/thawing and 10,000 g centrifugation. The resulting lysate (100 μl) was then incubated with 150 μl GSH-Sepharose beads and 100 μl assay buffer for 1 h at 4 °C. The beads were then recovered (Flow-through), washed thoroughly and eluted in 20 mM glutathione (Elution). Samples of the flow-through and elution were then separated by SDS-PAGE and immunoblotted for Apaf-1 and GST (**B**).

proteins eluted in 20 mM GSH (Figure 4.2.4B). This purification revealed that despite the expression of GTC-Casp9$^{1-130}$ in HeLa cells and capture onto the GSH Sepharose beads (Figure 4.2.4B, lower panel), GTC-Casp9$^{1-130}$ was unable to bind to Apaf-1 (upper panel). This abrogated interaction could possibly be due to steric hindrance caused by the GTC tag around the N-terminus of Casp9$^{1-130}$, close to the region where Apaf-1 is known to bind (Qin *et al*, 1999).

4.2.4 Recombinant GTC-Casp9$^{1-130}$ does not bind to Apaf-1 in HeLa cell lysates following dATP activation.

To analyse whether the absence of any interaction between Apaf-1 and GTC-Casp9$^{1-130}$ was solely a transfection artefact or due to steric hindrance by the GTC tag, a dATP activation of cellular lysate was performed in the presence of increasing concentrations of recombinant GTC-Casp9$^{1-130}$ (recGTC-Casp9$^{1-130}$). Purification of recGTC-Casp9$^{1-130}$ involved both stages of the TAP protocol and resulted in a very clean preparation (Materials and Methods, Figure 2.17.1). In order to evaluate whether the larger GTC affinity-tag was causing the interference, a parallel experiment was performed using recombinant GST-Casp9$^{1-130}$ (recGST-Casp9$^{1-130}$). HeLa cell lysates were activated with dATP and cytochrome *c* in the presence of GST (data not shown), recGST-Casp$^{1-130}$ or recGTC-Casp9$^{1-130}$ for 30 min, and the resulting DEVDase activity was measured (Figure 4.2.5A). Whereas 2 μM GST-Casp9$^{1-130}$ was sufficient to inhibit 93% of the DEVDase activity demonstrated by the GST control, the equivalent concentration of recGTC-Casp9$^{1-130}$ was only able to inhibit DEVDase activity by 37% (Figure 4.2.5 A). In addition, although recGTC-Casp9$^{1-130}$ was able to inhibit the DEVDase activity in a concentration-dependent manner, it was a considerably inferior inhibitor compared to recGST-Casp9$^{1-130}$. This result correlated with the inability of GTC-Casp9$^{1-130}$ to capture significant amounts of Apaf-1 despite using concentrations 4-fold higher than those used for GST-Casp9$^{1-130}$ (Figure 4.2.5B, lanes 13-14 compared with lanes 15-18).

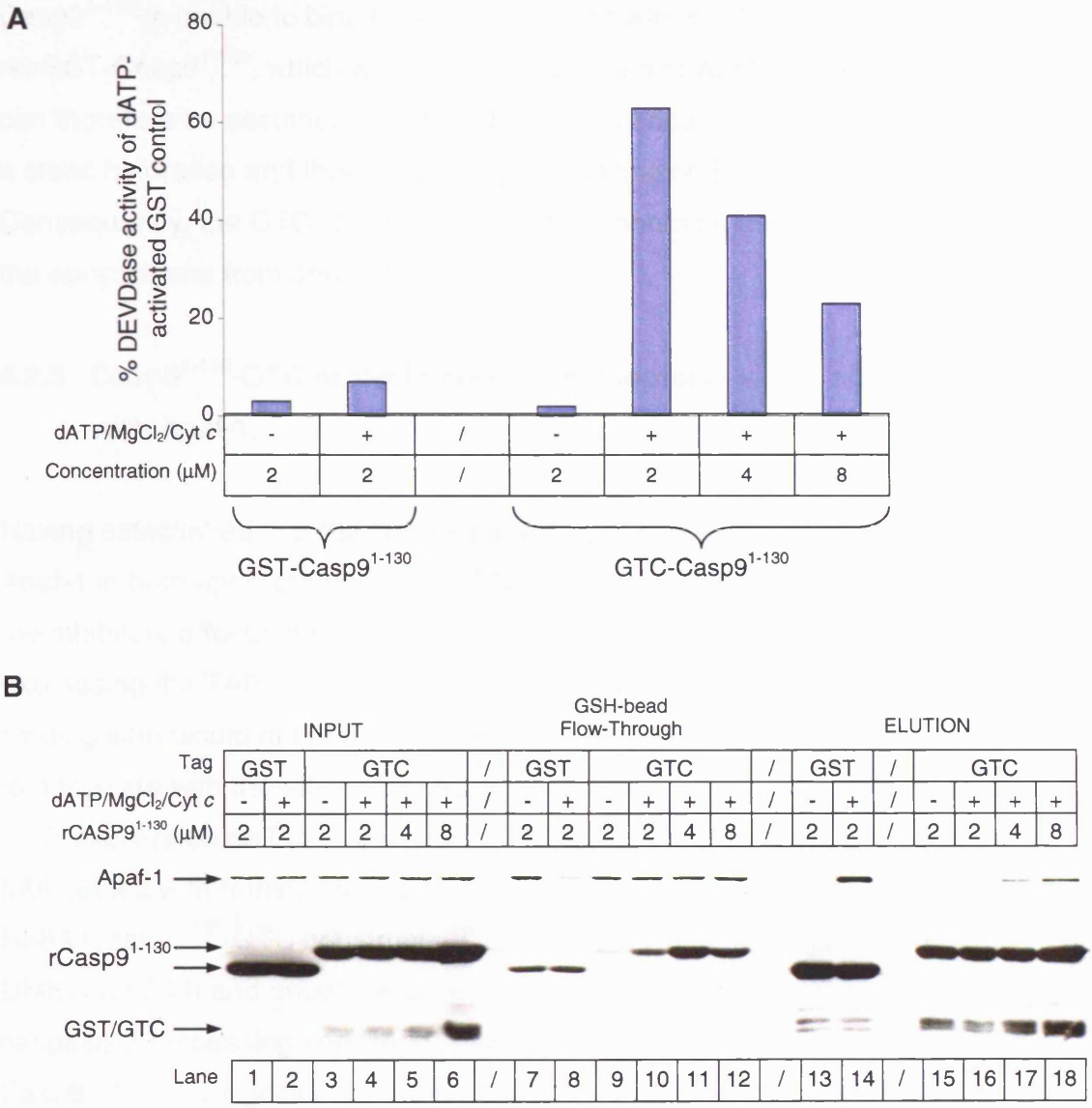

Figure 4.2.5: Recombinant GTC-Casp9$^{1-130}$ does not associate with Apaf-1 in HeLa cell lysates following dATP activation, unlike recGST-Casp9$^{1-130}$. Recombinant GTC-Casp9$^{1-130}$ was produced as described in Materials and Methods. HeLa cell lysates (10 mg/ml) were activated in the presence of 2 mM dATP/$MgCl_2$, 1.7 μM cytochrome *c* and either GST (data not shown), GST-Casp9$^{1-130}$ or GTC-Casp9$^{1-130}$ for 30 min at 37 °C. The DEVDase activity of each sample (100 μg) was then assayed (**A**). A sample from the activated lysates was taken for Western blot analysis (input) and the remainder (850 μg) was incubated with GSH-Sepharose beads for 1 h at 4 °C. The beads were then recovered (flow-through) and washed thoroughly before elution with 2 x SDS sample loading buffer. Proteins were separated by SDS-PAGE (20 μg input, 20 μg flow-though, 50% elution) and Apaf-1 and GST detected by immunoblotting (**B**).

Taken together with the data from the transient transfections, it appears that GTC-Casp9$^{1-130}$ is unable to bind to Apaf-1 with high affinity. This is in contrast to recGST-Casp9$^{1-130}$, which was able to stably bind to Apaf-1 in cellular lysates. It can therefore be assumed that the additional calmodulin binding protein is causing a steric hindrance and thus preventing the binding of GTC-Casp9$^{1-130}$ to Apaf-1. Consequently, the GTC-Casp9$^{1-130}$ construct cannot be used for the purification of the apoptosome from apoptotic cells.

4.2.5 Casp9$^{1-130}$-GTC protects cells from apoptosis via its ability to interact with Apaf-1.

Having established that the N-terminally tagged Casp9$^{1-130}$ was unable to bind to Apaf-1 in both apoptotic cells and dATP-activated cell lysates, I then investigated the inhibitory effects of the C-terminally tagged variant. It was predicted that expressing the TAP-tag at the C-terminus of Casp9$^{1-130}$ (distal to the Apaf-1 binding site) would remove the likelihood of any steric hindrance and allow Apaf-1 to associate with the affinity-tagged protein. To investigate the effect of Casp9$^{1-130}$-GTC expression on Etoposide-induced apoptosis, HeLa cells were transiently transfected with transfection controls, wild-type (wt) or the Apaf-1 binding mutant R56A Casp9$^{1-130}$-GTC constructs. These cells were then treated with Etoposide or DMSO for 24 h and apoptosis assessed by PS exposure (Annexin V binding), caspase-3 processing and PARP cleavage (Figure 4.2.6A). Transfection of Casp9$^{1-130}$-GTC significantly attenuated Etoposide-induced apoptosis to 39.9%, compared with 76.3% in vector control transfections (Figure 4.2.6A, red bars). Significantly, this effect was observed when measuring cell death in the total cell population and not just in the cells expressing Casp9$^{1-130}$-GTC (~40%). These data indicate that virtually all of the Casp9$^{1-130}$-GTC transfected cells were protected from Etoposide-induced apoptosis. The anti-apoptotic effect of Casp9$^{1-130}$-GTC was attenuated with the introduction of the point mutation R56A (Figure 4.2.6A). This mutation prevents caspase-9 from interacting with Apaf-1 via their respective CARD domains (Qin *et al*, 1999). This observation therefore suggests that the anti-apoptotic effects of Casp9$^{1-130}$-GTC were mediated through its ability to bind to Apaf-1, and form an inactive apoptosome. Interestingly, transfection with Casp9$^{1-130}$-GTC also suppressed spontaneous apoptosis, unlike the R56A mutant (Figure 4.2.6A, blue bars).

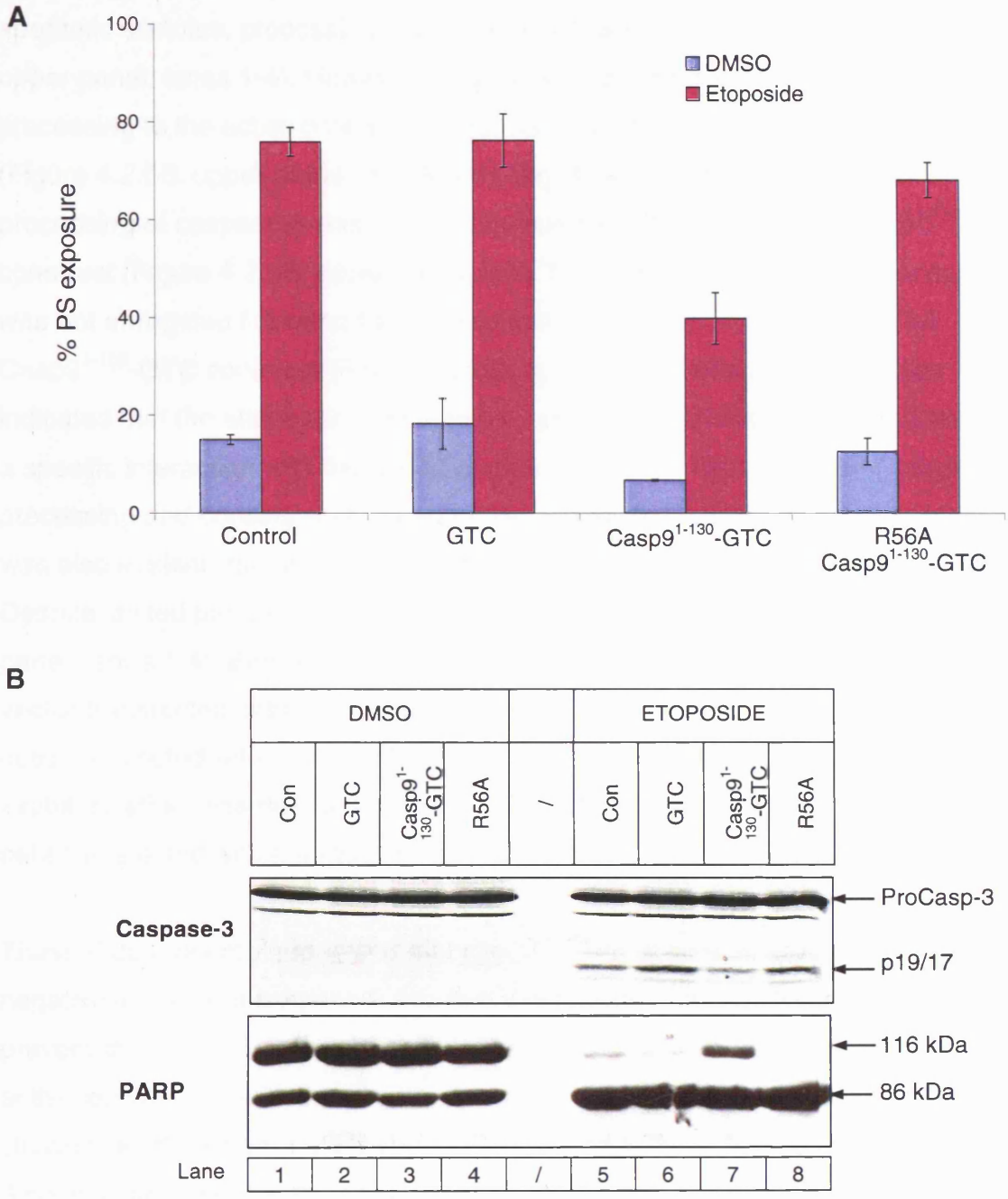

Figure 4.2.6: Casp9$^{1-130}$-GTC inhibits Etoposide-induced apoptosis. HeLa cells were transfected with FuGENE alone (Control), vector (GTC), Casp9$^{1-130}$-GTC, or R56A Casp9$^{1-130}$-GTC for 18 h prior to treatment with DMSO alone or Etoposide (200 μM). Cells were harvested after 24 h and PS exposure measured by Annexin V binding (**A**). Data expressed as mean ± SEM, n=3. Cell lysates were prepared by freeze/thawing and 10,000 x g centrifugation. The cytosol (20 μg) was analysed for caspase-3 processing by SDS-PAGE /Western blotting (**B**, upper panel). The membrane fraction was resuspended in PBS, sonicated and 20 μg protein/sample analysed by SDS-PAGE/ immunoblotting for PARP (**B**, lower panel).

The anti-apoptotic effect of Casp9$^{1-130}$-GTC was also apparent when caspase-3 processing and activity (PARP cleavage) were investigated. In the absence of an apoptotic stimulus, processing of procaspase-3 was not detected (Figure 4.2.6B, upper panel, lanes 1-4). However, Etoposide-treatment induced caspase-3 processing to the active p19 and p17 forms in control and vector-transfected cells (Figure 4.2.6B, upper panel, lane 5 & 6). Significantly, the Etoposide-induced processing of caspase-3 was inhibited in cells transfected with the Casp9$^{1-130}$-GTC construct (Figure 4.2.6B, upper panel, lane 7). In contrast, caspase-3 processing was not abrogated following transfection with the CARD point mutant R56A Casp9$^{1-130}$-GTC construct (Figure 4.2.6B, upper panel, lane 8). These data indicated that the attenuation of caspase-3 processing by Casp9$^{1-130}$-GTC was via a specific interaction with the CARD domain of Apaf-1. The absence of caspase-3 processing and consequently its activation in Casp9$^{1-130}$-GTC transfected cells, was also evident from the reduced PARP cleavage (Figure 4.2.6B, lower panel). Despite limited processing of PARP in DMSO-treated cells (Figure 4.2.6B, lower panel, lanes 1-4), Etoposide-induced complete processing of PARP in control and vector-transfected cells (lanes 5 & 6). However, PARP cleavage was abrogated in cells transfected with Casp9$^{1-130}$-GTC (Figure 4.2.6B, lower panel, lane 7). This inhibitory effect was due to the ability to bind Apaf-1, as this was not observed in cells transfected with the R56A Casp9$^{1-130}$-GTC construct (lane 8).

These data indirectly suggested that Casp9$^{1-130}$-GTC was acting as a dominant negative inhibitor of caspase-9 and that it was able to bind to the apoptosome and prevent the activation of endogenous caspase-9. Consequently, effector caspase activation was prevented and subsequently key apoptotic substrates were not cleaved. As the R56A mutant was unable to bind to Apaf-1, endogenous caspase-9 could instead bind to the apoptosome in Etoposide-treated R56A mutant transfected cells, and then promote cell death. The R56A mutant cannot therefore influence the progression of the intrinsic pathway and thus provides further evidence that the protective action of Casp9$^{1-130}$-GTC is mediated specifically via its ability to bind to the apoptosome.

4.2.6 Casp9$^{1-130}$-GTC binds to Apaf-1 in transfected HeLa cells in the absence of an apoptotic stimulus

Having indirectly determined that the inhibitory effect of Casp9$^{1-130}$-GTC is via its interaction with Apaf-1, a pull-down experiment was performed to confirm the binding of Apaf-1 with Casp9$^{1-130}$-GTC. Cells were transfected with GTC vector alone, Casp9$^{1-130}$-GTC, or R56A Casp9$^{1-130}$-GTC for 18 h prior to treatment with Etoposide for 24 h. The cells were then harvested and cell lysates produced by freeze/thawing cell lysis and 10,000 x g centrifugation. The Casp9$^{1-130}$-GTC-containing complexes were then purified using GSH-Sepharose beads, and the bound proteins identified by Western blot analysis.

Analysis of the GSH-coated Sepharose beads showed that Apaf-1 only binds to the wt Casp9$^{1-130}$-GTC variant (Figure 4.2.7, upper panel) even though equivalent amounts of each fusion protein were detected in the cells (lower panel). However, Apaf-1 unexpectedly bound to Casp9$^{1-130}$-GTC in both vehicle- and Etoposide-treated cells (Figure 4.2.7, upper panel). This agreed with the previous observation that Casp9$^{1-130}$-GTC attenuated spontaneous apoptosis (Figure 4.2.6A, blue bars). Furthermore, having previously established that Apaf-1 requires both dATP and cytochrome *c* to allow a conformational change and permit binding of GST-Casp9$^{1-130}$ (Chapter 3), it was assumed that binding of Casp9$^{1-130}$-GTC to Apaf-1 would require the same co-factors. However, in the absence of an apoptotic stimulus, (and presumably an absence of cytochrome *c*), Casp9$^{1-130}$-GTC was able to bind to Apaf-1. Significantly, the inability of R56A Casp9$^{1-130}$-GTC to capture Apaf-1 confirmed that the point mutation abrogated the CARD:CARD interaction between Casp9$^{1-130}$ and Apaf-1 (Figure 4.2.7).

4.2.7 Casp9$^{1-130}$-GTC associates with Apaf-1 in a ~700 kDa complex in DMSO-treated cells in the absence of cytochrome *c* release.

As Apaf-1 was able to bind to Casp9$^{1-130}$-GTC in the absence of an apoptotic stimulus, this raised the question of whether an apoptosome was being formed in transfected non-apoptotic cells. To answer this question, control-transfected and Casp9$^{1-130}$-GTC transfected cells were treated with DMSO or Etoposide for 24 h. Cell lysates were then produced and separated by Superose-6 gel filtration to

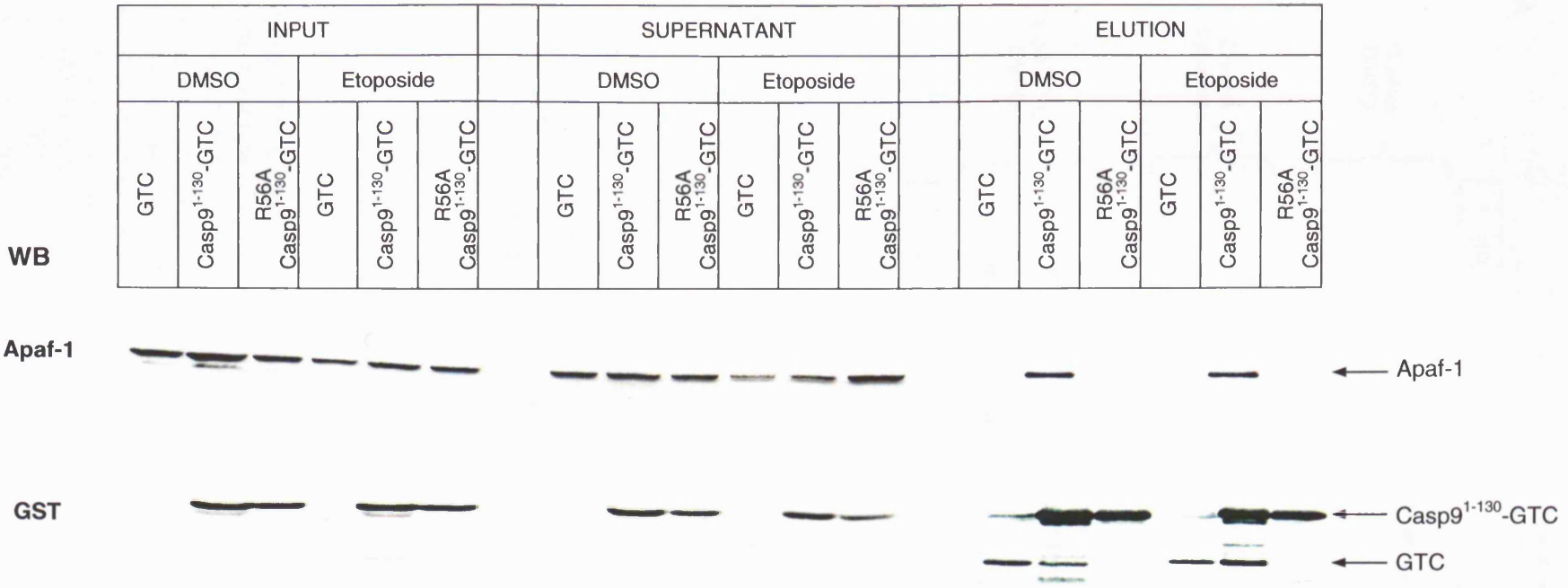

Figure 4.2.7: Casp9$^{1-130}$-GTC binds to Apaf-1 in transfected HeLa cells in the absence of an apoptotic stimulus. HeLa cells were transfected with empty vector (GTC), Casp9$^{1-130}$-GTC, or the R56A mutant for 18 h prior to treatment with vehicle (DMSO) or Etoposide (200 μM). Cells were then harvested and PS exposure determined by Annexin V binding (data not shown). Cell lysates were produced by freeze/thawing the cells and a 10,000 x g centrifugation step. The lysate (100 μl) was then incubated with 150 μl washed GSH-Sepharose beads and 100 μl assay buffer, at 4 °C for 1 h with continuous motion. The beads were then washed and eluted in 20 mM GSH. Samples were taken prior to bead incubation (input ~20 μg), after incubation (supernatant ~20 μg) and from the elution. Samples were separated by SDS-PAGE on 10% gels and immunoblotted for Apaf-1 and GST.

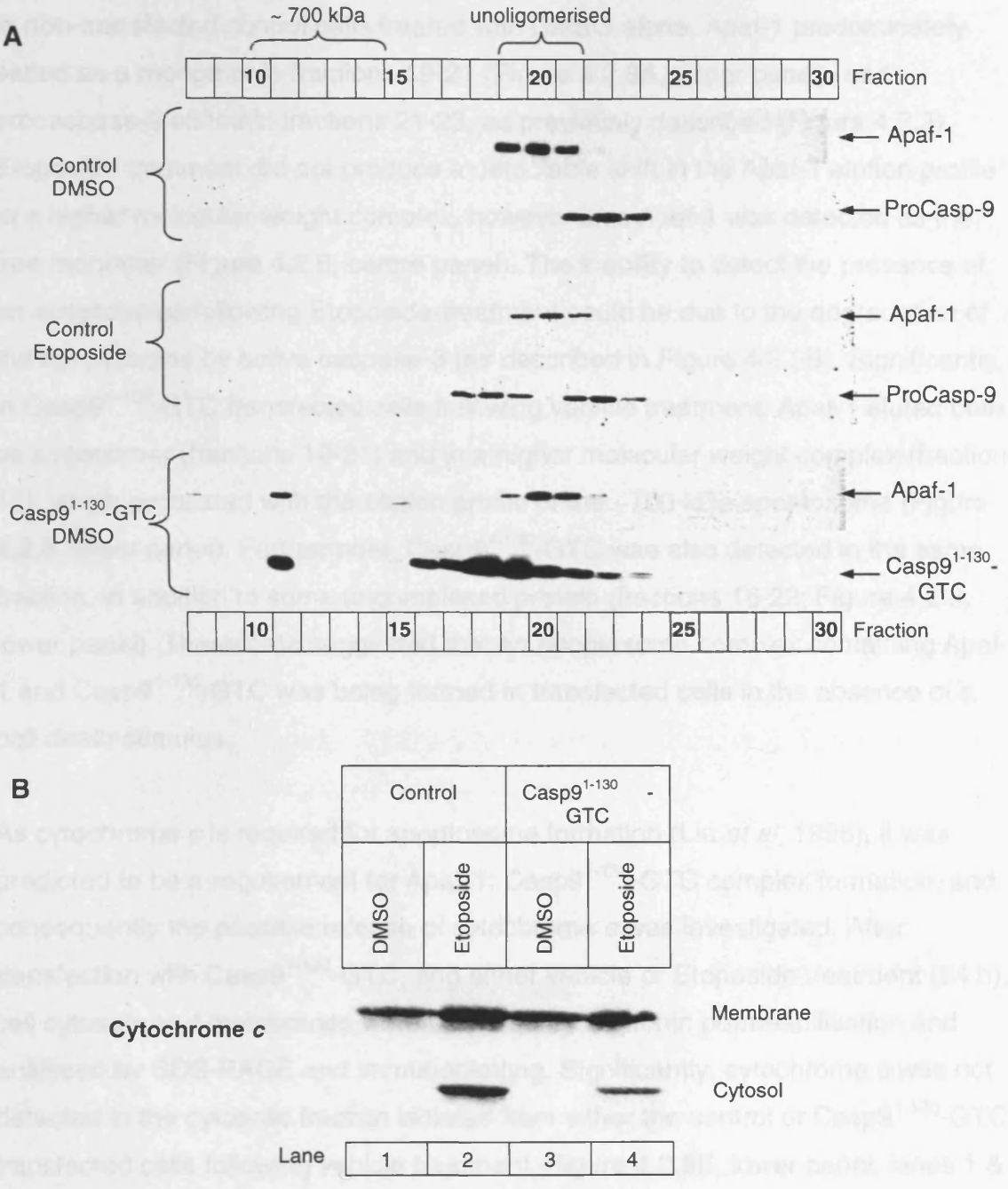

Figure 4.2.8: Casp9$^{1-130}$-GTC associates with Apaf-1 in an apoptosome of ~700 kDa, in the absence of apoptotic stimuli and cytochrome *c* release. HeLa cells were either transfected with FuGENE/optimem (control) or with Casp9$^{1-130}$-GTC for 18 h. Cells were treated with DMSO alone or Etoposide (200 μM) for 24 h. Cells were then harvested and cell lysates prepared by freeze/thawing and 10,000 x g centrifugation. Samples were then loaded onto a Superose-6 gel filtration column and eluted in 0.5 ml fractions. An aliquot of each fraction was analysed by SDS-PAGE/immunoblotting for Apaf-1, caspase-9 and GST (**A**). Prior to freeze/thawing the lysate a small sample of cells were treated with Digitonin (0.05%, 7 min) on ice and centrifuged at 13,000 rpm to separate the membranous fraction from the cytosol. Proteins (15 μg/lane) were then separated and analysed by SDS-PAGE/ immunoblotting for cytochrome *c* (**B**).

detect Apaf-1: caspase-9 and Apaf-1: Casp9$^{1-130}$-GTC complexes (Figure 4.2.8A). In non-transfected control cells treated with DMSO alone, Apaf-1 predominately eluted as a monomer in fractions 19-21 (Figure 4.2.8A, upper panel), and procaspase-9 eluted in fractions 21-23, as previously described (Figure 4.2.3). Etoposide treatment did not produce a detectable shift in the Apaf-1 elution profile to a higher molecular weight complex, however less Apaf-1 was detected as the free monomer (Figure 4.2.6, centre panel). The inability to detect the presence of an apoptosome following Etoposide-treatment could be due to the degradation of the apoptosome by active caspase-3 (as described in Figure 4.2.3B). Significantly, in Casp9$^{1-130}$-GTC transfected cells following vehicle treatment, Apaf-1 eluted both as a monomer (fractions 19-21) and in a higher molecular weight complex (fraction 11), which correlated with the elution profile of the ~700 kDa apoptosome (Figure 4.2.8, lower panel). Furthermore, Casp9$^{1-130}$-GTC was also detected in the same fraction, in addition to some uncomplexed protein (fractions 16-22; Figure 4.2.8, lower panel). These data suggested that an apoptosome complex containing Apaf-1 and Casp9$^{1-130}$-GTC was being formed in transfected cells in the absence of a cell death stimulus.

As cytochrome *c* is required for apoptosome formation (Liu *et al*, 1996), it was predicted to be a requirement for Apaf-1: Casp9$^{1-130}$-GTC complex formation, and consequently the possible release of cytochrome *c* was investigated. After transfection with Casp9$^{1-130}$-GTC, and either vehicle or Etoposide treatment (24 h), cell cytosols and membranes were prepared by Digitonin permeabilisation and analysed by SDS-PAGE and immunoblotting. Significantly, cytochrome *c* was not detected in the cytosolic fraction isolated from either the control or Casp9$^{1-130}$-GTC transfected cells following vehicle treatment (Figure 4.2.8B, lower panel, lanes 1 & 3). However, the Etoposide-induced release of cytochrome *c* from the mitochondria was substantially reduced in Casp9$^{1-130}$-GTC transfected cells compared to controls (Figure 4.2.8B, lower panel, lanes 2 & 4). This observation suggests that Etoposide induces an initial release of cytochrome *c* which is caspase-independent (Sun *et al*, 1999a), followed by secondary release occurring in the latter stages of apoptosis, which is a caspase-dependent event (Chen *et al*, 2000b). As caspase activation is inhibited in cells transfected with the Casp9$^{1-130}$-GTC construct, this secondary release of cytochrome *c* is not observed.

The formation of an apoptosome in vehicle-treated Casp9$^{1-130}$-GTC transfected cells could have resulted from a sufficient but undetectable level of cytochrome *c* in the cytosol. Alternatively, the TAP tagged truncated caspase-9 variant could induce unfolding of Apaf-1 and circumvent the need for cytochrome *c* for apoptosome formation. Unfortunately, unlike GTC-Casp9$^{1-130}$, a recombinant version of Casp9$^{1-130}$-GTC could not be produced from the available plasmids and therefore the requirement for cytochrome *c* in Apaf-1:Casp9$^{1-130}$ association could not be assessed *in vitro*.

In order to identify apoptosome-specific interacting proteins it was compulsory that the affinity-tagged construct bound specifically to Apaf-1 only upon apoptotic stimulation. However, the results described above suggest that a Casp$^{1-130}$-GTC: Apaf-1 complex was being formed in the absence of an apoptotic stimulus and therefore Casp9$^{1-130}$-GTC would not be suitable for the specific purification of the apoptosome and any modulatory partners from apoptotic cells. Importantly, transfection of Casp9$^{1-130}$-GTC acted as a very powerful dominant negative inhibitor of the mitochondrial-apoptotic pathway and therefore could be used as a specific inhibitor of this form of cell death.

4.3 Discussion

To effectively purify a protein complex and be certain of any interactions observed, the use of a single affinity tag is often not sufficiently specific. This problem has been addressed by the development of multiple-affinity tags (Rigaut *et al*, 1999, Honey *et al*, 2001). The TAP (tandem-affinity purification) method of protein purification was first developed with the IgG binding domains of Protein A and a calmodulin binding peptide (CBP) (Rigaut *et al*, 1999). This was improved by our collaborators in London, who modified the TAP to include GST and CBP domains expressed on either the N- or C-terminus of any given target protein (T. Tenev, P. Meier, Breakthrough Breast Cancer Research, London). This enabled us to evaluate caspase-9 constructs with a similar tag to that which we had used previously in the *in vitro* system (described in Chapter 3). The initial aim of this study was to assess whether an association between a TAP-tagged Casp9$^{1-130}$ and Apaf-1 could be specifically induced upon apoptotic stimulation. The ultimate aim was to produce cells that stably expressed a selected construct, either constitutively or inducibly, and would thus potentially increase the probability of detecting novel proteins by mass spectrometry.

Although the topoisomerase II inhibitor, Etoposide, has been widely used to induce apoptosis via DNA damage (Mizumoto *et al*, 1994; Kaufmann, 1998), the cellular and biochemical features of apoptosis induced by Etoposide were characterised in the experimental cell line chosen for this study. In order to evaluate the effects of Casp9$^{1-130}$ *in vivo*, it was essential that treatment of HeLa cells with Etoposide resulted in apoptosis induced via the intrinsic pathway. Following 24 h treatment with Etoposide (200 μM), changes synonymous with activation of the intrinsic apoptotic pathway were observed. Cytochrome *c*, a prerequisite for apoptosome formation (Liu *et al*, 1996), was released into the cytosol; caspase-9 was also autocatalytically processed within the apoptosome to form the p35 fragment (Li *et al*, 1997; Srinivasula *et al*, 1998), which in turn led to the cleavage of caspase-3 to form the p20 fragment (Li *et al*, 1997; Slee *et al*, 1999). The active p19/p17 fragments of caspase-3 were then produced by autocatalytic processing (Fernandes-Alnemri *et al*, 1996; Han *et al*, 1997; Slee *et al*, 1999) and amplified the apoptotic signal by further processing caspase-9 to form the p37 fragment (Srinivasula *et al*, 1998; 2001; Slee *et al*, 1999). Finally, effector caspase

substrates, i.e. PARP (Tewari *et al*, 1995) were cleaved and PS was externalised on the cell membrane, thus providing an engulfment signal for phagocytes (Fadok *et al*, 1992; 1998). Importantly, Etoposide treatment of HeLa cells resulted in the formation of a ~700 kDa apoptosome complex, although this was only detected in the presence of zVAD.FMK. Taken together these data confirmed that Etoposide was inducing apoptosis via the intrinsic pathway, with the formation of an apoptosome.

The effect of a dominant negative inhibitor on apoptosome formation and apoptosis was investigated by generating constructs containing Casp9$^{1-130}$ with the TAP tag at either the N or the C terminus. This allowed us to determine the most effective configuration for isolating the apoptosome from apoptotic cells. The N-terminally tagged Casp9$^{1-130}$ is similar but not identical to the GST-Casp9$^{1-130}$ fusion protein used previously in the *in vitro* study (Chapter 3), where GST-Casp9 $^{1-130}$ was able to inhibit dATP-dependent caspase activation. However, when transfected into cells, GTC-Casp9$^{1-130}$ lacked the ability to bind to Apaf-1 and inhibit Etoposide-induced apoptosis. This was surprising as it only differs from GST-Casp9$^{1-130}$ by the presence of the CBP domain (~9 kDa). To further assess the ability of GTC-Casp9$^{1-130}$ to bind to Apaf-1, a recombinant form of this protein was produced and used in an *in vitro* study. Recombinant GTC-Casp9$^{1-130}$ did not associate with Apaf-1 in dATP-activated HeLa cell lysates, nor did it prevent effector caspase activation. This result is contrary to the results obtained with the GST tagged Casp9$^{1-130}$ variant, which significantly attenuated caspase activation via its interaction with Apaf-1. This confirmed that the addition of the CBP domain was preventing Apaf-1 association with GTC-Casp9$^{1-130}$, possibly by steric hindrance due to the larger affinity-tag. In addition, other residues apart from Arginine 56 are involved in the CARD: CARD interaction between Apaf-1 and caspase-9, and the presence of the CBP domain at the N-terminus could be preventing these stabilising interactions (Qin *et al*, 1999). For example, Arginine 13 on caspase-9 forms hydrogen bonds with Glu40 and Asp27 on Apaf-1 (Qin *et al*, 1999). As this critical residue on caspase-9 resides so close to the N-terminus, it is possible that a charged residue on the CBP domain could prevent the formation of these hydrogen bonds and result in destabilising the caspase-9/Apaf-1 interaction.

With the TAP-tag located at the C-terminus of Casp9$^{1-130}$, and distal to the critical regions required for Apaf-1 binding, it was predicted that the tag would not affect the interaction between Apaf-1 and Casp9$^{1-130}$. Indeed, transient transfection of HeLa cells followed by an apoptotic stimulus revealed that the Casp9$^{1-130}$-GTC could significantly attenuate both spontaneous- and Etoposide-induced apoptosis. The mechanism of inhibition appeared to be via the ability of Casp9$^{1-130}$-GTC to bind to Apaf-1, as a point mutation at Arginine 56 (R56A) abrogated the anti-apoptotic function by prevented the association of Casp9$^{1-130}$-GTC with Apaf-1. The dominant negative effect of Casp9$^{1-130}$-GTC is in accordance with previous studies characterising the role of the native endogenous caspase-9 dominant negative isoform, caspase-9b. Expression of this 31 kDa caspase-9 isoform (which lacks the catalytic domain) suppressed apoptosis in MCF-7 cells, induced via a range of stimuli, including TRAIL, UV damage and Bak treatment (Srinivasula *et al*, 1999; Seol & Billiar, 1999).

One of the most significant findings of the current study was that Casp9$^{1-130}$-GTC and Apaf-1 associated in a ~700 kDa complex in the absence of detectable cytochrome *c* release. The mechanism by which Casp9$^{1-130}$-GTC is binding to Apaf-1 under these conditions remains unclear. Many studies have previously been performed to determine the requirements for apoptosome formation in cellular lysates i.e. dATP and cytochrome *c* (Liu *et al*, 1996; Zou *et al*, 1997; Li *et al*, 1997; Saleh *et al*, 1999; Adrain *et al*, 1999). The addition of these co-factors results in the 'opening' of the Apaf-1 conformation, oligomerisation and recruitment of caspase-9. In addition, various cell culture studies have highlighted the importance of cytochrome *c* in stress-mediated apoptosis, either by using cytochrome *c* null cells (Li *et al*, 2000a), or Bcl-2 over-expressing cells to prevent cytochrome *c* involvement (Yang *et al*, 1997; Kluck *et al*, 1997). It is therefore probable that cytochrome *c* is also required for the formation of an active apoptosome *in vivo*. Consequently, the Apaf-1: Casp9$^{1-130}$-GTC complex produced in the absence of cytochrome *c* is likely to be a transfection-induced artefact resulting from the over-expression of this truncated and tagged protein. Alternatively, this complex is produced as a result of a small release of cytochrome *c*, below the level of detection of the immunoblotting antibody, but sufficient to induce oligomerisation of Apaf-1.

This transfection study and the previous *in vitro* study (Chapter 3) have demonstrated that Casp9$^{1-130}$ can inhibit apoptosis induced by Etoposide, and dATP-dependent caspase activation in cell lysates, respectively, by forming an inactive apoptosome. As the TAP-tagged Casp9$^{1-130}$ constructs could not specifically bind to Apaf-1 under apoptotic conditions, they are not suited for the production of stably transfected cells from which to isolate an apoptosome. However, Casp9$^{1-130}$-GTC does act as a dominant negative inhibitor and could therefore still be used as a tool to inhibit the mitochondrial pathway downstream of cytochrome *c* release. This could help elucidate the mechanism of action of agents which in some cells induce apoptosis primarily via the death receptor pathway but require the intrinsic pathway for amplification (e.g. TRAIL).

Nevertheless, the Casp9$^{1-130}$ construct lacks the binding domains through which other proteins are known to bind to caspase-9 and the apoptosome, i.e. caspase-3 and XIAP. Thus, isolation of an apoptosome using this construct would have only enabled identification of protein associating with Apaf-1. Consequently, a series of full-length caspase-9 TAP-tagged constructs were designed and produced, with a view to isolating an intact apoptosome from apoptotic cells (Chapter 5).

Chapter 5

Tandem-Affinity Tagged Caspase-9 Variants Induce Apoptotic Cell Death In Hela Cells

5.1 Introduction

In the two previous chapters I have characterised the interaction between an affinity-tagged truncated caspase-9 fusion protein ($Casp9^{1-130}$) and Apaf-1 in both cell lysates (Chapter 3) and in apoptotic cells (Chapter 4). Briefly, in cell lysates GST-$Casp9^{1-130}$ binds to Apaf-1 after oligomerisation induced by dATP and cytochrome *c*. This results in the formation of an inactive apoptosome, which can no longer recruit and process caspases. When transfected into HeLa cells, $Casp9^{1-130}$-GTC effectively inhibits spontaneous and Etoposide-induced apoptosis by selectively binding to Apaf-1 via CARD:CARD interactions, albeit independently of detectable cytochrome *c* release.

The proteomic studies performed in cell lysates revealed that the GST-$Casp9^{1-130}$-inhibited apoptosome only contained Apaf-1 and cytochrome *c* (Chapter 3). However, the truncated form of caspase-9 used in that study did not allow protein interactions with the large and small subunits of caspase-9 to be detected. Furthermore, it appeared that the truncated nature of this fusion protein might result in its constitutive binding to Apaf-1 when expressed in HeLa cells (Chapter 4). It was therefore logical to produce TAP-tagged full-length caspase-9 constructs, which could then be transfected into cells. Their effects on apoptotic cell death could then be evaluated, with a view to producing stably expressing cells from which to isolate and characterise an apoptosome from an apoptotic cell.

A series of constructs were designed and produced as shown in Figure 5.1.1. These constructs include those containing point mutations in order to characterise any potential effects on apoptosis, and any protein-protein interactions. A caspase-3 non-cleavable caspase-9 construct (D330A Caspase-9) was produced to suppress apoptosis by preventing the feed-back amplification loop (Srinivasula *et al*, 1998). A catalytically inactive caspase-9 mutant (C287A Caspase-9) was also created and was predicted to act as a dominant negative inhibitor (Li *et al*, 1997; Pan *et al*, 1998b; Srinivasula *et al*, 1998). This variant could potentially be used to identify any proteins associating with the apoptosome in the absence of effector caspase activation. Furthermore, the point mutation in the CARD domain which abrogates Apaf-1 binding was introduced (R56A, Qin *et al*, 1999; Chapter 4). This mutation is crucial as it allows the dissection of apoptosome-dependent

interactions or events. The predicted outcomes of transient expression of the constructs on apoptosis are shown in Figure 5.1.1, and in this chapter their effects on apoptotic cell death were investigated.

Full-length caspase-9

Caspase-9 variant	Structure	Mutation effect and predicted biological consequence
Caspase-9	1 416	Binds to Apaf-1 Enhances apoptosis
R56A Caspase-9	1 R56A 416	Does not bind to Apaf-1 No effect on apoptosis
D330A Caspase-9	1 D330A 416	Binds to Apaf-1 Not processed to p37 Apoptosis retarded
R56A D330A Caspase-9	1 R56A D330A 416	Does not bind to Apaf-1 Not processed to p37 No effect on apoptosis
C287A Caspase-9	1 C287A 416	Binds to Apaf-1 No catalytic activity
R56A C287A Caspase-9	1 R56A C287A 416	Does not bind to Apaf-1 No catalytic activity

Figure 5.1.1: Mutations created and cloned into GTC expression vectors.
These variants were used investigate any effects on apoptosis and protein interactions resulting from their expression.

5.2 Results

5.2.1 Transient transfection of wt/D330A Caspase-9-GTC results in processing of the fusion protein.

Based on the results from Chapter 4, I designed and prepared both N- and C-terminally tagged caspase-9 constructs and initial experiments were performed to determine the expression levels of these TAP-tagged variants (Figure 5.2.1). Transient transfection experiments revealed that the N-terminally tagged wild-type (wt) and D330A Caspase-9 variants were expressed at very low levels compared with the C-terminally tagged versions (Figure 5.2.1, lanes 2 & 3 compare with lanes 5 & 6). Due to the low expression of the N-terminally tagged Caspase-9-GTCs and the abrogated binding previously observed between Apaf-1 and the N-terminally tagged $Casp9^{1-130}$ variant (Chapter 4), I decided to concentrate only on the C-terminally TAP-tagged caspase-9 constructs (Caspase-9-GTC). Significantly, it was observed that whilst the full-length p78 form of Caspase-9-GTC was being efficiently expressed in the transfected cells, the wt and D330A fusion proteins had also been processed (Figure 5.2.1, lanes 4-6). This processing resulted in the appearance of smaller sized fragments (p34/p35) correlating to processing at Ser306 and Asp315, respectively (Li *et al*, 1997; Srinivasula *et al*, 1998). In addition, wt Caspase-9-GTC was also processed to form the p37 fragment (Figure 5.2.1, lane 5), which was not observed in cells transfected with the D330A non-cleavable mutant form (lane 6). For clarity, the different cleavage permutations of the TAP tagged constructs are depicted in Figure 5.2.2.

5.2.2 The processing of wt/D330A Caspase-9-GTCs results in apoptosis of transfected cells with cytochrome *c* release and caspase activation.

As the Caspase-9-GTC variants were being processed, it was important to establish whether this was resulting in caspase-3 activation and thus inducing apoptosis in the transfected cells. In order to specifically measure apoptosis in cells expressing the caspase-9-GTC variants, HeLa cells were co-transfected with GFP, which fluoresces green under UV light. Cell counting was performed on >300 green fluorescent cells and cell death determined as cell rounding and detachment (as described in Srinivasula *et al*, 2000). Compared to vector-transfected cells,

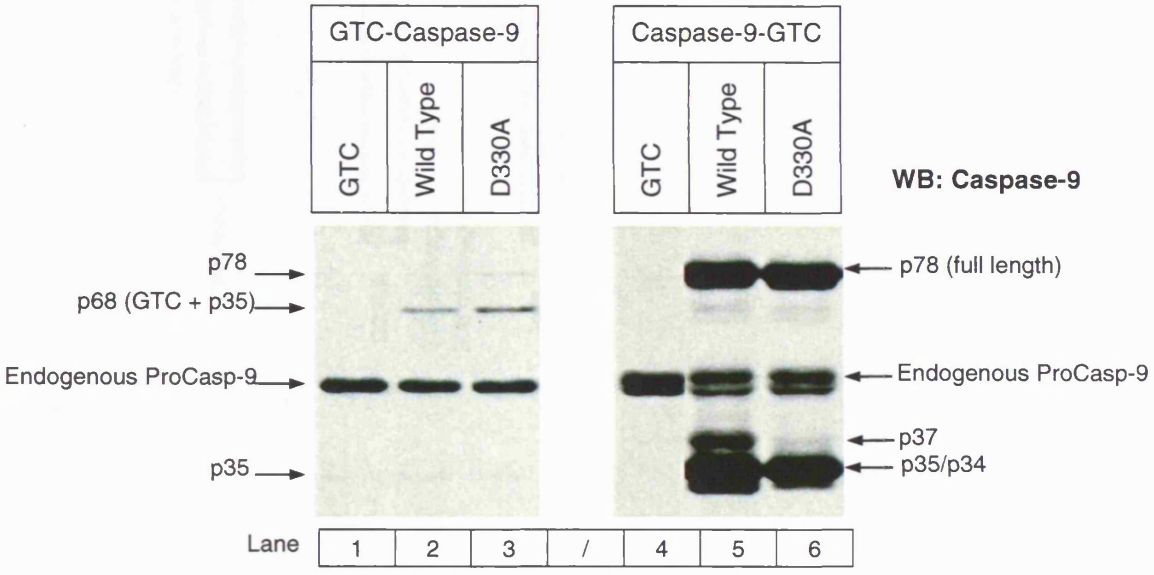

Figure 5.2.1: Expression of Caspase-9-GTC variants is considerably higher than that of the GTC-Caspase-9 fusion proteins. HeLa cells were seeded at 8 x 10^4 cells/well for 24 h, and then transfected with either N-terminally or C-terminally tagged GTC, wt Caspase-9 or D330A Caspase-9 for a further 18 h. Cells were harvested and cell lysates produced by freeze/thawing and 10,000 x g centrifugation. Protein samples (20 µg/lane) were then separated by SDS-PAGE and analysed by immunoblotting for caspase-9.

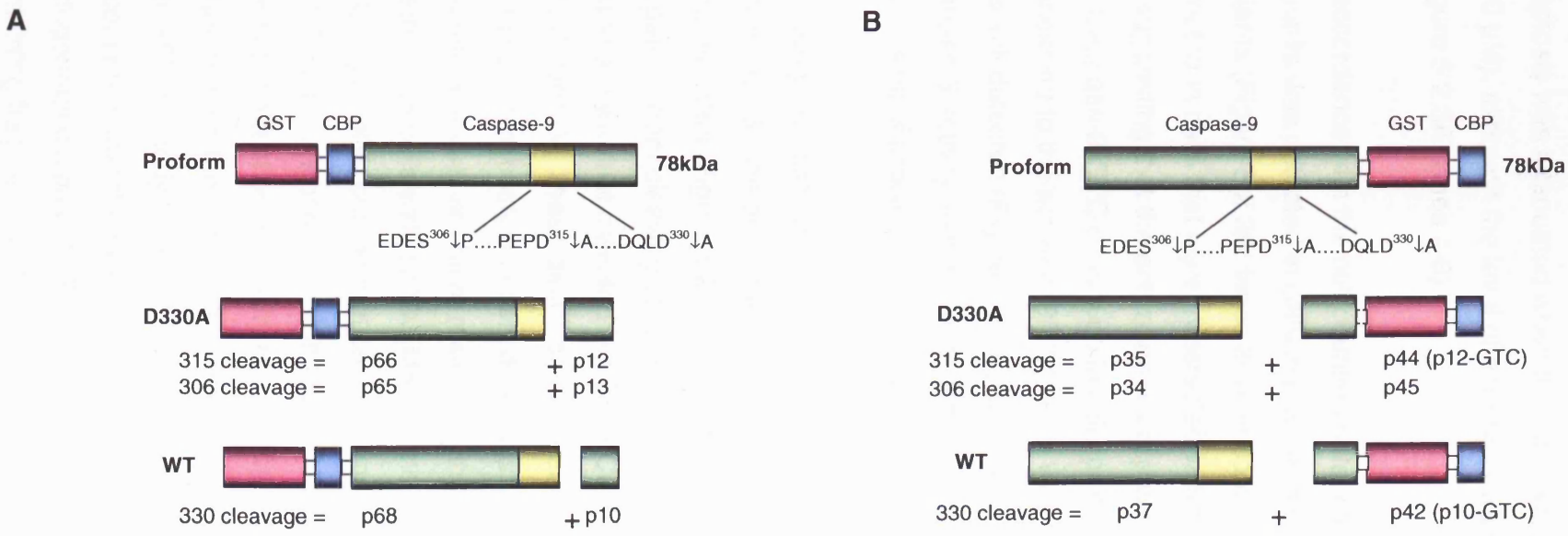

Figure 5.2.2: Schematic of how the GTC tagged caspase-9 constructs can be processed. A, GTC-Caspase-9 forms large molecular weight fragments when processed (66-69 kDa). **B**, In contrast, Caspase-9-GTC forms fragments usually seen by caspase-9 processing (p35, p37) and in addition the p12/p10 subunits can be detected as they now form p44/p42 fragments due to the addition of the GTC tag.

transfection of both the wt and D330A Caspase-9-GTC variants induced substantial apoptosis (Figure 5.2.3A, lanes 1-3). This transfection-induced apoptosis was attenuated when the cells were pretreated with zVAD.FMK (100 μM), although the level of apoptosis was still not reduced to basal levels (Figure 5.2.3A, lanes 4-6).

In accordance with the cell counting data, caspase-3 processing to the p19/p17 subunits was detected in cells that were transfected with the Caspase-9-GTC variants (Figure 5.2.3B, lanes 2-3). In contrast, processing of caspase-3 was not detected in cells that were transfected with the vector alone (Figure 5.2.3B, lane 1), suggesting that the activation of caspase-3 was as a result of transfection of the Caspase-9-GTC construct. In cells pretreated with zVAD.FMK, caspase-3 processing to the active p19/p17 forms was inhibited, although the p20 fragment was still detected (Figure 5.2.3B, lanes 4-6). These observations suggest that caspase-3 activity was markedly inhibited by zVAD.FMK, but that caspase-9 processing of procaspase-3 to the p20 subunit was less affected.

As seen previously, in addition to the full-length wt and D330A Caspase-9-GTC variants (p78), the processed caspase-9 fragments p37 (wt only) and p35/p34 were detected (Figure 5.2.3C, lanes 1-3). The mutation at Asp330 prevented caspase-3 from cleaving caspase-9 at this position and therefore the p37 form of caspase-9 was not detected in D330A Caspase-9-GTC transfected cells (Figure 5.2.3C, lane 3). These data also suggested that the Caspase-9-GTC variants were being spontaneously processed, because any processing of endogenous caspase-9 should still have resulted in the formation of the p37 fragment. Pre-treatment of cells with zVAD.FMK had no affect on the processing of Caspase-9-GTC to p35/p34, but did reduce the amount of p37 detected (Figure 5.2.3C, lanes 4-6). This is in accordance with the fact that zVAD.FMK was having a more significant effect on the ability of caspase-3 to feed back and process caspase-9, rather than on the autocatalytic activity of Caspase-9-GTC. Immunoblotting with an anti-GST antibody to detect the Caspase-9-GTC variants (Figure 5.2.3D, lanes 1-3) confirmed that the fusion proteins were being processed rather than endogenous caspase-9. Expression of wt Caspase-9-GTC produced a GST-containing fragment of 42 kDa (p10-GTC) whereas the D330A mutant produced a 44 kDa fragment (p12-GTC). In the presence of zVAD.FMK, only the p44 form was

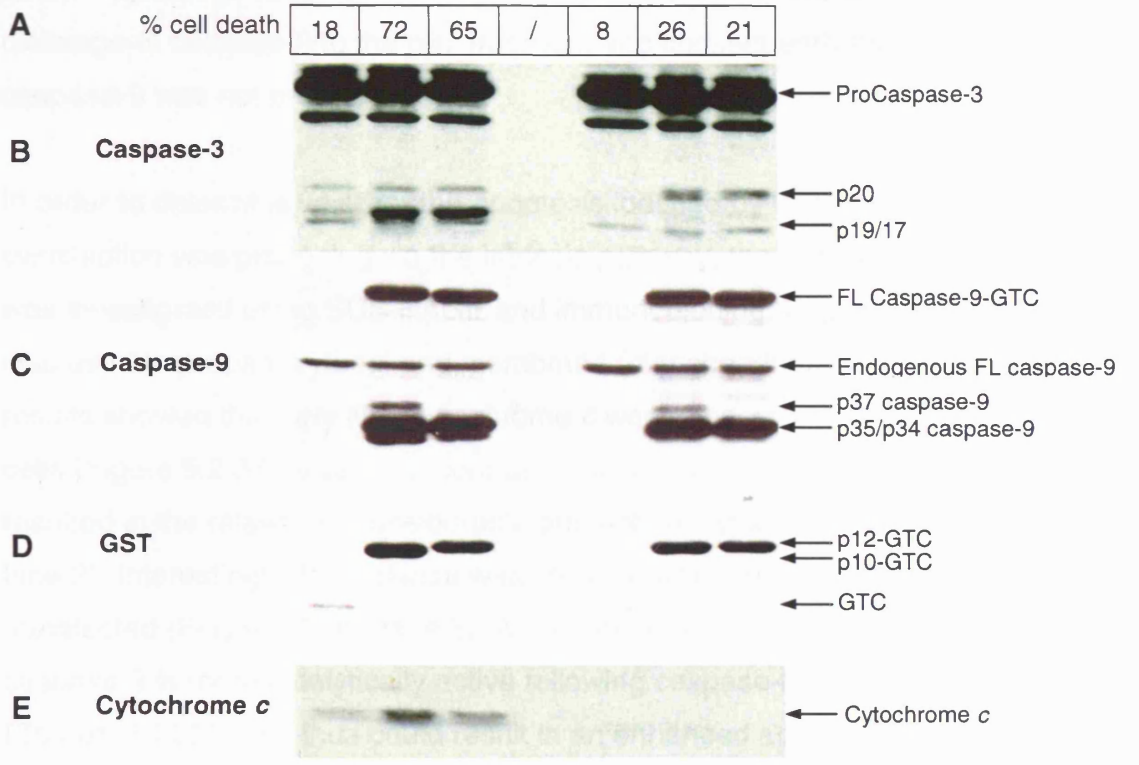

Lane	1	2	3		4	5	6
GTC	+	-	-		+	-	-
Casp-9-GTC	-	+	-		-	+	-
D330A Casp-9-GTC	-	-	+		-	-	+
100 μM zVAD.FMK	-	-	-		+	+	+

Figure 5.2.3: Transient transfection of Caspase-9-GTC (WT and D330A) induced cell death, accompanied by caspase activation and cytochrome *c* release. HeLa cells (1.25×10^5) were co-transfected with GFP (0.25 μg) and either GTC, Caspase-9-GTC, or D330A caspase-9-GTC (0.75 μg) for 18 h. Cell death was measured by counting the rounded and detached GFP-expressing cells. Data expressed as mean (n=3) for control transfections and the average (n=2) for zVAD.FMK pretreated cells (**A**). Cell lysates were then produced by freeze/thawing and 10,000 x g centrifugation (**B-D**), or by Digitonin treatment and 13,000 rpm centrifugation (**E**). Lysates (20 μg) were separated by SDS-PAGE and immunoblotted for caspase-3, caspase-9 and GST (**B-D**). Cytochrome *c* was detected in 15 μg of cytosolic protein following SDS-PAGE (**E**).

detected for both the wt and mutant Caspase-9-GTC variants (Figure 5.2.3D, lanes 4-6). These observations confirm that zVAD.FMK inhibited caspase-3 cleavage of caspase-9 to the p37 fragment and consequently the p10 subunit of caspase-9 was not produced.

In order to determine whether the apoptosis induced by Caspase-9-GTC transfection was preceding via the intrinsic pathway, the release of cytochrome *c* was investigated using SDS-PAGE and immunoblotting. Digitonin permeabilisation was used to prepare cytosol and membrane (mitochondrial) fractions, and the results showed that very little cytochrome *c* was released in vector-transfected cells (Figure 5.2.3E, lane 1). In contrast, transfection of the wt Caspase-9-GTC resulted in the release of considerable amounts of cytochrome *c* (Figure 5.2.3E, lane 2). Interestingly, this release was reduced when the D330A mutant was transfected (Figure 5.2.3E, lane 3). A possible reason for this could be that caspase-9 is more catalytically active following caspase-3 cleavage at Asp330 (Zou *et al*, 2003) and thus could result in an enhanced apoptotic response. However, this was a result from a single experiment and therefore may not truly reflect the impact of the D330A mutant on cytochrome *c* release. Pre-treatment with zVAD.FMK completely abrogated the release of cytochrome *c* induced by Caspase-9-GTC transfection (Figure 5.2.3E, lanes 4-6). This suggested that the release of cytochrome *c* was a caspase-dependent event and occurred secondarily to the activation and initial processing of the Caspase-9-GTC variants.

5.2.3 A point mutation at Arg56 in the CARD domain of caspase-9 suppresses apoptosis induced by the Caspase-9-GTC variants

As shown previously in Chapter 4 and independently by others (Qin *et al*, 1999) the R56A mutant of caspase-9 is unable to bind to the CARD domain of Apaf-1. This therefore provides a tool with which to investigate whether the effects seen above with the Caspase-9-GTC variants are due to the formation of an apoptosome. The spontaneous apoptosis induced by the transfection of the Caspase-9-GTC construct was suppressed by ~50% by introduction of the R56A mutation (Figure 5.2.4A, lower panel). In accordance with the cell death data, cleavage of PARP to the p86 fragment was also significantly reduced in R56A

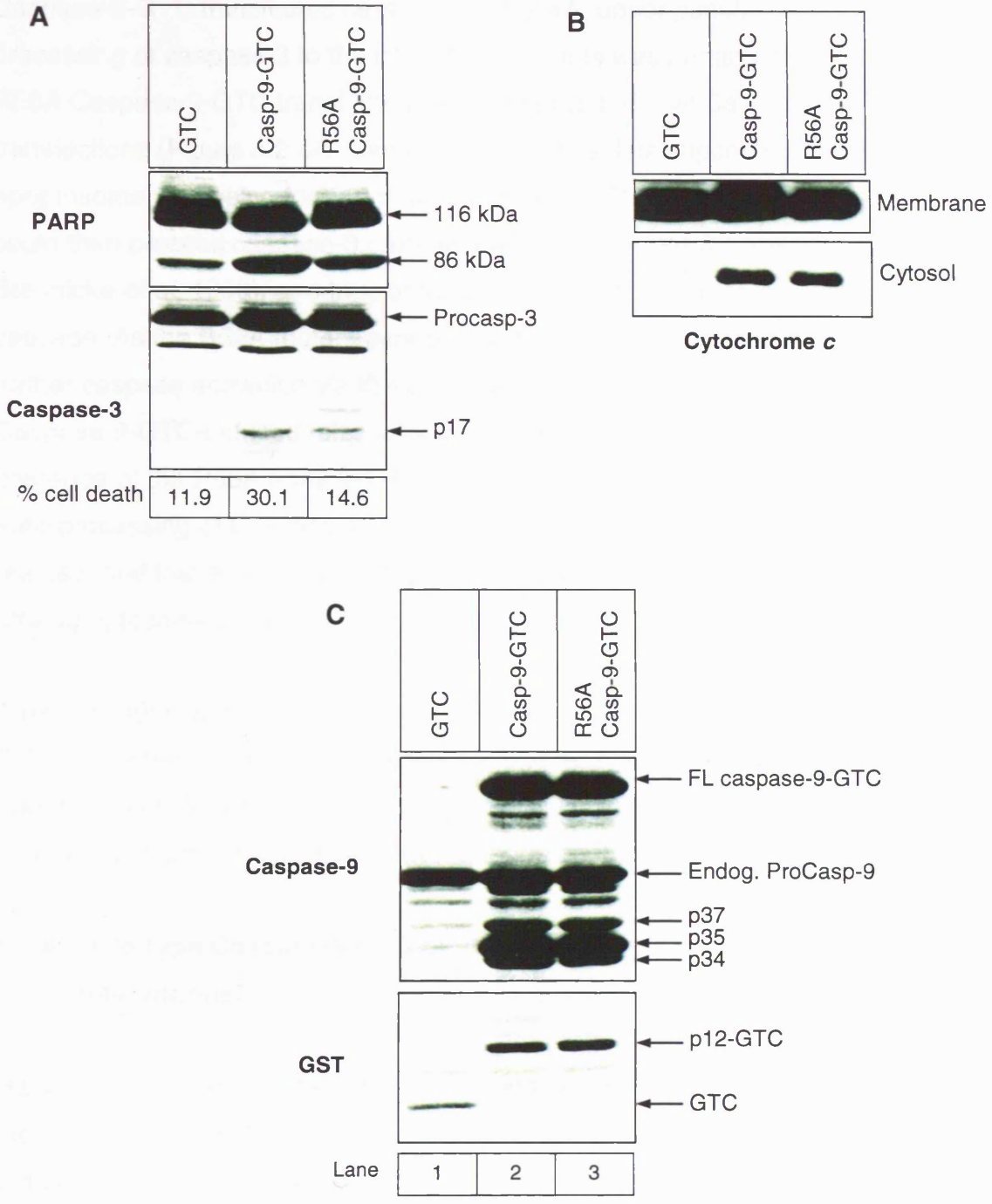

Figure 5.2.4: R56A Caspase-9-GTC suppresses apoptosis, but still results in cytochrome *c* release and Caspase-9-GTC processing. HeLa cells (1.25×10^5) were co-transfected with GFP and either GTC, Caspase-9-GTC or R56A Caspase-9-GTC for 18 h. Apoptosis in transfected cells was determined as described previously. Data expressed as the average of two representative experiments. Cells were then harvested and cell lysates produced by Digitonin treatment. The membranous fraction was resuspended in PBS, sonicated and 20 μg separated by SDS-PAGE and immunoblotted for PARP (**A**, top panel). The cytosol (20 μg) was analysed for caspase-3 processing (**A**, bottom panel). The release of cytochrome *c* was assessed by SDS-PAGE of cytosol (15 μg) and membrane (15 μg) and immunoblotting for cytochrome *c* (**B**). Caspase-9 and GST were detected in 20 μg cytosolic protein (**C**).

Caspase-9-GTC transfected cells (Figure 5.2.4A, upper panel). Furthermore, the processing of caspase-3 to the p19/p17 fragments was partially attenuated in R56A Caspase-9-GTC transfected cells compared with wt Caspase-9-GTC transfections (Figure 5.2.4A, centre panel). These data suggested that an apoptosome was being formed in wt Caspase-9-GTC transfected cells, which could then process caspase-3 more efficiently (Rodriguez & Lazebnik, 1999; Stennicke *et al*, 1999), and thus amplify the initial activation of the caspase cascade. As the R56A mutant cannot bind to Apaf-1, it was unable to promote further caspase activation via this caspase-activating complex. Interestingly, the Caspase-9-GTC-induced release of cytochrome *c* was partially attenuated by the presence of the R56A mutation (Figure 5.2.4B). This observation suggests that the auto-processing of Caspase-9-GTC is sufficient to promote the initial cytochrome *c* release, and that a secondary caspase-dependent release of cytochrome *c* occurs after apoptosome formation.

Taken together with the equivalent processing of the wt and R56A Caspase-9-GTCs detected (Figure 5.2.4C, lanes 2 & 3), these observations suggest that an apoptosome is formed subsequent to the initial processing of Caspase-9-GTC and that this is in turn enhancing the spontaneous apoptosis observed.

5.2.4 Wild-type Caspase-9-GTC binds to Apaf-1 via CARD: CARD interactions.

Having established that the initial processing of Caspase-9-GTCs is occurring independently from the apoptosome and inducing apoptosis, the subsequent predicted association between Apaf-1 and the Caspase-9-GTC variants was investigated. A GSH pull-down experiment was consequently performed on lysates from transfected cells (Figure 5.2.5). When comparable expression and processing of wt and R56A Caspase-9-GTC variants was achieved (Figure 5.2.5, centre and lower panel), only the wt Caspase-9-GTC was able to bind to Apaf-1 (top panel). These observations showed that only the wt variant could form an active apoptosome with Apaf-1 and subsequently activate caspase-3 to induce PARP cleavage and cell death. In contrast, the R56A mutant could induce autocatalytic processing of itself outside of an apoptosome, and in this way could

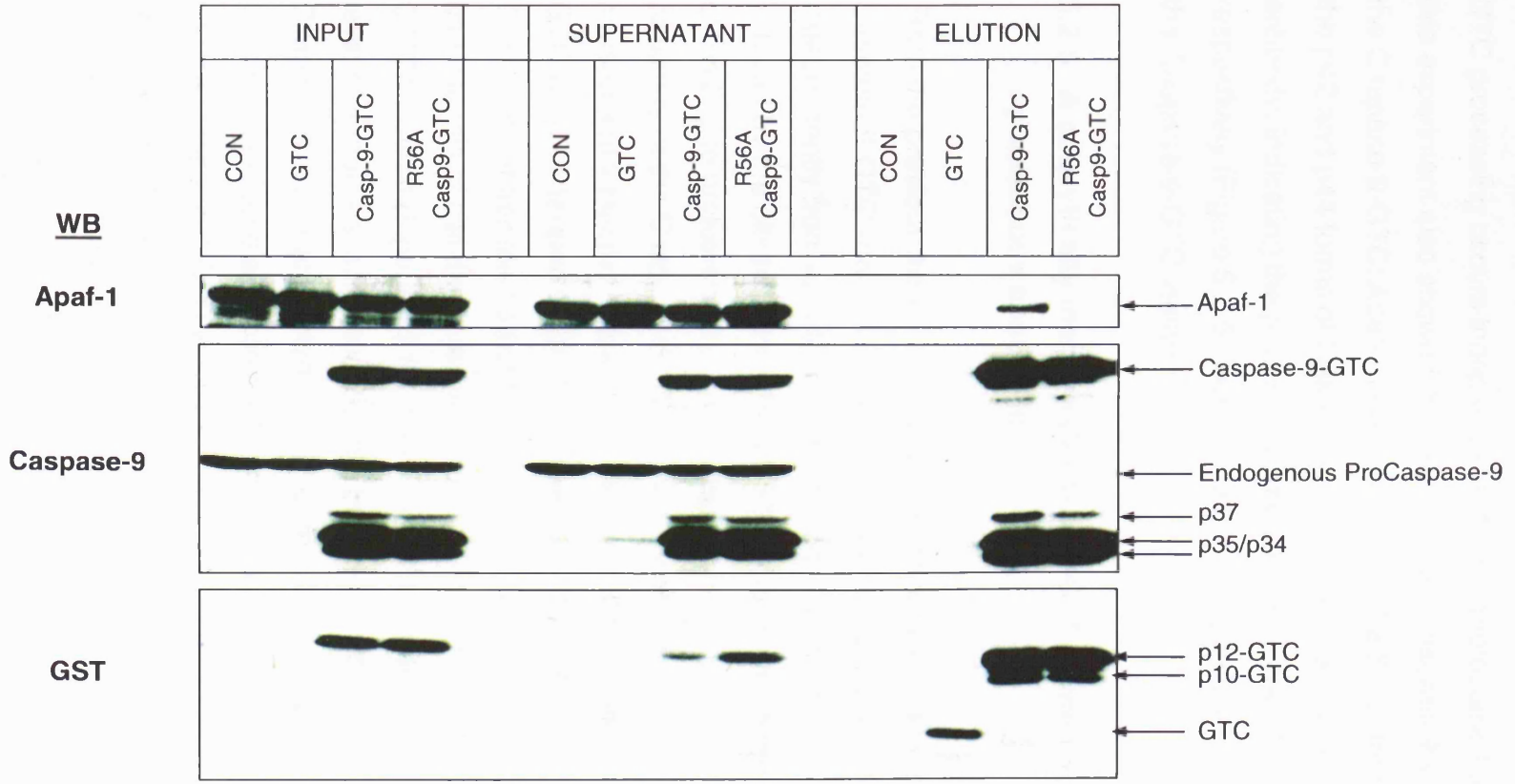

Figure 5.2.5: Wild type Caspase-9-GTC is able to bind to Apaf-1, but not Caspase-9-GTC containing a mutated R56 residue. HeLa cells (3.75×10^5) were transfected with FuGENE/optimem (control), GTC, Caspase-9-GTC or R56A Caspase-9-GTC for 18 h. The cells were then harvested and cell lysates produced by freeze/thawing and 10,000 x g centrifugation (input). The lysates (100 µl) were then incubated with 150 µl GSH-Sepharose beads and 100 µl assay buffer for 1 h at 4 °C. The beads were recovered (supernatant) and washed thoroughly before eluting in SDS sample buffer (elution). Samples were then separated by SDS-PAGE and Apaf-1, caspase-9 and GST detected by immunoblotting.

still activate small amounts of caspase-3. These data also confirm that Caspase-9-GTC processing occurs independently from apoptosome formation. Significantly, this experiment also showed that endogenous caspase-9 was not associated with the Caspase-9-GTC: Apaf-1 complex (Figure 5.2.5, centre panel). Furthermore, the p42 and p44 forms of Caspase-9-GTC were detectable with the anti-GST antibody, indicating the presence of the p10-GTC and p12-GTC fragments, respectively (Figure 5.2.5, lower panel), thus again confirming the processing of the Caspase-9-GTC variants.

5.2.5 A catalytically inactive Caspase-9-GTC mutant is unable to induce spontaneous apoptosis.

From the previous experiments it can be concluded that the processing of the Caspase-9-GTC variants is occurring via an autocatalytic process occurring independently from apoptosome formation. This autoactivation could potentially be induced by the dimerisation of the GST domains within the TAP tag, or as a result of binding to proteins that can dimerise. To investigate whether the induced proximity of the Caspase-9-GTC variants was resulting in their activation and consequently leading to apoptosis, catalytically inactive mutants of Caspase-9-GTC were generated (C287A Caspase-9-GTC/ R56A C287A Caspase-9-GTC). The transient transfection of these constructs did not induce apoptosis, with only basal levels of cell death detected for C287A Caspase-9-GTC and the R56A C287A mutant (Figure 5.2.6A, lanes 1-3). Following an apoptotic stimulus, the level of apoptosis increased 2-3 fold in vector controls and in R56A C287A Caspase-9-GTC transfected cells (Figure 5.2.6A, lanes 4 & 6). However, Etoposide-induced apoptosis was completely inhibited in cells expressing the C287A Caspase-9-GTC variant (Figure 5.2.6A, lane 5). This observation was in accordance with the caspase-3 processing data (Figure 5.2.6B). Although caspase-3 was not processed in DMSO-treated cells (Figure 5.2.6B, upper panel lanes 1-3), it was significantly processed to the p19/17 fragments following treatment with Etoposide in both vector control and R56A C287A Caspase-9-GTC transfected cells (Figure 5.2.6B, upper panel lanes 4 & 6). Significantly, the expression of the C287A Caspase-9-GTC variant substantially reduced the Etoposide-induced processing of caspase-3 (Figure 5.2.6B, upper panel, lane 5). These data suggest that the C287A Caspase-9-GTC variant is acting as a

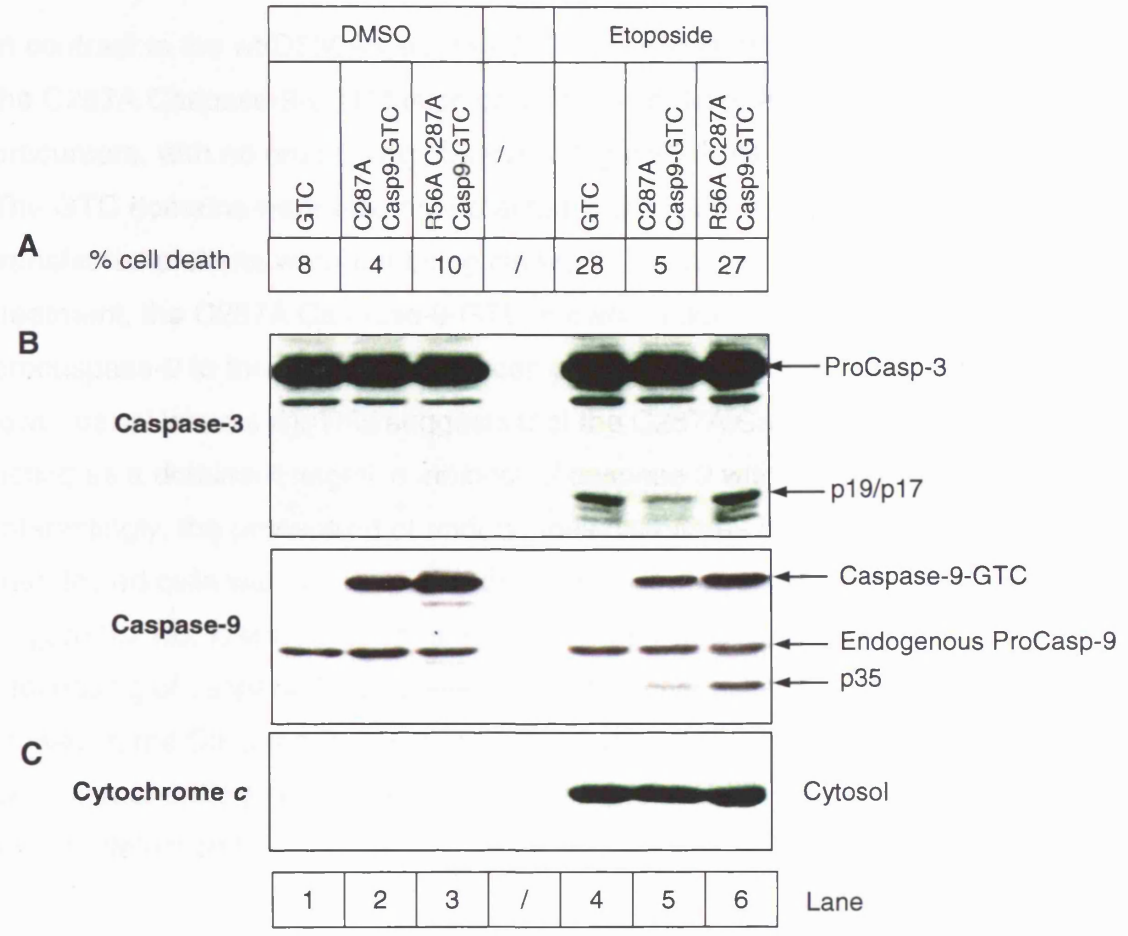

Figure 5.2.6: A catalytically inactive Caspase-9-GTC (C287A) is unable to induce spontaneous apoptosis, and also suppresses Etoposide-induced apoptosis.
HeLa cells (1.25 x 10^5) were co-transfected with GFP and either GTC, C287A Caspase-9-GTC or R56A C287A Caspase-9-GTC for 18 h prior to treatment with either vehicle (DMSO) or Etoposide (200 μM) for a further 24 h. Cell death was measured as previously described and data expressed as the average, n=2 (**A**). Cells were then harvested and cell lysates produced by Digitonin treatment and 13,000 rpm centrifugation. Processing of caspase-3 and caspase-9 was assessed in the cell lysates (20 μg protein/lane) via separation by SDS-PAGE and immunoblotting (**B**). Cytochrome *c* release was detected in the cell cytosol (15 μg), by immunoblotting (**C**).

dominant negative inhibitor. This would be predicted to occur via its ability to bind to Apaf-1, thereby preventing the activation of endogenous caspase-9 and subsequent initiation of the caspase cascade.

In contrast to the wt/D330A Caspase-9-GTC variants, the transient expression of the C287A Caspase-9-GTC fusion proteins were detected as their 78 kDa precursors, with no processing observed (Figure 5.2.6B, lower panel lanes 1-3). The GTC domains were also not detected in the lysates, confirming that the transfected proteins were not being cleaved (data not shown). Following Etoposide treatment, the C287A Caspase-9-GTC showed reduced processing of procaspase-9 to the p35 form when compared to the R56A mutant (Figure 5.2.6B, lower panel lanes 4-6). This suggests that the C287A Caspase-9-GTC is also acting as a dominant negative inhibitor of caspase-9 within the apoptosome. Interestingly, the processing of endogenous caspase-9 in vector-control transfected cells was not markedly detected following an apoptotic stimulus (Figure 5.2.6B, lower panel, lane 4). This result was unexpected, as the processing of caspase-3 suggested that active caspase-9 had been produced. However, the Caspase-9-GTC variants are over-expressed, and therefore the detection of endogenous caspase-9 processing could on comparison be below the level of detection.

In accordance with the absence of both spontaneous apoptosis and C287A Caspase-9-GTC processing, cytochrome *c* was not released in DMSO-treated cells (Figure 5.2.6C, lanes 1-3). However, the release of cytochrome *c* was induced following Etoposide treatment (Figure 5.2.6C, lanes 4-6). This observation suggested that the C287A/ R56A C287A Caspase-9-GTC variants had prevented activation of the caspase cascade via alternative pathways (i.e. autocatalytic activation via possible dimerisation), and instead could only be activated by an external apoptotic stimulus (Etoposide) that induced apoptosis via the formation of an apoptosome.

5.2.6 The catalytically inactive Caspase-9-GTC is able to bind Apaf-1 in the absence of cytochrome *c* release.

As the C287A Caspase-9-GTC was acting as a dominant negative inhibitor it could potentially be used to isolate the apoptosome for subsequent proteomic analysis, in a similar way as was initially proposed for the Casp9$^{1-130}$-GTC construct. However, to investigate apoptosis-induced apoptosome-specific interactions it is vital that the C287A Caspase-9-GTC variant only binds to Apaf-1 under Etoposide treatment conditions. Therefore the association between C287A Caspase-9-GTC and Apaf-1 was investigated with a GSH pull-down experiment in lysates from vehicle- and Etoposide-treated cells. On equivalent over-expression of C287A Caspase-9-GTC and the R56A mutant (Figure 5.2.7, bottom panel), Apaf-1 only bound to C287A Caspase-9-GTC (top panel). However, as had been seen previously with Casp9$^{1-130}$-GTC (Figure 4.2.6) this association was evident in both the DMSO and the Etoposide-treated cell samples (Figure 5.2.7), and again significantly in the absence of cytochrome *c* release (Figure 5.2.6C).

From the studies described above it can therefore be concluded that the wt/D330A Caspase-9-GTC variants can induce autocatalytic processing independently from the apoptosome, and can induce cell death by amplifying this apoptotic signal via the apoptosome. In contrast, the C287A Caspase-9-GTC variant acts as a dominant negative inhibitor of caspase-9 and inhibits apoptosome-mediated apoptosis. However, like the Casp9$^{1-130}$-GTC construct in Chapter 4, C287A Caspase-9-GTC can bind to Apaf-1 following both DMSO and Etoposide treatment.

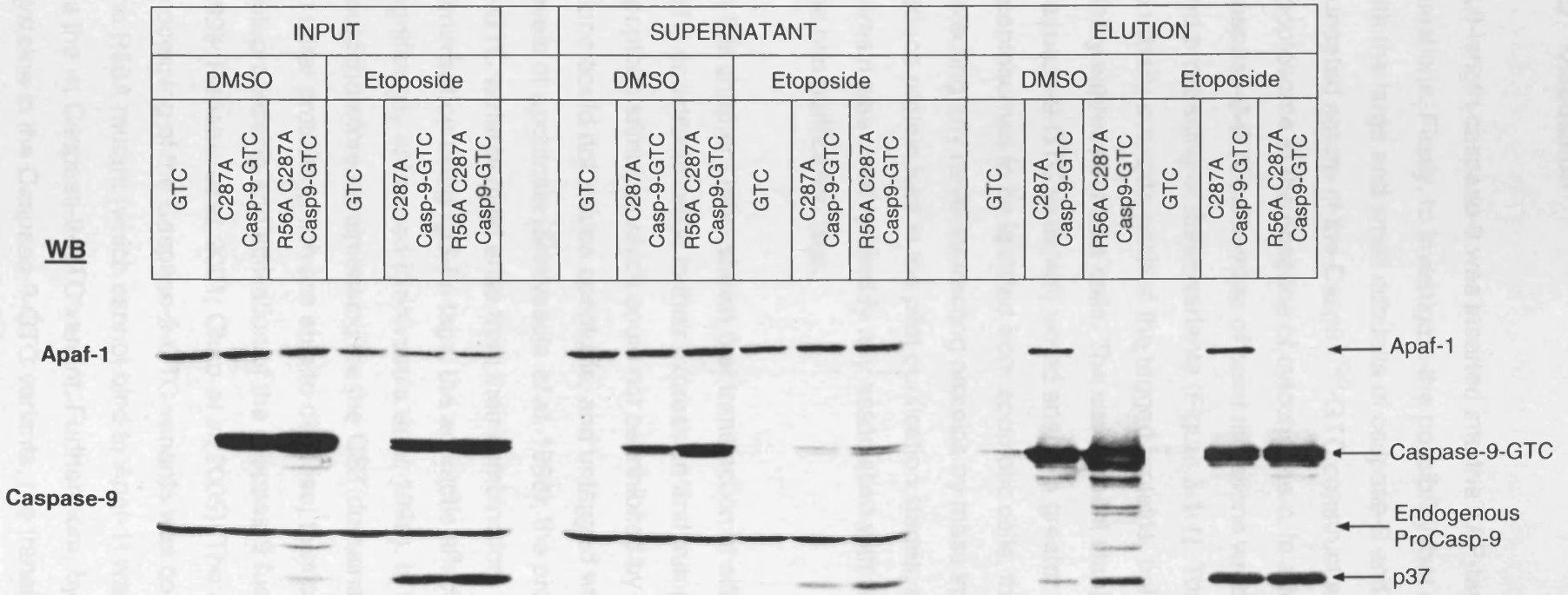

Figure 5.2.7: C287A Caspase-9-GTC binds to Apaf-1 in transfected HeLa cells in the absence of apoptotic stimuli. HeLa cells were transfected with empty vector (GTC), C287A Caspase-9-GTC, or the R56A mutant for 18 h prior to treatment with vehicle (DMSO) or Etoposide (200 μM). Following treatment cells were harvested and the PS exposure determined (data not shown). Cell lysates were then produced by freeze/thawing and 10,000 x g centrifugation. The lysate (100 μl) was then incubated 4 °C for 1 h with 150 μl washed GSH-Sepharose beads and 100 μl assay buffer, with continuous motion. The beads were then washed and eluted in 20 mM GSH. Samples were taken prior to bead incubation (input ~20 μg), after incubation (supernatant, ~20 μg) and the elution. Samples were separated by SDS-PAGE on 10% gels and immunoblotted for Apaf-1 and caspase-9.

5.3 Discussion

Full-length caspase-9 was inserted into the TAP-tag vector in order to address two questions. Firstly, to investigate the possibility that other proteins are interacting with the large and small subunits of caspase-9 and secondly, to see whether the truncated nature of the Casp9$^{1-130}$-GTC construct was permitting formation of an apoptosome in the absence of cytochrome *c*. In addition to wild-type (wt) Caspase-9-GTC, a number of point mutations were made to assess the binding and processing of these variants (Figure 5.1.1). This study was therefore designed to initially evaluate each of the tagged proteins, before deciding on which to then stably express in HeLa cells. The subsequent stable expression of the chosen Caspase-9-GTC variant(s) would enable a greater quantity of purified apoptosomes to be isolated from apoptotic cells, thus improving the probability of detecting any novel interacting proteins by mass spectrometry. However, to reduce protein loss in the pilot purification stages, only purification via the GST domain was used to identify any association with Apaf-1, despite the presence of the two purification tags.

In this chapter I have shown that transfection of either wt or D330A Caspase-9-GTC constructs result in their expression and autoprocessing in the absence of an apoptotic stimulus, which could not be inhibited by zVAD.FMK. As the GTC vector alone could not induce apoptosis, and untagged wt caspase-9 only induces low levels of apoptosis (Srinivasula *et al*, 1998), the proapoptotic effect of the caspase-9-GTC variants must arise from their combination. By inducing caspase-9 dimerisation using IgG-Fc tags, the apoptotic effect of caspase-9 could be significantly enhanced (Srinivasula *et al*, 1998). In the present study, the GTC tag could therefore be dimerising via the GST domains (Parker *et al*, 1990) or binding to other proteins which are able to dimerise, thus providing a scaffold for the autoprocessing and activation of the caspase-9 fusion proteins (Salvesen & Dixit, 1999; Renatus *et al*, 2001; Chao *et al*, 2005). The apoptosome-independent processing of the Caspase-9-GTC variants was confirmed by the observation that the R56A mutant (which cannot bind to Apaf-1) was processed to the same extent as the wt Caspase-9-GTC variant. Furthermore, by mutating the active site cysteine in the Caspase-9-GTC variants, the transfection-induced auto-processing

was averted, indicating that the Caspase-9-GTC variants were processed by autocatalytic cleavage and not via endogenous caspase-9.

Whereas the inactive caspase-9 zymogen exists as a monomer (Boatright *et al*, 2003), the active form of the caspase is a dimer (Renatus *et al*, 2001). However, unlike effector caspases, processing of caspase-9 is unnecessary and insufficient to produce a fully active enzyme (Stennicke *et al*, 1999; Bratton *et al*, 2001b). Instead caspase-9 requires allosteric changes to allow the formation of a fully active site, which occurs when bound to oligomerised Apaf-1 (Rodriguez & Lazebnik, 1999). Caspase-9 and Apaf-1 form an active holoenzyme, which is significantly more effective at processing caspase-3 than uncomplexed processed caspase-9 (Rodriguez & Lazebnik, 1999; Stennicke *et al*, 1999). In accordance, the autocatalytic processing of the Caspase-9-GTC variants resulted in the limited processing of caspase-3, and required the formation of the apoptosome to induce significant caspase-3 processing and apoptotic cell death. The R56A mutant couldn't bind to the apoptosome and thus suppressed the transfection-induced apoptosis.

The process via which the processed Caspase-9-GTC variants were inducing apoptosome formation was not clearly defined in this study. However, caspase-3 can cleave the proapoptotic Bcl-2 family member Bid, either directly or indirectly via caspase-8 (Li *et al*, 1998; Bossy-Wetzel & Green, 1999; Tang *et al*, 2000). Truncated Bid (tBid) can then induce the release of cytochrome *c* from the mitochondria (Gross *et al*, 1999a), required for the formation of the apoptosome (Liu *et al*, 1996). In support of this hypothesis, zVAD.FMK prevented the release of cytochrome *c* in cells transfected with either wt or D330A Caspase-9-GTC constructs, indicating that its release was caspase-dependent and not as a result of direct insult on the mitochondria. The resulting apoptosome can then either recruit Caspase-9-GTC variants or endogenous caspase-9. As caspase-9 has greater catalytic activity when bound to Apaf-1 (Rodriguez & Lazebnik, 1999; Stennicke *et al*, 1999), the active apoptosome can then result in significant caspase-3 processing and subsequently cell death. For clarity, a schematic of this hypothesis is depicted in Figure 5.2.8. However, when the active site cysteine was abrogated (C287A), Caspase-9-GTC was no longer spontaneously processed and instead acted as a dominant negative inhibitor in the Etoposide-induced

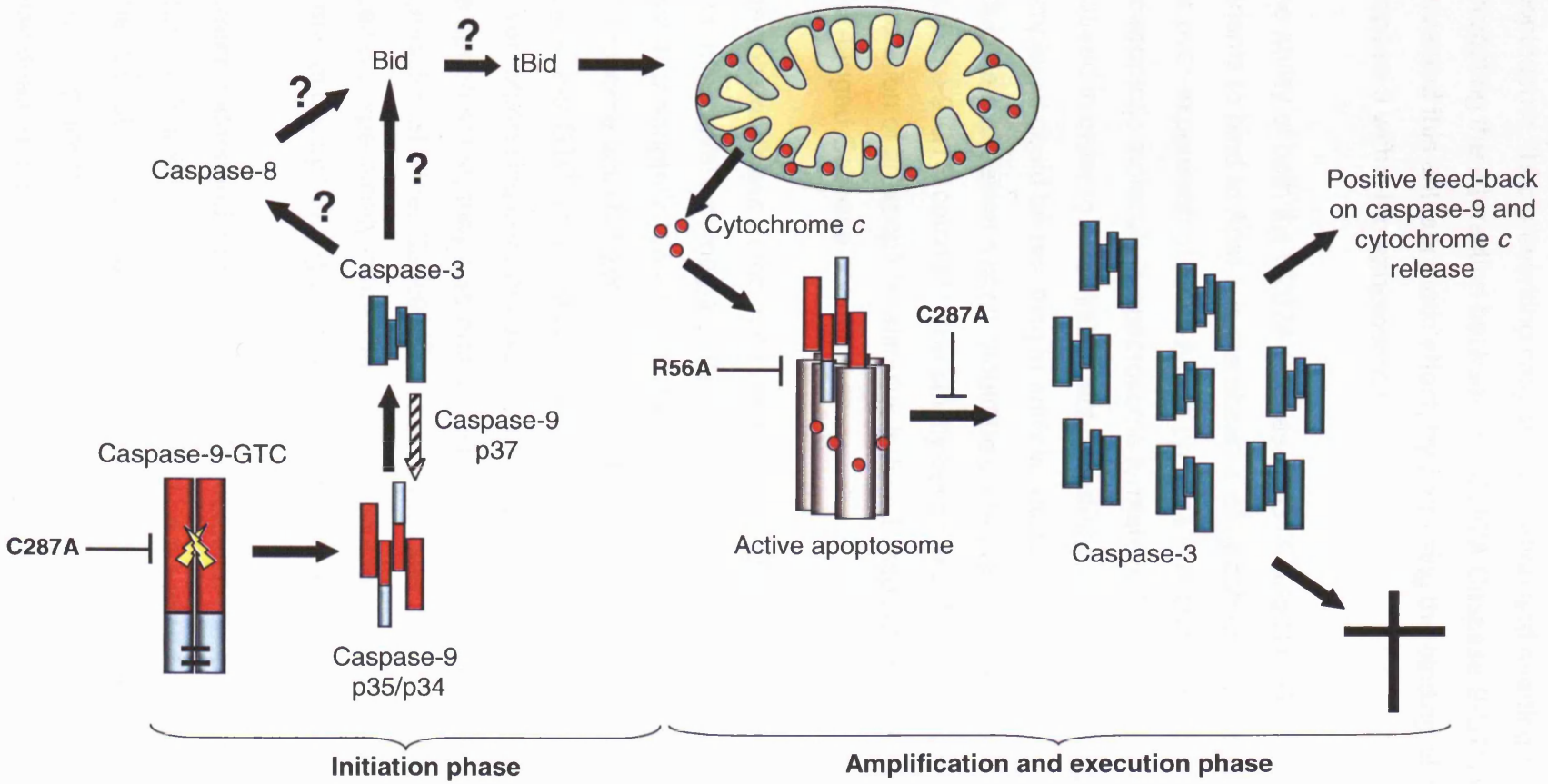

Figure 5.3.1: Schematic of how Caspase-9-GTC's are affecting the intrinsic apoptotic pathway. GST domains in the GTC are possibly dimerising and inducing Caspase-9-GTC autoprocessing (prevented in C287A mutants). This is followed by limited caspase-3 activation that then induces cytochrome *c* release via cleavage of Bid either directly, or through the activation of caspase-8. The formation of an apoptosome with the Caspase-9-GTC (but not in R56A mutants) can then occur and in turn can enhance apoptosis by processing more caspase-3 and downstream targets such as PARP. Binding of C287A Caspase-9-GTC results in the formation of an inactive apoptosome, preventing activation of effector caspases and consequently inhibits apoptosis.

apoptosome, thus preventing caspase activation and averting cell death. Abrogating the interaction between the C287A Caspase-9-GTC variant and Apaf-1 prevented this anti-apoptotic effect, by permitting the binding of endogenous caspase-9 within the apoptosome.

The ability of both the C287A Caspase-9-GTC and Casp9$^{1-130}$-GTC (Chapter 4) variants to bind to Apaf-1 in the absence of cytochrome *c* release, suggests that the over-expression of these fusion proteins is circumventing the need for this proapoptotic molecule in apoptosome formation. Thus, although high expression is required in order to potentially identify proteins associated with the apoptosome complex, it could be resulting in artificial interactions. It therefore appears that an inducible expression system would be preferable, as the levels of expression of Caspase-9-GTC could then be strictly controlled. This could result in the generation of an apoptotic stimulus-induced association between Apaf-1 and a TAP-tagged Caspase-9 variant.

The constructs evaluated in this chapter (and in Chapter 4) will not be used further to identify novel binding partners of the apoptosome (due to constitutive binding to Apaf-1 or apoptotic tendencies). However, two dominant negative inhibitors of apoptosome activity have been characterised (Casp9$^{1-130}$-GTC or C287A Caspase-9-GTC) and could be used to dissect the intrinsic pathway. Although Bcl-2 over-expressing cells are available to evaluate observations in the absence of the apoptosome, they also prohibit mitochondrial involvement. In contrast, the expression of either Casp9$^{1-130}$ or the catalytically inactive mutant caspase-9 within a cell can specifically inhibit the intrinsic apoptotic pathway, after mitochondrial perturbation, by forming an inactive apoptosome.

Current understanding of the Fas or TRAIL death receptor pathways that use the mitochondrial arm for amplification, could be advanced by using cells expressing either Casp9$^{1-130}$-GTC or C287A Caspase-9-GTC. Furthermore, the role of sensitising agents (such as HDAC inhibitors) in potentiating apoptosis induced by these death receptors could also be further assessed in cells transfected with these dominant negative inhibitors. In such studies where the dominant negative nature of these proteins is their main role, the TAP tag could be removed in order to prevent autoactivation or any steric hindrances from occurring.

Chapter 6

Characterisation of the Apoptosome and a Novel Active Caspase-7 Complex in MCF-7 Cells

6.1 Introduction

The MCF-7 cell line was derived from a patient with metastatic breast cancer in 1970, and was established as the first hormone-responsive breast cancer cell line (Reviewed in Simstein *et al*, 2003). Not only has this cell line advanced the understanding and treatment of oestrogen receptor-positive breast cancer, but it is also a model system for the study of apoptosis. As resistance to chemotherapy has become a major problem in the treatment of breast cancer, MCF-7 cells have been widely used to investigate the potential mechanisms of apoptosis in breast cancer cells.

Interestingly, it was discovered that MCF-7 cells do not express caspase-3 due to a 47-base pair deletion within exon 3 of the *CASP3* gene (Janicke *et al*, 1998a). This deletion results in abrogated translation of caspase-3 mRNA due to a frame shift and consequently the formation of a premature stop codon. This was initially thought to be the reason why these cells were increasingly resistant to apoptosis. However, MCF-7 cells have subsequently been shown to undergo apoptosis following activation of the intrinsic apoptotic pathway (Tang *et al*, 2000; Liang *et al*, 2001) and the death receptor-mediated pathway (MacFarlane *et al*, 2000). These findings suggest that in MCF-7 cells another effector caspase must be compensating for caspase-3 during the execution phase of apoptosis, and one potential candidate is caspase-7. Further to this, in caspase-3-null mice, strains that express higher levels of caspase-7 can inactivate the inhibitor of caspase-activated DNase (ICAD) (Houde *et al*, 2004), resulting in normal apoptotic DNA fragmentation in response to an apoptotic stimulus. However, although caspase-7 is able to compensate for caspase-3 in the cleavage of certain substrates (i.e. PARP, Germain *et al*, 1999; Slee *et al*, 2001; ICAD, Houde *et al*, 2004) it cannot compensate in the cleavage of certain other proteins (i.e. RIP, Topoisomerase I, STAT1 and vimentin, Slee *et al*, 1999; and Bid, Bossy-Wetzel & Green, 1999; Thornberry *et al*, 1997), despite caspase-3 and caspase-7 possessing a shared substrate recognition sequence (Thornberry *et al*, 1997).

Many anti-cancer drugs induce apoptosis via the intrinsic pathway (Reviewed in Simstein *et al*, 2003) with the formation of an apoptosome (Zou *et al*, 1999; Saleh *et al*, 1999; Cain *et al*, 1999), which in turn directly processes and activates the

inactive caspase-9 zymogen (Li *et al*, 1997; Srinivasula *et al*, 1998). Caspase-9 can then activate effector caspases, such as caspase-3 (which subsequently cleaves caspase-6) and caspase-7 (Li *et al*, 1997; Slee *et al*, 1999) resulting in cleavage of specific substrates, which leads to the dismantling of the cell. Interestingly, although caspase-7 is processed in dATP-activated cell lysates (Cain *et al*, 1999; Slee *et al*, 1999; Bratton *et al*, 2001a), and in cells treated with a range of apoptotic stimuli (Tang *et al*, 2000; MacFarlane *et al*, 2000; Liang *et al*, 2001), to date no-one has reported whether caspase-7 is activated at the apoptosome, in a manner analogous to that shown previously for caspase-3 activation (Cain *et al*, 1999; Bratton *et al*, 2001b; Twiddy *et al*, 2004; Chapter 3).

Therefore the main aims of this study were two fold; first, to establish whether an apoptosome is formed in the absence of caspase-3, and second, to ascertain whether caspase-7 is directly activated by the apoptosome. These aims were addressed using both an *in vitro* model of dATP activation in MCF-7 S-100 cell lysates and by examining the mechanism of caspase-7 activation in staurosporine (STS)-treated MCF-7 cells. In this study I show that following dATP activation, the ~700 kDa active apoptosome is formed in cell lysates and that it can directly process and activate caspase-7. The ~700 kDa apoptosome complex is also formed in MCF-7/WT cells treated with STS. Furthermore, in both dATP-activated cell lysates and in STS-treated MCF-7 cells, active caspase-7 is not freely available but is released from the apoptosome and forms a stable ~200 kDa complex comprising both active caspase-7 and XIAP.

6.2 Results

6.2.1 The dATP activation of MCF-7 cell lysates results in caspase processing.

The main aim of this project was to characterise the activity and function of the apoptosome in caspase-3-deficient cells. Initial experiments were therefore carried out to determine whether dATP activation could result in caspase processing in MCF-7/WT cell lysates. In order to identify any caspase-3-dependent events two additional MCF-7 cell lysates were produced: one from MCF-7 cells stably transfected with the caspase-3 gene (MCF-7/CASP3) and another from vector-only transfected MCF-7 cells (MCF-7/pcDNA3).

MCF-7 cell lysates were activated with dATP and cytochrome *c*, and the caspase-processing profiles analysed by SDS-PAGE and immunoblotting (Figure 6.2.1A-D). In addition, the DEVDase activity of the activated lysates was measured fluorometrically using Ac-DEVD.AFC (Figure 6.2.1E). Upon dATP activation, the caspase processing and DEVDase activity observed in MCF-7/WT and pcDNA3 cell lysates was comparable (Figure 6.2.1A-E, lanes 1-6). This observation showed that the stable transfection of the empty pcDNA3 vector does not alter the caspase activation mechanism of the cells, and therefore provides an excellent control cell line. In the absence of caspase-3, the dATP/cytochrome *c*-dependent processing of caspase-9 only produced the p35/p34 fragments (Figure 6.2.1A, lanes 1-6). However, when MCF-7/CASP3 cell lysates were activated in the presence of dATP and cytochrome *c*, caspase-9 was also processed to the p37 form (Figure 6.2.1A, lanes 7-9). This correlated with the processing of caspase-3 to the p20 and p19/p17 fragments (Figure 6.2.1C, Lanes 7-9). In accordance with the literature, caspase-3 was not detected in MCF-7/WT or MCF-7/pcDNA3 cell lysates (Jänicke *et al*, 1998; Figure 6.2.1C, lanes 1-6). Furthermore, caspase-8 was not processed under any of the lysate activation conditions tested (Figure 6.2.1B, lanes 1-9), thus suggesting that the caspase cascade was initiated by caspase-9 and the apoptosome, and not via caspase-8 activation.

In the absence of caspase-3, procaspase-7 was incompletely processed to produce only the p19 form of the caspase following dATP and cytochrome *c*

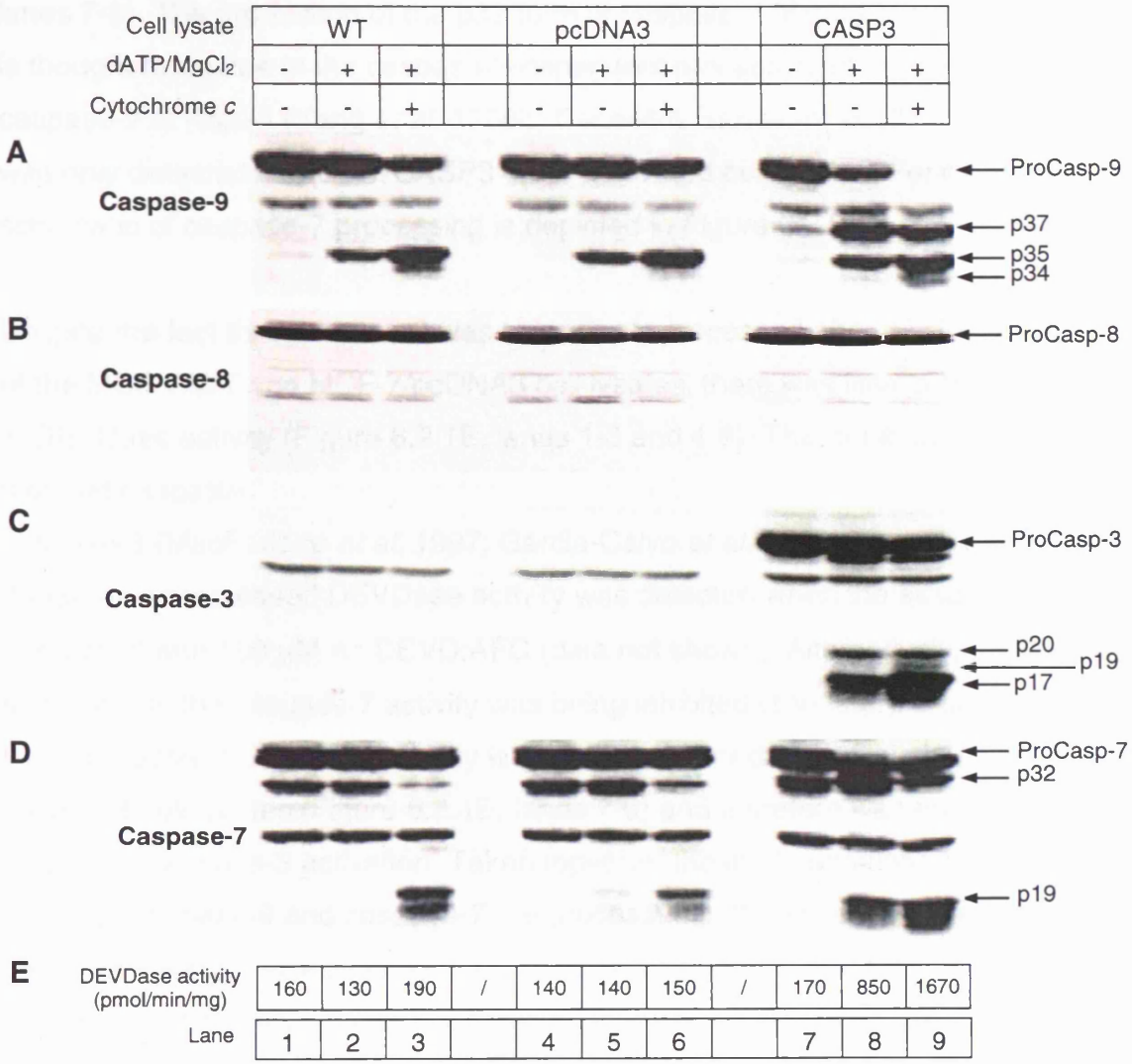

Figure 6.2.1: Comparison of dATP-induced caspase processing in MCF7/WT, pcDNA3 and CASP3 cell lysates. MCF-7 cell lysates (10 mg/ml) were activated with dATP/$MgCl_2$ (2 mM) in the presence/absence of cytochrome *c* (1.7 μM) for 30 min at 37 °C. The processing of apical and effector caspases was then analysed in each sample (20 μg of protein/lane) by SDS-PAGE and immunoblotting for caspase-9 (**A**), caspase-8 (**B**), caspase-3 (**C**) and caspase-7 (**D**). The caspase-3/-7 (DEVDase) activity was measured using the fluorescent substrate Ac-DEVD.AFC (20 μM, as described in Materials and Methods).

incubation (Figure 6.2.1D, lanes 1-3 and 4-6). In contrast, in MCF-7/CASP3 cell lysates, caspase-7 was fully processed to the p32 and p19 forms (Figure 6.2.1D, lanes 7-9). The production of the p32 form of caspase-7 (Figure 6.2.1D, lanes 8-9) is thought to be due to the caspase-3-dependent processing of the prodomain of caspase-7 at Asp23 (Yang *et al*, 1998b; Denault & Salvesen, 2003) and as such was only detected in MCF-7/CASP3 dATP-activated cell lysates. For clarity, a schematic of caspase-7 processing is depicted in Figure 6.2.2.

Despite the fact that caspase-7 was extensively processed after dATP activation of the MCF-7/WT and MCF-7/pcDNA3 cell lysates, there was little or no increase in DEVDase activity (Figure 6.2.1E, lanes 1-3 and 4-6). This could be due to the fact that caspase-7 has a higher Km for the Ac-DEVD.AFC substrate than caspase-3 (MacFarlane *et al*, 1997; Garcia-Calvo *et al*, 1999; Denault & Salvesen, 2003), as an increased DEVDase activity was detected when the assay was performed with 100 μM Ac.DEVD.AFC (data not shown). Alternatively, these data suggest that the caspase-7 activity was being inhibited (see later). Significantly, a large increase in DEVDase activity was detected after dATP activation of MCF-7/CASP3 cell lysates (Figure 6.2.1E, lanes 7-9) and therefore was presumably as a result of caspase-3 activation. Taken together, these observations suggest that although caspase-9 and caspase-7 are processed in the absence of caspase-3, their processing is greatly enhanced when caspase-3 is present. In contrast, processing of caspase-6 was not detected in the absence of caspase-3 (data not shown), in agreement with previous studies (Slee *et al*, 1999; Denault & Salvesen, 2003).

6.2.2 Caspase-3 accelerates processing of caspase-9 and caspase-7 in dATP activated cell lysates.

Having established that caspase-9 and caspase-7 are both processed in MCF-7/WT cell lysates following dATP activation, but to a lesser extent than occurs in caspase-3-containing MCF-7 cell lysates, the rate of caspase processing was then assessed. MCF-7/pcDNA3 and MCF-7/CASP3 cell lysates were dATP-activated for the indicated times and SDS-PAGE and immunoblotting were then used to analyse the time-dependent caspase processing (Figure 6.2.3A and B). In the

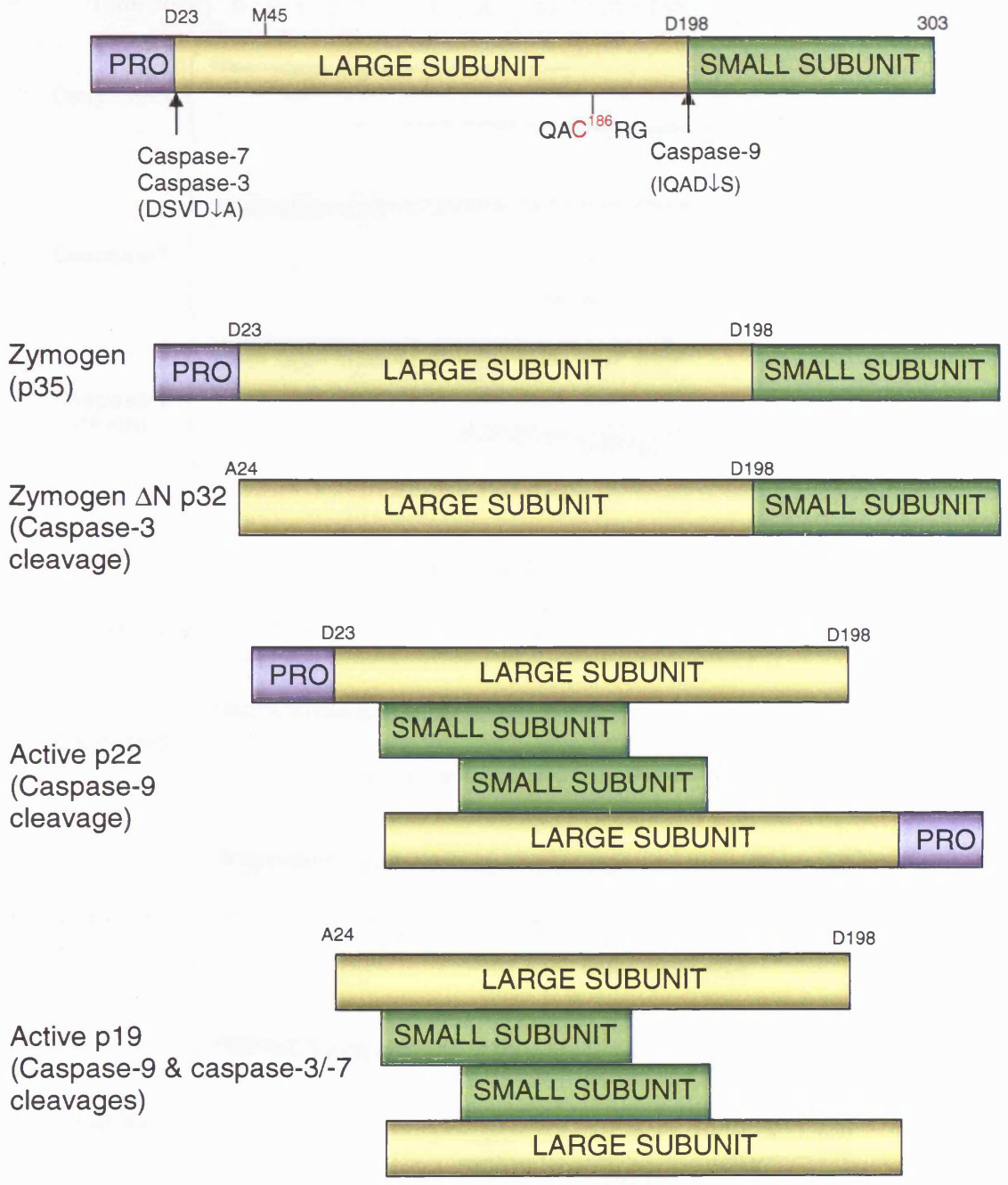

Figure 6.2.2: Alternative processing of caspase-7. A schematic to illustrate the possible combinations of caspase-7 processing and the second translational start codon (Met45) used by bacteria.

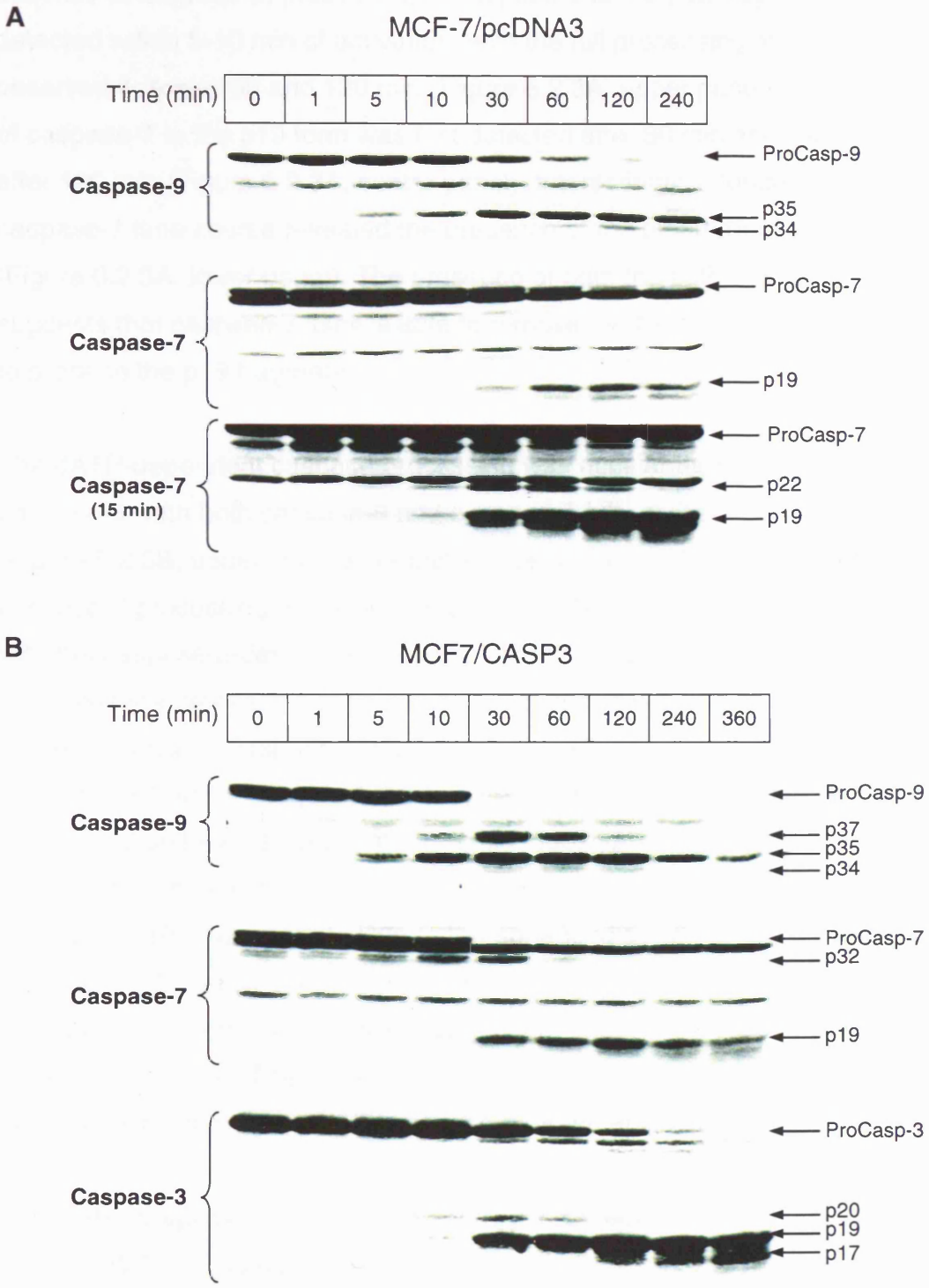

Figure 6.2.3: Caspase-3 accelerates processing of caspase-9 and caspase-7. MCF-7/pcDNA3 (**A**) and MCF-7/CASP3 cell lysates (**B**) (10 mg/ml) were activated with dATP, $MgCl_2$ and cytochrome *c* (as described previously) for the indicated times. The zero time point represents control activation (no cofactors present). At each time point, 10 µl of lysate was removed and added to 90 µl SDS loading buffer. SDS-PAGE was then used to separate 20 µg protein/lane and immunoblotted for caspase-9, caspase-7 and caspase-3 (MCF-7/CASP3 only). A longer exposure was used for caspase-7 MCF-7/WT to illustrate the presence of the p22 fragment.

absence of caspase-3, processing of caspase-9 to the p35 fragment was initially detected within 5-10 min of activation, with the full processing of this procaspase observed between 60 and 120 min (Figure 6.2.3A, upper panel). The processing of caspase-7 to the p19 form was first detected after 30 min and was maximal after 120 min (Figure 6.2.3A, centre panel). Interestingly, a longer exposure of the caspase-7 time course revealed the presence of the p22 form of caspase-7 (Figure 6.2.3A, lower panel). The presence of both the p22 and the p19 forms suggests that caspase-7 itself is able to remove the N-peptide from the p22 form to produce the p19 fragment.

The dATP-dependent caspase processing was accelerated in the presence of caspase-3, with both caspase-9 and caspase-7 fully processed after 30 min (Figure 6.2.3B, upper and centre panels, respectively). An intermediate product of caspase-7 processing was also detected after 10 min activation (p32), consistent with the caspase-3-dependent removal of the caspase-7 prodomain, which enhances the processing of caspase-7 by caspase-9 (Denault & Salvesen, 2003). In the presence of caspase-3, caspase-9 was additionally processed to the p37 form after 10-30 min (Figure 6.2.3B, upper panel). The processing of caspase-3 to the p20 subunit was detected after 10 min (subsequent to the formation of p35 caspase-9), and the p19/p17 forms were detected after 30 min dATP-activation (Figure 6.2.3B, lower panel). Due to the enhanced activity of the p37 form of caspase-9 (Zou *et al*, 2003), the processing of all of the caspases analysed was increased. Furthermore, the processing of both effector caspases-3 and -7 was subsequent to that of caspase-9 processing, therefore suggesting a sequence of caspase activation events, with caspase-9 as the apical caspase.

6.2.3 Procaspase-3 processing activity is detected in dATP-activated MCF-7/WT cell lysates.

Given that caspase-9 is the apical caspase following dATP activation in MCF-7 cells, it was logical to assume that an apoptosome was being formed. To investigate this possibility, recombinant procaspase-3 was incubated with dATP-activated MCF-7/WT cell lysates and caspase-3 processing and activity was assayed (Figure 6.2.4). As shown in Figure 6.2.1, dATP activation of MCF-7 cell lysates in the absence of caspase-3 resulted in only a small increase in DEVDase

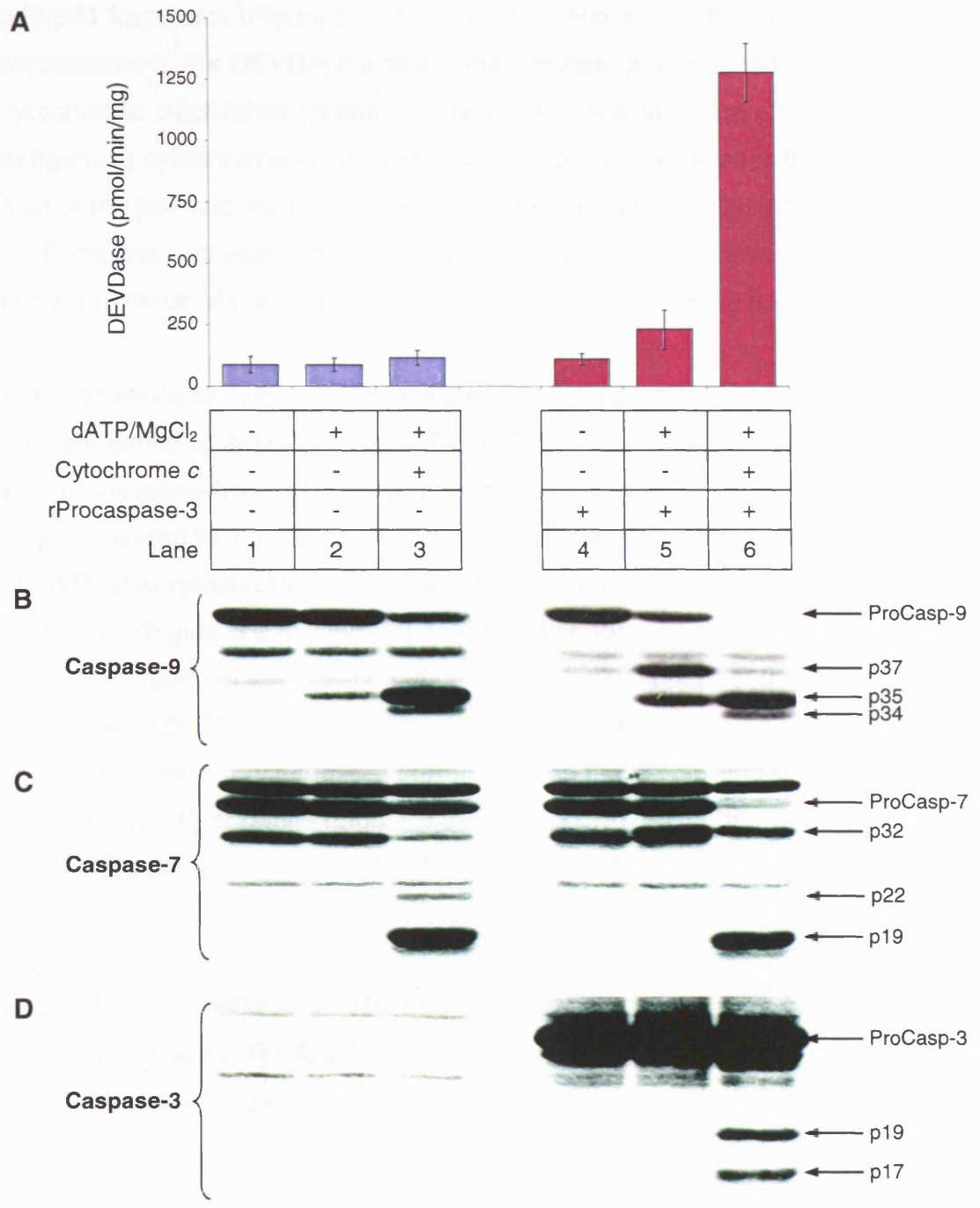

Figure 6.2.4: Addition of caspase-3 reveals the presence of an active apoptosome. MCF-7/ WT cell lysates (10 mg/ml) were activated with dATP and $MgCl_2$ in the presence or absence of cytochrome *c* and incubated at 37 °C for 30 min (as described previously). The DEVDase activity was then measured using Ac-DEVD.AFC (20 μM, blue bars (**A**)). To assess the caspase cleaving activity of the lysates, recombinant procaspase-3 (0.2 μM) was added to the activated lysate and incubated for a further 1 h. The DEVDase activity was then assessed as above (red bars, (**A**)). Data expressed as mean ± SEM, n=3. Caspase processing was then detected in the activated lysates by SDS-PAGE and immunoblotting for caspase-9, caspase-7 (20 μg/lane, **B** and **C**, respectively) and caspase-3 (7.5 μg/lane) (**D**).

activity (Figure 6.2.4A, lane 3) and incomplete processing of caspase-9 to the p35/p34 fragments (Figure 6.2.4B, lanes 1-3). However, after incubation with procaspase-3, the DEVDase activity was significantly enhanced in the dATP/ cytochrome *c*-activated lysates (Figure 6.2.4A, lane 6). In the absence of exogenous cytochrome *c*, caspase-9 was partially processed to the p35 form and also to the p37 subunit in the presence of procaspase-3 (Figure 6.2.4B, lanes 2 & 5). Complete processing of procaspase-9 to the p35/p34 forms was only detected in the presence of both cytochrome *c* and caspase-3 (Figure 6.2.4B, lane 6).

In the absence of caspase-3, procaspase-7 was processed to the p19 form and to a lesser extent to the p22 subunit (Figure 6.2.4C, lane 3). Following incubation with procaspase-3 in dATP alone-activated cell lysates, some of the procaspase-7 was processed to the p32 form (Figure 6.2.4C, lane 5). However, in the presence of dATP and cytochrome *c*, procaspase-7 was fully processed to both the p32 and p19 forms (Figure 6.2.4C, lane 6). Interestingly, the p22 cleavage fragment of caspase-7 (seen in the absence of caspase-3) was no longer detected (Figure 6.2.4C, lane 6). The enhanced DEVDase activity detected following incubation with recombinant procaspase-3 correlated with the processing of the proform to the p19 and p17 subunits (Figure 6.2.4D, lane 6). These observations suggest that the dATP/cytochrome *c*-activated MCF-7/WT cell lysate is capable of processing exogenous procaspase-3, most likely in an apoptosome-dependent mechanism.

6.2.4 The ~1.4 MDa and ~700 kDa apoptosome complexes are formed in dATP-activated MCF-7/WT cell lysates, in addition to a ~200 kDa active caspase-7 complex.

The ability of dATP/cytochrome *c*-activated MCF-7/WT cell lysates to process and activate recombinant procaspase-3 suggested that a caspase activating apoptosome complex was being formed. This possibility was therefore examined using Superose-6 gel-filtration. MCF-7/WT cell lysates were activated for 30 min in the absence or presence of dATP and cytochrome *c*, and separated by Superose-6 gel-filtration. In control lysates, Apaf-1 eluted as a monomer in fractions 18-21 (Figure 6.2.5A), but eluted in fractions 5-7 (~1.4 MDa) and fractions 9-14 (~700 kDa) after activation with dATP/ cytochrome *c* (Figure 6.2.5A). Thus, both the ~1.4 MDa and ~700 kDa apoptosome complexes are formed in dATP-

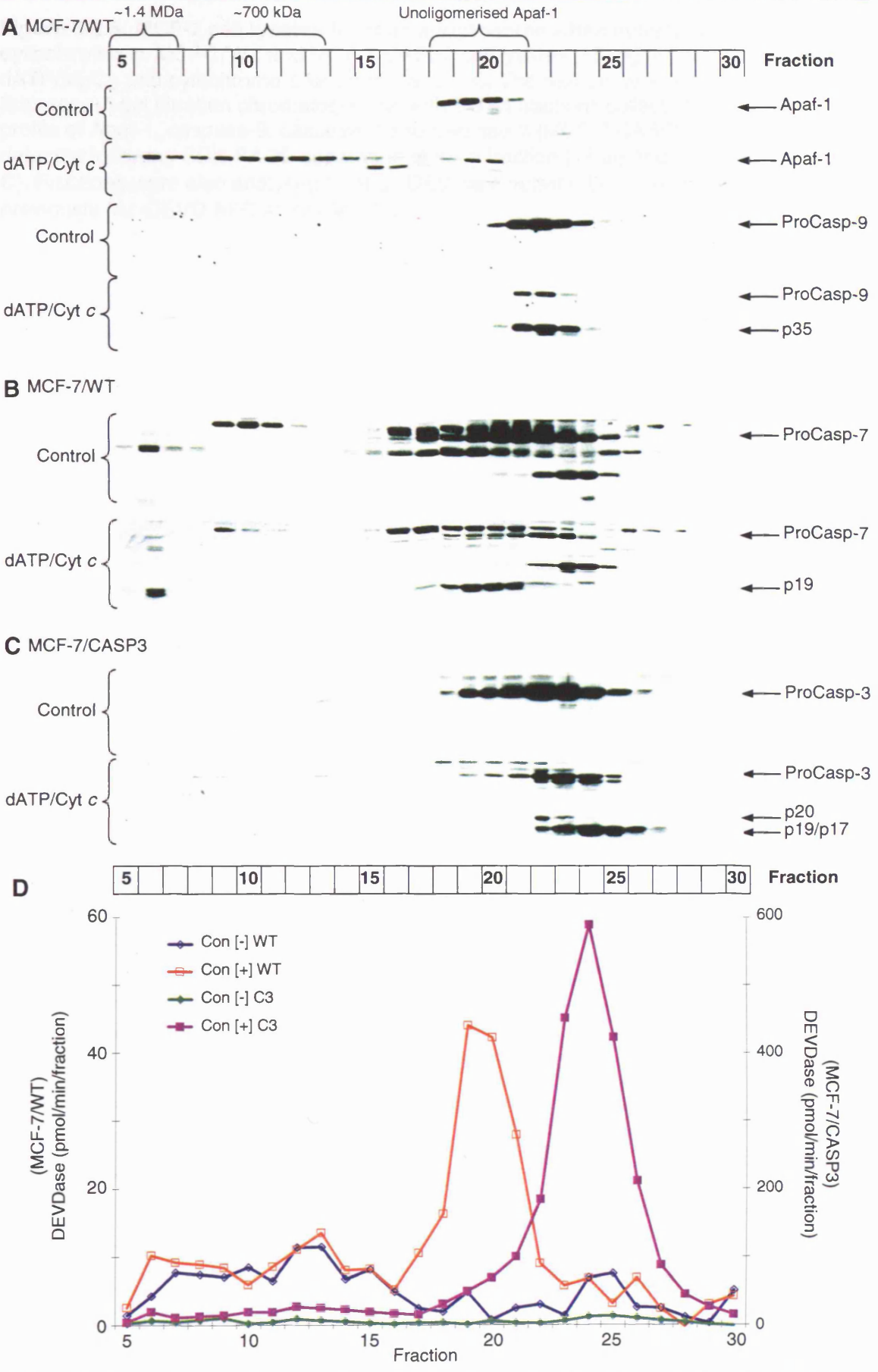

Figure 6.2.5: MCF-7 cell lysates form an apoptosome when activated with dATP/ cytochrome *c*.

Figure 6.2.5: MCF-7 cell lysates form an apoptosome when activated with dATP/ cytochrome *c*. MCF-7/WT and MCF-7/CASP3 cell lysates (15 mg/ml) were activated with dATP/$MgCl_2$ and cytochrome *c* for 30 min at 37 °C. The lysates were then separated by Superose-6 gel filtration chromatography, with 0.5 ml fractions collected. The elution profile of Apaf-1, caspase-9, caspase-7 and caspase-3 (MCF-7/CASP3 only) were detected following SDS-PAGE separation of each fraction (18 µl) and immunoblotting (**A-C**). Fractions were also analysed for their DEVDase activity (50 µl) as described previously (Ac-DEVD.AFC at 20 µM) (**D**).

activated MCF-7 cell lysates. Although, caspase-9 was not detected in the ~700 kDa apoptosome, it was still processed to the p35 fragment and was detected as the free caspase in fractions 22-23 (i.e. the same fractions which contained procaspase-9 in the control lysates) (Figure 6.2.5A). These data confirm that dATP activation of MCF-7/WT cell lysates induces the oligomerisation of Apaf-1 to form two large apoptosome complexes.

Interestingly, active caspase-7 (p19) eluted from the Superose-6 column in fractions 18-21 (Figure 6.2.5B), whereas procaspase-7 was detected in fractions 19-22. The elution profile of active caspase-7 suggests that this is a much larger form of active caspase-7 than would be predicted as a dimer. Active caspase-3, for example, forms an active heterotetramer (~60 kDa) in MCF-7/CASP3 cell lysates, and is eluted from the Superose-6 column in fractions 23-26 (Figure 6.2.5C). Furthermore, the separation of recombinant procaspase-7 by gel-filtration revealed an elution profile predominantly in fractions 21-24, similar to those containing active caspase-3 (data not shown). This shift in elution pattern upon dATP activation and processing suggests that active caspase-7 is associating with other proteins, or is forming a larger oligomerised complex of itself. The presence of the active caspase-7 complex was not dependent on the absence of caspase-3, as it was also seen in MCF-7/CASP3 cell lysates separated by Superose-6 gel-filtration (data not shown).

A peak of DEVDase activity in the Superose-6 gel-filtration fractions of MCF-7/WT cell lysates, corresponded to the location of active caspase-7 and confirmed the presence of a larger molecular weight active caspase-7 complex in fractions 18-21 (Figure 6.2.5D, orange line). The DEVDase activity of caspase-3 (using MCF-7/CASP3 cell lysates) was detected in fractions 23-26 (Figure 6.2.5D, purple line), in accordance with the position of caspase-3 from the Western blot data. As seen previously, caspase-7 does not have a high affinity for the Ac-DEVD.AFC substrate, and the peak of DEVDase activity was ~15 fold lower than that detected for caspase-3. Interestingly, caspase-7 was not detected in the fractions corresponding to the apoptosome, presumably because the concentration of sodium chloride (50 mM) in the column elution buffer was too high to sustain the interaction, as has been shown previously for caspase-3 (Bratton *et al*, 2001a).

6.2.5 The dATP activation of MCF-7 cell lysates results in the formation of an active apoptosome.

Having established that dATP activation results in the oligomerisation of Apaf-1 into ~1.4 MDa and ~700 kDa apoptosome complexes, it was necessary to determine whether these complexes were able to sustain caspase processing. As Western blot analysis of the gel-filtration experiment failed to detect any caspase-9 in the ~700 kDa apoptosome, further experiments were performed to investigate the interaction between Apaf-1 and caspase-9 in this complex. Following Superose-6 gel-filtration, the fractions corresponding to the ~1.4 MDa (5-7) and the ~700 kDa (10-15) apoptosome complexes were pooled (input) and immunoprecipitated overnight with anti-caspase-9 antibody-coated Dyna-beads. The supernatants and elutions from the beads were then separated by SDS-PAGE and immunoblotted for Apaf-1 and caspase-9 (Figure 6.2.6A).

Apaf-1 and caspase-9 were scarcely detected in the fractions from the ~1.4 MDa apoptosome complex (Figure 6.2.6A, lanes 1-2), and were not seen to associate with each other in the immunoprecipitation (lanes 9-10). Conversely, Apaf-1 was detected in the ~700 kDa apoptosome fractions in both control and dATP-activated cell lysates (Figure 6.2.6A, upper panel, lanes 3-4). However, Apaf-1 is only captured onto the beads via its association with caspase-9, and accordingly Apaf-1 was only seen in the elution from the dATP-activated ~700 kDa apoptosome fractions (Figure 6.2.6A, upper panel, lanes 9-12). The active p35 fragment of caspase-9 was also detected in the fractions of the dATP-activated ~700 kDa apoptosome complex, with little detected in any of the controls (Figure 6.2.6A, lower panel, lane 1-4). As expected, immunoprecipitation only revealed the presence of the p35 and p34 forms of caspase-9 in the dATP-activated ~700 kDa apoptosome complex (Figure 6.2.6A, lower panel, lanes 9-12). These data confirm that Apaf-1 and caspase-9 had formed an association in the ~700 kDa apoptosome, which should therefore be able to process and activate effector caspases.

The caspase processing ability of the ~1.4 MDa and ~700 kDa apoptosome complexes was then investigated by incubating the complexes with either recombinant procaspase-3 (Figure 6.2.6B, left panel) or procaspase-7 (right panel)

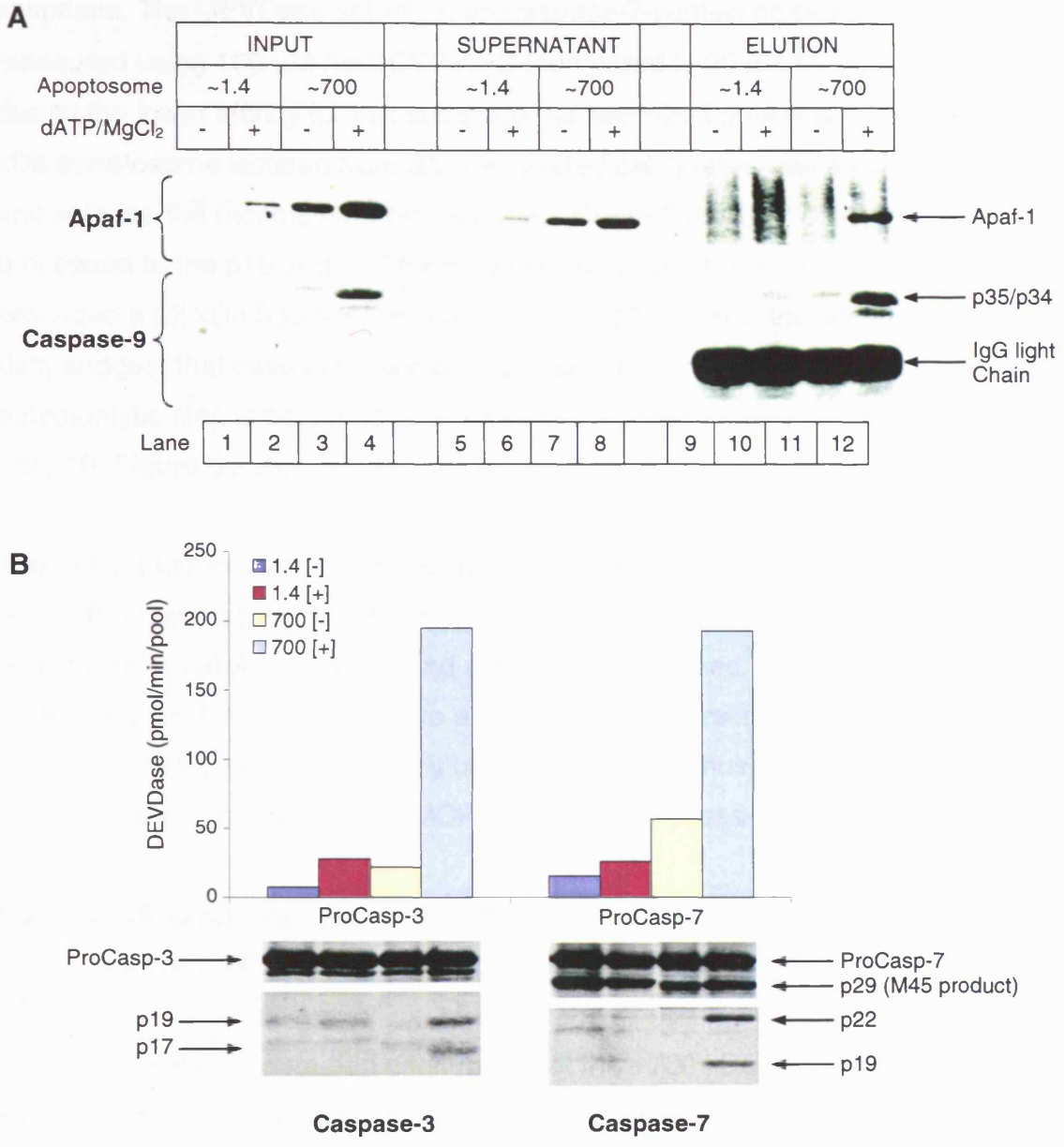

Figure 6.2.6: The MCF-7/WT ~700 kDa apoptosome complex directly processes both procaspase-7 and procaspase-3. MCF-7/WT cell lysates (15 mg/ml) were activated for 30 min with dATP/Cyt *c* and separated on a Superose-6 gel-filtration column. Pooled fractions 5-7 (~1.4 MDa) and 10-15 (~700 kDa) were concentrated and immunoprecipitated overnight with the addition of cross-linked anti-caspase-9 monoclonal antibody-coated Dyna-beads. The beads were then washed (4x) and eluted in SDS sample buffer (**A**). From a separate experiment, 50 µl pooled fraction was incubated alone (data not shown), or with 0.2 µM procaspase-3 or 0.2 µM procaspase-7 or 1 h at 37 °C. Ac-DEVD.AFC was then added to each sample (20 µM for caspase-3, 100 µM for caspase-7) and the DEVDase activity measured (**B**). The DEVDase reaction was then diluted in SDS sample buffer, separated by SDS-PAGE and immunoblotting for caspase-3 and caspase-7. A longer exposure was used to detect the cleavage fragments. The immunoreactive band at 29 kDa is the secondary translational product (initiating at Met45) resulting from the bacterial expression of caspase-7, and not a result of caspase-7 cleavage.

and assaying for both DEVDase activity and cleavage of the recombinant caspases. The DEVDase activity in procaspase-7-containing samples was measured using 100 μM Ac-DEVD.AFC (compared to 20 μM for procaspase-3), due to the lower affinity for this substrate (as described previously). Only the ~700 kDa apoptosome isolated from dATP-activated cell lysates was able to process and activate the recombinant procaspases (Figure 6.2.6B). Procaspase-3 was processed to the p19 and p17 forms, while cleavage of recombinant caspase-7 produced a 22 kDa fragment, in addition to the p19 form of the caspase. These data suggest that caspase-9 is cleaving caspase-7 at Asp198, and that an autocatalytic step is occurring to process the caspase-7 from the p22 fragment to the p19 (Figure 6.2.2).

These data are in accordance with previous studies in THP-1 cell lysates (Cain *et al*, 2000) showing that the ~700 kDa and not the ~1.4 MDa apoptosome complex, possesses the ability to cleave and activate procaspases. This also demonstrates for the first time that the ~700 kDa apoptosome can directly process procaspase-7, a concept that previously has only been implied, and thus provides a mechanism for activation of this caspase in MCF-7 cells during stress-mediated apoptosis.

6.2.6 XIAP is rapidly recruited to the apoptosome following dATP activation in MCF-7/WT cell lysates with reduced levels of SMAC and Omi.

Although the above data had confirmed that the ~700 kDa apoptosome processes exogenous caspase-7 directly, the transient association between caspase-7 and the apoptosome had yet to be proven. In order to demonstrate this, a gentler method of cell disruption than freeze/thawing was employed, namely Digitonin permeabilisation followed by homogenisation (Dig/Hom). As shown in Chapter 3, this method preserves the integrity of the mitochondria and removes these organelles from the lysate without releasing SMAC and Omi (Figure 6.2.7A, lanes 2-3). As XIAP is not thought to interact with active caspases in the presence of SMAC and Omi, the Dig/Hom cell lysate allows the interactions between XIAP and the apoptosome to be investigated. In accordance with data from dATP-activated THP-1 cell lysates (Twiddy *et al*, 2004), the DEVDase activity was reduced in MCF-7 Dig/Hom cell lysates compared with lysates produced by freeze/thawing (Figure 6.2.7B). This is presumably because XIAP binds to active caspases and

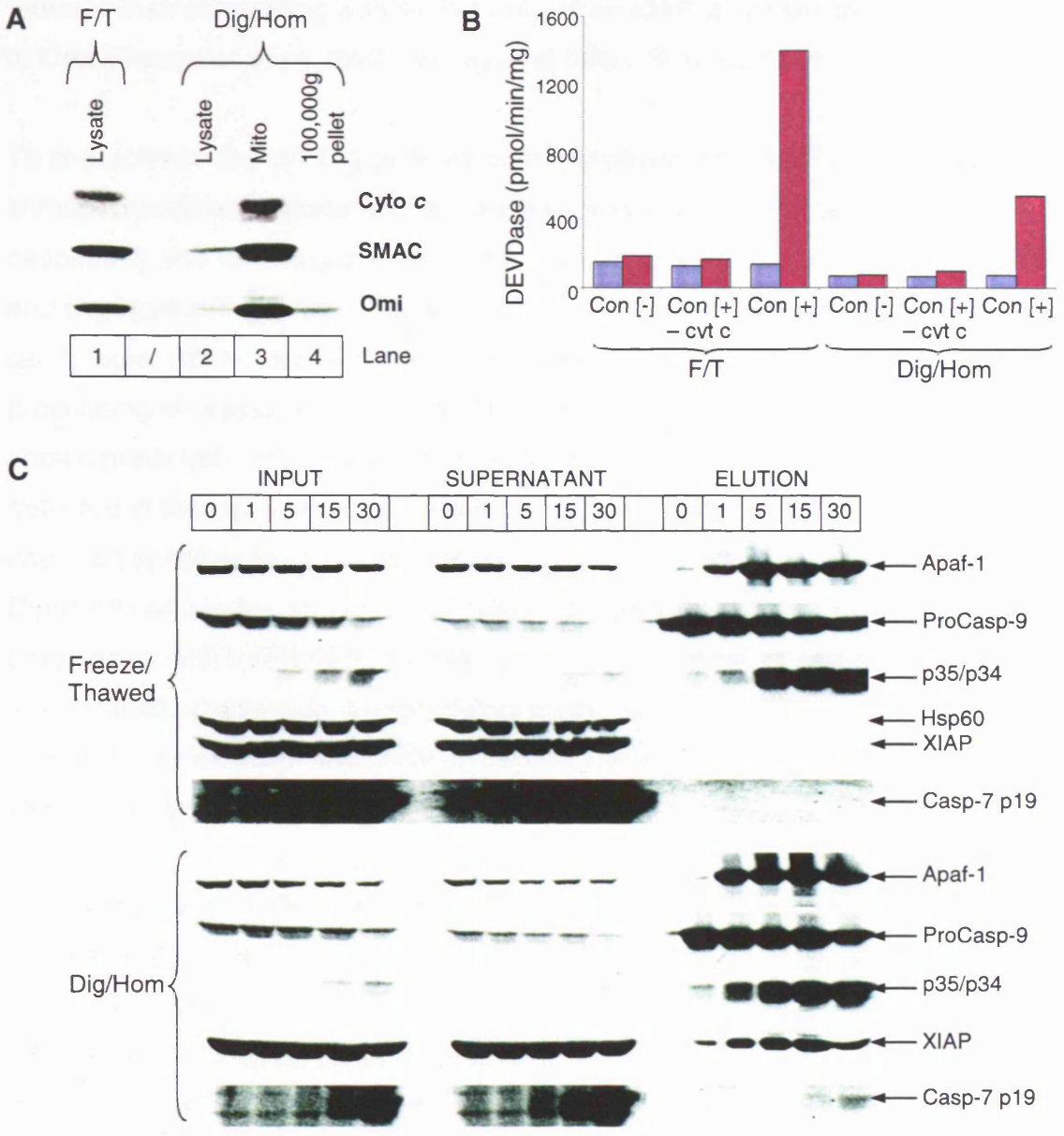

Figure 6.2.7: XIAP is rapidly recruited to the apoptosome, where it suppresses caspase activity. The presence of mitochondrial proteins was compared in MCF-7/WT F/T cell lysate, Dig/Hom cell lysate and centrifugal pellets produced in the production of Dig/Hom lysate. Protein samples (20 μg protein/lane) were analyzed by SDS-PAGE/immunoblotting for cytochrome *c*, SMAC and Omi (**A**). F/T and Dig/Hom MCF-7/WT cell lysate (10 mg/ml) were activated for 30 min in the absence /presence of dATP and cytochrome *c*, and the DEVDase activity was subsequently measured (20 μM Ac-DEVD.AFC) (**B**, blue bars). In addition, an aliquot of activated lysate was incubated with procaspase-3 for 1 h, and the DEVDase activity remeasured (**B**, red bars). Data shown is representative of three experiments. MCF-7/WT F/T and Dig/Hom cell lysates (15 mg/ml) were activated as above, for the indicated times, and the reaction stopped with zVAD.FMK (20 μM) prior to overnight immunoprecipitation with anti-caspase-9 monoclonal antibody-coated Dyna-beads. The supernatant was recovered and the beads washed (4x) and eluted in 30 μl SDS sample buffer. Proteins were separated by SDS-PAGE (input 20 μg, supernatant 20 μg, and elution 20 μl) and immunoblotted for Apaf-1, caspase-9, XIAP and caspase-7 (**C**).

reduces their processing activity, but only when XIAP is not sequestered by SMAC or Omi (Deveraux *et al*, 1997, Huang *et al*, 2001, Srinivasula *et al*, 2001).

To characterise the binding partners of the apoptosome in MCF-7 cell lysates, an immunoprecipitation study was carried out using a monoclonal antibody to caspase-9 and following a time course of dATP activation in both freeze/thawed and Dig/Hom cell lysates, (Figure 6.2.7 C). In both freeze/thawed and Dig/Hom cell lysates, Apaf-1 was seen to rapidly associate with caspase-9 (1 min) with processing of caspase-9 detected at the same time point (Figure 6.2.7C). As shown previously in Chapter 3, XIAP (and the mitochondrial protein, Hsp60) were detected in the input and flow-through of freeze/thawed cell lysates but not in the captured apoptosome complex (Figure 6.2.7C, upper panel). In contrast, XIAP in Dig/Hom cell lysates was able to interact with the apoptosome complex at early time points, with a reduction in captured XIAP detected at 30 min (Figure 6.2.7C, lower panel). These data demonstrate that the absence of SMAC and Omi the Dig/Hom lysate has allowed XIAP to bind to the apoptosome via its interactions with caspase-9, and possibly with caspase-7.

The presence of caspase-7 in immunoprecipitations from the freeze/thawed cell lysates could not be detected, even when heavily over-exposing the immunoblotting film (Figure 6.2.7C, upper panel). By contrast, in Dig/Hom cell lysates, active caspase-7 was initially detected in the apoptosome at 15 min and then increased further by 30 min (lower panel). However, only a very small amount of the total active caspase-7 detected in dATP-activated cell lysates was present in the apoptosome. The large active caspase-7 complex seen in the Superose-6 gel-filtration studies could therefore account for the reduced levels of caspase-7 that were detected in the apoptosome (when compared to caspase-3, Chapter 3; Twiddy *et al*, 2004).

6.2.7 Activation of the intrinsic apoptotic pathway in MCF-7 cells induces the formation of a ~700 kDa apoptosome.

Having established that dATP activation in MCF-7 cell lysates results in the formation of apoptosome complexes, it was necessary to ensure that this phenomenon was also occurring in cells undergoing chemical-induced apoptosis.

To determine the optimal treatment conditions, MCF-7/WT cells were treated with either vehicle alone (DMSO), or staurosporine (STS) in the presence or absence of zVAD.FMK for the indicated times. Apoptosis was measured by PS exposure (Annexin V binding), loss of mitochondrial membrane potential (MMP) (determined by TMRE release), cytochrome *c* release and PARP cleavage (Figure 6.2.8A). DMSO-treated cells did not show any signs of apoptosis at any of the time points analysed (Figure 6.2.8A). However, STS induced a time-dependent apoptosis as measured by a number of techniques. After 3 h, PARP cleavage was initially detected, with a modest increase in Annexin V binding and a loss of MMP (Figure 6.2.8A, lanes 3-5), with little caspase-7 processed. However, after 6 h, over 50% of the cells were Annexin V positive and had lost their MMP. Cytochrome *c* was released from the mitochondria and detected in the cytosol and PARP was substantially cleaved at this time point (Figure 6.2.8A, lanes 7-9). Processing of caspase-7 was also maximal after 6 h STS treatment. When the cells were pretreated with zVAD.FMK for 1 h, PARP cleavage was inhibited (lane 9), as well as the PS exposure, the loss of MMP and caspase-7 processing, suggesting that these events are all caspase-dependent. However, the release of cytochrome *c* was not affected by the presence of zVAD.FMK, suggesting that this is a caspase-independent event (Figure 6.2.8A, lanes 9 & 13). After 24 h, there was poor cell integrity, with no greater effect on the apoptotic parameters than that seen at 6 h and therefore subsequent experiments involving apoptotic MCF-7 cells were treated with STS (1 μM) for 6 h.

Having determined the treatment conditions required to produce sufficient apoptosis, but not cell disintegration, the formation of an apoptosome within these cells was then investigated. MCF-7 cells were treated with DMSO or STS with/without pre-treatment with zVAD.FMK. After harvesting the treated cells, cell lysates were produced and applied to a Superose-6 gel filtration column. The fractions corresponding to the ~1.4 MDa (fractions 6-7) and the ~700 kDa apoptosomes (11-14) were then pooled, concentrated and immunoprecipitated with an anti-caspase-9 monoclonal antibody. The presence of Apaf-1 and caspase-9 in the captured apoptosome was then assessed by SDS-PAGE and immunoblotting (Figure 6.2.8B). The immunoprecipitation step was necessary as neither Apaf-1 nor caspase-9 could be detected in the unconcentrated column fractions (data not shown).

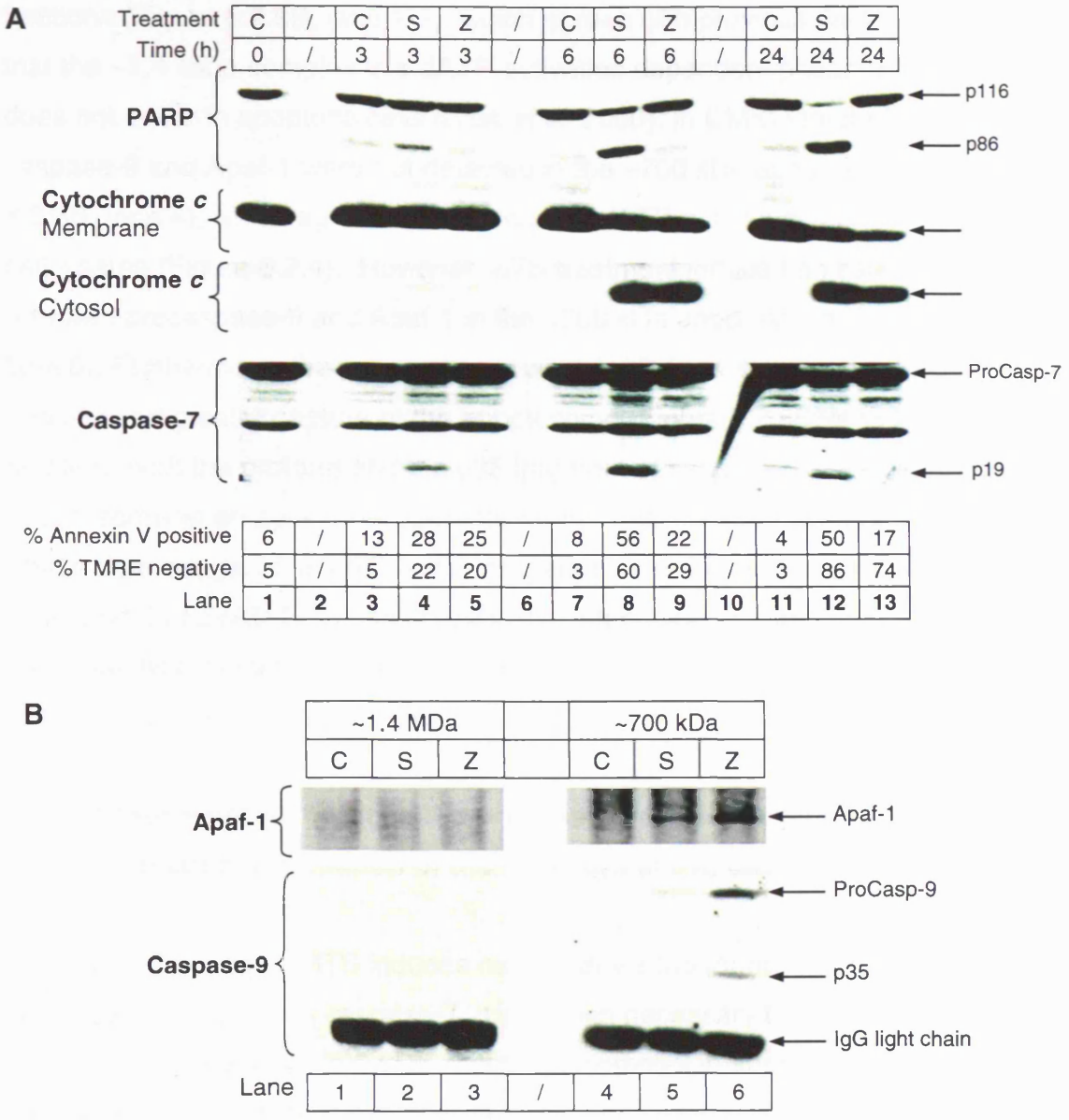

Figure 6.2.8: Staurosporine (STS) induces apoptosis in MCF-7 cells via the formation of an apoptosome. MCF-7/WT cells (2 x 10^5) were treated with either vehicle alone (DMSO) (C) or STS (1 μM) (S) in the absence or presence of a 1 h pre-treatment with zVAD.FMK (100 μM; Z). At the indicated times TMRE retention and Annexin V binding were assessed as described in Materials and Methods. The treated cells were also pelleted and washed prior to permeabilisation with Digitonin. The membrane fraction and cytosol were then separated and immunoblotted for PARP (20 μg membrane protein/lane), cytochrome *c* (15 μg cytosol and membrane protein/lane) and caspase-7 (20 μg cytosolic protein/lane) following SDS-PAGE protein separation. (**A**). MCF-7/WT cells (5 x 10^6) were treated as in A, for 6 h. Cell lysates were then produced by freeze/thawing, followed by centrifugation at 20,000 x g. The lysate was then separated on a Superose-6 gel-filtration column and 0.5 ml fractions were collected. Fractions 6 & 7 (~1.4 MDa) and 11-14 (~700 kDa) were pooled, concentrated and immunoprecipitated overnight with anti-caspase-9 monoclonal antibody-coated Dyna-beads. The beads were then recovered, washed in PBS (4x) and eluted in 30 μl SDS sample buffer. Apaf-1 and caspase-9 were then detected in the eluate by SDS-PAGE and immunoblotting (**B**).

Neither caspase-9 nor Apaf-1 were detected in the ~1.4 MDa apoptosome fractions (Figure 6.2.8B, lane 1-3), which agrees with previous data suggesting that the ~1.4 MDa complex is a dATP-activation dependent phenomenon and does not occur in apoptotic cells (Cain *et al*, 2000). In DMSO-treated cells, caspase-9 and Apaf-1 were not detected in the ~700 kDa apoptosome (Figure 6.2.8B, lane 4), which agrees with the control dATP-activation data from MCF-7 cell lysates (Figure 6.2.4). However, STS treatment induced an association between procaspase-9 and Apaf-1 in the ~700 kDa apoptosome (Figure 6.2.8B, lane 5). Furthermore, the pre-treatment with zVAD.FMK stabilised this complex and allowed greater capture of the apoptosome (Figure 6.2.8B, lane 6). In addition, both the proform and the p35 fragment of caspase-9 were detected in the apoptosome when cells were co-treated with zVAD.FMK (Figure 6.2.8B, lane 6). These data suggest that STS is inducing apoptosis via the apoptosome in MCF-7 cells, and that zVAD.FMK can stabilise this interaction, presumably by preventing the proteolytic cleavage of Apaf-1 by active effector caspases and the subsequent release of processed caspase-9.

6.2.8 Staurosporine induces the processing of caspase-7 and the subsequent formation of the ~200 kDa active caspase-7 complex.

Having confirmed that STS induces cell death via the formation of an apoptosome, which can then process caspase-7, it was then necessary to investigate the presence of the active ~200 kDa caspase-7 complex in apoptotic cells. Cell lysates were therefore produced from control or STS-treated cells in the presence or absence of zVAD.FMK, separated by Superose-6 gel-filtration and the column fractions then immunoblotted for caspase-7 (Figure 6.2.9A). As seen in the time course experiment (Figure 6.2.8), active caspase-7 was not detected in control or zVAD.FMK treated cells (Figure 6.2.9A, upper and lower panels). However, an ~200-300 kDa caspase-7 complex was detected in STS treated cells, which eluted in fractions 19-21 (Figure 6.2.9A, centre panel). This observation showed that the ~200 kDa complex, previously detected in MCF-7 cell lysates, was not an artefact of dATP activation and therefore suggests that active caspase-7 could potentially be binding to other proteins.

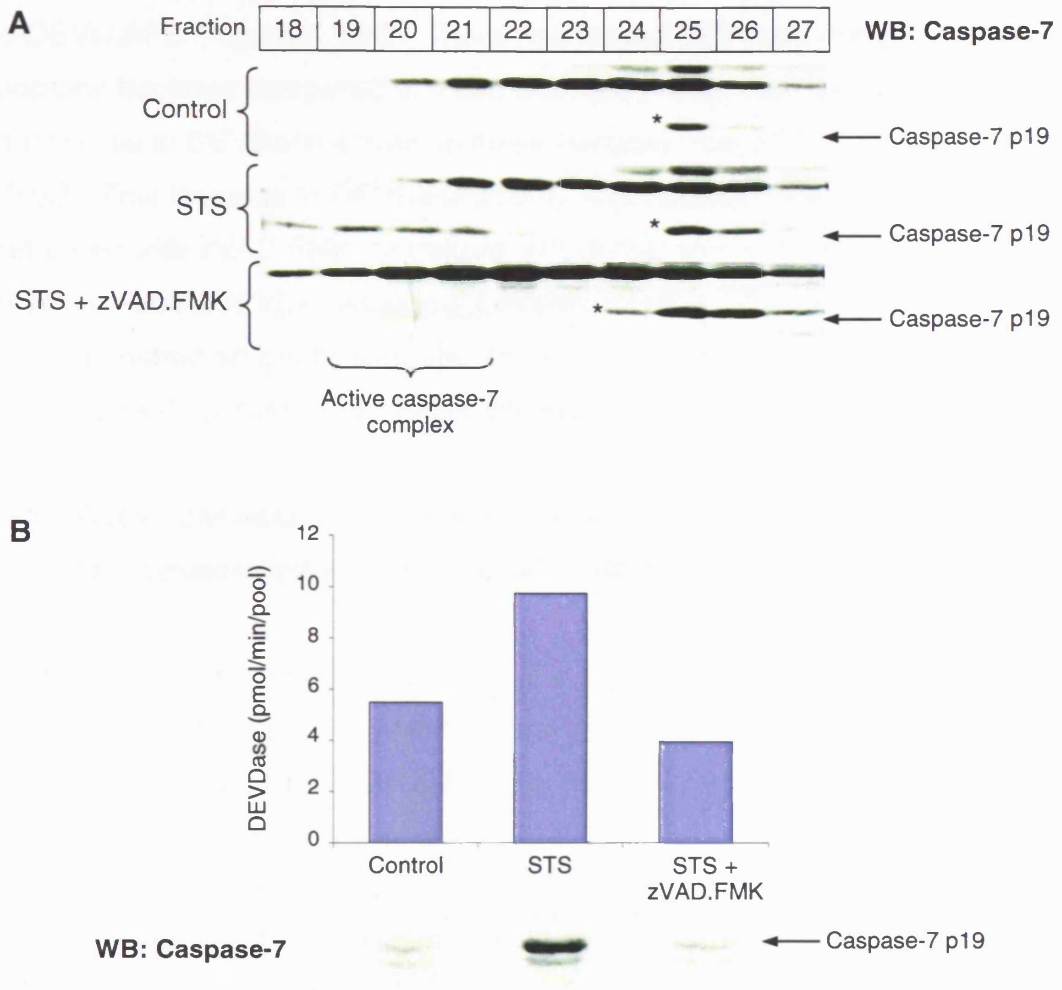

Figure 6.2.9: STS induces caspase-7 processing and the formation of the active caspase-7 complex. MCF-7/WT cells (5 x 10^5) were treated with vehicle alone, STS or STS following a 1 h pre-treatment with zVAD.FMK for 6 h. Cell lysates were then produced by freeze/thawing, followed by centrifugation at 20,000 x g. The lysate was then separated on a Superose-6 column with 0.5 ml fractions collected, which were immunoblotted for caspase-7. Asterisk denotes non-specific antibody cross-reactive band (**A**). Fractions 19-21 were then pooled, concentrated and assayed for DEVDase activity (100 μM Ac-DEVD.AFC) (**B**). The presence of active caspase-7 in the pooled fractions was also detected by SDS-PAGE and immunoblotting (lower panel).

To examine whether the ~200 kDa complex containing the processed caspase-7 was active, fractions 19-21 from the Superose-6 gel-filtration column (from Figure 6.2.9A) were pooled and concentrated and their DEVDase activity measured using Ac-DEVD.AFC (Figure 6.2.9B). There was limited DEVDase detected in the apoptotic fractions compared to those from dATP activation, however, there was an increase in DEVDase activity in these fractions from STS-treated cells (Figure 6.2.9B). This increase in DEVDase activity was inhibited when the cells had been pretreated with zVAD.FMK, or treated with DMSO alone. These data suggest that an active ~200-300 kDa caspase-7 complex exists in apoptotic cells following a stress-mediated apoptotic stimulus, and confirms the data obtained previously following dATP activation of cellular lysates (Figure 6.2.5).

6.2.9 Active caspase-7 does not associate with IAPs following immunoprecipitation with an anti-active caspase-7 antibody.

Having established that the ~200-300 kDa active caspase-7 complex was formed in both dATP-activated cell lysates and in apoptotic cells, it was necessary to try and determine the protein composition of the complex. As the IAP family members are known to bind to active caspase-7 (Deveraux *et al*, 1997; 1999; Huang *et al*, 2001; Roy *et al*, 1997), the binding of IAPs to caspase-7 was first investigated. In order to purify only the active caspase-7 complex, an immunoprecipitation antibody was used that recognised an epitope within the cleavage site of caspase-7 at Asp198 (Cell Signalling). The immunoprecipitation was carried out from both S-100 MCF-7 cell lysates and Superose-6 column fractions corresponding to the eluted ~200 kDa complex (fractions 19-21), using anti-active caspase-7 antibody-coated Dyna-beads. In order to maximise the amount of active caspase-7 produced, the cell lysates were dATP-activated for 2 h (Figure 6.2.10), resulting in almost the complete processing of procaspase-7 to p19 (Figure 6.2.10A, lane 1-2). In both whole cell lysates and the concentrated gel filtration columns, only the active form of caspase-7 was captured onto the antibody (Figure 6.2.10A and B, lane 6). This demonstrates the specificity of the antibody for the cleaved p19 form of caspase-7. There was however, a small amount of p19 detected in the immunoprecipitation from the non-dATP-activated control, which could have arisen from the overnight incubation of the lysate with the antibody-coated beads (Figure 6.2.10B, lane 5).

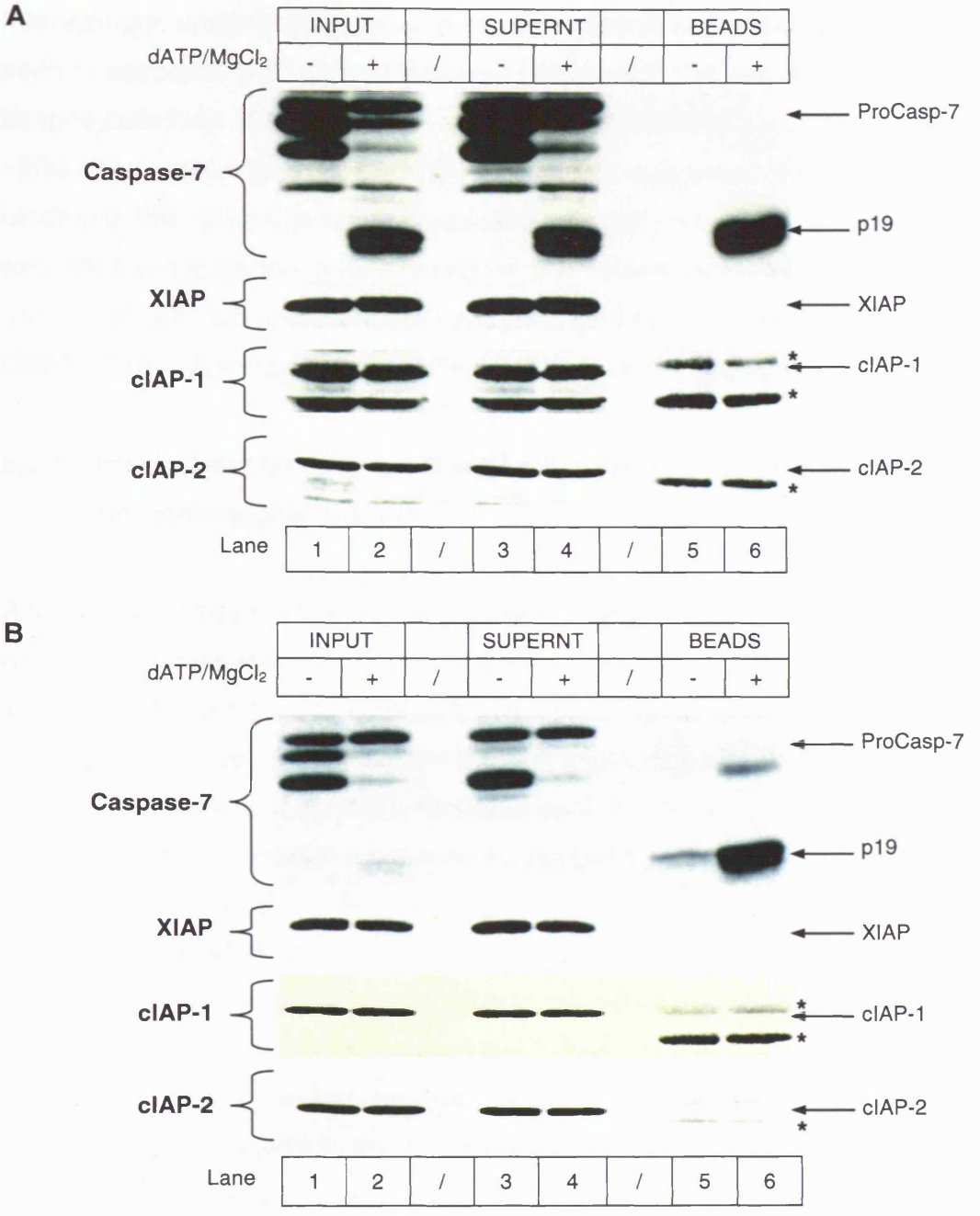

Figure 6.2.10: Active caspase-7 does not associate with XIAP, cIAP-1 or cIAP-2 when immunoprecipiated with an anti-active caspase-7 antibody. Precleared MCF-7/WT cell lysates (15 mg/ml) were activated with dATP and cytochrome *c* for 2 h and immunoprecipitated overnight with anti-caspase-7 antibody-coated Protein A Dyna-beads. The beads were then washed thoroughly in PBS and eluted in SDS sample buffer. The input (1%, 20 µg protein), supernatant (1%, ~20 µg protein) and the elution (20%) were then analysed for the presence of caspase-7, XIAP, cIAP-1 and cIAP-2. (**A**). MCF-7/WT cell lysates (15 mg/ml) were activated as in A, and separated on a Superose-6 gel-filtration column. Fractions 19 & 20, containing the ~200 kDa active caspase-7 complex (determined by DEVDase activity, data not shown) were then pooled and concentrated. Anti-active caspase-7 antibody-coated Dyna-beads were then incubated overnight with the concentrate. The beads were recovered, washed 4x in PBS and eluted in SDS sample buffer. The input (6.25%), supernatant (7%) and elution (36%) samples were then loaded onto SDS-PAGE gels and immunoblotted for caspase-7, XIAP, cIAP-1 and cIAP-2 (**B**). Asterisks denote non-specific band due to antibody cross-reactivity.

Interestingly, under both of these immunoprecipitation conditions no IAPs were seen to associate with active caspase-7 (Figure 6.2.10A and B, lane 6). This was despite detection of XIAP, cIAP-1 and cIAP-2 in the fractions corresponding to the ~200 kDa complex (Figure 6.2.10B). These data suggested that an IAP was not binding to the ~200 kDa active caspase-7 complex. This result is somewhat expected as the cellular lysates used were produced by the freeze/thawing method of cell lysis and therefore contained mitochondrial proapoptotic factors (SMAC/Omi), which sequester IAPs away from active caspases.

6.2.10 The anti-active caspase-7 antibody could have displaced XIAP during the immunoprecipiation.

Although a member of the IAP family was not detected in the immunoprecipitation of the active caspase-7 complex using an anti-active caspase-7 antibody, their involvement could not be completely ruled out. XIAP is known to bind to effector caspases via competitive inhibition through interaction with the active site of the caspase (Deveraux *et al*, 1997; Huang *et al*, 2001). Previous reports have suggested that the interaction between caspase-3 and XIAP can be inhibited if the active site is occluded by the presence of a peptide inhibitor (i.e. DEVD.CHO, Sun *et al*, 1999b; zVAD.FMK, Suzuki *et al*, 2001a; Riedl *et al*, 2001a). However, conflicting evidence exists for caspase-7; one report has shown that zVAD.FMK does not inhibit XIAP binding to caspase-7 (Suzuki *et al*, 2001a) an observation which is in direct contrast to another report (Tenev *et al*, 2005). As the antibody used to immunoprecipitate the active caspase-7 complex was directed against the active site of caspase-7 it was possible that XIAP was being displaced during the immunoprecipitation (Figure 6.2.11A). By contrast, cIAP-1 has been suggested to bind to caspase-7 via both competitive (via the active site, Deveraux *et al*, 1997; Huang *et al*, 2001) and non-competitive inhibition (via cleavage at Asp23, Tenev *et al*, 2005). It was therefore predicted the capture antibody should not have displaced cIAP-1 if the IAP was associating with the caspase independantly from the active site. Indeed, cIAP-1 was shown not to be associated with caspase-7 in the ~200 kDa complex, in the presence of an occluded active site (Figure 6.2.10).

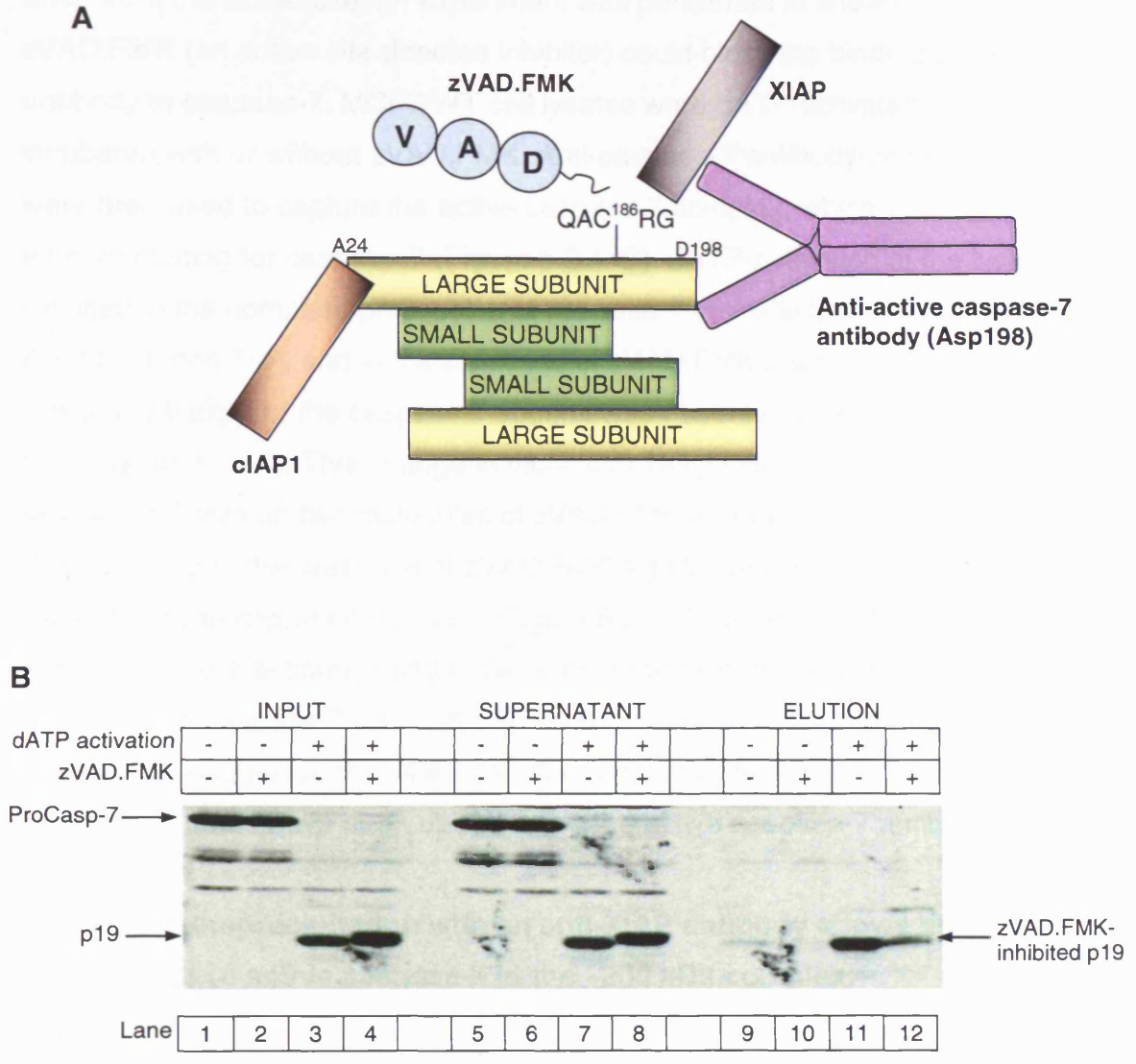

Figure 6.2.11: zVAD.FMK and the immunoprecipitation antibody interact with the same site on caspase-7. A schematic which illustrates the competition for the active site of caspase-7 between XIAP, zVAD.FMK and the anti-active caspase-7 antibody (**A**). MCF-7/WT cell lysates (15 mg/ml) were either activated with dATP and cytochrome *c*, or with heat activation alone for 2 h. The poly-caspase inhibitor, zVAD.FMK (200 μM) was added as indicated after the lysate was activated. The active caspase-7 complex was then immunoprecipitated for 4 h with anti-active caspase-7 antibody-coated Dyna-beads. The beads were then washed repeatedly and eluted in SDS sample buffer. The inputs (20 μg), supernatants (4%, ~20 μg) and elutions (40%) were then analysed by SDS-PAGE and immunoblotted for caspase-7 (**B**).

In order to establish whether the active caspase-7 antibody could be displacing XIAP from the active site, an experiment was performed to show whether zVAD.FMK (an active site directed inhibitor) could block the binding of the antibody to caspase-7. MCF7/WT cell lysates were dATP activated and then incubated with or without zVAD.FMK. Anti-caspase-7 antibody-coated Dyna-beads were then used to capture the active caspase-7 complex, which was analysed by immunoblotting for caspase-7 (Figure 6.2.11B). dATP-activation of the lysates resulted in the complete processing of caspase-7 to the active p19 form (Figure 6.2.11B, lanes 1-4), and in the presence of zVAD.FMK a small shift in the molecular weight of the caspase-7 subunit was observed (from p19 to p20; Figure 6.2.11B, lanes 3-4). This change in molecular weight was due to a covalent interaction between two molecules of zVAD.FMK and the active sites of caspase-7. Furthermore, the presence of zVAD.FMK significantly attenuated the ability of the antibody to capture caspase-7 (Figure 6.2.11B, lanes 4, 8, 12). This result showed that the antibody used in the immunoprecipitation was binding to the active site of caspase-7 and that this binding could be abrogated by zVAD.FMK. These data suggested that XIAP (or other proteins interacting at the active site of caspase-7) could have been displaced by the active caspase-7 antibody.

6.2.11 Immunoprecipitation with an anti-XIAP antibody shows that XIAP binds to active caspase-7 in the ~200 kDa complex.

Having established that XIAP might have been displaced from the ~200 kDa caspase-7 complex by the anti-active caspase-7 antibody, a reverse immunoprecipitation was performed. An anti-XIAP antibody (Transduction Labs) was cross-linked to Protein G Dyna-beads and then used for immunoprecipitation from the partially purified ~200 kDa caspase-7 complex. In order to capture only XIAP from the fractions containing the ~200 kDa complex, a Sephacryl S300 column was used to initially fractionate this complex. This column would also allow separation of a larger amount of cell lysate compared to the Superose-6 gel-filtration system, and therefore should enhance the possibility of detecting any protein interactions.

MCF-7/WT cell lysates were activated with dATP/cytochrome *c*, as described previously, and separated by Sephacryl S300 gel-filtration chromatography. In

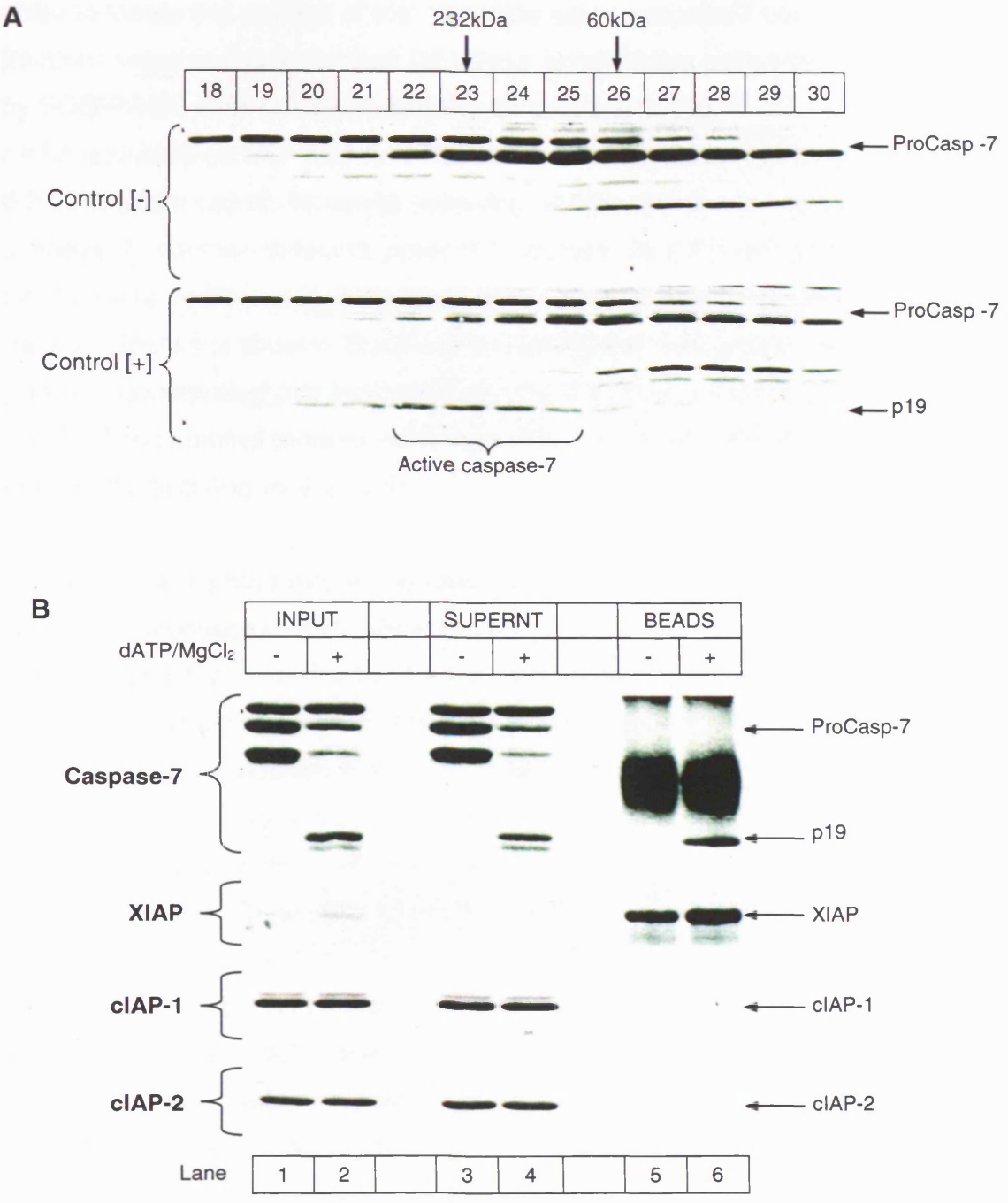

Figure 6.2.12: XIAP and caspase-7 are associated in a ~200 kDa complex following dATP activation. MCF-7/WT cell lysates (15 mg/ml, 10 mg) were activated at 37 °C in the presence or absence of dATP and cytochrome *c* for 2 h. Sephacryl S300 gel-filtration was used to isolate the active caspase-7 complex from cell lysates. The active caspase-7 complex was identified by assaying the DEVDase activity (data not shown) and immunoblotting the fractions for caspase-7 (**A**). Fractions 22-25 were then pooled and immunoprecipitated with anti-XIAP antibody-coated Dyna-beads for 4 h. The beads were then washed extensively (6x), eluted with 75 µl SDS sample buffer and analysed for caspase-7, XIAP, cIAP-1 and cIAP-2 by Western blotting (**B**). The input, supernatant and elution volumes loaded onto the SDS-PAGE gels were 1%, 1% and 13% respectively of the total volume.

order to locate the position of the ~200 kDa active caspase-7 complex the eluted fractions were analysed for their DEVDase activity (data not shown) and separated by SDS-PAGE prior to immunoblotting for caspase-7 (Figure 6.2.12A). In the non-dATP-activated control, caspase-7 eluted in the proform in fractions 23-26 (Figure 6.2.12A, upper panel). However, following dATP-activation the active form of caspase-7 was then detected, present in fractions 22-25 (lower panel). This location was confirmed by the presence of a peak of DEVDase activity in these fractions (data not shown). Fractions containing active caspase-7 were then pooled, concentrated and incubated with the anti-XIAP antibody-coated Dyna-beads. The captured proteins were then analysed by SDS-PAGE and immunoblotting (Figure 6.2.12B).

Caspase-7 was processed to the active p19 form following the dATP activation, with some procaspase-7 detected in the negative control fraction input (Figure 6.2.12B, lane 1-2). Importantly, the p19 form of caspase-7 was only detected in the elution sample from dATP-activated column fractions (Figure 6.2.12B, lane 6), suggesting an association with XIAP. The association between XIAP and active caspase-7 was confirmed by the capture of XIAP, which was greater in the immunoprecipitation from dATP-activated fractions compared with the non-dATP-activated control. These data suggested that more XIAP had shifted to these fractions following dATP-activation, possibly due to the production of the p19 caspase-7 fragment and subsequent formation of the ~200 kDa complex. In addition, although cIAP-1 and cIAP-2 were both detected in the ~200 kDa complex fractions (input), neither was detected in the elution. These data suggest that cIAP-1 is not only bound to active caspase-7 in a non-competitive manner via interactions with the N-terminal region of the large subunit (Tenev *et al*, 2005). Although cIAP-1 could be interacting with the active site of caspase-7, a reverse immunoprecipiation using an anti-cIAP-1 antibody was not performed due to the lack of a suitable commercial antibody, and consequently cIAP-1 cannot be ruled out as a potential binding partner for active caspase-7.

These observations show that once caspase-7 is activated at the apoptosome, XIAP sequesters active caspase-7 by forming an ~200 kDa complex, even in the presence of SMAC and Omi. This complex would be predicted to reduce the

processing activity of caspase-7 and thus suppress apoptosis in MCF-7 cells (Figure 6.2.13).

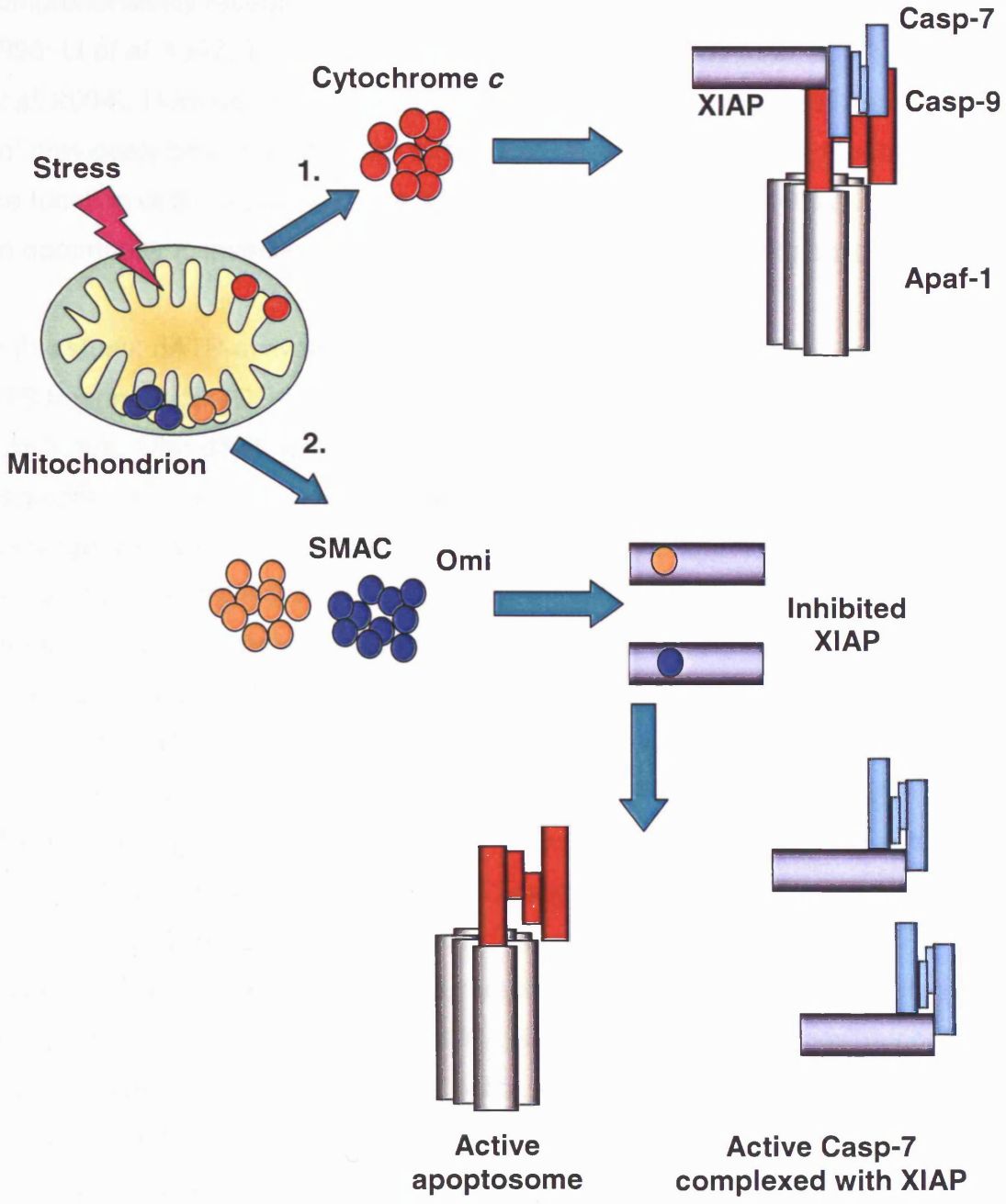

Figure 6.2.13: Schematic of caspase-7 activation and sequestration in MCF-7 cells. The formation of an apoptosome results in the cleavage and activation of caspase-7, but the interaction is transient as active caspase-7 is quickly sequestered by XIAP into a ~200 kDa complex, even in the presence of SMAC and Omi.

6.3 Discussion

The formation and activity of the ~700 kDa apoptosome complex has been comprehensively researched in caspase-3 containing cell lysates (HeLa, Liu *et al*, 1996; Li *et al*, 1997; THP-1, Cain *et al*, 1999; 2000; Twiddy *et al*, 2004; Jurkat, Hill *et al*, 2004). However, the role of the apoptosome in caspase-3 deficient cells has not previously been investigated. MCF-7 cells not only provided a model to look at the function of the apoptosome in the absence of caspase-3, but also presented an opportunity to investigate the role of caspase-7 as an effector caspase.

In this study, dATP-activation of MCF-7/WT or MCF-7/pcDNA3 cell lysates, and STS treatment of MCF-7/WT cells has confirmed some caspase-3 specific substrates. After dATP activation, caspase-9 was processed only to the p35/p34 fragments. The p37 form of caspase-9 is produced by a caspase-3-dependent cleavage (Srinivasula *et al*, 1998) and thus was only observed in MCF-7/CASP3 cell lysates or in MCF-7/WT cell lysates after the addition of exogenous procaspase-3. Caspase-7 was unable to be processed to the p32 fragment in the absence of caspase-3, due to the absence of a flexible linker region between the large and small subunits (Yang *et al*, 1998b). However, both the p22 and p19 forms of caspase-7 are present in dATP-activated MCF-7/WT cell lysates. This observation suggests that after cleavage between the large and small subunits of caspase-7 by caspase-9 to form the p22 fragment, caspase-7 can then autocatalytically remove the prodomain to produce the active p19 form. The processing of procaspase-6 was not detected in MCF-7/WT dATP-activated cell lysates, but was processed in MCF-7/CASP3 lysates (data not shown), confirming that caspase-6 is only processed by caspase-3 and that this is a downstream event in caspase activation (Slee *et al*, 1999; Denault & Salvesen, 2003). Caspase-7 was also unable to compensate for caspase-3 in inducing the exposure of PS in STS-treated MCF-7/WT cells, and therefore the loss of the mitochondrial membrane potential was used to measure apoptosis in these cells. In contrast, in apoptotic MCF-7/WT cells caspase-7 can cleave PARP to produce the characteristic p86 fragment, showing that some caspase-3 targets are also potential substrates for caspase-7. Collectively these data show that caspase-7 lacks the ability to compensate for caspase-3 in the cleavage of some known

substrates, despite having an identical substrate cleavage site recognition sequence (DEXD↓A; Thornberry *et al*, 1997).

The time course experiments have illustrated the sequence of caspase activation in MCF-7 cell lysates following activation with dATP/cytochrome *c*. The first caspase to be processed is the apical caspase, caspase-9, which then cleaves the effector caspase-7. When caspase-3 is also present (MCF-7/CASP3) the processing of caspase-7 is accelerated by the initial cleavage of caspase-7 to the p32 form, which appears to aid subsequent cleavage by caspase-9 (Figure 6.2.2B; Denault & Salvesen, 2003). This is in accordance with the production of the p32 fragment prior to cleavage and activation of caspase-7 by Granzyme B (Yang *et al*, 1998b). However, in MCF-7/WT as in caspase-3 containing cell lysates, the apical caspase, caspase-9, is activated first, followed by the activation of the effector caspase-7.

Both *in vitro* dATP-activation and *in vivo* treatment of MCF-7/WT cells with staurosporine resulted in the formation of an active ~700 kDa apoptosome. Immunoprecipitation of the ~700 kDa apoptosome from both of these models identified the component proteins as Apaf-1 and caspase-9. This interaction was strengthened by the presence of zVAD.FMK, preventing the release of active caspase-9 and preserving the integrity of the apoptosome. These results have shown that the formation of the apoptosome is not dependent on caspase-3 and occurs readily in MCF-7 cells. Furthermore, despite circumstantial evidence suggesting that the apoptosome processes procaspase-7 directly, this is the first study to show that the MCF-7/WT ~700 kDa apoptosome complex directly processes and activates both procaspase-3 and -7. Not only can the apoptosome process exogenous caspase-7, but this study has also shown that endogenous caspase-7 is recruited to the apoptosome following dATP activation. However, in Dig/Hom cell lysates only a small amount of caspase-7 was bound to the apoptosome as its association with the apoptosome is only transient, due to removal and sequestration by XIAP.

Interestingly, a large proportion of active caspase-7 was detected eluting as a ~200 kDa complex. The approach to identify the active caspase-7 binding partner(s) was made more difficult as it required an active caspase-7 specific

antibody, as even following Superose-6 gel-filtration some of the proform and active caspase-7 co-eluted. However, the disadvantage in using this method came to light during investigations into the effect of zVAD.FMK co-incubation. It appeared that binding of active caspase-7 to the active site-specific antibody was reduced in the presence of zVAD.FMK, suggesting that the antibody and zVAD.FMK were both interacting with the active site on caspase-7 and disrupting binding of one another by steric hindrance (Figure 6.2.11). As XIAP is known to only interact with, and inhibit activity of the active form of caspase-7 (Deveraux *et al*, 1997), via reverse binding in the active site (Huang *et al*, 2001), we therefore postulated that the anti-active caspase-7 antibody could have displaced XIAP during immunoprecipitation. By instead using an anti-XIAP antibody to immunoprecipiate the ~200 kDa active caspase-7 complex this revealed an interaction between XIAP and the active caspase-7. Taken together, these results confirm previous observations that the main inhibitory interaction between XIAP and caspase-7 centres on the accessibility of the active site of caspase-7 and the BIR1-BIR2 linker of XIAP (Deveraux *et al*, 1997; 1999; Huang *et al*, 2001; Tenev *et al*, 2005). However, it has been suggested that the BIR2 domain of XIAP can inhibit caspase-7 by non-competitive mechanisms; by binding to the N-terminal region exposed by cleavage at Asp23 (Suzuki *et al*, 2001a), or to the neoepitope generated at the N-terminus of the small subunit of caspase-7, following a predominantly caspase-8 mediated-cleavage at Asp206 (Scott *et al*, 2005). My study is in disagreement with these two hypotheses, as the antibody to the active site of caspase-7 could displace XIAP binding, therefore suggesting that XIAP is inhibiting active caspase-7 by a competitive mechanism.

cIAP-1 and cIAP-2 can also bind to and inhibit the activity of active effector caspases (Roy *et al*, 1997), however the mechanism by which the inhibition occurs has not yet been clarified. Recent data (Tenev *et al*, 2005) has suggested that cIAP-1 binds to active caspase-7 in a non-competitive manner, similar to that initially suggested for the BIR2 domain of XIAP (Suzuki *et al*, 2001a), and that this effect is independent of an accessible active site. This interaction initially appeared unlikely in the MCF-7/WT cell lysates due to the absence of caspase-3 and thus the lack of the p32 fragment of caspase-7. However, Ala24 was exposed by the removal of the N-terminal peptide from the p22 fragment of caspase-7 to form the p19 fragment. Therefore, if this hypothesis is correct the presence of cIAP-1 would

still have been expected in the immunoprecipitations using the anti-active caspase-7 antibody. However, neither cIAP-1 nor cIAP-2 were detected in the immunoprecipitations of the active caspase-7 complex and the displacement study using zVAD.FMK further confirmed that XIAP was the IAP binding in the active caspase-7 complex.

Although there appears to be a complex containing caspase-7 and XIAP of ~200 kDa, the different relative ratios between caspase-7 and XIAP in the complex (Figure 6.2.12) could imply that other proteins could also be associated with caspase-7. Furthermore, in the absence of adequate antibodies to immunoprecipitate cIAP-1 and cIAP-2, stable association of these proteins and caspase-7 could not be discluded. In contrast, the antibodies used to immunodetect cIAP-1 and -2 have been verified in our laboratory, and we are confident that these antibodies are detecting these IAPs. However, cIAP-1 and -2 could be acting as protein sinks to sequester SMAC and Omi to preserve the interaction between XIAP and caspase-7, as previously shown for ML-IAP (melanoma inhibitor of apoptosis; Vucic *et al* 2002; 2005). Interestingly, Survivin has been shown to bind to XIAP and increase its binding affinity for effector caspases (Dohi *et al*, 2004), and could therefore also be present in the ~200 kDa caspase-7 complex.

Furthermore, to strengthen the evidence for the caspase-7/XIAP complex, RNAi against XIAP should be performed to show whether the caspase-7 complex is dependent upon the presence of this IAP. This technique could also be used to confirm that cIAP-1 and -2 do not affect the formation of this complex. Interestingly, the residual caspase-7 proteolytic activity found within this complex raises questions as to how the binding of IAPs inhibit caspase activity. It has recently been shown that cIAP-1 and -2 bind to caspase-7 but do not inhibit its activity (Eckelman & Salvesen, in press). It is also possible that another protein is associating with caspase-7 in a ~200 kDa complex and not inhibiting its DEVDase activity, resulting in a cross-over of results. To investigate this possibility further a TAP-tagged caspase-7 variant could be produced, removing the difficulties faced with the immunoprecipitation of active caspase-7.

It has been suggested that the prodomain of caspase-7 stabilizes the zymogen conformation. Thus the removal of the N-peptide of caspase-7 enhances the ability of caspase-7 to be cleaved by caspase-9, but does not the affect the activity of the active effector caspase (Denault & Salvesen, 2003). This hypothesis agrees with the time course experiments in this study, where the processing of caspase-7 by caspase-9 was greatly enhanced in the presence of caspase-3 (Figure 6.2.3). Interestingly, the study by Denault and Salvesen suggested a role for sequestration via the N-peptide *in vivo*, a concept that would also support the theory of cIAP-1 binding to this domain (Denault & Salvesen, 2003; Tenev *et al*, 2005).

The present study has shown that a ~700 kDa active apoptosome is formed in both dATP-activated MCF-7 cell lysates and in STS-treated MCF-7 cells. The MCF-7 cell apoptosome can recruit and process procaspase-9, which in turn activates caspase-7, via cleavage at Asp198. Caspase-7 is then autocatalytically processed to the p19 form and released from the apoptosome where it is then sequestered by XIAP (Figure 6.2.13). This interaction decreases the proteolytic activity of caspase-7 and reduces the extent of apoptosis observed. This could in part account for why MCF-7 cells are more resistant to apoptosis than caspase-3-containing cells, as in caspase-3 containing cells caspase-3 is still able to cleave downstream targets and execute apoptosis, even when caspase-7 has been sequestered by XIAP.

Chapter 7

General Discussion

7.1 General Discussion

The assembly of the apoptosome forms the initiation step for the activation of caspases in mitochondrially-mediated apoptosis. The apoptosome can be reconstituted *in vitro* with recombinant Apaf-1, caspase-9 and cytochrome *c* and is a fully active caspase-processing complex (Saleh *et al*, 1999; Zou *et al*, 1999). However, the apoptosomes formed in dATP-activated cell lysates range in size from ~700 kDa to ~1.4 MDa (Cain *et al*, 1999; 2000; Zou *et al*, 1999; Jiang *et al*, 2003) with the ~700 kDa apoptosome predominating in apoptotic cells (Cain *et al*, 2000; Freathy *et al*, 2000; Almond *et al*, 2001). This apparent variation in the size of the apoptosome could be as a result of proteins associating with the apoptosome and modulating its activity. The main aim of my thesis was to isolate and characterise the apoptosome from lysates activated *in vitro* with dATP and cytochrome *c*. This *in vitro* study would allow sufficient material to be analysed to obtain identification of modulatory proteins by proteomics. Any candidate proteins could then be verified by isolating the apoptosome from apoptotic cells, using affinity-tagged caspase-9 constructs. A further aim was to investigate the role of the apoptosome in MCF-7 cells, which lack caspase-3 and are widely used in breast cancer research and in apoptotic studies.

The methods of apoptosome isolation employed in this study either involved affinity-tagging or immunoprecipitation of caspase-9 (Chapter 3), which eliminates the possibility of finding binding partners to monomeric Apaf-1, as caspase-9 is only known to bind to Apaf-1 in an apoptosome complex (Saleh *et al*, 1999). Many of the proposed modulators of the apoptosome appear to be involved in regulating the oligomerisation of Apaf-1 and formation of the apoptosome. These proteins include Hsp70, Hsp90, Aven, ProT and Bcl-2 family members (Saleh *et al*, 2000; Beere *et al*, 2000; Pandey *et al*, 2000; Chau *et al*, 2000; Jiang *et al*, 2003; Fang *et al*, 1998; Hu *et al*, 1998a; Pan *et al*, 1998a). These proteins may bind to Apaf-1 and prevent the conformational change essential for oligomerisation to occur and consequently prevent caspase-9 (either endogenous or affinity-tagged) recruitment. However, recent studies have shown that Hsp70 and Hsp90 are not stably associated with the native apoptosome isolated from Jurkat cell lysates (Hill *et al*, 2004). Furthermore, it appears that Hsp70 cannot directly inhibit the formation of the apoptosome, and it may be that the high salt concentration in the

Hsp70 (and Hsp90) preparations used in the original studies resulted in the observed attenuation of apoptosome formation and activity (Steel *et al*, 2004). This is in agreement with previous data from our laboratory showing that apoptosome formation is abrogated in a high salt environment (Cain *et al*, 2001), which can be overcome with increasing concentrations of cytochrome *c*. A direct association between ProT and Apaf-1 was also not demonstrated in the original paper, and ProT only inhibited the formation of the apoptosome in the presence of cell cytosols (Jiang *et al*, 2003). Similarly, Aven, which binds to the CARD domain of Apaf-1, requires the presence of cell cytosol in order to elicit its effects. These data suggest that both ProT and Aven are indirectly affecting apoptosome function and are not associated at endogenous levels. The importance of these proteins in modulating the formation of the apoptosome could be addressed by immunoprecipitating monomeric Apaf-1 under conditions of endogenous protein expression, as used previously to disprove the association between Apaf-1 and Bcl-2 family members (Moriishi *et al*, 1999).

Interestingly, proteins that promote apoptosome activity (PHAP) or enhance caspase-9 recruitment (DEFCAP/NAC) are also not present following isolation of the native apoptosomes from THP-1 (Twiddy *et al*, 2004) or Jurkat cell lysates (Hill *et al*, 2004). However, a direct association between PHAP and Apaf-1 was not shown in the original paper, and furthermore requires the presence of cell cytosol (Jiang *et al*, 2003). DEFCAP/NAC cannot be excluded as an apoptosome modulator, as it is thought to bind to Apaf-1 in the inactive ~1.4 MDa complex, thus promoting caspase-9 recruitment to the active ~700 kDa apoptosome (Chu *et al*, 2001). As both the immunoprecipitation and affinity-tagged purification of the apoptosome from cell lysates used in this study involved an initial fractionation step to isolate the ~700 kDa apoptosome, the ~1.4 MDa complex was consequently not analysed (Chapter 3; Twiddy *et al*, 2004). In conclusion, using the affinity-tagged CARD region of caspase-9 (GST-Casp9$^{1-130}$) which only binds to Apaf-1 in the apoptosome, in conjunction with the immunoprecipitation of the native apoptosome via an anti-caspase-9 antibody, the only components of the dATP-induced ~700 kDa apoptosome complex are Apaf-1$_{XL}$ and caspase-9 (Chapter 3, Twiddy *et al*, 2004).

Mitochondria are central to apoptosis induced by chemicals, cellular-stress and when amplification of the death-receptor mediated pathway is required. My studies show that in addition to cytochrome *c*, the IAP-interacting proteins SMAC and Omi modulate the composition of the apoptosome in both THP-1 (Chapter 3) and MCF-7 cell lysates (Chapter 6). These proapoptotic proteins modulate the apoptosome composition by sequestering XIAP, as in their absence, both XIAP and caspase-3 associate with the native THP-1 apoptosome, via their interaction with the catalytic subunits of caspase-9 (Chapter 3; Figure 7.1.1). Thus, these data demonstrate that when XIAP binds to the apoptosome via caspase-9, it can also bind to caspase-3 and stabilise its interaction with the apoptosome. This stabilising interaction has also been shown independently in other studies with dATP-activated Jurkat cell lysates (Hill *et al*, 2004). The data presented in this thesis show that when cytochrome *c* is released from the mitochondria it induces the formation of the apoptosome, which initially consists of Apaf-1, caspase-9, cytochrome *c*, XIAP and caspase-3. The release of SMAC and Omi then results in the removal and sequestration of XIAP and the release of caspase-3 from the apoptosome (Figure 7.1.1).

This study is also the first to demonstrate that an active ~700 kDa Apaf-1/caspase-9 apoptosome is formed both in dATP-activated MCF-7 cell lysates and in apoptotic MCF-7 cells, that processes and activates procaspase-7 directly (Chapter 6). The components of the MCF-7 apoptosome are also modulated by the presence of SMAC and Omi, in a similar manner to the THP-1 apoptosome, with the native MCF-7 apoptosome comprising of Apaf-1 and caspase-9. In the absence of SMAC and Omi, the MCF-7 apoptosome also contains XIAP, but with only negligible amounts of caspase-7 (Figure 7.1.1). The lack of caspase-7 in the apoptosome complex is due to its sequestration by XIAP, which forms a caspase-7/XIAP ~200-300 kDa complex (Chapter 6; Figure 7.1.1). The association between XIAP and active caspase-7 is evident in both dATP-activated cell lysates and in apoptotic MCF-7/WT cells, even in the presence of SMAC and Omi (Chapter 6). This association is not observed when immunoprecipitating the complex with an anti-active caspase-7 antibody as this antibody displaces XIAP from the active site of caspase-7. The sequestration of active caspase-7 by XIAP also provides a probable reason for the low DEVDase activity which was detected in the ~200-300 kDa complex. These results show that the apoptosome complex is formed in the

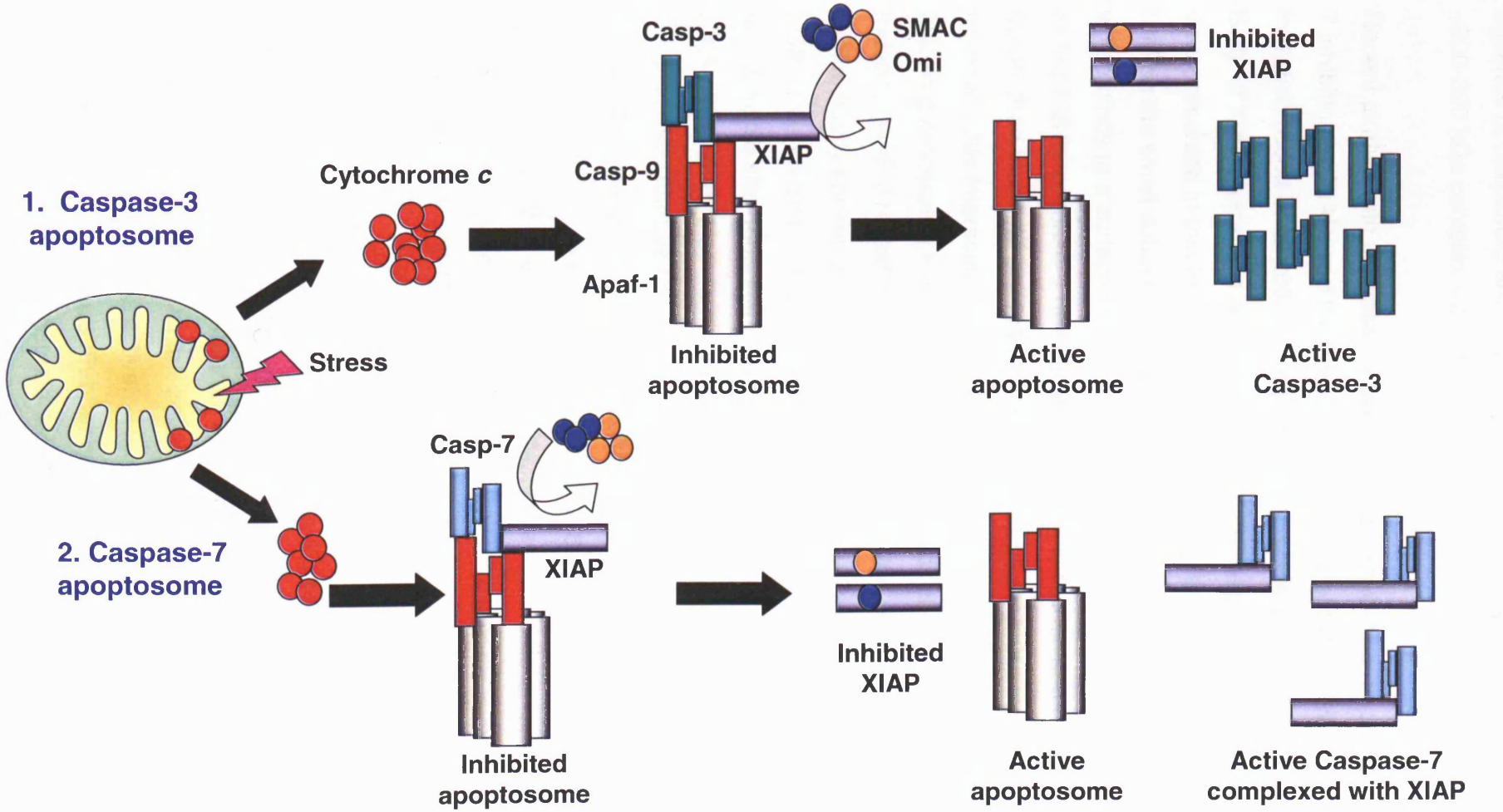

Figure 7.1.1: Modulation of apoptosome and effector caspase activity by XIAP. 1) In the presence of caspase-3, the apoptosome forms in the presence of dATP and cytochrome *c* but is initially inhibited by XIAP. After the release of SMAC and Omi from the mitochondria XIAP is then sequestered, resulting in an active apoptosome complex. 2) Caspase-7 is also directly recruited to the apoptosome where it is processed and binds XIAP. However, the association with the apoptosome is only transient as XIAP and caspase-7 are released from the apoptosome and form an independent stable ~200 kDa complex, in the presence of SMAC and Omi.

absence of caspase-3 and readily processes caspase-7, which then forms a stable ~200-300 kDa complex with XIAP (Figure 7.1.1).

Recent studies with caspase-7 have proposed a two-step mechanism for caspase-7 inhibition by XIAP, and the potential importance of the cleavage site for caspase inhibition (Scott *et al*, 2005). The first mechanism is via the N-terminal linker to BIR2 of XIAP interacting with the active site on caspase-7, in agreement with the data presented in this thesis. The second mechanism involves the exposure of an IBM on the small subunit of caspase-7, following processing in the linker region, which binds to a surface-interacting groove on XIAP (Scott *et al*, 2005). Cleavage at Asp198 by caspase-9 reveals an IBM which is recognised by XIAP with more avidity than the motif exposed following cleavage at Q196 (by Cathepsin G). However, this interaction is weaker than that demonstrated for the IBM exposed following processing at Asp206 (predominantly by caspase-8) (Scott *et al*, 2005). Indeed, the IBM revealed after cleavage at Asp206 (Ala-Asn-Pro) is similar to the evolutionarily conserved IBMs. In *Drosophila*, DIAP-1 also binds to drICE (and DCP-1) via an IBM exposed on the N-terminus of the large subunit (Ala-Leu-Gly) and is active site-dependent, again suggested a two-pronged attack (Tenev *et al*, 2005). This study also demonstrated that cIAP-1 binds to caspase-7 via the N-terminal IBM (Ala-Lys-Pro) exposed following cleavage at Asp23, in an active-site independent manner (Tenev *et al*, 2005). In contrast, my results demonstrate that in MCF-7 cells, following processing at Asp198, caspase-7 can remove the N-terminal peptide thus exposing this IBM. However, this does not result in an association between caspase-7 and cIAP-1 via the IBM motif in the absence of an accessible active site (Chapter 6).

Caspase-7 differs from caspase-3 in a number of ways; the subcellular distribution of active caspase-7 induced by CD95 ligation (Chandler *et al*, 1998), the dramatic shift in pI associated with its activation (Denault & Salvesen, 2003), and its sequestration by XIAP (Chapter 6). MCF-7 cells are also more resistant to apoptosis than those containing caspase-3, with the ability of XIAP to sequester caspase-7 as soon as it is activated at the apoptosome providing one mechanism for this increased resistance. Further potential mechanisms could result from the lack of processing of key caspase-3-dependent substrates, such as XIAP, Bcl-2/Bcl_{XL}, Bid and caspase-8 (Deveraux *et al*, 1999; Slee *et al*, 1999; Cheng *et al*,

1997; Kirsch *et al*, 1999; Figueroa *et al*, 2003; Tang *et al*, 2000). The cleavage of such proteins results in the amplification of the apoptotic signal via removal of sequestering proteins and enhancement of cytochrome *c* release with other proapoptotic factors from the mitochondria.

As SMAC and Omi can modulate the composition of the apoptosome *in vitro*, other compartmentalised proteins could interact with the apoptosome during apoptosis *in vivo*. Therefore, affinity-tagged caspase-9 constructs were developed and expressed in HeLa cells in order to isolate the apoptosome from apoptotic cells. One of the acknowledged difficulties of using affinity-tagged proteins is the possibility of identifying false or artefactual interactions, due to non-specific interactions with the affinity-tag. In this respect, GST, a commonly used affinity-tag is potentially problematic, and thus in my studies was used in tandem with CBP to provide a very selective approach to affinity purification. However, this affinity-tag has raised other potential problems, which have produced some surprising and interesting results. Firstly, the location and size of the TAP-tag fundamentally effects the function of caspase-9. Thus, expression of the GTC-tag at the N-terminus of Casp9$^{1-130}$ prevents access to the CARD domain of Apaf-1 and consequently does not protect against Etoposide-induced apoptosis (Chapter 4). However, expressing the TAP-tag at the C-terminus, distal to the Apaf-1 interaction site, allows the fusion protein to bind to Apaf-1 and inhibit apoptosis. Interestingly, Casp9$^{1-130}$-GTC is able to bind to Apaf-1 in the absence of an apoptotic stimulus, which is in stark contrast to the dATP and cytochrome *c*-dependent mechanism for GST-Casp9$^{1-130}$ inhibition in cellular lysates. There are two hypotheses that may explain this observation: firstly, that given the absolute requirement for cytochrome *c* in the formation of an *in vitro* apoptosome, it is possible that a small but sufficient amount of cytochrome *c* was released into the cytosol, thus allowing apoptosome formation. Alternatively, the TAP-tagged truncated caspase-9 variant could have circumvented the need for cytochrome *c* in apoptosome formation, possibly as a result of over-expression.

The possibility that the affinity-tag used can induce activation of the tagged protein, either through a direct or indirect mechanism, needs to be investigated prior to any large-scale experimentation or production of stable cell lines. Similar to Fc-fused caspase-9 (Srinivasula *et al*, 1998), the expression of full-length

caspase-9-GTC proteins results in their auto-activation and apoptosis in HeLa cells, which in part involves the formation of an active apoptosome (Chapter 5). As caspase-9 can be activated by dimerisation, other affinity tags could be employed which are not known to associate, thus reducing the likelihood of dimerisation and autocatalytic activation. In this respect, FLAG tags and c-myc tags are also widely used for purification and are not known to dimerise, unlike GST (Parker *et al*, 1990) and His tags (Wu & Filutowicz, 1999). However, the auto-activation observed in this study, would only be predicted to occur when over-expressing an apical caspase, as these caspases can be activated by an induced-proximity mechanism (Salvesen & Dixit, 1999). Effector caspases, by contrast, undergo a two-step processing to produce an active caspase (Fernandes-Alnemri *et al*, 1996; Han *et al*, 1997) and therefore the over-expression of effector caspase TAP-tagged constructs should not result in their spontaneous processing and subsequent apoptosis. In accordance, autocatalytic processing and subsequent apoptosis is not observed in transient transfection experiments of various TAP-tagged caspase-7 constructs (WT, Δ199-202, and C186A) in MCF-7 cells (data not shown). Collectively, the information obtained from TAP-tagging caspase-9 to isolate the apoptosome has revealed many important factors to consider when undertaking tandem-affinity purification.

7.2 Future Work

I have shown in this thesis that affinity-tagging caspase-9 is an appropriate strategy to use to isolate and characterise the apoptosome (Chapter 3). However, *in vivo* expression of the TAP-tagged caspase-9 variants resulted in experimental difficulties (Chapters 4 & 5), such as the auto-activation of full-length caspase-9 induced by the dimerisation of GST. While these problems prevented any further analysis of the apoptosome from apoptotic cells they could potentially be overcome by expressing alternative TAP-tags. In this regard, FLAG and c-myc are widely used affinity-tags and have not been shown to dimerise, and therefore could be used to TAP-tag caspase-9 and be transiently expressed. If, as predicted, this TAP-tag composition does not induce the autoactivation of caspase-9 in transient-transfection experiments, then stable cell lines could be produced. The stable expression (constitutive or inducible) of the selected TAP-

tagged caspase-9 variant should then allow purification of sufficient quantities of apoptotic apoptosomes to identify associated proteins by mass spectrometry.

Although I identified the ~200 kDa active caspase-7 complex in both dATP-activated MCF-7 cell lysates and in apoptotic MCF-7 cells, work in this thesis only characterised the formation of this complex *in vitro* (Chapter 6). The composition of the active caspase-7 complex could therefore be investigated in apoptotic cells by a combination of two strategies. Firstly, by using the anti-XIAP antibody to immunoprecipitate the complex, as previously used to isolate the ~200-300 kDa caspase-7/XIAP complex from dATP-activated cell lysates. Secondly, the complex could be affinity-purified by over-expressing caspase-7 TAP-tagged at the C-terminus. The affinity purification of wt and mutant forms (non-cleavable/ catalytically inactive) of caspase-7 from apoptotic cells should also help elucidate the mechanism by which XIAP is sequestering active caspase-7.

Not only does caspase-7 differ in its biochemical properties from caspase-3 (such as its subcellular localisation (Chandler *et al*, 1998) and its sequestration by XIAP in the presence of SMAC and Omi (Chapter 6)), but also the N-peptide domain of caspase-7 has been proposed to act as a negative regulator of the caspase *in vivo* (Denault & Salvesen, 2003). It is therefore possible that this N-peptide domain is interacting with a sequestering protein and affecting the function of caspase-7. This possibility could be investigated by TAP-tagging caspase-7 at either the N- or the C-terminus. Following cleavage at Asp23, the N-terminal TAP-tag would remain associated with the N-peptide, whereas the C-terminal tag would track active caspase-7. Furthermore, this would allow a distinction to be drawn between proteins interacting with these specific domains. This study could be performed in MCF-7/WT and MCF-7/CASP3 cells to observe the role of caspase-3 in the regulation of caspase-7 by its N-peptide domain.

Overexpression of the ΔN-caspase-7 protein is significantly more proapoptotic than similar overexpression of the wild-type protein (Duan *et al*, 1996a; Denault & Salvesen, 2003). However, many of these previous studies have expressed ΔN-caspase-7 with a methionine residue substituting for alanine at the N-terminus (Denault & Salvesen, 2003; Yaoita, 2002). Significantly, the presence of a methionine at the N-terminus could prevent any likely interactions with potential

binding partners, as the exposed alanine has been suggested to mediate IAP binding and modulation of caspase activity (Tenev *et al*, 2005). To address this, ΔN-caspase-7 could be expressed with an N-terminal ubiquitin motif, which can subsequently be removed by proteolytic cleavage, to reveal the N-terminal alanine residue. This approach has already been successfully used to induce expression of cytosolic SMAC (Hunter *et al*, 2003). The presence of a C-terminal TAP-tag would then allow purification of this form of caspase-7 and the identification of any interacting proteins.

Many caspase-3-specific substrates have previously been identified, however, little is known about the substrates of caspase-7. In order to identify caspase-7 substrates, a technique could be employed which has previously enabled the identification of NDUFS1 as a caspase-3 substrate (Ricci *et al*, 2004). Briefly, this technique would require cell cytosols to be extracted from apoptotic MCF-7 cells and separated by SDS-PAGE. The gels would then be incubated with recombinant active caspase-7, rotated 90° to the initial SDS-PAGE and re-electrophorised, thus allowing the identification of potential cleavage products along the diagonal axis. Furthermore, as active caspase-7 undergoes subcellular translocation during apoptosis (Chandler *et al*, 1998), apoptotic MCF-7 cells could initially be fractionated into membrane, nuclear, mitochondrial/microsomal and cytosolic fractions, prior to analysis, thus increasing the likelihood of identifying potential caspase-7-specific substrates.

Appendix

Publications arising from this work

1) Twiddy, D., Brown, D.G., Adrain, C., Jukes, R., Martin, S.J., Cohen, G.M., MacFarlane, M. and Cain, K. (2004) Pro-apoptotic proteins released from the mitochondria regulate the protein composition and caspase-processing activity of the native Apaf-1/caspase-9 apoptosome complex. *J. Biol. Chem.* **279**, 19665-19682.

2) Twiddy, D., Cohen, G.M., MacFarlane, M. and Cain, K. (2005) Caspase-7 is directly activated by the ~700 kDa apoptosome complex and is released as a stable XIAP/caspase-7 ~200 kDa complex. *J. Biol. Chem.* In press.

Awards received from this work

'Best Student Poster Presentation' at the 5th International Cell Death Symposium, Maynooth, Ireland, 2004.

References

Acehan D., Jiang X. J., Morgan D. G., Heuser J. E., Wang X. D. and Akey C. W. (2002) Three-dimensional structure of the apoptosome: Implications for assembly, procaspase-9 binding, and activation. *Mol Cell* **9,** 423-432.

Adachi S., Cross A. R., Babior B. M. and Gottlieb R. A. (1997) Bcl-2 and the outer mitochondrial membrane in the inactivation of cytochrome c during Fas-mediated apoptosis. *J Biol Chem* **272,** 21878-21882.

Adrain C., Slee E. A., Harte M. T. and Martin S. J. (1999) Regulation of apoptotic protease activating factor-1 oligomerization and apoptosis by the WD-40 repeat region. *J Biol Chem* **274,** 20855-20860.

Adrain C., Creagh E. M. and Martin S. J. (2001) Apoptosis-associated release of Smac/DIABLO from mitochondria requires active caspases and is blocked by Bcl-2. *EMBO J.* **20,** 6627-6636.

Allan L. A., Morrice N., Brady S., Magee G., Pathak S. and Clarke P. R. (2003) Inhibition of caspase-9 through phosphorylation at Thr 125 by ERK MAPK. *Nature Cell Biology* **5,** 647-654.

Almond J. B., Snowden R. T., Hunter A., Dinsdale D., Cain K. and Cohen G. M. (2001) Proteasome inhibitor-induced apoptosis of B-chronic lymphocytic leukaemia cells involves cytochrome c release and caspase activation, accompanied by formation of an approximately 700 kDa Apaf-1 containing apoptosome complex. *Leukemia* **15,** 1388-1397.

Andree H. A., Reutelingsperger C. P., Hauptmann R., Hemker H. C., Hermens W. T. and Willems G. M. (1990) Binding of vascular anticoagulant alpha (VAC alpha) to planar phospholipid bilayers. *J Biol Chem* **265,** 4923-4928.

Beere H. M., Wolf B. B., Cain K., Mosser D. D., Mahboubi A., Kuwana T., Tailor P., Morimoto R. I., Cohen G. M. and Green D. R. (2000) Heat-shock protein 70 inhibits apoptosis by preventing recruitment of procaspase-9 to the Apaf-1 apoptosome. *Nature Cell Biology* **2,** 469-475.

Benedict M. A., Hu Y. M., Inohara N. and Nunez G. (2000) Expression and functional analysis of Apaf-1 isoforms - Extra WD-40 repeat is required for cytochrome c binding and regulated activation of procaspase-9. *J Biol Chem* **275,** 8461-8468.

Boatright K. M., Renatus M., Scott F. L., Sperandio S., Shin H., Pedersen I. M., Ricci J. E., Edris W. A., Sutherlin D. P., Green D. R. and Salvesen G. S. (2003) A unified model for apical caspase activation. *Mol Cell* **11,** 529-541.

Boldin M. P., Varfolomeev E. E., Pancer Z., Mett I. L., Camonis J. H. and Wallach D. (1995) A novel protein that interacts with the death domain of Fas/APO1 contains a sequence motif related to the death domain. *J Biol Chem* **270,** 7795-7798.

Boldin M. P., Goncharov T. M., Goltsev Y. V. and Wallach D. (1996) Involvement of MACH, a novel MORT1/FADD-interacting protease, in Fas/APO-1- and TNF receptor-induced cell death. *Cell* **85,** 803-815.

Bossy-Wetzel E. and Green D. R. (1999) Caspases induce cytochrome c release from mitochondria by activating cytosolic factors. *J Biol Chem* **274,** 17484-17490.

Bradford M. M. (1976) Rapid and Sensitive Method for Quantitation of Microgram Quantities of Protein Utilizing Principle of Protein-Dye Binding. *Anal Biochem* **72,** 248-254.

Bratton S. B., Walker G., Roberts D. L., Cain K. and Cohen G. M. (2001a) Caspase-3 cleaves Apaf-1 into an approximately 30 kDa fragment that associates with an inappropriately oligomerized and biologically inactive approximately 1.4 MDa apoptosome complex. *Cell Death Differ* **8,** 425-433.

Bratton S. B., Walker G., Srinivasula S. M., Sun X. M., Butterworth M., Alnemri E. S. and Cohen G. M. (2001b) Recruitment, activation and retention of caspases-9 and -3 by Apaf-1 apoptosome and associated XIAP complexes. *EMBO J* **20,** 998-1009.

Bratton S. B., Lewis J., Butterworth M., Duckett C. S. and Cohen G. M. (2002) XIAP inhibition of caspase-3 preserves its association with the Apaf-1 apoptosome and prevents CD95- and Bax-induced apoptosis. *Cell Death Differ* **9,** 881-892.

Bruey J. M., Ducasse C., Bonniaud P., Ravagnan L., Susin S. A., Diaz-Latoud C., Gurbuxani S., Arrigo A. P., Kroemer G., Solary E. and Garrido C. (2000) Hsp27 negatively regulates cell death by interacting with cytochrome c. *Nature Cell Biology* **2,** 645-652.

Cain K., Brown D. G., Langlais C. and Cohen G. M. (1999) Caspase activation involves the formation of the aposome, a large (approximately 700 kDa) caspase-activating complex. *J Biol Chem* **274,** 22686-22692.

Cain K., Bratton S. B., Langlais C., Walker G., Brown D. G., Sun X. M. and Cohen G. M. (2000) Apaf-1 oligomerizes into biologically active approximately 700-kDa and inactive approximately 1.4-MDa apoptosome complexes. *J Biol Chem* **275,** 6067-6070.

Cain K., Langlais C., Sun X. M., Brown D. G. and Cohen G. M. (2001) Physiological concentrations of K+ inhibit cytochrome c-dependent formation of the apoptosome. *J Biol Chem* **276,** 41985-41990.

Cain K., Bratton S. B. and Cohen G. M. (2002) The Apaf-1 apoptosome: a large caspase-activating complex. *Biochimie* **84,** 203-214.

Casciola-Rosen L. A., Miller D. K., Anhalt G. J. and Rosen A. (1994) Specific cleavage of the 70-kDa protein component of the U1 small nuclear ribonucleoprotein is a characteristic biochemical feature of apoptotic cell death. *J Biol Chem* **269,** 30757-30760.

Casciola-Rosen L., Nicholson D. W., Chong T., Rowan K. R., Thornberry N. A., Miller D. K. and Rosen A. (1996) Apopain/CPP32 cleaves proteins that are essential for cellular repair: a fundamental principle of apoptotic death. *J Exp Med* **183,** 1957-1964.

Cecconi F., Alvarez-Bolado G., Meyer B. I., Roth K. A. and Gruss P. (1998) Apaf1 (CED-4 Homolog) Regulates Programmed Cell Death in Mammalian Development. *Cell* **94,** 727-737.

Cerretti D. P., Kozlosky C. J., Mosley B., Nelson N., Van Ness K., Greenstreet T. A., March C. J., Kronheim S. R., Druck T. and Cannizzaro L. A. (1992) Molecular cloning of the interleukin-1 beta converting enzyme. *Science* **256,** 97-100.

Chai J., Du C., Wu J.-W., Kyin S., Wang X. and Shi Y. (2000) Structural and biochemical basis of apoptotic activation by Smac/DIABLO. *Nature* **406,** 855-862.

Chai J., Shiozaki E., Srinivasula S. M., Wu Q., Datta P., Alnemri E. S. and Shi Y. (2001) Structural basis of caspase-7 inhibition by XIAP. *Cell* **104,** 769-780.

Chandler J. M., Alnemri E. S., Cohen G. M. and MacFarlane M. (1997) Activation of CPP32 and Mch3 alpha in wild-type p53-induced apoptosis. *Biochem J* **322,** 19-23.

Chandler J. M., Cohen G. M. and MacFarlane M. (1998) Different subcellular distribution of caspase-3 and caspase-7 following Fas-induced apoptosis in mouse liver. *J Biol Chem* **273,** 10815-10818.

Chang D. W., Xing Z., Pan Y., Algeciras-Schimnich A., Barnhart B. C., Yaish-Ohad S., Peter M. E. and Yang X. (2002) c-FLIP(L) is a dual function regulator for caspase-8 activation and CD95-mediated apoptosis. *EMBO J* **21,** 3704-3714.

Chao Y., Shiozaki E. N., Srinivasula S. M., Rigotti D. J, Fairman R. and Shi Y. G. (2005) Engineering a dimeric caspase-9: A re-evaluation of the induced proximity model for caspase activation. *Plos Biol.* **3**,1079-1087.

Chau B. N., Cheng E. H.-Y., Kerr D. A. and Hardwick J. M. (2000) Aven, a Novel Inhibitor of Caspase Activation, Binds Bcl-xL and Apaf-1. *Mol Cell* **6,** 31-40.

Chen F. L., Hersh B. M., Conradt B., Zhou Z., Riemer D., Gruenbaum Y. and Horvitz H. R. (2000a) Translocation of C. elegans CED-4 to nuclear membranes during programmed cell death. *Science* **287,** 1485-1489.

Chen Q., Gong B. and Almasan A. (2000b) Distinct stages of cytochrome c release from mitochondria: evidence for a feedback amplification loop linking caspase activation to mitochondrial dysfunction in genotoxic stress induced apoptosis. *Cell Death Differ* **7,** 227-233.

Cheng E. H. Y., Kirsch D. G., Clem R. J., Ravi R., Kastan M. B., Bedi A., Ueno K. and Hardwick J. M. (1997) Conversion of Bcl-2 to a Bax-like death effector by caspases. *Science* **278,** 1966-1968.

Chinnaiyan A. M., O'Rourke K., Tewari M. and Dixit V. M. (1995) FADD, a novel death domain-containing protein, interacts with the death domain of Fas and initiates apoptosis. *Cell* **81,** 505-512.

Chinnaiyan A. M., ORourke K., Lane B. R. and Dixit V. M. (1997a) Interaction of CED-4 with CED-3 and CED-9: A molecular framework for cell death. *Science* **275,** 1122-1126.

Chinnaiyan A. M., Chaudhary D., O'Rourke K., Koonin E. V. and Dixit V. M. (1997b) Role of CED-4 in the activation of CED-3. *Nature* **388,** 728-729.

Chou J. J., Matsuo H., Duan H. and Wagner G. (1998) Solution structure of the RAIDD CARD and model for CARD/CARD interaction in caspase-2 and caspase-9 recruitment. *Cell* **94,** 171-180.

Chow S. C., Weis M., Kass G. E., Holmstrom T. H., Eriksson J. E. and Orrenius S. (1995) Involvement of multiple proteases during Fas-mediated apoptosis in T lymphocytes. *FEBS Letters* **364,** 134-138.

Chu Z.-L., Pio F., Xie Z., Welsh K., Krajewska M., Krajewski S., Godzik A. and Reed J. C. (2001) A Novel Enhancer of the Apaf1 Apoptosome Involved in Cytochrome c-dependent Caspase Activation and Apoptosis. *J Biol Chem* **276,** 9239-9245.

Cohen G. M. (1997) Caspases: the executioners of apoptosis. *Biochem J* **326,** 1-16.

Conradt B. and Horvitz H. R. (1998) The C-elegans protein EGL-1 is required for programmed cell death and interacts with the Bcl-2-like protein CED-9. *Cell* **93,** 519-529.

Danial N. N. and Korsmeyer S. J. (2004) Cell death: Critical control points. *Cell* **116,** 205-219.

Darmon A. J., Nicholson D. W. and Bleackley R. C. (1995) Activation of the apoptotic protease CPP32 by cytotoxic T-cell-derived granzyme B. *Nature* **377,** 446-448.

Deming P. B., Schafer Z. T., Tashker J. S., Potts M. B., Deshmukh M. and Kornbluth S. (2004) Bcr-Abl-mediated protection from apoptosis downstream of mitochondrial cytochrome c release. *Mol Cell Biol* **24,** 10289-10299.

Denault J. B. and Salvesen G. S. (2003) Human caspase-7 activity and regulation by its N-terminal peptide. *J Biol Chem* **278,** 34042-34050.

Desagher S., Osen-Sand A., Nichols A., Eskes R., Montessuit S., Lauper S., Maundrell K., Antonsson B. and Martinou J. C. (1999) Bid-induced conformational change of Bax is responsible for mitochondrial cytochrome c release during apoptosis. *J Cell Biol* **144,** 891-901.

Desagher S., Osen-Sand A., Montessuit S., Magnenat E., Vilbois F., Hochmann A., Journot L., Antonsson B. and Martinou J.-C. (2001) Phosphorylation of Bid by Casein Kinases I and II Regulates Its Cleavage by Caspase 8. *Mol Cell* **8,** 601-611.

Dohi T., Okada K., Xia F., Wilford C. E., Samuel T., Welsh K., Marusawa H., Zou H., Armstrong R., Matsuzawa S., Salvesen G. S., Reed J. C. and Altieri D. C. (2004) An IAP-IAP complex inhibits apoptosis. *J. Biol. Chem.* **279**, 34087-34090.

Deveraux Q. L. and Reed J. C. (1999) IAP family proteins--suppressors of apoptosis. *Genes & Development* **13,** 239-252.

Deveraux Q. L., Takahashi R., Salvesen G. S. and Reed J. C. (1997) X-linked IAP is a direct inhibitor of cell-death proteases. *Nature* **388,** 300-304.

Deveraux Q. L., Leo E., Stennicke H. R., Welsh K., Salvesen G. S. and Reed J. C. (1999) Cleavage of human inhibitor of apoptosis protein XIAP results in fragments with distinct specificities for caspases. *EMBO J* **18,** 5242-5251.

Dorstyn L., Colussi P. A., Quinn L. M., Richardson H. and Kumar S. (1999) DRONC, an ecdysone-inducible Drosophila caspase. *P Natl Acad Sci USA* **96,** 4307-4312.

Dorstyn L., Read S., Cakouros D., Huh J. R., Hay B. A. and Kumar S. (2002) The role of cytochrome c in caspase activation in Drosophila melanogaster cells. *J Cell Biol* **156,** 1089-1098.

Du C., Fang M., Li Y., Li L. and Wang X. (2000) Smac, a mitochondrial protein that promotes cytochrome c-dependent caspase activation by eliminating IAP inhibition. *Cell* **102,** 33-42.

Duan H. J., Chinnaiyan A. M., Hudson P. L., Wing J. P., He W. W. and Dixit V. M. (1996a) ICE-LAP3, a novel mammalian homologue of the Caenorhabditis elegans cell death protein ced-3 is activated during fas- and tumor necrosis factor-induced apoptosis. *J Biol Chem* **271,** 1621-1625.

Duan H. J., Orth K., Chinnaiyan A. M., Poirier G. G., Froelich C. J., He W. W. and Dixit V. M. (1996b) ICE-LAP6, a novel member of the ICE/Ced-3 gene family, is activated by the cytotoxic T cell protease granzyme B. *J Biol Chem* **271,** 16720-16724.

Eckelman B.P. and Salvesen G.S. (2005) The human anti-apoptotic proteins, cIAP1 and cIAP2 bind but do not inhibit caspases. *J. Biol. Chem.* In press.

Ehrenberg B., Montana V., Wei M. D., Wuskell J. P. and Loew L. M. (1988) Membrane-Potential Can Be Determined in Individual Cells from the Nernstian Distribution of Cationic Dyes. *Biophys J* **53,** 785-794.

Ekert P. G., Silke J. and Vaux D. L. (1999) Caspase inhibitors. *Cell Death Differ* **6,** 1081-1086.

Ekert P. G., Silke J., Hawkins C. J., Verhagen A. M. and Vaux D. L. (2001) DIABLO promotes apoptosis by removing MIHA/XIAP from processed caspase 9. *J Cell Biol* **152,** 483-490.

Ellis H. M. and Horvitz H. R. (1986) Genetic-Control of Programmed Cell-Death in the Nematode C-Elegans. *Cell* **44,** 817-829.

Enari M., Sakahira H., Yokoyama H., Okawa K., Iwamatsu A. and Nagata S. (1998) A caspase-activated DNase that degrades DNA during apoptosis, and its inhibitor ICAD. *Nature* **391,** 43-50.

Fadok V. A., Voelker D. R., Campbell P. A., Cohen J. J., Bratton D. L. and Henson P. M. (1992) Exposure of phosphatidylserine on the surface of apoptotic lymphocytes triggers specific recognition and removal by macrophages. *J Immunology* **148,** 2207-2216.

Fadok V. A., Bratton D. L., Frasch S. C., Warner M. L. and Henson P. M. (1998) The role of phosphatidylserine in recognition of apoptotic cells by phagocytes. *Cell Death Differ* **5,** 551-562.

Fang G. F., Chang B. S., Kim C. N., Perkins C., Thompson C. B. and Bhalla K. N. (1998) "Loop" domain is necessary for taxol-induced mobility shift and phosphorylation of Bcl-2 as well as for inhibiting taxol-induced cytosolic Accumulation of cytochrome c and apoptosis. *Cancer Res* **58,** 3202-3208.

Fearnhead H. O., Dinsdale D. and Cohen G. M. (1995) An interleukin-1 beta-converting enzyme-like protease is a common mediator of apoptosis in thymocytes. *FEBS Letters* **375,** 283-288.

Fernandes-Alnemri T., Litwack G. and Alnemri E. (1994) CPP32, a novel human apoptotic protein with homology to Caenorhabditis elegans cell death protein Ced-3 and mammalian interleukin-1 beta- converting enzyme. *J Biol Chem* **269,** 30761-30764.

Fernandes-Alnemri T., Takahashi A., Armstrong R., Krebs J., Fritz L., Tomaselli K. J., Wang L., Yu Z., Croce C. M. and Salveson G. (1995) Mch3, a novel human apoptotic cysteine protease highly related to CPP32. *Cancer Res* **55,** 6045-6052.

Fernandes-Alnemri T., Armstrong R. C., Krebs J., Srinivasula S. M., Wang L., Bullrich F., Fritz L. C., Trapani J. A., Tomaselli K. J., Litwack G. and Alnemri E. S. (1996) In vitro activation of CPP32 and Mch3 by Mch4, a novel human apoptotic cysteine protease containing two FADD-like domains. *P Natl Acad Sci USA* **93,** 7464-7469.

Fesik S. W. and Shi Y. G. (2001) Structural biology - Controlling the caspases. *Science* **294,** 1477-1478.

Figueroa B., Jr., Sauerwald T. M., Oyler G. A., Hardwick J. M. and Betenbaugh M. J. (2003) A comparison of the properties of a Bcl-xL variant to the wild-type anti-apoptosis inhibitor in mammalian cell cultures. *Metabolic Engineering* **5,** 230-245.

Freathy C., Brown D. G., Roberts R. A. and Cain K. (2000) Transforming growth factor-beta(1) induces apoptosis in rat FaO hepatoma cells via cytochrome c release and oligomerization of Apaf-1 to form a similar to 700-kd apoptosome caspase-processing complex. *Hepatology* **32,** 750-760.

Fuentes-Prior P. and Salvesen G. S. (2004) The protein structures that shape caspase activity, specificity, activation and inhibition. *Biochem J* **384,** 201-232.

Garcia-Calvo M., Peterson E. P., Rasper D. M., Vaillancourt J. P., Zamboni R., Nicholson D. W. and Thornberry N. A. (1999) Purification and catalytic properties of human caspase family members. *Cell Death Differ* **6,** 362-369.

Garrido C., Bruey J.-M., Fromentin A., Hammann A., Arrigo A. P. and Solary E. (1999) HSP27 inhibits cytochrome c-dependent activation of procaspase-9. *FASEB J.* **13,** 2061-2070.

Germain M., Affar E. B., D'Amours D., Dixit V. M., Salvesen G. S. and Poirier G. G. (1999) Cleavage of automodified poly(ADP-ribose) polymerase during apoptosis. Evidence for involvement of caspase-7. *J Biol Chem* **274,** 28379-28384.

Gonzales D. H. and Neupert W. (1990) Biogenesis of mitochondrial c-type cytochromes. *J Bioenerg & Biomembr* **22,** 753-768.

Gross A., Yin X. M., Wang K., Wei M. C., Jockel J., Milliman C., Erdjument-Bromage H., Tempst P. and Korsmeyer S. J. (1999a) Caspase cleaved BID targets mitochondria and is required for cytochrome c release, while BCL-XL prevents this release but not tumor necrosis factor-R1/Fas death. *J Biol Chem* **274,** 1156-1163.

Gross A., McDonnell J. M. and Korsmeyer S. J. (1999b) BCL-2 family members and the mitochondria in apoptosis. *Genes & Development* **13,** 1899-1911.

Gu Y., Sarnecki C., Fleming M. A., Lippke J. A., Bleackley R. C. and Su M. S. (1996) Processing and activation of CMH-1 by granzyme B. *J Biol Chem* **271,** 10816-10820.

Hahn C., Hirsch B., Jahnke D., Durkop H. and Stein H. (1999) Three new types of Apaf-1 in mammalian cells. *Biochem Bioph Res Co* **261,** 746-749.

Hakem R., Hakem A., Duncan G. S., Henderson J. T., Woo M., Soengas M. S., Elia A., de la Pompa J. L., Kagi D., Khoo W., Potter J., Yoshida R., Kaufman S. A., Lowe S. W., Penninger J. M. and Mak T. W. (1998) Differential requirement for caspase 9 in apoptotic pathways in vivo. *Cell* **94,** 339-352.

Han Z. Y., Hendrickson E. A., Bremner T. A. and Wyche J. H. (1997) A sequential two-step mechanism for the production of the mature p17:p12 form of caspase-3 in vitro. *J Biol Chem* **272,** 13432-13436.

Harper N., Hughes M., MacFarlane M. and Cohen G. M. (2003) Fas-associated death domain protein and caspase-8 are not recruited to the tumor necrosis factor receptor 1 signaling complex during tumor necrosis factor-induced apoptosis. *J Biol Chem* **278,** 25534-25541.

Hausmann G., O'Reilly L. A., van Driel R., Beaumont J. G., Strasser A., Adams J. M. and Huang D. C. S. (2000) Pro-apoptotic Apoptosis Protease-activating Factor 1 (Apaf-1) Has a Cytoplasmic Localization Distinct from Bcl-2 or Bcl-xL. *J Cell Biol* **149,** 623-634.

Hawkins C. J., Yoo S. J., Peterson E. P., Wang S. L., Vernooy S. Y. and Hay B. A. (2000) The Drosophila caspase DRONC cleaves following glutamate or aspartate and is regulated by DIAP1, HID, and GRIM. *J Biol Chem* **275,** 27084-27093.

Hay B. A., Wassarman D. A. and Rubin G. M. (1995) Drosophila homologs of baculovirus inhibitor of apoptosis proteins function to block cell death. *Cell* **83,** 1253-1262.

Hegde R., Srinivasula S. M., Zhang Z. J., Wassell R., Mukattash R., Cilenti L., DuBois G., Lazebnik Y., Zervos A. S., Fernandes-Alnemri T. and Alnemri E. S. (2002) Identification of Omi/HtrA-2 as a mitochondrial apoptotic serine protease that disrupts inhibitor of apoptosis protein-caspase interaction. *J Biol Chem* **277,** 432-438.

Heibein J. A., Goping I. S., Barry M., Pinkoski M. J., Shore G. C., Green D. R. and Bleackley R. C. (2000) Granzyme B-mediated cytochrome c release is regulated by the Bcl-2 family members bid and Bax. *J Exp Med.* **192,** 1391-1402.

Heiskanen K. M., Bhat M. B., Wang H. W., Ma J. and Nieminen A. L. (1999) Mitochondrial depolarization accompanies cytochrome c release during apoptosis in PC6 cells. *J Biol Chem* **274,** 5654-5658.

Hengartner M. O. and Horvitz H. R. (1994) C-Elegans Cell-Survival Gene Ced-9 Encodes a Functional Homolog of the Mammalian Protooncogene Bcl-2. *Cell* **76,** 665-676.

Hengartner M. O., Ellis R. E. and Horvitz H. R. (1992) Caenorhabditis elegans gene ced-9 protects cells from programmed cell death. *Nature* **356,** 494-499.

Hill M. M., Adrain C., Duriez P. J., Creagh E. M. and Martin S. J. (2004) Analysis of the composition, assembly kinetics and activity of native Apaf-1 apoptosomes. *EMBO J* **23,** 2134-2145.

Hlaing T., Guo R.-F., Dilley K. A., Loussia J. M., Morrish T. A., Shi M. M., Vincenz C. and Ward P. A. (2001) Molecular Cloning and Characterization of DEFCAP-L and -S, Two Isoforms of a Novel Member of the Mammalian Ced-4 Family of Apoptosis Proteins. *J Biol Chem* **276,** 9230-9238.

Hofmann K., Bucher P. and Tschopp J. (1997) The CARD domain: a new apoptotic signalling motif. *Trends Biochem Sci* **22,** 155-156.

Holcik M. and Korneluk R. G. (2001) XIAP, the guardian angel. *Nat Rev Mol Cell Biol* **2,** 550-556.

Honey S., Schneider B. L., Schieltz D. M., Yates J. R. and Futcher B. (2001) A novel multiple affinity purification tag and its use in identification of proteins associated with a cyclin-CDK complex. *Nucl Acids Res* **29,** e24, 1-9.

Houde C., Banks K. G., Coulombe N., Rasper D., Grimm E., Roy S., Simpson E. M. and Nicholson D. W. (2004) Caspase-7 expanded function and intrinsic expression level underlies strain-specific brain phenotype of caspase-3-null mice. *J Neuroscience* **24,** 9977-9984.

Hsu H., Shu H. B., Pan M. G. and Goeddel D. V. (1996a) TRADD-TRAF2 and TRADD-FADD interactions define two distinct TNF receptor 1 signal transduction pathways. *Cell* **84,** 299-308.

Hsu H., Huang J., Shu H. B., Baichwal V. and Goeddel D. V. (1996b) TNF-dependent recruitment of the protein kinase RIP to the TNF receptor-1 signaling complex. *Immunity* **4,** 387-396.

Hu Y., Benedict M. A., Wu D., Inohara N. and Nunez G. (1998a) Bcl-XL interacts with Apaf-1 and inhibits Apaf-1-dependent caspase-9 activation. *P Natl Acad Sci USA* **95,** 4386-4391.

Hu Y. M., Ding L. Y., Spencer D. M. and Nunez G. (1998b) WD-40 repeat region regulates Apaf-1 self-association and procaspase-9 activation. *J Biol Chem* **273,** 33489-33494.

Hu Y., Benedict M. A., Ding L. and Nunez G. (1999) Role of cytochrome c and dATP/ATP hydrolysis in Apaf-1-mediated caspase-9 activation and apoptosis. *EMBO J* **18,** 3586-3595.

Huang Y., Park Y. C., Rich R. L., Segal D., Myszka D. G. and Wu H. (2001) Structural basis of caspase inhibition by XIAP: differential roles of the linker versus the BIR domain. *Cell* **104,** 781-790.

Hunter A. M., Kottachchi D., Lewis J., Duckett C. S., Korneluk R. G. and Liston P. (2003) A novel ubiquitin fusion system bypasses the mitochondria and generates biologically active Smac/DIABLO. *J Biol Chem* **278,** 7494-7499.

Igney F. H. and Krammer P. H. (2002) Death and anti-death: tumour resistance to apoptosis. *Nature Reviews. Cancer* **2,** 277-288.

Irmler M., Thome M., Hahne M., Schneider P., Hofmann K., Steiner V., Bodmer J. L., Schroter M., Burns K., Mattmann C., Rimoldi D., French L. E. and Tschopp J. (1997) Inhibition of death receptor signals by cellular FLIP. *Nature* **388,** 190-195.

Itoh N., Yonehara S., Ishii A., Yonehara M., Mizushima S., Sameshima M., Hase A., Seto Y. and Nagata S. (1991) The polypeptide encoded by the cDNA for human cell surface antigen Fas can mediate apoptosis. *Cell* **66,** 233-243.

Jacobson M. D., Weil M. and Raff M. C. (1996) Role of Ced3/ICE-family proteases in staurosporine-induced programmed cell death. *J Cell Biol* **133,** 1041-1051.

Jacobson M. D., Weil M. and Raff M. C. (1997) Programmed cell death in animal development. *Cell* **88,** 347-354.

Janicke R. U., Sprengart M. L., Wati M. R. and Porter A. G. (1998) Caspase-3 is required for DNA fragmentation and morphological changes associated with apoptosis. *J Biol Chem* **273,** 9357-9360.

Jiang X. J. and Wang X. D. (2000) Cytochrome c promotes caspase-9 activation by inducing nucleotide binding to Apaf-1. *J Biol Chem* **275,** 31199-31203.

Jiang X., Kim H.-E., Shu H., Zhao Y., Zhang H., Kofron J., Donnelly J., Burns D., Ng S.-c., Rosenberg S. and Wang X. (2003) Distinctive Roles of PHAP Proteins and Prothymosin-alpha in a Death Regulatory Pathway. *Science* **299,** 223-226.

Juo P., Kuo C. J., Yuan J. and Blenis J. (1998) Essential requirement for caspase-8/FLICE in the initiation of the Fas-induced apoptotic cascade. *Curr Biol* **8,** 1001-1008.

Kagi D., Ledermann B., Burki K., Seiler P., Odermatt B., Olsen K. J., Podack E. R., Zinkernagel R. M. and Hengartner H. (1994) Cytotoxicity mediated by T cells and natural killer cells is greatly impaired in perforin-deficient mice. *Nature* **369,** 31-37.

Kaiser W. J., Vucic D. and Miller L. K. (1998) The Drosophila inhibitor of apoptosis D-IAP1 suppresses cell death induced by the caspase drICE. *FEBS Letters* **440,** 243-248.

Kanuka H., Sawamoto K., Inohara N., Matsuno K., Okano H. and Miura M. (1999) Control of the cell death pathway by Dapaf-1, a Drosophila Apaf-1/CED-4-related caspase activator. *Mol Cell* **4,** 757-769.

Kaufmann S. H. (1998) Cell death induced by topoisomerase-targeted drugs: more questions than answers. *Biochimica et Biophysica Acta (BBA) - Gene Structure and Expression* **1400,** 195-211.

Kaufmann S. H., Desnoyers S., Ottaviano Y., Davidson N. E. and Poirier G. G. (1993) Specific proteolytic cleavage of poly(ADP-ribose) polymerase: an early marker of chemotherapy-induced apoptosis. *Cancer Res* **53,** 3976-3985.

Kerr J. F., Wyllie A. H. and Currie A. R. (1972) Apoptosis: a basic biological phenomenon with wide-ranging implications in tissue kinetics. *Br J Cancer* **26,** 239-257.

Kharbanda S., Pandey P., Schofield L., Israels S., Roncinske R., Yoshida K., Bharti A., Yuan Z.-M., Saxena S., Weichselbaum R., Nalin C. and Kufe D. (1997) Role for Bcl-xL as an inhibitor of cytosolic cytochrome C accumulation in DNA damage-induced apoptosis. *P Natl Acad Sci USA* **94,** 6939-6942.

Kirsch D. G., Doseff A., Chau B. N., Lim D. S., de Souza-Pinto N. C., Hansford R., Kastan M. B., Lazebnik Y. A. and Hardwick J. M. (1999) Caspase-3-dependent cleavage of Bcl-2 promotes release of cytochrome c. *J Biol Chem* **274,** 21155-21161.

Kluck R. M., Bossy-Wetzel E., Green D. R. and Newmeyer D. D. (1997) The release of cytochrome c from mitochondria: A primary site for Bcl-2 regulation of apoptosis. *Science* **275,** 1132-1136.

Kluck R. M., Esposti M. D., Perkins G., Renken C., Kuwana T., Bossy-Wetzel E., Goldberg M., Allen T., Barber M. J., Green D. R. and Newmeyer D. D. (1999) The pro-apoptotic proteins, Bid and Bax, cause a limited permeabilization of the mitochondrial outer membrane that is enhanced by cytosol. *J Cell Biol* **147,** 809-822.

Kothakota S., Azuma T., Reinhard C., Klippel A., Tang J., Chu K., McGarry T. J., Kirschner M. W., Koths K., Kwiatkowski D. J. and Williams L. T. (1997) Caspase-3-generated fragment of gelsolin: effector of morphological change in apoptosis. *Science* **278,** 294-298.

Krippner A., MatsunoYagi A., Gottlieb R. A. and Babior B. M. (1996) Loss of function of cytochrome c in Jurkat cells undergoing Fas-mediated apoptosis. *J Biol Chem* **271,** 21629-21636.

Krueger A., Baumann S., Krammer P. H. and Kirchhoff S. (2001) FLICE-inhibitory proteins: Regulators of death receptor-mediated apoptosis. *Mol Cell Biol* **21,** 8247-8254.

Kuida K., Haydar T. F., Kuan C. Y., Gu Y., Taya C., Karasuyama H., Su M. S., Rakic P. and Flavell R. A. (1998) Reduced apoptosis and cytochrome c-mediated caspase activation in mice lacking caspase 9. *Cell* **94,** 325-337.

Kumar S. and Doumanis J. (2000) The fly caspases. *Cell Death Differ* **7,** 1039-1044.

Langlais C. (2002) Characterisation of the ~700 kDa apoptosome complex from THP.1 cells. PhD Thesis.

Lauber K., Appel H. A., Schlosser S. F., Gregor M., Schulze-Osthoff K. and Wesselborg S. (2001) The adapter protein apoptotic protease-activating factor-1 (Apaf-1) is proteolytically processed during apoptosis. *J Biol Chem* **276,** 29772-29781.

Lazebnik Y. A., Kaufmann S. H., Desnoyers S., Poirier G. G. and Earnshaw W. C. (1994) Cleavage of poly(ADP-ribose) polymerase by a proteinase with properties like ICE. *Nature* **371,** 346-347.

Li P., Nijhawan D., Budihardjo I., Srinivasula S. M., Ahmad M., Alnemri E. S. and Wang X. (1997) Cytochrome c and dATP-dependent formation of Apaf-1/caspase-9 complex initiates an apoptotic protease cascade. *Cell* **91,** 479-489.

Li H., Zhu H., Xu C. J. and Yuan J. (1998) Cleavage of BID by caspase 8 mediates the mitochondrial damage in the Fas pathway of apoptosis. *Cell* **94,** 491-501.

Li K., Li Y. C., Shelton J. M., Richardson J. A., Spencer E., Chen Z. J., Wang X. D. and Williams R. S. (2000a) Cytochrome c deficiency causes embryonic lethality and attenuates stress-induced apoptosis. *Cell* **101,** 389-399.

Li C. Y., Lee J. S., Ko Y. G., Kim J. I. and Seo J. S. (2000b) Heat shock protein 70 inhibits apoptosis downstream of cytochrome c release and upstream of caspase-3 activation. *J Biol Chem* **275,** 25665-25671.

Li W. Y., Srinivasula S. M., Chai J. J., Li P. W., Wu J. W., Zhang Z. J., Alnemri E. S. and Shi Y. G. (2002) Structural insights into the pro-apoptotic function of mitochondrial serine protease HtrA2/Omi. *Nat Struct Biol* **9,** 436-441.

Liang Y., Yan C. and Schor N. F. (2001) Apoptosis in the absence of caspase 3. *Oncogene* **20,** 6570-6578.

Lippke J. A., Gu Y., Sarnecki C., Caron P. R. and Su M. S. (1996) Identification and characterization of CPP32/Mch2 homolog 1, a novel cysteine protease similar to CPP32. *J Biol Chem* **271,** 1825-1828.

Liu X. S., Kim C. N., Yang J., Jemmerson R. and Wang X. D. (1996) Induction of apoptotic program in cell-free extracts: Requirement for dATP and cytochrome c. *Cell* **86,** 147-157.

Liu X. S., Zou H., Slaughter C. and Wang X. D. (1997) DFF, a heterodimeric protein that functions downstream of caspase-3 to trigger DNA fragmentation during apoptosis. *Cell* **89,** 175-184.

Liu Z., Sun C., Olejniczak E. T., Meadows R. P., Betz S. F., Oost T., Herrmann J., Wu J. C. and Fesik S. W. (2000) Structural basis for binding of Smac/DIABLO to the XIAP BIR3 domain. *Nature* **408,** 1004-1008.

Los M. and Walczak H. (2002) *Caspases-Their Role in Cell Death and Cell Survival*, Vol. 24. Landes Bioscience, Georgetown, Texas.

Luo X., Budihardjo I., Zou H., Slaughter C. and Wang X. (1998) Bid, a Bcl2 interacting protein, mediates cytochrome c release from mitochondria in response to activation of cell surface death receptors. *Cell* **94,** 481-490.

MacFarlane M., Cain K., Sun X. M., Alnemri E. S. and Cohen G. M. (1997) Processing/activation of at least four interleukin-1beta converting enzyme-like proteases occurs during the execution phase of apoptosis in human monocytic tumor cells. *J Cell Biol* **137,** 469-479.

MacFarlane M., Merrison W., Dinsdale D. and Cohen G. M. (2000) Active caspases and cleaved cytokeratins are sequestered into cytoplasmic inclusions in TRAIL-induced apoptosis. *J Cell Biol* **148,** 1239-1254.

Martin M. C., Allan L. A., Lickrish M., Sampson C., Morrice N. and Clarke P. R. (2005) Protein Kinase A Regulates Caspase-9 Activation by Apaf-1 Downstream of Cytochrome c. *J Biol Chem.* **280,** 15449-15455.

Martin S. J., Obrien G. A., Nishioka W. K., Mcgahon A. J., Mahboubi A., Saido T. C. and Green D. R. (1995a) Proteolysis of Fodrin (Nonerythroid Spectrin) During Apoptosis. *J Biol Chem* **270,** 6425-6428.

Martin S. J., Newmeyer D. D., Mathias S., Farschon D. M., Wang H. G., Reed J. C., Kolesnick R. N. and Green D. R. (1995b) Cell-Free Reconstitution of Fas-Induced, UV-Radiation-Induced and Ceramide-Induced Apoptosis. *EMBO J* **14,** 5191-5200.

Martin S. J., AmaranteMendes G. P., Shi L. F., Chuang T. H., Casiano C. A., OBrien G. A., Fitzgerald P., Tan E. M., Bokoch G. M., Greenberg A. H. and Green D. R. (1996) The cytotoxic cell protease granzyme B initiates apoptosis in a cell-free system by proteolytic processing and activation of the ICE/CED-3 family protease, CPP32, via a novel two-step mechanism. *EMBO J* **15,** 2407-2416.

Martins L. M., Iaccarino I., Tenev T., Gschmeissner S., Totty N. F., Lemoine N. R., Savopoulos J., Gray C. W., Creasy C. L., Dingwall C. and Downward J. (2002) The serine protease Omi/HtrA2 regulates apoptosis by binding XIAP through a reaper-like motif. *J Biol Chem* **277,** 439-444.

Meier P., Silke J., Leevers S. J. and Evan G. I. (2000) The Drosophila caspase DRONC is regulated by DIAP1. *EMBO J* **19,** 598-611.

Micheau O. and Tschopp J. (2003) Induction of TNF receptor I-mediated apoptosis via two sequential signaling complexes. *Cell* **114,** 181-190.

Micheau O., Thome M., Schneider P., Holler N., Tschopp J., Nicholson D. W., Briand C. and Grutter M. G. (2002) The long form of FLIP is an activator of caspase-8 at the Fas death-inducing signaling complex. *J Biol Chem* **277,** 45162-45171.

Mittl P. R., Di Marco S., Krebs J. F., Bai X., Karanewsky D. S., Priestle J. P., Tomaselli K. J. and Grutter M. G. (1997) Structure of recombinant human CPP32 in complex with the tetrapeptide acetyl-Asp-Val-Ala-Asp fluoromethyl ketone. *J Biol Chem* **272,** 6539-6547.

Mizumoto K., Rothman R. J. and Farber J. L. (1994) Programmed cell death (apoptosis) of mouse fibroblasts is induced by the topoisomerase II inhibitor etoposide. *Mol Pharmacology* **46,** 890-895.

Moriishi K., Huang D. C. S., Cory S. and Adams J. M. (1999) Bcl-2 family members do not inhibit apoptosis by binding the caspase activator Apaf-1. *P Natl Acad Sci* **96,** 9683-9688.

Muro I., Hay B. A. and Clem R. J. (2002) The Drosophila DIAP1 Protein Is Required to Prevent Accumulation of a Continuously Generated, Processed Form of the Apical Caspase DRONC. *J Biol Chem.* **277,** 49644-49650.

Muzio M., Chinnaiyan A. M., Kischkel F. C., O'Rourke K., Shevchenko A., Ni J., Scaffidi C., Bretz J. D., Zhang M., Gentz R., Mann M., Krammer P. H., Peter M. E. and Dixit V. M. (1996) FLICE, a novel FADD-homologous ICE/CED-3-like protease, is recruited to the CD95 (Fas/APO-1) death--inducing signaling complex. *Cell* **85,** 817-827.

Muzio M., Salvesen G. S. and Dixit V. M. (1997) FLICE induced apoptosis in a cell-free system. Cleavage of caspase zymogens. *J Biol Chem* **272,** 2952-2956.

Muzio M., Stockwell B. R., Stennicke H. R., Salvesen G. S. and Dixit V. M. (1998) An induced proximity model for caspase-8 activation. *J Biol Chem* **273,** 2926-2930.

Nagata S. (1997) Apoptosis by death factor. *Cell* **88,** 355-365.

Neer E. J., Schmidt C. J., Nambudripad R. and Smith T. F. (1994) The Ancient Regulatory-Protein Family of Wd-Repeat Proteins. *Nature* **371,** 297-300.

Nicholson D. W. and Thornberry N. A. (1997) Caspases: killer proteases. *Trends Biochem Sci* **22,** 299-306.

Nicholson D. W., Ali A., Thornberry N. A., Vaillancourt J. P., Ding C. K., Gallant M., Gareau Y., Griffin P. R., Labelle M., Lazebnik Y. A., Munday N. A., Raju S. M., Smulson M. E., Yamin T. T., Yu V. L. and Miller D. K. (1995) Identification and Inhibition of the Ice/Ced-3 Protease Necessary for Mammalian Apoptosis. *Nature* **376,** 37-43.

Oehm A., Behrmann I., Falk W., Pawlita M., Maier G., Klas C., Li-Weber M., Richards S., Dhein J. and Trauth B. C. (1992) Purification and molecular cloning of the APO-1 cell surface antigen, a member of the tumor necrosis factor/nerve growth factor receptor superfamily. Sequence identity with the Fas antigen. *J Biol Chem* **267,** 10709-10715.

Ogawa T., Shiga K., Hashinioto S., Kobayashi T., Horii A. and Furukawa T. (2003) APAF-1-ALT, a novel alternative splicing form of Apaf-1, potentially causes impeded ability of undergoing DNA damage-induced apoptosis in the LNCaP human prostate cancer cell line. *Biochem Bioph Res Co* **306,** 537-543.

Op den Kamp J. A. F. (1979) Lipid Asymmetry in Membranes. *Annu Rev Biochem* **48,** 47-71.

Oppenheim R. W., Prevette D., Yin Q. W., Collins F. and MacDonald J. (1991) Control of embryonic motoneuron survival in vivo by ciliary neurotrophic factor. *Science* **251,** 1616-1618.

O'Reilly L. A., Ekert P., Harvey N., Marsden V., Cullen L., Vaux D. L., Hacker G., Magnusson C., Pakusch M., Cecconi F., Kuida K., Strasser A., Huang D. C. S. and Kumar S. (2002) Caspase-2 is not required for thymocyte or neuronal apoptosis even though cleavage of caspase-2 is dependent on both Apaf-1 and caspase-9. *Cell Death Differ* **9,** 832-841.

Pan G., O'Rourke K. and Dixit V. M. (1998a) Caspase-9, Bcl-XL, and Apaf-1 Form a Ternary Complex. *J Biol Chem.* **273,** 5841-5845.

Pan G. H., Humke E. W. and Dixit V. M. (1998b) Activation of caspases triggered by cytochrome c in vitro. *Febs Letters* **426,** 151-154.

Pandey P., Saleh A., Nakazawa A., Kumar S., Srinivasula S. M., Kumar V., Weichselbaum R., Nalin C., Alnemri E. S., Kufe D. and Kharbanda S. (2000) Negative regulation of cytochrome c-mediated oligomerization of Apaf-1 and activation of procaspase-9 by heat shock protein 90. *EMBO J* **19,** 4310-4322.

Park S. E., Kim N. D. and Yoo Y. H. (2004) Acetylcholinesterase plays a pivotal role in apoptosome formation. *Cancer Res* **64,** 2652-2655.

Parker M. W., Lobello M. and Federici G. (1990) Crystallization of Glutathione S-Transferase from Human Placenta. *J Mol Biol* **213,** 221-222.

Purring-Koch C. and McLendon G. (2000) Cytochrome c binding to Apaf-1: the effects of dATP and ionic strength. *P Natl Acad Sci USA* **97,** 11928-11931.

Qin H., Srinivasula S. M., Wu G., Fernandes-Alnemri T., Alnemri E. S. and Shi Y. (1999) Structural basis of procaspase-9 recruitment by the apoptotic protease-activating factor 1. *Nature* **399,** 549-557.

Quinn L. M., Dorstyn L., Mills K., Colussi P. A., Chen P., Coombe M., Abrams J., Kumar S. and Richardson H. (2000) An essential role for the caspase dronc in developmentally programmed cell death in Drosophila. *J Biol Chem* **275,** 40416-40424.

Raina D., Pandey P., Ahmad R., Bharti A., Ren J., Kharbanda S., Weichselbaum R. and Kufe D. (2005) c-Abl Tyrosine Kinase Regulates Caspase-9 Autocleavage in the Apoptotic Response to DNA Damage. *J Biol Chem.* **280,** 11147-11151.

Read S. H., Baliga B. C., Ekert P. G., Vaux D. L. and Kumar S. (2002) A novel Apaf-1-independent putative caspase-2 activation complex. *J Cell Biol* **159,** 739-745.

Renatus M., Stennicke H. R., Scott F. L., Liddington R. C. and Salvesen G. S. (2001) Dimer formation drives the activation of the cell death protease caspase 9. *P Natl Acad Sci USA* **98,** 14250-14255.

Ricci J. E., Munoz-Pinedo C., Fitzgerald P., Bailly-Maitre B., Perkins G. A., Yadava N., Scheffler I. E., Ellisman M. H. and Green D. R. (2004) Disruption of mitochondrial function during apoptosis is mediated by caspase cleavage of the p75 subunit of complex I of the electron transport chain. *Cell* **117,** 773-786.

Riedl S. J. and Shi Y. (2004) Molecular mechanisms of caspase regulation during apoptosis. *Nat Rev Mol Cell Biol* **5,** 897-907.

Riedl S. J., Renatus M., Schwarzenbacher R., Zhou Q., Sun C. H., Fesik S. W., Liddington R. C. and Salvesen G. S. (2001a) Structural basis for the inhibition of caspase-3 by XIAP. *Cell* **104,** 791-800.

Riedl S. J., Fuentes-Prior P., Renatus M., Kairies N., Krapp S., Huber R., Salvesen G. S. and Bode W. (2001b) Structural basis for the activation of human procaspase-7. *P Natl Acad Sci USA* **98,** 14790-14795.

Rigaut G., Shevchenko A., Rutz B., Wilm M., Mann M. and Seraphin B. (1999) A generic protein purification method for protein complex characterization and proteome exploration. *Nat Biotechnol* **17,** 1030-1032.

Rodriguez J. and Lazebnik Y. (1999) Caspase-9 and APAF-1 form an active holoenzyme. *Genes & Development* **13,** 3179-3184.

Rodriguez A., Oliver H., Zou H., Chen P., Wang X. and Abrams J. M. (1999) Dark is a Drosophila homologue of Apaf-1/CED-4 and functions in an evolutionarily conserved death pathway. *Nat Cell Biology* **1,** 272-279.

Rothe M., Pan M. G., Henzel W. J., Ayres T. M. and Goeddel D. V. (1995) The TNFR2-TRAF signaling complex contains two novel proteins related to baculoviral inhibitor of apoptosis proteins. *Cell* **83,** 1243-1252.

Rotonda J., Nicholson D. W., Fazil K. M., Gallant M., Gareau Y., Labelle M., Peterson E. P., Rasper D. M., Ruel R., Vaillancourt J. P., Thornberry N. A. and Becker J. W. (1996) The three-dimensional structure of apopain/CPP32, a key mediator of apoptosis. *Nat Struct Biol* **3,** 619-625.

Roy N., Deveraux Q. L., Takahashi R., Salvesen G. S. and Reed J. C. (1997) The c-IAP-1 and c-IAP-2 proteins are direct inhibitors of specific caspases. *EMBO J* **16,** 6914-6925.

Sakahira H., Enari M. and Nagata S. (1998) Cleavage of CAD inhibitor in CAD activation and DNA degradation during apoptosis. *Nature* **391,** 96-99.

Saleh A., Srinivasula S. M., Acharya S., Fishel R. and Alnemri E. S. (1999) Cytochrome c and dATP-mediated oligomerization of Apaf-1 is a prerequisite for procaspase-9 activation. *J Biol Chem* **274,** 17941-17945.

Saleh A., Srinivasula S. M., Balkir L., Robbins P. D. and Alnemri E. S. (2000) Negative regulation of the Apaf-1 apoptosome by Hsp70. *Nat Cell Biology* **2,** 476-483.

Salvesen G. S. and Dixit V. M. (1999) Caspase activation: the induced-proximity model. *P Natl Acad Sci USA* **96,** 10964-10967.

Salvesen G. S. and Duckett C. S. (2002) IAP proteins: blocking the road to death's door. *Nat Rev Mol Cell Biol* **3,** 401-410.

Scaffidi C., Schmitz I., Krammer P. H. and Peter M. E. (1999) The role of c-FLIP in modulation of CD95-induced apoptosis. *J Biol Chem* **274,** 1541-1548.

Scaffidi C., Fulda S., Srinivasan A., Friesen C., Li F., Tomaselli K. J., Debatin K. M., Krammer P. H. and Peter M. E. (1998) Two CD95 (APO-1/Fas) signaling pathways. *EMBO J* **17,** 1675-1687.

Schwarz A., Bhardwaj R., Aragane Y., Mahnke K., Riemann H., Metze D., Luger T. A. and Schwarz T. (1995) Ultraviolet-B-induced apoptosis of keratinocytes: evidence for partial involvement of tumor necrosis factor-alpha in the formation of sunburn cells. *J Invest Dermatol* **104,** 922-927.

Scott F. L., Denault J.-B., Riedl S. J., Shin H., Renatus M. and Salvesen G. S. (2005) XIAP inhibits caspase-3 and -7 using two binding sites: evolutionarily conserved mechanism of IAPs. *EMBO J* **24,** 645-655.

Seol D. W. and Billiar T. R. (1999) A caspase-9 variant missing the catalytic site is an endogenous inhibitor of apoptosis. *J Biol Chem* **274,** 2072-2076.

Seshagiri S. and Miller L. K. (1997) Caenorhabditis elegans CED-4 stimulates CED-3 processing and CED-3-induced apoptosis. *Curr Biol* **7,** 455-460.

Shi Y. G. (2002a) Apoptosome: The cellular engine for the activation of caspase-9. *Structure* **10,** 285-288.

Shi Y. (2002b) Mechanisms of caspase activation and inhibition during apoptosis. *Mol Cell* **9,** 459-470.

Shimizu S., Narita M. and Tsujimoto Y. (1999) Bcl-2 family proteins regulate the release of apoptogenic cytochrome c by the mitochondrial channel VDAC. *Nature* **399,** 483-487.

Shu H. B., Takeuchi M. and Goeddel D. V. (1996) The tumor necrosis factor receptor 2 signal transducers TRAF2 and c-IAP1 are components of the tumor necrosis factor receptor 1 signaling complex. *P Natl Acad Sci USA* **93,** 13973-13978.

Shu H. B., Halpin D. R. and Goeddel D. V. (1997) Casper is a FADD- and caspase-related inducer of apoptosis. *Immunity* **6,** 751-763.

Simstein R., Burow M., Parker A., Weldon C. and Beckman B. (2003) Apoptosis, Chemoresistance, and Breast Cancer: Insights From the MCF-7 Cell Model System. *Exp Biol and Medicine* **228,** 995-1003.

Slee E. A., Zhu H., Chow S. C., MacFarlane M., Nicholson D. W. and Cohen G. M. (1996) Benzyloxycarbonyl-Val-Ala-Asp (OMe) fluoromethylketone (Z-VAD.FMK) inhibits apoptosis by blocking the processing of CPP32. *Biochem J* **315,** 21-24.

Slee E. A., Harte M. T., Kluck R. M., Wolf B. B., Casiano C. A., Newmeyer D. D., Wang H. G., Reed J. C., Nicholson D. W., Alnemri E. S., Green D. R. and Martin S. J. (1999) Ordering the cytochrome c-initiated caspase cascade: hierarchical activation of caspases-2, -3, -6, -7, -8, and -10 in a caspase-9-dependent manner. *J Cell Biol* **144,** 281-292.

Slee E. A., Adrain C. and Martin S. J. (2001) Executioner caspase-3,-6, and-7 perform distinct, non-redundant roles during the demolition phase of apoptosis. *J Biol Chem* **276,** 7320-7326.

Sondek J., Bohm A., Lambright D. G., Hamm H. E. and Sigler P. B. (1996) Crystal structure of a G(A) protein beta gamma dimer at 2.1 angstrom resolution. *Nature* **379,** 369-374.

Spierings D. C., de Vries E. G., Vellenga E., van den Heuvel F. A., Koornstra J. J., Wesseling J., Hollema H. and de Jong S. (2004) Tissue distribution of the death ligand TRAIL and its receptors. *J Histochem Cytochem* **52,** 821-831.

Srinivasula S. M., Ahmad M., Fernandes-Alnemri T., Litwack G. and Alnemri E. S. (1996a) Molecular ordering of the Fas-apoptotic pathway: the Fas/APO-1 protease Mch5 is a CrmA-inhibitable protease that activates multiple Ced-3/ICE-like cysteine proteases. *P Natl Acad Sci USA* **93,** 14486-14491.

Srinivasula S. M., FernandesAlnemri T., Zangrilli J., Robertson N., Armstrong R. C., Wang L. J., Trapani J. A., Tomaselli K. J., Litwack G. and Alnemri E. S. (1996b) The Ced-3/interleukin 1 beta converting enzyme-like homolog Mch6 and the lamin-cleaving enzyme Mch2 alpha are substrates for the apoptotic mediator CPP32. *J Biol Chem* **271,** 27099-27106.

Srinivasula S. M., Ahmad M., Fernandes-Alnemri T. and Alnemri E. S. (1998) Autoactivation of procaspase-9 by Apaf-1-mediated oligomerization. *Mol Cell* **1,** 949-957.

Srinivasula S. M., Ahmad M., Guo Y., Zhan Y., Lazebnik Y., Fernandes-Alnemri T. and Alnemri E. S. (1999) Identification of an endogenous dominant-negative short isoform of caspase-9 that can regulate apoptosis. *Cancer Res* **59,** 999-1002.

Srinivasula S. M., Datta P., Fan X. J., Fernandes-Alnemri T., Huang Z. and Alnemri E. S. (2000) Molecular determinants of the caspase-promoting activity of Smac/DIABLO and its role in the death receptor pathway. *J Biol Chem* **275,** 36152-36157.

Srinivasula S. M., Hegde R., Saleh A., Datta P., Shiozaki E., Chai J., Lee R. A., Robbins P. D., Fernandes-Alnemri T., Shi Y. and Alnemri E. S. (2001) A conserved XIAP-interaction motif in caspase-9 and Smac/DIABLO regulates caspase activity and apoptosis. *Nature* **410,** 112-116.

Steel R., Doherty J. P., Buzzard K., Clemons N., Hawkins C. J. and Anderson R. L. (2004) Hsp72 inhibits apoptosis upstream of the mitochondria and not through interactions with Apaf-1. *J Biol Chem* **279,** 51490-51499.

Stennicke H. R., Jurgensmeier J. M., Shin H., Deveraux Q., Wolf B. B., Yang X., Zhou Q., Ellerby H. M., Ellerby L. M., Bredesen D., Green D. R., Reed J. C., Froelich C. J. and Salvesen G. S. (1998) Pro-caspase-3 is a major physiologic target of caspase-8. *J Biol Chem* **273,** 27084-27090.

Stennicke H. R., Deveraux Q. L., Humke E. W., Reed J. C., Dixit V. M. and Salvesen G. S. (1999) Caspase-9 can be activated without proteolytic processing. *J Biol Chem* **274,** 8359-8362.

Strasser A., O'Connor L. and Dixit V. M. (2000) Apoptosis signaling. *Annu Rev Biochem* **69,** 217-245.

Sun X. M., MacFarlane M., Zhuang J. G., Wolf B. B., Green D. R. and Cohen G. M. (1999a) Distinct caspase cascades are initiated in receptor-mediated and chemical-induced apoptosis. *J Biol Chem* **274,** 5053-5060.

Sun C., Cai M., Gunasekera A. H., Meadows R. P., Wang H., Chen J., Zhang H., Wu W., Xu N., Ng S. C. and Fesik S. W. (1999b) NMR structure and mutagenesis of the inhibitor-of-apoptosis protein XIAP. *Nature* **401,** 818-822.

Sun C., Cai M., Meadows R. P., Xu N., Gunasekera A. H., Herrmann J., Wu J. C. and Fesik S. W. (2000) NMR structure and mutagenesis of the third Bir domain of the inhibitor of apoptosis protein XIAP. *J Biol Chem* **275,** 33777-33781.

Suzuki Y., Nakabayashi Y., Nakata K., Reed J. C. and Takahashi R. (2001a) X-linked inhibitor of apoptosis protein (XIAP) inhibits caspase-3 and-7 in distinct modes. *J Biol Chem* **276,** 27058-27063.

Suzuki Y., Nakabayashi Y. and Takahashi R. (2001b) Ubiquitin-protein ligase activity of X-linked inhibitor of apoptosis protein promotes proteasomal degradation of caspase-3 and enhances its anti-apoptotic effect in Fas-induced cell death. *P Natl Acad Sci USA* **98,** 8662-8667.

Suzuki Y., Imai Y., Nakayama H., Takahashi K., Takio K. and Takahashi R. (2001c) A serine protease, HtrA2, is released from the mitochondria and interacts with XIAP, inducing cell death. *Mol Cell* **8,** 613-621.

Tait J. F., Gibson D. and Fujikawa K. (1989) Phospholipid Binding-Properties of Human Placental Anticoagulant Protein-I, a Member of the Lipocortin Family. *J Biol Chem* **264,** 7944-7949.

Takahashi R., Deveraux Q., Tamm I., Welsh K., Assa-Munt N., Salvesen G. S. and Reed J. C. (1998) A single BIR domain of XIAP sufficient for inhibiting caspases. *J Biol Chem* **273,** 7787-7790.

Tang D., Lahti J. M. and Kidd V. J. (2000) Caspase-8 activation and bid cleavage contribute to MCF7 cellular execution in a caspase-3-dependent manner during staurosporine-mediated apoptosis. *J Biol Chem* **275,** 9303-9307.

Tenev T., Zachariou A., Wilson R., Paul A. and Meier P. (2002) Jafrac2 is an IAP antagonist that promotes cell death by liberating Dronc from DIAP1. *EMBO J* **21,** 5118-5129.

Tenev T., Zachariou A., Wilson R., Ditzel M. and Meier P. (2005) IAPs are functionally non-equivalent and regulate effector caspases through distinct mechanisms. *Nat Cell Biology* **7,** 70-77.

Tewari M., Quan L. T., O'Rourke K., Desnoyers S., Zeng Z., Beidler D. R., Poirier G. G., Salvesen G. S. and Dixit V. M. (1995) Yama/CPP32 beta, a mammalian homolog of CED-3, is a CrmA-inhibitable protease that cleaves the death substrate poly(ADP-ribose) polymerase. *Cell* **81,** 801-809.

Thornberry N. A. and Lazebnik Y. (1998) Caspases: Enemies within. *Science* **281,** 1312-1316.

Thornberry N. A., Bull H. G., Calaycay J. R., Chapman K. T., Howard A. D., Kostura M. J., Miller D. K., Molineaux S. M., Weidner J. R. and Aunins J. (1992) A novel heterodimeric cysteine protease is required for interleukin-1 beta processing in monocytes. *Nature* **356,** 768-774.

Thornberry N. A., Rano T. A., Peterson E. P., Rasper D. M., Timkey T., Garcia-Calvo M., Houtzager V. M., Nordstrom P. A., Roy S., Vaillancourt J. P., Chapman K. T. and Nicholson D. W. (1997) A combinatorial approach defines specificities of members of the caspase family and granzyme B. Functional relationships established for key mediators of apoptosis. *J Biol Chem* **272,** 17907-17911.

Twiddy D., Brown D. G., Adrain C., Jukes R., Martin S. J., Cohen G. M., MacFarlane M. and Cain K. (2004) Pro-apoptotic proteins released from the mitochondria regulate the protein composition and caspase-processing activity of the native Apaf-1/caspase-9 apoptosome complex. *J Biol Chem* **279,** 19665-19682.

Uren A. G., Pakusch M., Hawkins C. J., Puls K. L. and Vaux D. L. (1996) Cloning and expression of apoptosis inhibitory protein homologs that function to inhibit apoptosis and/or bind tumor necrosis factor receptor-associated factors. *P Natl Acad Sci USA* **93,** 4974-4978.

Uren A. G., Coulson E. J. and Vaux D. L. (1998) Conservation of baculovirus inhibitor of apoptosis repeat proteins (BIRPs) in viruses, nematodes, vertebrates and yeasts. *Trends Biochem Sci* **23,** 159-162.

Varfolomeev E. E., Schuchmann M., Luria V., Chiannilkulchai N., Beckmann J. S., Mett I. L., Rebrikov D., Brodianski V. M., Kemper O. C., Kollet O., Lapidot T., Soffer D., Sobe T., Avraham K. B., Goncharov T., Holtmann H., Lonai P. and Wallach D. (1998) Targeted disruption of the mouse Caspase 8 gene ablates cell death induction by the TNF receptors, Fas/Apo1, and DR3 and is lethal prenatally. *Immunity* **9,** 267-276.

Varkey J., Chen P., Jemmerson R. and Abrams J. M. (1999) Altered cytochrome c display precedes apoptotic cell death in Drosophila. *J Cell Biol* **144,** 701-710.

Verhagen A. M., Ekert P. G., Pakusch M., Silke J., Connolly L. M., Reid G. E., Moritz R. L., Simpson R. J. and Vaux D. L. (2000) Identification of DIABLO, a mammalian protein that promotes apoptosis by binding to and antagonizing IAP proteins. *Cell* **102,** 43-53.

Verhagen A. M., Coulson E. J. and Vaux D. L. (2001) Inhibitor of apoptosis proteins and their relatives: IAPs and other BIRPs. *Genome Biology* **2,** REVIEWS 3009.1-3009.10.

Verhagen A. M., Silke J., Ekert P. G., Pakusch M., Kaufmann H., Connolly L. M., Day C. L., Tikoo A., Burke R., Wrobel C., Moritz R. L., Simpson R. J. and Vaux D. L. (2002) HtrA2 promotes cell death through its serine protease activity and its ability to antagonize inhibitor of apoptosis proteins. *J Biol Chem* **277,** 445-454.

Vermes I., Haanen C., Steffens-Nakken H. and Reutelingsperger C. (1995) A novel assay for apoptosis. Flow cytometric detection of phosphatidylserine expression on early apoptotic cells using fluorescein labelled Annexin V. *J Immunol Methods* **184,** 39-51.

Vucic D., Deshayes K., Ackerly H., Pisabarro M. T., Kadkhodayan S., Fairbrother W. J. and Dixit V. M. (2002) SMAC negatively regulates the anti-apoptotic activity of melanoma inhibitor of apoptosis (ML-LAP). *J Biol Chem* **277**, 12275-12279.

Vucic D., Franklin M. C., Wallweber H. J. A., Das K., Eckelman B. P., Shin H., Elliott L. O., Kadkhodayan S., Deshayes K., Salvesen G. S. and Fairbrother W. J. (2005) Engineering ML-IAP to produce an extraordinarily potent caspase 9 inhibitor: implications for Smac-dependent anti-apoptotic activity of ML-IAP. *Biochem J* **385**, 11-20.

Walker J. E., Saraste M., Runswick M. J. and Gay N. J. (1982) Distantly related sequences in the alpha- and beta-subunits of ATP synthase, myosin, kinases and other ATP-requiring enzymes and a common nucleotide binding fold. *EMBO J* **1,** 945-951.

Walker N. P., Talanian R. V., Brady K. D., Dang L. C., Bump N. J., Ferenz C. R., Franklin S., Ghayur T., Hackett M. C. and Hammill L. D. (1994) Crystal structure of the cysteine protease interleukin-1 beta-converting enzyme: a (p20/p10)2 homodimer. *Cell* **78,** 343-352.

Wall M. A., Coleman D. E., Lee E., Iniguez-Lluhi J. A., Posner B. A., Gilman A. G. and Sprang S. R. (1995) The structure of the G protein heterotrimer Gi alpha 1 beta 1 gamma 2. *Cell* **83,** 1047-1058.

Wang C. Y., Mayo M. W., Korneluk R. G., Goeddel D. V. and Baldwin A. S., Jr. (1998) NF-kappaB antiapoptosis: induction of TRAF1 and TRAF2 and c-IAP1 and c-IAP2 to suppress caspase-8 activation. *Science* **281,** 1680-1683.

Wei M. C., Lindsten T., Mootha V. K., Weiler S., Gross A., Ashiya M., Thompson C. B. and Korsmeyer S. J. (2000) tBID, a membrane-targeted death ligand, oligomerizes BAK to release cytochrome c. *Genes & Development* **14,** 2060-2071.

Wei M. C., Zong W. X., Cheng E. H., Lindsten T., Panoutsakopoulou V., Ross A. J., Roth K. A., MacGregor G. R., Thompson C. B. and Korsmeyer S. J. (2001) Proapoptotic BAX and BAK: a requisite gateway to mitochondrial dysfunction and death. *Science* **292,** 727-730.

Weil M., Jacobson M. D., Coles H. S. R., Davies T. J., Gardner R. L., Raff K. D. and Raff M. C. (1996) Constitutive expression of the machinery for programmed cell death. *J Cell Biol* **133,** 1053-1059.

Wilson K. P., Black J. A. F., Thomson J. A., Kim E. E., Griffith J. P., Navia M. A., Murcko M. A., Chambers S. P., Aldape R. A., Raybuck S. A. and Livingston D. J. (1994) Structure and Mechanism of Interleukin-1-Beta Converting-Enzyme. *Nature* **370,** 270-275.

Wilson R., Goyal L., Ditzel M., Zachariou A., Baker D. A., Agapite J., Steller H. and Meier P. (2002) The DIAP1 RING finger mediates ubiquitination of Dronc and is indispensable for regulating apoptosis. *Nat Cell Biology* **4,** 445-450.

Wu D., Wallen H. D. and Nunez G. (1997) Interaction and Regulation of Subcellular Localization of CED-4 by CED-9. *Science* **275,** 1126-1129.

Wu J. and Filutowicz M. (1999) Hexahistidine (His6)-tag dependent protein dimerization: a cautionary tale. *Acta Biochim Pol* **46,** 591-599.

Wu G., Chai J., Suber T. L., Wu J.-W., Du C., Wang X. and Shi Y. (2000) Structural basis of IAP recognition by Smac/DIABLO. *Nature* **408,** 1008-1012.

Yan N., Wu J. W., Chai J., Li W. and Shi Y. (2004) Molecular mechanisms of DrICE inhibition by DIAP1 and removal of inhibition by Reaper, Hid and Grim. *Nat Struct Mol Biol* **11,** 420-428.

Yang J., Liu X., Bhalla K., Kim C. N., Ibrado A. M., Cai J., Peng T. I., Jones D. P. and Wang X. (1997) Prevention of apoptosis by Bcl-2: release of cytochrome c from mitochondria blocked. *Science* **275,** 1129-1132.

Yang X., Chang H. Y. and Baltimore D. (1998a) Essential role of CED-4 oligomerization in CED-3 activation and apoptosis. *Science* **281,** 1355-1357.

Yang X., Stennicke H. R., Wang B., Green D. R., Janicke R. U., Srinivasan A., Seth P., Salvesen G. S. and Froelich C. J. (1998b) Granzyme B mimics apical caspases. Description of a unified pathway for trans-activation of executioner caspase-3 and -7. *J Biol Chem* **273,** 34278-34283.

Yang Q. H., Church-Hajduk R., Ren J., Newton M. L. and Du C. (2003) Omi/HtrA2 catalytic cleavage of inhibitor of apoptosis (IAP) irreversibly inactivates IAPs and facilitates caspase activity in apoptosis. *Genes & Development* **17,** 1487-1496.

Yoshida H., Kong Y.-Y., Yoshida R., Elia A. J., Hakem A., Hakem R., Penninger J. M. and Mak T. W. (1998) Apaf1 Is Required for Mitochondrial Pathways of Apoptosis and Brain Development. *Cell* **94,** 739-750.

Yuan J. and Horvitz H. R. (1992) The Caenorhabditis elegans cell death gene ced-4 encodes a novel protein and is expressed during the period of extensive programmed cell death. *Development* **116,** 309-320.

Yuan J. Y., Shaham S., Ledoux S., Ellis H. M. and Horvitz H. R. (1993) The C-Elegans Cell-Death Gene Ced-3 Encodes a Protein Similar to Mammalian Interleukin-1-Beta-Converting Enzyme. *Cell* **75,** 641-652.

Zhang X, J., Yang L., Zhao Q., Caen J. P., He H. Y., Jin Q. H., Guo L. H., Alemany M., Zhang L. Y. and Shi Y. F. (2002) Induction of acetylcholinesterase expression during apoptosis in various cell types. *Cell Death Differ* **9,** 790-800.

Zhou L., Song Z. W., Tittel J. and Steller H. (1999) HAC-1, a Drosophila homolog of APAF-1 and CED-4 functions in developmental and radiation-induced apoptosis. *Mol Cell* **4,** 745-755.

Zhu H., Fearnhead H. O. and Cohen G. M. (1995) An ICE-like protease is a common mediator of apoptosis induced by diverse stimuli in human monocytic THP.1 cells. *FEBS Letters* **374,** 303-308.

Zimmermann K. C., Ricci J. E., Droin N. M. and Green D. R. (2002) The role of ARK in stress-induced apoptosis in Drosophila cells. *J Cell Biol* **156,** 1077-1087.

Zou H., Henzel W. J., Liu X. S., Lutschg A. and Wang X. D. (1997) Apaf-1, a human protein homologous to C-elegans CED-4, participates in cytochrome c-dependent activation of caspase-3. *Cell* **90,** 405-413.

Zou H., Li Y., Liu X. and Wang X. (1999) An APAF-1.cytochrome c multimeric complex is a functional apoptosome that activates procaspase-9. *J Biol Chem* **274,** 11549-11556.

Zou H., Yang R., Hao J., Wang J., Sun C., Fesik S. W., Wu J. C., Tomaselli K. J. and Armstrong R. C. (2003) Regulation of the Apaf-1/caspase-9 apoptosome by caspase-3 and XIAP. *J Biol Chem* **278,** 8091-8098.

Publications

THE JOURNAL OF BIOLOGICAL CHEMISTRY
© 2004 by The American Society for Biochemistry and Molecular Biology, Inc.

Vol. 279, No. 19, Issue of May 7, pp. 19665–19682, 2004
Printed in U.S.A.

Pro-apoptotic Proteins Released from the Mitochondria Regulate the Protein Composition and Caspase-processing Activity of the Native Apaf-1/Caspase-9 Apoptosome Complex*

Received for publication, October 16, 2003, and in revised form, February 26, 2004
Published, JBC Papers in Press, March 1, 2004, DOI 10.1074/jbc.M311388200

Davina Twiddy‡, David G. Brown‡, Colin Adrain§, Rebekah Jukes, Seamus J. Martin§, Gerald M. Cohen, Marion MacFarlane, and Kelvin Cain¶

From the Medical Research Council Toxicology Unit, Hodgkin Building, University of Leicester, Leicester LE1 9HN, United Kingdom and the §Department of Genetics, The Smurfit Institute, Trinity College, Dublin 2, Ireland

The apoptosome is a large caspase-activating (~700–1400 kDa) complex, which is assembled from Apaf-1 and caspase-9 when cytochrome *c* is released during mitochondrial-dependent apoptotic cell death. Apaf-1 the core scaffold protein is ~135 kDa and contains CARD (caspase recruitment domain), CED-4, and multiple (13) WD40 repeat domains, which can potentially interact with a variety of unknown regulatory proteins. To identify such proteins we activated THP.1 lysates with dATP/cytochrome *c* and used sucrose density centrifugation and affinity-based methods to purify the apoptosome for analysis by MALDI-TOF mass spectrometry. First, we used a glutathione *S*-transferase (GST) fusion protein (GST-casp9$^{1-130}$) containing the CARD domain of caspase-9-(1–130), which binds to the CARD domain of Apaf-1 when it is in the apoptosome and blocks recruitment/activation of caspase-9. This affinity-purified apoptosome complex contained only Apaf-1XL and GST-casp9$^{1-130}$, demonstrating that the WD40 and CED-4 domains of Apaf-1 do not stably bind other cytosolic proteins. Next we used a monoclonal antibody to caspase-9 to immunopurify the native active apoptosome complex from cell lysates, containing negligible levels of cytochrome *c*, second mitochondria-derived activator of caspase (Smac), or Omi/HtrA2. This apoptosome complex exhibited low caspase-processing activity and contained four stably associated proteins, namely Apaf-1, pro-p35/34 forms of caspase-9, pro-p20 forms of caspase-3, X-linked inhibitor of apoptosis (XIAP), and cytochrome *c*, which was only bound transiently to the complex. However, in lysates containing Smac and Omi/HtrA2, the caspase-processing activity of the purified apoptosome complex increased 6–8-fold and contained only Apaf-1 and the p35/p34-processed subunits of caspase-9. During apoptosis, Smac, Omi/HtrA2, and cytochrome *c* are released simultaneously from mitochondria, and thus it is likely that the functional apoptosome complex in apoptotic cells consists primarily of Apaf-1 and processed caspase-9.

The morphological and biochemical changes of apoptotic cell death largely result from the activation of a group of cysteine aspartic acid-specific proteases known as caspases (for review see Refs. 1–3). The activation of caspases is a central feature of apoptosis, and key components of this mechanism are highly conserved throughout evolution from *Caenorhabditis elegans* to *Drosophila melanogaster* and ultimately to mammals. In *C. elegans* there are at least four genes, *ced-3, ced-4, ced-9*, and *egl-1*, which are critical for the execution of apoptotic cell death. In *C. elegans*, CED-4 is normally bound to mitochondria and cell membranes by CED-9 (4). Up-regulation of EGL-1 inactivates CED-9, releasing CED-4, which oligomerizes/recruits and induces autocatalytic processing and activation of CED-3 (5). *ced-3* encodes for a cysteine protease, which is homologous to interleukin-1β-converting enzyme or ICE, now known as caspase-1. Thirteen other caspases have now been identified in mammals, some of which are involved in cell death (CED-3 subfamily), whereas others are involved in inflammation (ICE subfamily).

Caspases are synthesized as inactive procaspases or zymogens, which in mammals are activated in a cascade mechanism, involving an initiator or activating caspase that cleaves/activates a downstream caspase, which in turn activates the next caspase and so on. There are at least two primary (extrinsic and intrinsic) caspase activation pathways, involving either stimulation of cell surface death receptors or perturbation of mitochondria (for review see Ref. 6). The intrinsic pathway is essentially homologous to *C. elegans* in that it involves the formation of the apoptosome, a large caspase-processing complex (for review see Refs. 7, 8). Mammalian homologues of CED-3, CED-9, and EGL-1 have been identified by conventional cloning strategies, but Apaf-1 a mammalian homologue of CED-4 was only identified by a classical biochemical approach. In these cell-free studies, caspase activation was induced in cell lysates by dATP, and three apoptotic protease-activating factors (Apaf-1–3) were isolated (9). Apaf-1 was identified as a CED-4 homologue (10), Apaf-2 as cytochrome *c* (9) and Apaf-3 as caspase-9 (11). Apaf-1 is a large ~135 kDa protein, which consists of an N-terminal caspase recruitment domain (CARD),[1] a region homologous to CED-4 followed by a large C-terminal domain containing 12–13 WD40 repeats. The CARD domain interacts with a similar domain on procaspase-9 and the central CED-4-(98–412) region contains a putative

* This work was supported in part by European Union Grant QLG1-1999-00739. The costs of publication of this article were defrayed in part by the payment of page charges. This article must therefore be hereby marked "*advertisement*" in accordance with 18 U.S.C. Section 1734 solely to indicate this fact.

‡ These authors contributed equally to this work.

¶ To whom correspondence should be addressed. Tel.: 44-116-252-5547; Fax: 44-116-252-5616; E-mail: kc5@le.ac.uk.

[1] The abbreviations used are: CARD, caspase recruitment domain; GST, glutathione *S*-transferase; MALDI-TOF, matrix-assisted laser desorption/ionization time-of-flight; Smac, second mitochondria-derived activator of caspase; PBS, phosphate-buffered saline; DTT, dithiothreitol; Z, benzyloxycarbonyl; FMK, fluoromethylketone; CHAPS, 3-[(3-cholamidopropyl)dimethylammonio]-1-propanesulfonic acid; XIAP, X-linked inhibitor of apoptosis; IEF, isoelectrofocusing; F/T, freeze-thaw; ProT, prothymosin α; PHAP, putative HLA-DR-associated proteins.

ATPase domain with conserved Walker's A (P-loop) and B boxes forming nucleotide binding sites (11, 12). The function of the WD40 regions is largely unknown although a critical number of 13 WD40 repeats is required for cytochrome *c* binding as Apaf-1 splice forms containing only 12 WD40 repeats do not bind cytochrome *c* and do not activate caspases (13). WD40 repeats usually form β-propeller structures arranged in a rigid circular structure and in the case of Apaf-1 it is likely that these would be arranged as two asymmetric (7- and 6-bladed) structures (8).

Apaf-1 has been shown to oligomerize in the presence of cytochrome *c* and dATP to form a very large apoptosome complex with a molecular weight between ~700 kDa and ~1.4 MDa (14–17). The size of the apoptosome complex varies from ~1.4 MDa when reconstituted from recombinant proteins (16) to >1.3 MDa (17) and ~1.0 MDa (18) when isolated from HeLa cell lysates, However, in dATP-activated THP.1 and B chronic lymphocytic leukemia cell lysates we have identified both an ~700-kDa and an ~1.4-MDa apoptosome complex (15, 19). The ~700-kDa complex predominates in apoptotic cells and is the most active complex in processing exogenous procaspase-9 and -3 (15, 19).

These studies suggest that the size of the apoptosome complex may vary according to cell type and/or the conditions in which the apoptosome is formed, and it is possible that other cellular proteins can bind to the Apaf-1/caspase-9 holo-enzyme complex. We therefore decided to purify the native ~700-kDa apoptosome complex to homogeneity in order to identify the additional components of the apoptosome. However, our attempts to purify the apoptosome by classical biochemical methodology using multistep chromatography were unsuccessful because of the co-purification of other large ~700 kDa protein assemblies such as the IKK (20) and rabaptin-5/rabex 5 complexes (21). We have therefore developed two affinity-based techniques to purify the apoptosome from dATP-activated lysates. First, we used a GST-caspase-9-(1–130) (GST-casp9$^{1-130}$) construct, which does not contain the large and small subunits of caspase-9, and acts as a dominant negative inhibitor of caspase activation by occupying the Apaf-1 CARD domain in the apoptosome complex. We then sequentially purified the ~700-kDa complex tagged with GST-casp9$^{1-130}$ by sucrose density gradient purification and glutathione beads. Second, we have used a monoclonal anti-caspase-9 antibody to purify the intact fully functional ~700-kDa apoptosome complex, which contains Apaf-1 and processed caspase-9. The purified apoptosome complexes were analyzed by Western blotting and MALDI-TOF mass spectrometry (M@LDI R, Micromass, Manchester, UK), and surprisingly the respective apoptosome complexes contained only Apaf-1 and GST-casp9$^{1-130}$ or Apaf-1 and the p35 and p34 processed forms of caspase-9. Caspase-3 was not detected in the complex and appears to only interact transiently with the apoptosome complex in conditions of low (non-physiological) ionic strength. X-linked inhibitor of apoptosis (XIAP) was also not detected in the purified complex due to the presence of endogenous Smac (second mitochondria-derived activator of caspase) and Omi/HtrA2, which sequester free XIAP and thereby prevent it from interacting with the apoptosome complex. However, when the apoptosome was formed in lysates, which were essentially free of Smac and Omi/HtrA2, we demonstrated recruitment of XIAP and caspase-3 to the apoptosome complex. These studies indicate that when the apoptosome is formed in the apoptotic cell it initially can be inhibited by XIAP, but increasing cytosolic concentrations of Smac and Omi/HtrA2 remove XIAP from the apoptosome complex, which then achieves maximum caspase-activating activity.

EXPERIMENTAL PROCEDURES

Cell Culture, Apoptosis Assays, Preparation of Control and Caspase-activated Cell Lysates—Human monocytic tumor cell (THP.1) and cell lysates (100,000 × *g* supernatants) from control cells were prepared by freeze-thawing (F/T) as described previously (8, 15). In some experiments, to minimize mitochondrial breakage and release of pro-apoptotic proteins (see Fig. 9), THP.1 cell lysates (Dig/Hom) were prepared in an isotonic buffer (MSH), containing 210 mM mannitol, 70 mM sucrose, 5 mM Hepes, 1 mM EGTA, 1 mg/ml Pefabloc SCD, 1 tablet/10 ml protease inhibitor mixture (Roche Diagnostics), pH 7.4 using a modified digitonin/homogenization technique. In this procedure, THP.1 cells were pelleted and gently resuspended (10^8 cells/ml) in MSH buffer plus 0.05% w/v digitonin. The cells were incubated at 4 °C for 7 min, before adding 4 volumes of MSH buffer and homogenizing with a ball bearing homogenizer (5 cycles with an 8.002-mm ball, clearance 18 microns, HGM Laboratory equipment, EMBL, Germany). The cell lysates were then prepared as described for the freeze-thawed lysates and concentrated in Vivaspin columns (10,000 molecular weight cutoff) to a final protein concentration of 15–20 mg/ml. Caspase activation in lysates (10–15 mg/ml) was induced by incubation at 37 °C with 2 mM dATP, 2 mM $MgCl_2$, plus or minus 7 μM cytochrome *c*.

Preparation of Recombinant Procaspase-3 and SmacΔ55—BL21 (DE3) cells were transformed with a pET-21b (Novagen) plasmid expression vector containing pro-caspase-3 cDNA with a C-terminal His_6 purification tag and grown at 37 °C in terrific broth, 1% glucose, and ampicillin (100 μg/ml). Expression of the caspase-3 zymogen was optimal when the culture (OD_{600} = 0.6) was induced for 15 min at 30 °C with 1 mM isopropyl-1-thio-β-D-galactopyranoside. Bacterial lysates were prepared by sonication in 20 mM HEPES, 100 mM NaCl, 10 mM imidazole, one protease inhibitor-EDTA tablet (10 ml), pH 8.0, and procaspase-3 purified with nickel-coated Sepharose beads (Qiagen). The truncated form of Smac (*i.e.* lacking the mitochondrial targeting signal) was prepared in BL21 (DE3) cells in a similar manner using SmacΔ55 pET-15b as previously described (22).

Purification of GST-casp9$^{1-130}$ Fusion Protein—BL21 (DE3) cells were transformed with a pGEX4TK2 construct, encoding a fusion protein construct (GST-casp9$^{1-130}$), consisting of the prodomain (amino acids 1–130) of caspase-9 fused in-frame with glutathione *S*-transferase. Transformed cells were grown at 37 °C in TB broth containing 100 μg/ml ampicillin and at a culture density of 0.6 AU. GST-casp9$^{1-130}$ protein expression was induced at 22 °C for 3 h with 0.1 mM isopropyl-1-thio-β-D-galactopyranoside. The bacteria were sedimented and lysed by sonication in PBS containing Complete protease inhibitors (Roche Applied Science). The GST-tagged protein was affinity-purified from the bacterial lysate with GSH-Sepharose beads (Amersham Biosciences) for 30 min at 4 °C. The beads were washed three times in cold PBS and the GST-casp9$^{1-130}$ eluted with 20 mM reduced glutathione. The protein concentration and purity of the GST-casp9$^{1-130}$ was determined by Bradford assay and SDS-PAGE/Coomassie Blue, respectively.

Fluorometric Assays of Proteolytic Activity—DEVDase activity (i.e. primarily caspase-3 and -7) of lysates or column fractions was measured fluorometrically ($\lambda_{ex}/\lambda_{em}$ = 405/510 nm) at 37 °C in 96-well plates in 200 μl of assay buffer (20 μM Z-DEVD.AFC, 0.1% CHAPS, 10 mM DTT, 100 mM HEPES, and 10% sucrose, pH 7.0) using a Wallac Victor^2 1420 Multilabel counter (15). The protease activities were expressed as either pmol/min/mg protein or pmol/min/fraction. In some experiments, the chymotrypsin-like (LLVYase) activity of the 20 S proteasome was measured with 40 μM Suc-Leu-Leu-Val-Tyr-AMC (Peptide Institute Inc, Osaka, Japan). Liberation of AMC the substrate from was monitored continuously using an excitation/emission wavelength pair ($\lambda_{ex}/\lambda_{em}$) of 380/460 nm, respectively.

The caspase processing/activating activity of soluble apoptosome complexes was assayed essentially as previously described (15) except that purified recombinant procaspase-3 was used as an apoptosome substrate. Briefly, 200-μl aliquots of the column fractions were incubated with recombinant procaspase-3 (200 nM) for 1 h at 37 °C. The samples were then assayed for DEVDase activity, which is a measure of how much procaspase-3 has been processed and activated by the apoptosome. The caspase activating activity of apoptosome complexes bound to anti-caspase-9 antibody-labeled magnetic beads (see later) was assayed in a similar manner. Briefly, the purified apoptosome complexes bound to the Dyna beads were incubated/mixed with recombinant procaspase-3 (200 nM) for 1 h at 37 °C. The apoptosome/bead complexes were then removed, and the active caspase-3, which had been released into the supernatant, assayed for DEVDase activity. Aliquots of the DEVD assay mixtures were diluted 1:1 with 2× SDS loading buffer and analyzed for caspase-3 processing by SDS-PAGE and Western blotting.

Separation of Apoptosome Complexes—Lysates were fractionated by size-exclusion chromatography on Superose 6 columns using an FPLC (HR 10/30 column) protein purification system (Amersham Biosciences). Columns were eluted at 4 °C with 5% (w/v) sucrose, 0.1% (w/v) CHAPS, 20 mM HEPES/NaOH, 5 mM DTT, and 50 mM NaCl, pH 7.0 calibrated with protein standards as previously described (15). Large scale preparation of ~700-kDa apoptosome complexes were prepared by centrifuging THP.1 lysates (30–60 mg) at 25,000 rpm for 17 h at 4 °C on continuous sucrose gradients (10–40%), 0.1% (w/v) CHAPS, 20 mM HEPES/NaOH, 5 mM DTT, pH 7.0 at 4 °C (14). The gradients were collected in 2-ml fractions, which were analyzed for the LLVYase activity of the 20 S proteasome, which co-sediments with the ~700-kDa apoptosome complex (14). Aliquots of the gradient fractions were also analyzed by SDS-PAGE and Western blotting for Apaf-1 and appropriate fractions pooled and concentrated with Vivaspin concentrators (Millipore).

Affinity Purification of Apoptosome Complexes—GST-casp9$^{1-130}$-tagged apoptosome complexes were purified from lysates by incubating for 1 h at 4 °C with an equal volume of GSH-Sepharose beads (50% slurry in PBS). Column and sucrose density fractions were extracted in the same way except that a 1:5 bead/sample volume ratio was used. The beads were washed four times in PBS by centrifugation/resuspension and then eluted with 20 mM reduced glutathione. Immunoaffinity purification of ~700-kDa apoptosome complexes was carried out by first preclearing THP.1 cell lysates (~25 mg/ml) for 1 h at 4 °C with 400 μl/ml of lysate of protein G-Sepharose-coated beads, which had been prewashed three times in wash buffer (assay buffer supplemented with 0.5% bovine serum albumin and 0.05% Tween 20). Precleared lysates were diluted to 15 mg/ml with assay buffer, caspase was activated and treated as indicated under "Results," except that cytochrome *c* (7 μM) was included in the activation buffer. Apoptosome capture was then carried out by cooling to 4 °C and incubating with periodic mixing for 2 h with 10 μg of anti-caspase-9 monoclonal antibody (R&D mAb8301, Abingdon, UK). The apoptosome complexes were then incubated with constant mixing for 1 h at 4 °C with 400 μl of prewashed (three times in wash buffer) protein G-coated Dyna Beads® (Dynal Biotech Ltd., Cheshire, UK). Beads were then harvested magnetically and washed twice (1 ml) with wash buffer. Aliquots of the beads were either eluted for SDS-PAGE or IEF by incubating with the appropriate loading buffer and magnetic removal of the stripped Dyna beads.

In some experiments the anti-caspase-9 antibody was covalently attached to protein G Dyna Beads® as described by Dynal Biotech Ltd. Briefly, 100 μl of beads were washed three times with PBS, 0.05% Tween 20, and then roller-mixed for 1 h at 4 °C with 6.25 μg of anti-caspase-9 antibody. The labeled beads were washed three times with 1 ml of 0.2 M triethanolamine, pH 8.2 buffer before resuspending in 1 ml of cross-linking buffer containing 0.2 M ethanolamine, 20 mM dimethyl pimelimidate pH 8.2. The beads were roller-mixed for 30 min at room temperature, before terminating the cross-linking reaction by resuspending and incubating for 15 min in 1 ml of 50 mM Tris-HCL, pH 7.5 buffer. The beads were washed three times with PBS, 0.05% Tween 20 before resuspending in 100 μl of the same buffer. Apoptosome complexes were captured by adding 20 μl of cross-linked beads to 100 μl of dATP-activated THP.1 lysate and roller mixed overnight at 4 °C. Proteins were eluted from the beads as described above.

Two-dimensional Gel Electrophoresis Analysis of Purified Apoptosome Complexes—Protein complexes were eluted from the protein G-coated Dyna beads with IEF rehydration buffer (6 M urea, 2 M thiourea, 2% (w/v) CHAPS, 0.5% (w/v) ampholines (pH 3–10), IPG buffer (Amersham Biosciences), 18 mM DTT, and a trace amount of bromphenol blue. IPG strips (pH 5–8, Bio-Rad) were rehydrated overnight at 50 μA in 185 μl of rehydration buffer with the gel side face down. Protein aliquots dissolved in rehydration buffer (100 μl) were applied to the IPG strips using cup loading, and the strips run for 20,000 Vh with a terminal voltage of 8000 volts. For the second SDS-PAGE dimension, the IPG strips were incubated for 15 min in an equilibration buffer containing 50 mM Tris-HCl, 6 M urea, 30% glycerol (v/v), 2% SDS (w/v), bromphenol blue 0.002% (w/v), and 64 mM DTT, pH 8.8. The strips were then given a further 15-min incubation in a modified equilibration buffer in which the DTT was replaced by 135 mM iodacetamide. The strips were then immersed in Tris-glycine buffer, applied to 10% SDS-polyacrylamide gels, and electrophoresed under standard conditions. Gels were stained with either Coomassie Blue or SYPRO ruby and imaged using ProXPRESS proteomic imaging system (PerkinElmer Life Sciences) and Progenesis Work station image analysis software (Non-Linear Dynamics, Newcastle, UK).

Proteomic Analysis—Gel plugs (0.8 mm × 1 mm) were excised from stained SDS-PAGE or two-dimensional gels using an automated spot picker (ProPic, PerkinElmer Life Sciences). An automated digestion robot (ProGest, PerkinElmer Life Sciences) was used to perform *in situ* digestion on the plugs, which were sequentially reduced with 10 mM dithiothreitol, alkylated with 100 mM iodacetamide, and digested with modified sequencing-grade porcine trypsin (Promega). Peptides were extracted from the digested gel plugs with 21 μl of 0.1% formic acid, and aliquots (5 μl) of the extracted peptides desalted with C18 Zip tips (Millipore). Aliquots (0.5 μl) of the desalted peptide extracts were combined with equal volumes of a saturated solution of α-cyano-4-hydroxycinammic acid in 1% trifluoroacetic acid, 50% acetonitrile and were loaded on to a MALDI target plate using an automated spotting robot (ProMS, PerkinElmer Life Sciences). Peptide mass analysis was then performed on a MALDI-TOF mass spectrometer using a mass range of 900–3000 Da. Mass spectrometric data were analyzed automatically or manually by ProteinLynx and MASCOT software, respectively. Protein identity was determined by submission to SWISS-PROT and TrEMBL data bases.

Reagents and Western Blot Analysis—The GST-casp9$^{1-130}$ construct was generated using conventional cloning strategies. Most other reagents, including antibodies to caspases-3, and -7 were obtained unless otherwise indicated from previously described sources (6, 15, 22–24). A mouse monoclonal antibody (clone 5B4) to caspase-9 was obtained from MBL laboratories (Nagoya, Japan) and used at 0.1 μg/ml concentration. Protein samples (~20 μg) were resolved on 10 or 12.5% SDS-polyacrylamide gels, transferred onto nitrocellulose membranes (Hybond C extra, Amersham Biosciences), and antibody binding was detected as described previously (15). Western blotting for XIAP was carried out, using a 0.125 μg/ml solution of a mouse monoclonal antibody (clone 48, BD Biosciences, PharMingen, San Diego, CA), which was raised to the C terminus (amino acids 268–426) of XIAP. The heavy chain of the IgG_1 monoclonal antibody to caspase-9 and XIAP have molecular weights of 57 and ~50 kDa, respectively and can be difficult to resolve with certainty using SDS gels and immunoblotting. Therefore in some experiments a triple sandwich (tertiary) detection method was used to identify XIAP. Briefly, the nitrocellulose blot was incubated for 1 h with a 1:2000 dilution of the primary XIAP antibody, and then blocked for 30 min with 4% bovine serum albumin in TBST (20 mM Tris-HCl, 137 mM NaCl, 0.05% Tween 20, pH 7.0). The blot was then incubated at 4 °C overnight with 2 μg/ml recombinant protein G-biotin conjugate (Sigma) in TBST buffer. The protein G-biotin conjugate does not cross-react with the separated heavy and light chains of the caspase-9 antibody, and only binds to the primary XIAP antibody. The protein G-biotin conjugate was detected with ECL using a 1:1500 dilution of streptavidin-horseradish peroxidase (Amersham Biosciences).

RESULTS

In previous studies we have shown that dATP activation of THP.1 cell lysates induces *de novo* formation of ~1.4-MDa and ~700-kDa Apaf-1/caspase-9-containing apoptosome complexes (15). The ~700-kDa apoptosome complex, which predominates in apoptotic cells, is the most active apoptosome when assessed by its ability to process and activate effector caspases (15). Other proteins such as caspase-3 and caspase-7 are transiently bound to the ~700-kDa apoptosome by virtue of the fact that the proforms are substrates for the apoptosome and form E·S complexes, which are easily disrupted by moderate ionic strength conditions (14, 15, 25). We initially attempted to purify the ~700-kDa apoptosome complex by conventional sequential multistep chromatographic techniques.[2] Although the 7-step procedure we subsequently developed substantially purified the apoptosome complex (~30-fold increase in caspase-processing activity), it was apparent from two-dimensional gel analysis and mass spectrometry that the purified preparation contained other similar sized assemblies such as the IKK (20) and rabaptin-5/rabex 5 complexes (21).

Immunoaffinity purification methods potentially provide a more selective purification strategy; however, the affinity method needs to be specific for the ~700-kDa apoptosome complex. In this respect we have tested without success a panel of Apaf-1 antibodies for their ability to discriminate between monomeric and oligomerized Apaf-1 (data not shown). There-

[2] K. Cain, C. Langlais, D. Brown, G. M. Cohen, unpublished results.

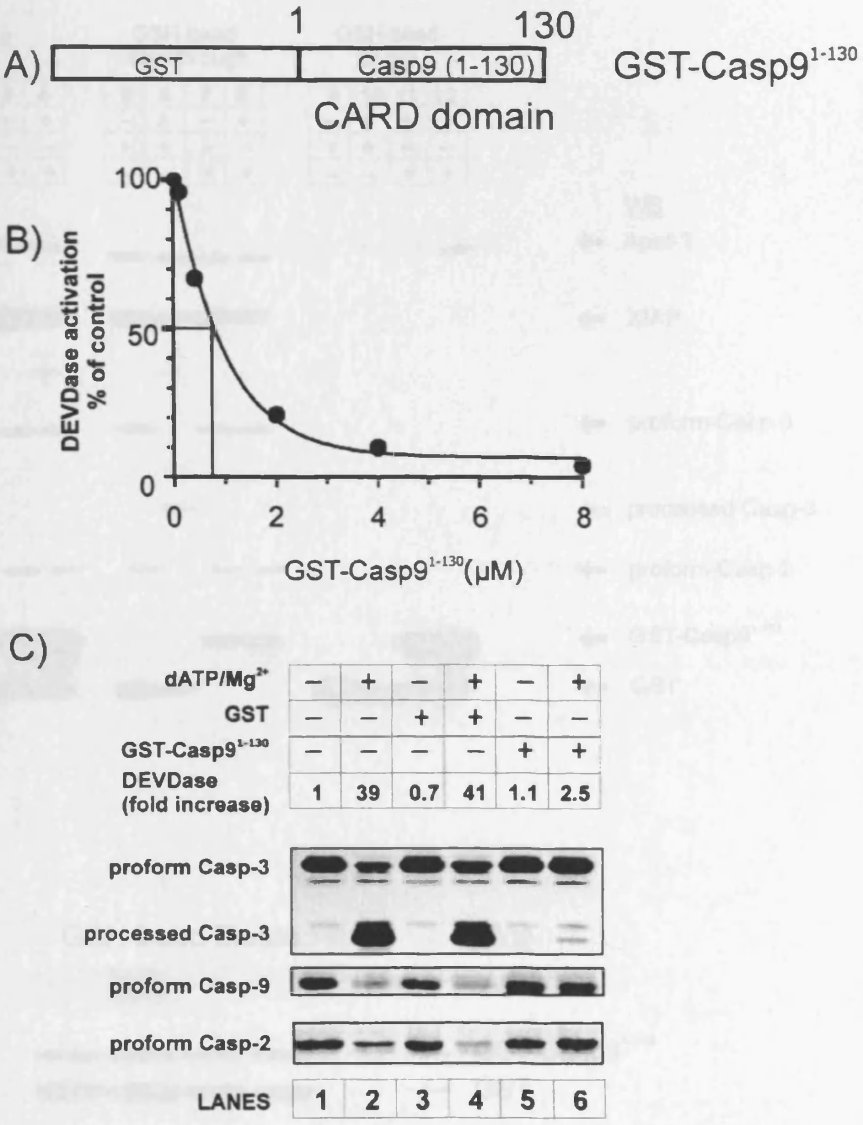

FIG. 1. **GST-casp9$^{1-130}$ acts as a dominant negative inhibitor of dATP activation in THP-1 cell lysates.** *A*, schematic representation of the fusion protein GST-casp9$^{1-130}$. *B*, caspase activation in THP-1 lysates (10 mg/ml) was induced with 2 mM dATP/$MgCl_2$ for 30 min at 37 °C in the presence of increasing concentrations of GST-casp9$^{1-130}$. Caspase activation was measured using DEVD.AFC as a substrate as described under "Experimental Procedures" and expressed as a percentage of the dATP-activated control. *C*, THP-1 lysates (10 mg/ml) either with (*lanes 2* and *6*) or without (*lanes 1* and *5*) 2 mM dATP/$MgCl_2$ were incubated for 30 min at 37 °C with either 2 μM GST (*lanes 3* and *4*) or 2 μM GST-casp9$^{1-130}$ (*lanes 5* and *6*). Each lysate sample was assayed for DEVDase activity (expressed as fold-increase over the nonactivated THP.1 lysate). The cell lysates (20 μg/lane) were also analyzed for caspase-3, caspase-9, and caspase-2 by SDS-PAGE/Western blotting as described under "Experimental Procedures." The proform and processed p19/p17 forms of caspase-3 are indicated, as are the proforms of caspase-9 and caspase-2.

fore we have instead developed two affinity-based approaches using caspase-9 to capture and purify the ~700-kDa apoptosome complex.

GST-casp9$^{1-130}$ Blocks dATP-dependent Caspase Activation in THP.1 Cell Lysates—The first approach was based on previous observations that the prodomain (residues 1–130) of caspase-9 inhibits caspase activation (26) by binding tightly to Apaf-1 via CARD-CARD interactions. Suitably tagged, the prodomain of caspase-9 should only bind to the CARD domain of Apaf-1 when it is accessible, *i.e.* after dATP activation, as in the apoptosome. We therefore reasoned that it should be possible to tag and purify the apoptosome complex with this construct, and this would allow us to identify any proteins that were interacting with the CED-4 and WD40 repeat domains. We therefore generated a recombinant GST-casp9$^{1-130}$ fusion protein (Fig. 1*A*) and showed that it inhibited dATP-activated effector caspase activation in THP.1 lysates with an $IC_{50} \cong 0.8$ μM (Fig. 1*B*). GST-casp9$^{1-130}$ had no effect on DEVDase activity when it was added after dATP activation (data not shown), demonstrating that it does not inhibit either caspase-3 or -7 enzymic activity. However, the inhibition of DEVDase activation by GST-casp9$^{1-130}$ was accompanied by blocking of caspase-9, and -3 processing (Fig. 1*C*, *lane 6*). In addition, GST-casp9$^{1-130}$ also completely inhibited the cleavage and processing of caspase-2 (Fig. 1*C*, *lane 6*), demonstrating that this caspase is only activated via the apoptosome-dependent activation of caspase-9 and caspase-3. Recombinant GST had no effect on dATP-dependent caspase activation (Fig. 1*C*, *lane 4*).

GST-casp9$^{1-130}$ Binding to Apaf-1 Requires dATP—We next determined under what conditions GST-casp9$^{1-130}$ would bind to Apaf-1. GSH-Sepharose beads were used to affinity capture GST-casp9$^{1-130}$ and any attendant binding proteins, which were then eluted from the beads with 20 mM GSH. Lysates were incubated for 30 min with and without dATP/Mg^{2+} in the presence of either GST-casp9$^{1-130}$ or GST as a control. Lysates were then extracted with the GSH-Sepharose beads, and GST and GST-casp9$^{1-130}$ detected in the lysates (input) (Fig. 2*A*, *lanes 1–4*) and also in the GSH-eluates (Fig. 2*A*, *lanes 9–12*) by SDS-PAGE and Western blotting. Small amounts of GST and GST-casp9$^{1-130}$ were not captured by the GSH-Sepharose beads but were detected in the flow-through fractions (Fig. 2*A*,

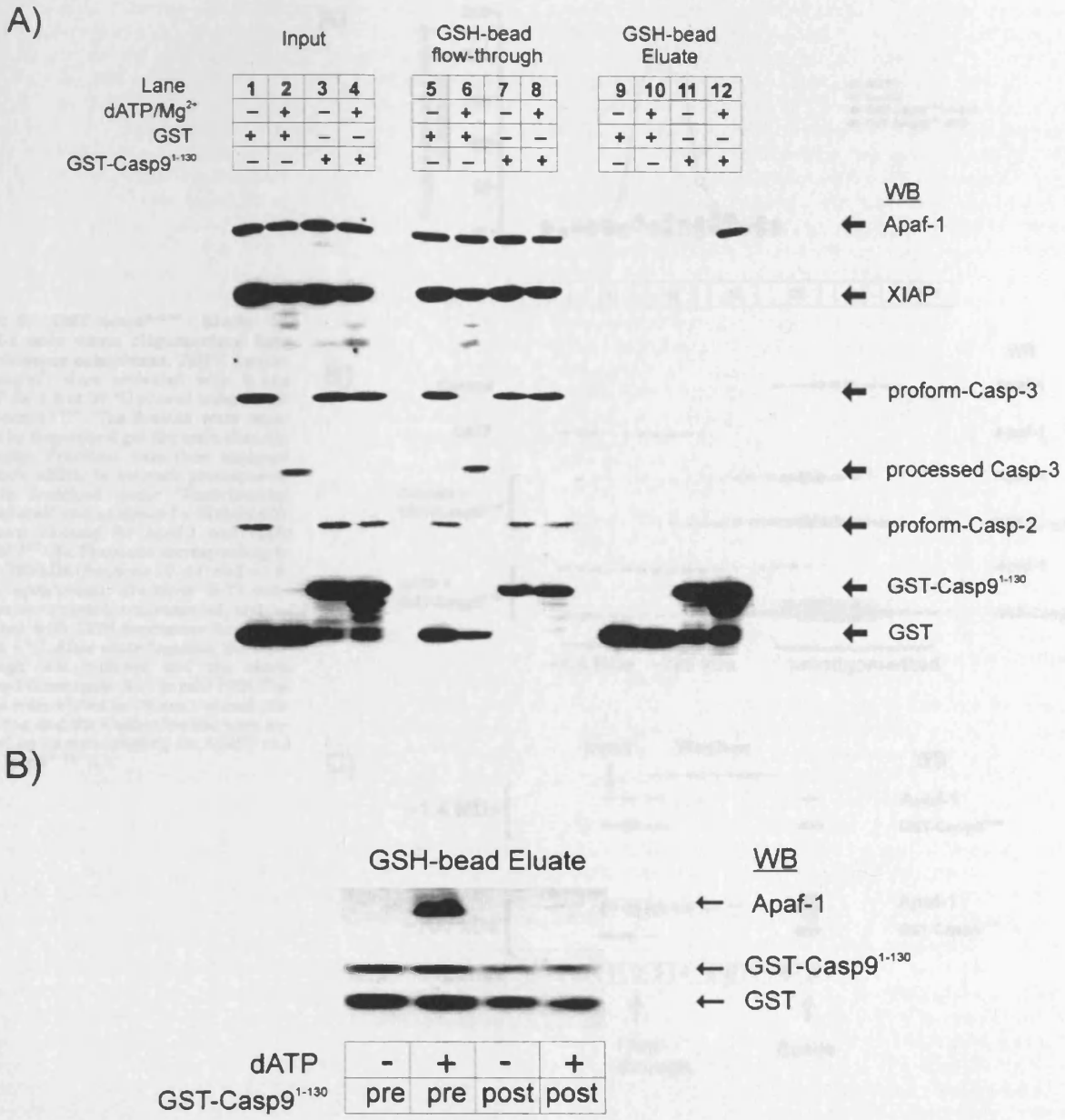

FIG. 2. **GST-casp9$^{1-130}$ binding to Apaf-1 is dATP-dependent and does not result in recruitment of XIAP, caspase-3, or caspase-2.** *A*, THP-1 lysate (10 mg/ml) was activated with 2 mM dATP and 2 μM GST (*lanes 1* and *2*) or 2 μM GST-casp9$^{1-130}$ (*lanes 3* and *4*) as described in Fig. 1*C*. The lysates were then incubated with glutathione (GSH)-Sepharose beads (100 μl) for 1 h at 4 °C, and the beads harvested by centrifugation. The flow-through was collected and the beads washed three times by resuspension and centrifugation in cold PBS. The beads were eluted with 20 mM reduced glutathione (50 μl) and the lysates (*input*), flow-through, and eluates analyzed by SDS-PAGE/Western blotting for Apaf-1, XIAP, caspase-3, caspase-2, and GST as described in Fig. 1*C*. *B*, THP-1 lysate (10 mg/ml) was either co-incubated (*pre*) with GST-casp9$^{1-130}$ (2 μM) alone, GST-casp9$^{1-130}$ plus 2 mM dATP for 30 min at 37 °C (*lanes 1* and *2*) or incubated with and without dATP for 30 min before incubating (*post*) for a further 30 min with GST-casp9$^{1-130}$ (*lanes 3* and *4*). The lysates were then incubated and extracted with GSH-Sepharose beads as described above and analyzed by immunoblotting for Apaf-1, GST-casp9$^{1-130}$, and GST.

lanes 5–8). Although, Apaf-1 was detected in the lysates (*Input*, Fig. 2*A*, *lanes 1–4*) and flow-through fractions (Fig. 2*A*, *lanes 5–8*), it was only captured in the presence of GST-casp9$^{1-130}$ and dATP/Mg^{2+} (Fig. 2*A*, *lane 12*). Thus, GST-casp9$^{1-130}$ only binds to Apaf-1 under conditions that promote apoptosome formation. Furthermore, when GST-casp9$^{1-130}$ was added to the lysates post-caspase activation, it did not inhibit DEVDase activity (results not shown) and was unable to displace the endogenous caspase-9, judged by its inability to bind Apaf-1 to the GSH-Sepharose beads (Fig. 2*B*, *lanes 3* and *4*). Thus, without dATP activation, GST-casp9$^{1-130}$ does not bind to Apaf-1, presumably because the conformation of monomeric Apaf-1 occludes the CARD binding site.

We then used Western blotting to determine whether XIAP and caspase-3 were associated with the GST-casp9$^{1-130}$-tagged apoptosome complex. Although, both proteins were detected in the lysates and flow-through fractions (Fig. 2*A*, *lanes 1–8*), they were not detected in the glutathione eluates (Fig. 2*A*, *lanes 9–12*). Thus, XIAP and caspase-3 do not bind directly to the GST-casp9$^{1-130}$/Apaf-1 complex or alternatively may be bind-

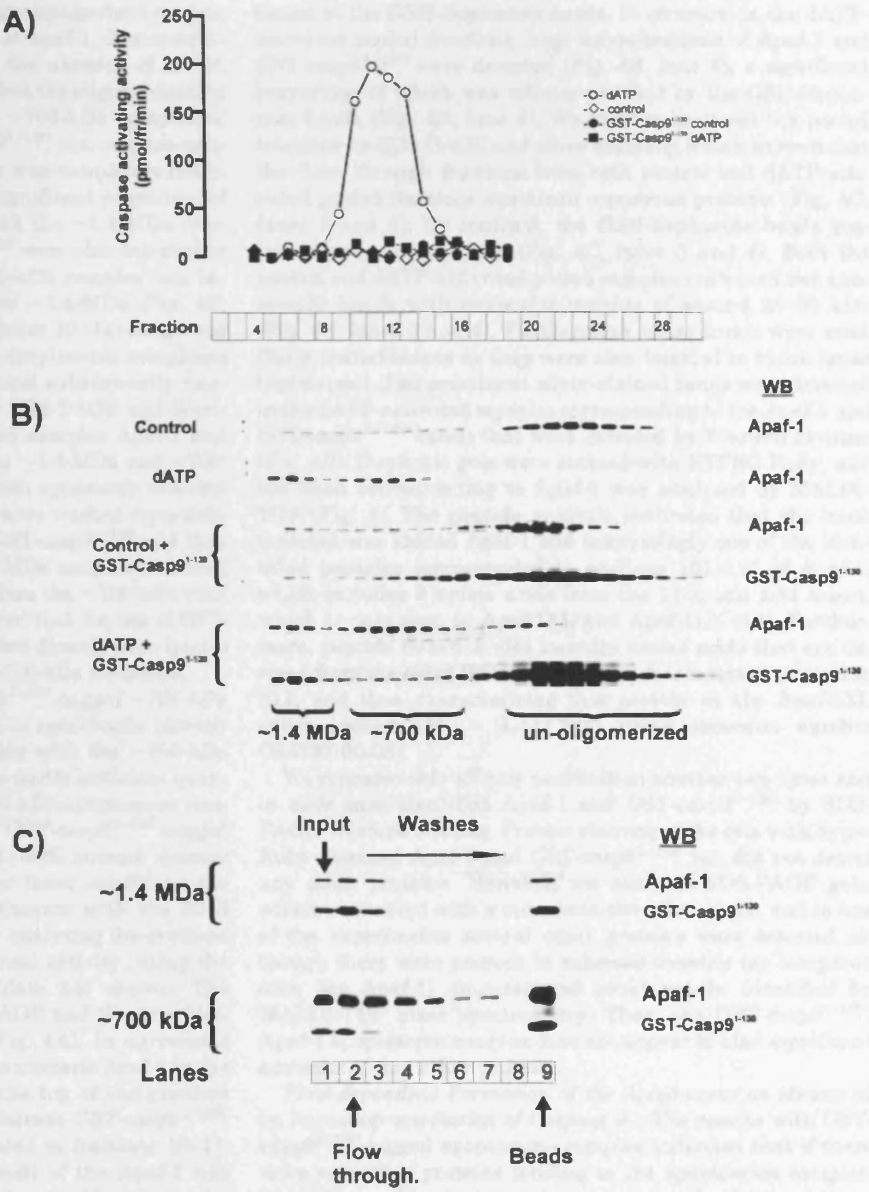

FIG. 3. **GST-casp9$^{1-130}$ binds to Apaf-1 only when oligomerized into apoptosome complexes.** THP-1 lysates (15 mg/ml) were activated with 2 mM dATP for 1 h at 37 °C plus or minus 2 μM GST-casp9$^{1-130}$. The lysates were separated by Superose-6 gel filtration chromatography. Fractions were then analyzed for their ability to activate procaspase-3 (*A*) as described under "Experimental Procedures" and analyzed by SDS-PAGE/Western blotting for Apaf-1 and GST-casp9$^{1-130}$ (*B*). Fractions corresponding to the ~700-kDa (*fractions 10–14*) and ~1.4-MDa apoptosome (*fractions 5–7*) complexes were pooled, concentrated, and incubated with GSH-Sepharose beads for 1 h at 4 °C. After centrifugation, the flow-through was removed and the beads washed thoroughly (5×) in cold PBS. The beads were eluted in 20 mM reduced glutathione, and the eluates (*beads*) were analyzed by immunoblotting for Apaf-1 and GST-casp9$^{1-130}$ (*C*).

ing to complexes in the flow-through fractions that have not been captured by the GSH-Sepharose beads. Previously, XIAP and caspase-3 have been shown to bind to the native apoptosome complex via interactions with XIAP, which simultaneously binds caspase-9 and caspase-3 (27). The binding of the BIR3 domain of XIAP to caspase-9 requires the cleavage of caspase-9 at Asp^{315} to yield an N-terminal ATPF motif, which binds to a conserved surface groove on the XIAP-BIR3 domain (28). Although this interaction is important for inhibition, a second protein-protein interface between XIAP-BIR3 and the small subunit of caspase-9 has also been identified, which produces an inactive BIR3-caspase-9 dimeric complex instead of an active caspase-9 homodimer (29). In contrast the inhibition of caspase-3 and -7 by XIAP involves an 18-peptide sequence immediately preceding the BIR2 domain, which interacts with the catalytic groove and occupies the substrate binding pockets of caspase-3/7 (30, 31). Furthermore, catalytically active caspase-9 is required for recruitment of caspase-3 to the apoptosome (27). Thus, in the GST-casp9$^{1-130}$ apoptosome complex where the ATPF and caspase-9 active site binding motifs are absent it would be predicted that XIAP and caspase-3 would not be recruited to the apoptosome complex. Thus, these results show conclusively that without a fully functional and intact caspase-9 there is no direct interaction/binding of XIAP and caspase-3 to the apoptosome complex. Interestingly, caspase-2 also did not bind to the GST-casp9$^{1-130}$-tagged apoptosome complex (Fig. 2*A*), demonstrating that there is no interaction between caspase-2 and the apoptosome.

GST-casp9$^{1-130}$ Binds to Both the ~1.4-MDa and ~700-kDa Complexes—We next used Superose-6 gel filtration to characterize the binding of GST-casp9$^{1-130}$ to the ~1.4-MDa and ~700-kDa apoptosome complexes. Apaf-1 in control THP.1 lysates eluted as a monomeric protein (Fig. 3*B*, *fractions 16–23*) and after dATP activation oligomerized to form both ~700-kDa (Fig. 3*B*, *fractions 8–14*) and ~1.4-MDa (Fig. 3*B*, *fractions 5–7*) complexes. As shown previously (15) in dATP-activated lysates only the ~700-kDa complex is capable of processing and activating caspase-3 (Fig. 3*A*). In control THP.1 lysates, GST-

casp9$^{1-130}$ predominantly eluted as a non-oligomerized protein and did not affect the elution behavior of Apaf-1, demonstrating that it does not bind to Apaf-1 in the absence of dATP. Furthermore, GST-casp9$^{1-130}$ did not affect the oligomerization of Apaf-1 to form the ~1.4-MDa and ~700-kDa complexes. However, in the presence of GST-casp9$^{1-130}$ the caspase-activating activity of the ~700-kDa complex was completely inhibited (Fig. 3*A*). After dATP activation, a significant proportion of the GST-casp9$^{1-130}$ now co-migrated with the ~1.4-MDa complex. Smaller amounts of GST-casp9$^{1-130}$ were also detected in the fractions corresponding to the ~700-kDa complex (see below). The fractions corresponding to the ~1.4-MDa (Fig. 3*B*, *lanes 5–8*) and the ~700-kDa (Fig. 3*B*, *lanes 10–14*) complexes were pooled and concentrated, and the apoptosome complexes affinity-purified with GSH-Sepharose, and subsequently analyzed for Apaf-1 and GST-casp9$^{1-130}$ by SDS-PAGE and Western blotting. In the concentrated pooled samples Apaf-1 and GST-casp9$^{1-130}$ were detected in both the ~1.4-MDa and ~700-kDa complexes (Fig. 3*C*, *lane 9*), albeit with apparently different Apaf-1/GST-casp9$^{1-130}$ ratios. The beads were washed repeatedly to remove all loosely bound Apaf-1 and GST-casp9$^{1-130}$ and then eluted with 20 mM glutathione. The ~1.4-MDa complex contained more GST-casp9$^{1-130}$ per mol of Apaf-1 than the ~700-kDa complex (Fig. 3*C*, *lane 9*). The data also showed that the use of GST-casp9$^{1-130}$ to capture apoptosome complexes directly from lysates could co-purify both the ~1.4-MDa and ~700-kDa complexes.

Large Scale Purification of GST-casp9$^{1-130}$-tagged ~700-kDa Apoptosome Complexes—As we wished to specifically identify only those proteins that were interacting with the ~700-kDa apoptosome complex, it was necessary to purify sufficient quantities of the GST-casp9$^{1-130}$-tagged ~700-kDa apoptosome complex. Therefore, we prepared 30 mg of GST-casp9$^{1-130}$-tagged lysate that was fractionated on a 10–40% sucrose density gradient (25,000 rpm for 17 h). Under these conditions the ~700-kDa apoptosome complex co-sediments with the 20 S proteasome (14), which was detected by analyzing the gradient fractions for chymotrypsin-like (LLVYase) activity, using the synthetic substrate, suc-LLVY.AMC (data not shown). The fractions were also analyzed by SDS-PAGE and Western blotting for Apaf-1 and GST-casp9$^{1-130}$ (Fig. 4*A*). In agreement with our previous studies, most of the monomeric Apaf-1 in the nonactivated lysates was detected at the top of the gradient mainly in fractions 11–16 (Fig. 4*A*), whereas GST-casp9$^{1-130}$, which is smaller than Apaf-1, sedimented in fractions 13–17. However, in dATP-activated lysates most of the Apaf-1 was oligomerized and sedimented in fractions 8–11, which also contained LLVYase activity (data not shown). Residual amounts of nonoligomerized Apaf-1 were detected at the top of the gradient (fractions 13–16), whereas the ~1.4-MDa complexes were detected in the higher density fractions (1–7). Although small amounts of GST-casp9$^{1-130}$ were detected in the fractions corresponding to the ~700-kDa and ~1.4-MDa apoptosome complexes, the majority of the GST-casp9$^{1-130}$ was present as the uncomplexed form in fractions 13–16. In the nonactivated lysate, GST-casp9$^{1-130}$ was only detected in fractions 13–16, confirming that the construct only binds to Apaf-1 when it is incorporated into the apoptosome complex.

Fractions 8–10 were selected so as to exclude contamination from free Apaf-1 and the ~1.4 MDa apoptosome. We then combined and concentrated these fractions both from the control and dATP-activated sucrose density gradients and then affinity-purified the tagged complexes with GSH-Sepharose beads. In the pooled control fractions only trace amounts of Apaf-1 and GST-casp9$^{1-130}$ could be detected by SDS-PAGE/Western blotting (Fig. 4*B*, *lane 1*). Furthermore, Apaf-1 was also detected in the flow-through fraction (*lane 2*) but was not bound to the GSH-Sepharose beads. In contrast, in the dATP-activated pooled fractions, high concentrations of Apaf-1 and GST-casp9$^{1-130}$ were detected (Fig. 4*B*, *lane 5*), a significant proportion of which was affinity-purified by the GSH-Sepharose beads (Fig. 4*B*, *lane 8*). We further analyzed the pooled fractions by SDS-PAGE and silver staining, which showed that the flow- through fractions from both control and dATP-activated pooled fractions contained numerous proteins (Fig. 4*C*, *lanes 1* and *2*). By contrast, the GSH-Sepharose beads contained very few proteins (Fig. 4*C*, *lanes 3* and *4*). Both the control and dATP-activated pooled samples contained two nonspecific bands with molecular weights of around 25–30 kDa (Fig. 4*C*, *lanes 3* and *4*). Furthermore, these bands were most likely contaminants as they were also detected in blank lanes (not shown). Two prominent silver-stained bands were detected in the dATP-activated samples corresponding to the Apaf-1 and GST-casp9$^{1-130}$ bands that were detected by Western blotting (Fig. 4*B*). Duplicate gels were stained with SYPRO Ruby, and the band corresponding to Apaf-1 was analyzed by MALDI-TOF (Fig. 5). The peptide analysis confirmed that the band detected was indeed Apaf-1 and interestingly one of the identified peptides corresponded to residues 101–111 of Apaf-1, which includes 9 amino acids from the 11-amino acid insert, which is only seen in Apaf-1XL and Apaf-1LN (13). Furthermore, peptide 803–818 also includes amino acids that are derived from the extra WD40 repeat, which is inserted at residue 811, and thus characterizing this protein as the Apaf-1XL splice isoform (M_r = 1,417,333; HSSP accession number O14727-00-08).

We repeated this affinity purification another two times and in each case identified Apaf-1 and GST-casp9$^{1-130}$ by SDS-PAGE/Western blotting. Protein staining of the gels with Sypro Ruby detected Apaf-1 and GST-casp9$^{1-130}$ but did not detect any other proteins. However, we also ran SDS-PAGE gels, which we stained with a more sensitive silver stain, and in one of the experiments several other proteins were detected although these were present in substoichiometric (as compared with the Apaf-1) amounts and could not be identified by MALDI-TOF mass spectrometry. Thus, the GST-casp9$^{1-130}$/Apaf-1 apoptosome complex does not appear to bind significant amounts of any other proteins.

Time-dependent Formation of the Apoptosome as Measured by Immunoprecipitation of Caspase-9—The results with GST-casp9$^{1-130}$-tagged apoptosome complex indicated that if there were any other proteins binding to the apoptosome complex, then they could only do so via caspase-9 and associated interactions. It was therefore necessary to immunopurify the apoptosome complex with an intact caspase-9. Initially, we screened a panel of Apaf-1 and caspase-9 antibodies and finally selected an anti-caspase-9 antibody, which was raised to the CARD domain of caspase-9 and would only could capture Apaf-1 when it was bound to the apoptosome complex. Initial experiments confirmed that the antibody only captured Apaf-1 when the lysate was activated with dATP (data not shown). We have previously established using Superose 6 chromatography that formation of the ~700-kDa apoptosome complex in THP.1 lysates is maximal 10–15 min after dATP activation (15) and that after 30 min it decreases, presumably because caspase-3 cleavage of Apaf-1 degrades the complex (32). As we wished to establish the optimal time for analyzing the complex by two-dimensional gels we carried out a time course experiment in which we took samples and captured caspase-9 and associated proteins with the anti-caspase-9 monoclonal antibody. The lysates (inputs), unbound proteins (supernatants), and captured proteins (beads) were then analyzed by Western blotting for Apaf-1, caspase-9, XIAP, and caspase-3. The rate of formation

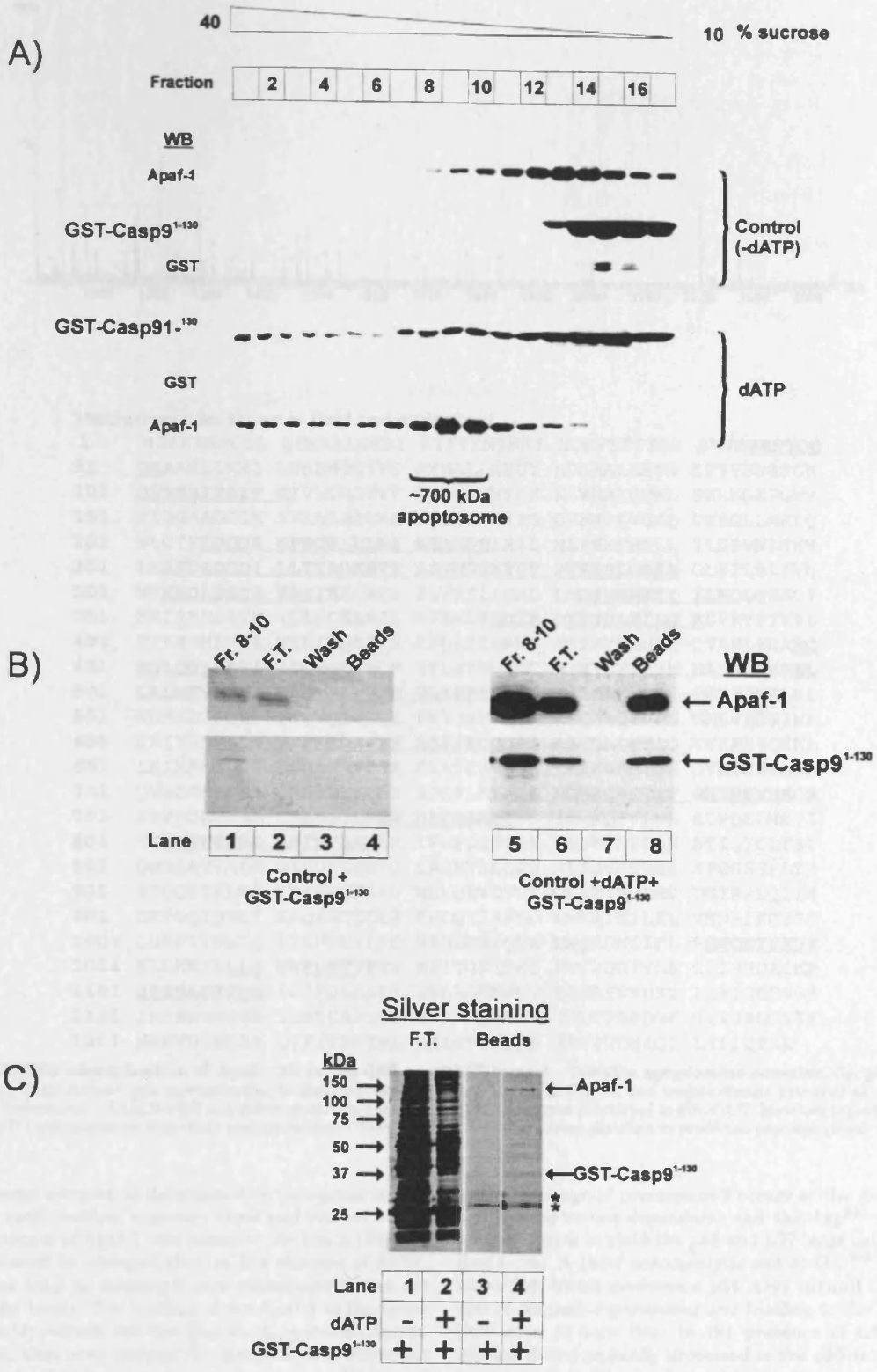

FIG. 4. **Only GST-casp9$^{1-130}$ and Apaf-1 can be detected in the purified GST-casp9$^{1-130}$- inhibited ~700-kDa apoptosome.** THP-1 lysates (15 mg/ml) were activated with 2 mM dATP in the presence of 2 μM GST-casp9$^{1-130}$ for 1 h at 37 °C. Lysates were layered onto 10–40% sucrose gradients and centrifuged at 25,000 rpm for 17 h. The fractionated gradients were analyzed for LLVYase activity (data not shown) and immunoblotted for Apaf-1, GST, and GST-casp9$^{1-130}$ (*A*). Fractions corresponding to the ~700-kDa apoptosome were pooled, concentrated, and incubated with GSH-Sepharose for 1 h at 4 °C. After centrifugation, the flow-through was removed, and the beads were washed in cold PBS (4×). The beads were then resuspended in 2× SDS loading buffer, heated at 50 °C for 30 min, and centrifuged to pellet the beads. The eluate from the beads was then analyzed by SDS-PAGE/Western blotting for Apaf-1 and GST-casp9$^{1-130}$ (*B*), and other proteins by silver staining (*C*). Duplicate samples were also run and stained with SYPRO Ruby and used for tryptic digestion and MALDI-TOF analysis.

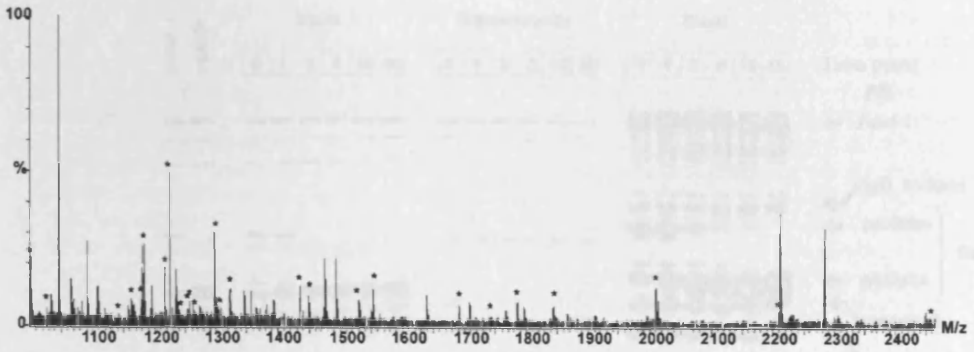

Matched peptides shown in **Bold and underlined.**

```
1     MDAKARNCLL QHREALEKDI KTSYIMDHMI SDGFLTISEE EKVRNEPTQQ
51    QRAAMLIKMI LKKDNDSYVS FYNALLHEGY KDLAALLHDG IPVVSSSSGK
101   DSVSGITSYV RTVLCEGGVP QRPVVFVTRK KLVNAIQQKL SKLKGEPGWV
151   TIHGMAGCGK SVLAAEAVRD HSLLEGCFPG GVHWVSVGKQ DKSGLLMKLQ
201   NLCTRLDQDE SFSQRLPLNI EEAKDRLRIL MLRKHPRSLL ILDDVWDSWV
251   LKAFDSQCQI LLTTRDKSVT DSVMGPKYVV PVESSLGKEK GLEILSLFVN
301   MKKADLPEQA HSIIKECKGS PLVVSLIGAL LRDFPNRWEY YLKQLQNKQF
351   KRIRKSSSYD YEALDEAMSI SVEMLREDIK DYYTDLSILQ KDVKVPTKVL
401   CILWDMETEE VEDILQEFVN KSLLFCDRNG KSFRYYLHDL QVDFLTEKNC
451   SQLQDLHKKI ITQFQRYHQP HTLSPDQEDC MYWYNFLAYH MASAKMHKEL
501   CALMFSLDWI KAKTELVGPA HLIHEFVEYR HILDEKDCAV SENFQEFLSL
551   NGHLLGRQPF PNIVQLGLCE PETSEVYQQA KLQAKQEVDN GMLYLEWINK
601   KNITNLSRLV VRPHTDAVYH ACFSEDGQRI ASCGADKTLQ VFKAETGEKL
651   LEIKAHEDEV LCCAFSTDDR FIATCSVDKK VKIWNSMTGE LVHTYDEHSE
701   QVNCCHFTNS SHHLLLATGS SDCFLKLWDL NQKECRNTMF GHTNSVNHCR
751   FSPDDKPLAS CSADGTLKLW DATSANERKS INVKQFFLNL EDPQEDMEVI
801   VKCCSWSADG ARIMVAAKNK IFLFDIHTSG LLGEIHTGHH STIQYCDFSP
851   QNHLAVVALS QYCVELWNTD SRSKVADCRG HLSWVHGVMF SPDGSSFLTS
901   SDDQTIRLWE TKKVCKNSAV MLKQEVDVVF QENEVMVLAV DHIRRLQLIN
951   GRTGQIDYLT EAQVSCCCLS PHLQYIAFGD ENGAIEILEL VNNRIFQSRF
1001  QHKKTVWHIQ FTADEKTLIS SSDDAEIQVW NWQLDKCIFL RGHQETVKDF
1051  RLLKNSRLLS WSFDGTVKVW NIITGNKEKD FVCHQGTVLS CDISHDATKF
1101  SSTSADKTAK IWSFDLLLPL HELRGHNGCV RCSAFSVDST LLATGDDNGE
1151  IRIWNVSNGE LLHLCAPLSE EGAATHGGWV TDLCFSPDGK MLISAGGYIK
1201  WWNVVTGESS QTFYTNGTNL KKIHVSPDFK TYVTVDNLGI LYILQTLE
```

FIG. 5. **MALDI-TOF identification of Apaf-1 XL in the GST-casp9$^{1-130}$-tagged ~700-kDa apoptosome complex.** Gel plugs were taken from the SYPRO Ruby stained gels corresponding to the silver-stained bands shown in Fig. 4*C* and tryptic digests prepared as described under "Experimental Procedures." MALDI-TOF analysis was carried out and the peptide masses submitted to MASCOT. Matched peptides are indicated in the spectrum (*) and sequence map (*bold* and *underlined*). Twenty-six mass values were matched to predicted peptides giving 21% coverage of the sequence.

of the apoptosome complex as determined by the appearance of Apaf-1 in the bead fraction, was very rapid and even at 0 min, significant amounts of Apaf-1 was bound to the beads (Fig. 6*A*, *lane 15*). It should be stressed that in the absence of dATP, Apaf-1 did not bind to caspase-9 and consequently was not captured by the beads. The binding of the Apaf-1 to the beads at 0 min probably reflects the fact that the apoptosome assembly is so rapid, that even cooling the lysate to 4 °C slows but does not completely stop apoptosome assembly. Binding of Apaf-1 to the beads was maximal at 5/10 min and remained relatively constant for up to 30 min (Fig. 6*A*, *lanes 18 -20*), before decreasing significantly at 60 min (data not shown). The binding of Apaf-1 to the beads was accompanied by a corresponding decrease in the level of Apaf-1 in the supernatants (Fig. 6*A*, *lanes 9–14*).

The cleavage of procaspase-9 occurs at the Asp^{315} (autocatalytic, apoptosome-dependent) and the Asp^{330} (caspase-3-dependent) sites to yield the p35 and p37 large subunits, respectively (28). A third autocatalytic site at Glu^{306} has also been identified, which produces a p34 large subunit (28). Our analysis of caspase-9 processing and binding to the beads showed that even at zero time in the presence of dATP, captured caspase-9 was partially processed to the p35 subunit (Fig. 6*A*, *lane 15*). At 5–10 min (*lanes 18* and *19*), caspase-9 was fully processed as only the p35 and p34 subunits were bound to the beads. From 10 to 30 min, there was little change in the levels of processed caspase-9 that bound to the beads, but thereafter there was a significant decrease in the amount of caspase-9 bound to the beads (data not shown). We did not detect the p37 form of caspase-9 in these experiments, which is to be expected

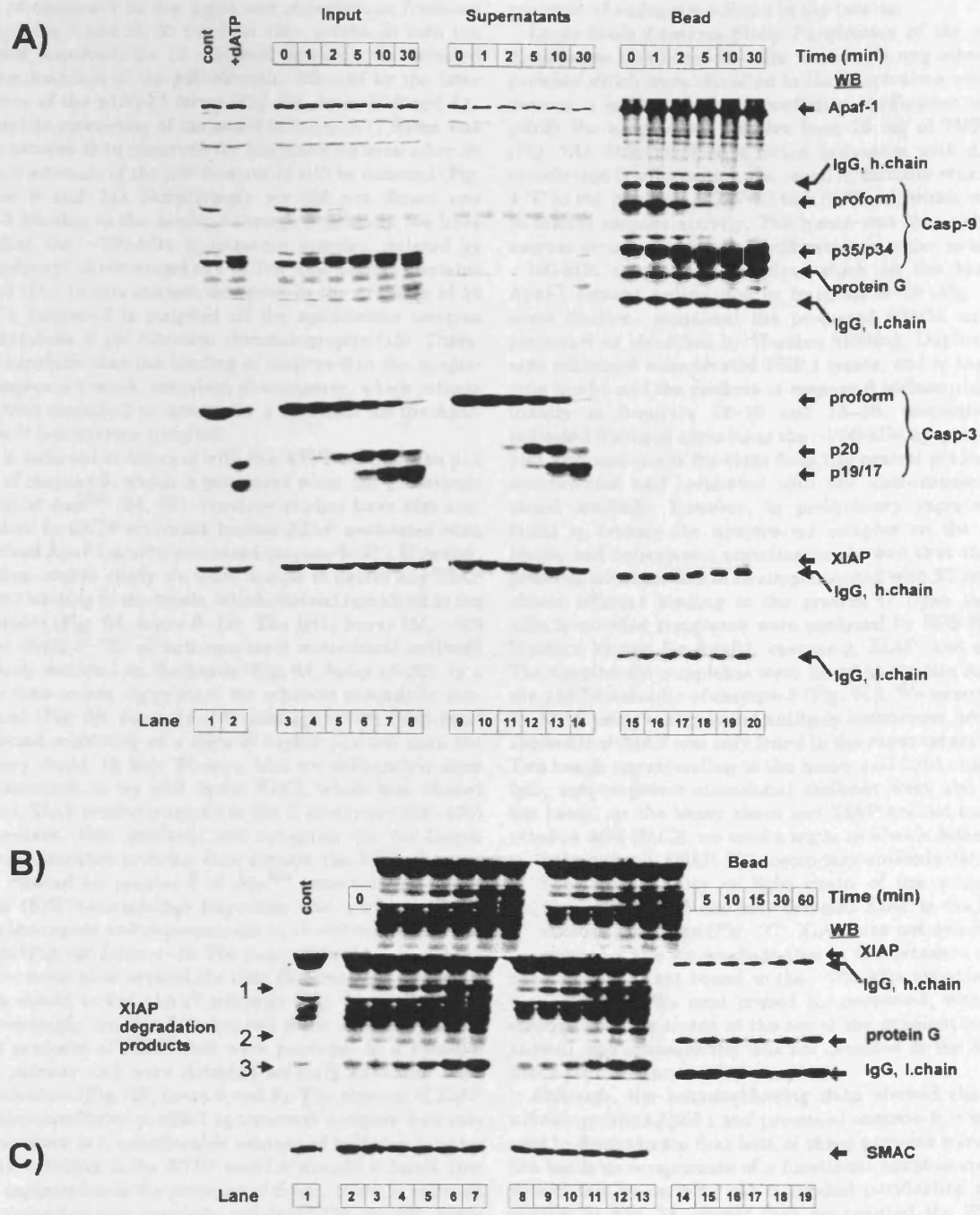

FIG. 6. **Time-dependent apoptosome formation as measured by immunoprecipitation of caspase-9.** Precleared THP.1 lysates were activated with dATP as described under "Experimental Procedures." At the indicated times, the lysates were treated with Z-VAD.fmk (200 μM) and transferred onto ice. Samples of the lysates (*Input*) were taken for the SDS-PAGE/Western blotting, and the remaining lysates then incubated with the anti-caspase-9 monoclonal antibody for 2 h at 4 °C. The lysates were then incubated overnight at 4 °C with Protein G Dyna beads. The beads were removed from the supernatants and washed before eluting with SDS-sample buffer (*bead*). The input (*lanes 3–8*), supernatants (*lanes 9–14*), and bead samples (*lanes 15–20*) were then separated by SDS-PAGE and immunoblotted for Apaf-1, caspase-9, caspase-3, and XIAP as described under "Experimental Procedures." *A*, a time course from 0 to 30 min is shown with a control and dATP (30 min)-activated lysate added as marker lanes (*1* and *2*) for the indicated proteins. The position of the heavy and light chains of the IgG_1 and protein G are as indicated. *B*, a longer time course for XIAP detection is shown in which the film has been overexposed so as to resolve the XIAP degradation products (*1–3*). *Band 2* corresponds to the ~29-kDa (BIR 3 ring containing) fragment, which is generated by caspase-3 cleavage at Asp^{242}. *C*, the time course samples shown in *B* were also probed with an antibody raised to Smac as described previously (22).

as caspase-9 processing appears to be so rapid that by the time the caspase-3 is activated (see below) there is very little procaspase-9 left to be cleaved at the Asp^{330} site.

The supernatant fractions contained only residual traces of caspase-9 (Fig. 6*A*, *lanes 9–14*), demonstrating that under the conditions employed there was almost complete binding of caspase-9 to the beads. We then looked at the recruitment and processing of caspase-3, and at zero time we only detected the

proform of caspase-3 in the input and supernatant fractions (Fig. 6*A*, *lanes 3* and *9*). At the later time points, in both the inputs and supernatants (2 min and onward), we detected increasing amounts of the p20 subunit, followed by the later appearance of the p19/p17 forms (Fig. 6*A*, *lanes 5–8* and *11–14*). Complete processing of caspase-3 to the p19/17 forms was a slower process than observed for caspase-9 as even after 30 min, small amounts of the p20 form could still be detected (Fig. 6*A*, *lanes 8* and *14*). Surprisingly we did not detect any caspase-3 binding to the beads, although previously, we have shown that the ~700-kDa apoptosome complex isolated by S300 Sephacryl chromatography in low salt buffers contains caspase-3 (14). In this context, however, in the presence of 50 mM NaCl, caspase-3 is stripped off the apoptosome complex during Superose 6 gel filtration chromatography (15). Therefore, we conclude that the binding of caspase-3 to the apoptosome complex is a weak, transient phenomenon, which reflects the fact that caspase-3 is essentially a substrate for the Apaf-1/caspase-9 holoenzyme complex.

XIAP is believed to interact with the ATPF motif of the p12 subunit of caspase-9, which is generated when the procaspase is cleaved at Asp^{315} (24, 28). Previous studies have also suggested that in dATP-activated lysates XIAP associates with oligomerized Apaf-1 and/or processed caspase-9 (27). However, in this time-course study we were unable to detect any XIAP (~57 kDa) binding to the beads, which instead remained in the supernatants (Fig. 6*A*, *lanes 9–14*). The IgG_1 heavy (M_r ~50) and light chain (~25) of anti-caspase-9 monoclonal antibody were clearly detected on the beads (Fig. 6*A*, *lanes 15–20*). In a separate time course experiment we achieved essentially similar results (Fig. 6*B*, *lanes 14–19*) although a very faint band was detected migrating at a slightly higher position than the IgG_1 heavy chain. In this Western blot we deliberately used longer exposures to try and detect XIAP, which was blotted against an XIAP antibody raised to the C terminus (268–426) of the protein. This antibody will recognize the full-length protein or truncated proteins that contain the BIR3 domain. XIAP is cleaved by caspase-3 at Asp^{242} generating ~27 and ~29 kDa (BIR 3-containing) fragments (33) which were detected in the inputs and supernatants at 10–60 min post dATP activation (Fig. 6*B*, *lanes 4–8*). The generation of this fragment appears to occur at or around the time that caspase-3 is extensively processed to the p19/17 subunits (Fig. 6*A*, *lanes 7* and *13*). Interestingly, we also detected two other immunoreactive/cleavage products of XIAP that were produced in a time-dependent manner and were detected as early as 5 min after dATP activation (Fig. 6*B*, *lanes 3* and *9*). The absence of XIAP in the immunoaffinity-purified apoptosome complex was surprising as there is a considerable amount of evidence to show that XIAP will bind to the ATPF motif of the p35 subunit. One possible explanation is the presence of Smac, which is released into the cytosol during apoptotic cell death (28, 34, 35). Smac binds to XIAP and relieves the inhibition of caspase-9, and in naïve 293 cell lysates, exogenous GST-XIAP immunoprecipitates Smac (24). We therefore probed the time course samples, for the presence of Smac, which was detected in the lysate (Fig. 6*B*, *lane 1*), inputs (Fig. 6*B*, *lanes 2–7*), and supernatant fractions (Fig. 6*C*, *lanes 8–13*). However, Smac was not detected in the bead eluates demonstrating that Smac was not binding to the apoptosome complex. The presence of Smac in the lysates strongly suggested that XIAP was sequestered by Smac. Therefore, we used Smac (22) and XIAP antibodies to immunoprecipitate Smac and XIAP, respectively, from THP.1 lysates and found that XIAP coprecipitated with Smac (data not shown). This result confirmed that the lack of XIAP in the complexes precipitated by the anti-caspase-9 antibody was due to the presence of endogenous Smac in the lysates.

Large Scale Immunoaffinity Purification of the ~700-kDa Apoptosome Complex—In order to identify any other binding proteins which were recruited to the apoptosome complex, we devised a large scale immunoaffinity purification scheme to purify the apoptosome complex from 75 mg of THP.1 lysate (Fig. 7*A*). This involved a 5-min activation with dATP and cytochrome *c*, after which the reaction mixture was cooled to 4 °C in the presence of Z-VAD.fmk (200 μM), which was added to inhibit caspase activity. The lysate was then subjected to sucrose density gradient centrifugation in order to isolate the ~700-kDa apoptosome complex, which on the basis of its Apaf-1 content sedimented in fractions 8–10 (Fig. 7*B*). The same fractions contained the processed p35/34 subunits of caspase-9 as identified by Western blotting. Duplicate gradients contained nonactivated THP.1 lysate, and in these gradients Apaf-1 and the proform of caspase-9 sedimented predominantly in fractions 12–16 and 15–18, respectively. The indicated fractions containing the ~700-kDa apoptosome complex and equivalent fractions from the control gradients were concentrated and incubated with the anti-caspase-9 monoclonal antibody. However, in preliminary experiments we failed to capture the apoptosome complex on the magnetic beads, and subsequent experiments showed that the sucrose gradient solutions had to be supplemented with 25 mM NaCl to obtain efficient binding to the protein G Dyna beads. The affinity-purified complexes were analyzed by SDS-PAGE and Western blotted for Apaf-1, caspase-9, XIAP, and caspase-3. The apoptosome complexes were found to contain Apaf-1 and the p35/34 subunits of caspase-9 (Fig. 7*C*). We immunoblotted for XIAP using conventional antibody techniques, which again showed that XIAP was only found in the supernatant (Fig. 7*C*). Two bands corresponding to the heavy and light chains of the IgG_1 anti-caspase-9 monoclonal antibody were also bound to the beads. As the heavy chain and XIAP are not easily separated on SDS-PAGE, we used a triple sandwich detection technique to probe for XIAP. This secondary antibody did not cross-react with the heavy or light chain of the anti-caspase-9 monoclonal antibody and only detected XIAP in the lysates or supernatant fractions (Fig. 7*C*). XIAP was not detected in the bead sample, and we conclude that in the presence of endogenous Smac it is not bound to the ~700-kDa apoptosome complex (Fig. 7*C*). We next probed for caspase-3, which on the sucrose gradient eluted at the top of the gradient (results not shown), and consequently was not detected in the immunoaffinity-purified apoptosome complex.

Although, the immunoblotting data showed that we had affinity-purified Apaf-1 and processed caspase-9, it was important to demonstrate that both of these proteins were bound to the beads as components of a functional apoptosome. We confirmed this by carrying out a parallel purification run as described in Fig. 7*A*, except that we omitted the ZVAD.FMK treatment. The apoptosome bead complexes were then incubated with recombinant procaspase-3 for 1 h at 37 °C, before magnetically separating the beads and the captured apoptosome complexes from the supernatants. The latter were assayed for DEVDase activity and caspase-3 processing. Significantly, a high DEVDase activity coupled with extensive processing of procaspase-3 to the p19 and p17 subunits was only detected in the supernatant, which was obtained from incubating the apoptosome-bead complexes with procaspase-3 (Fig. 7*D*, *lane 2*). In the absence of recombinant procaspase-3 there was little or no DEVDase activity and caspase-3 was not by detected by SDS-PAGE and immunoblotting (Fig. 7*D*, *lane 1*). Procaspase-3 in the absence of the apoptosome bead complex had a very low DEVDase activity, and only one band with

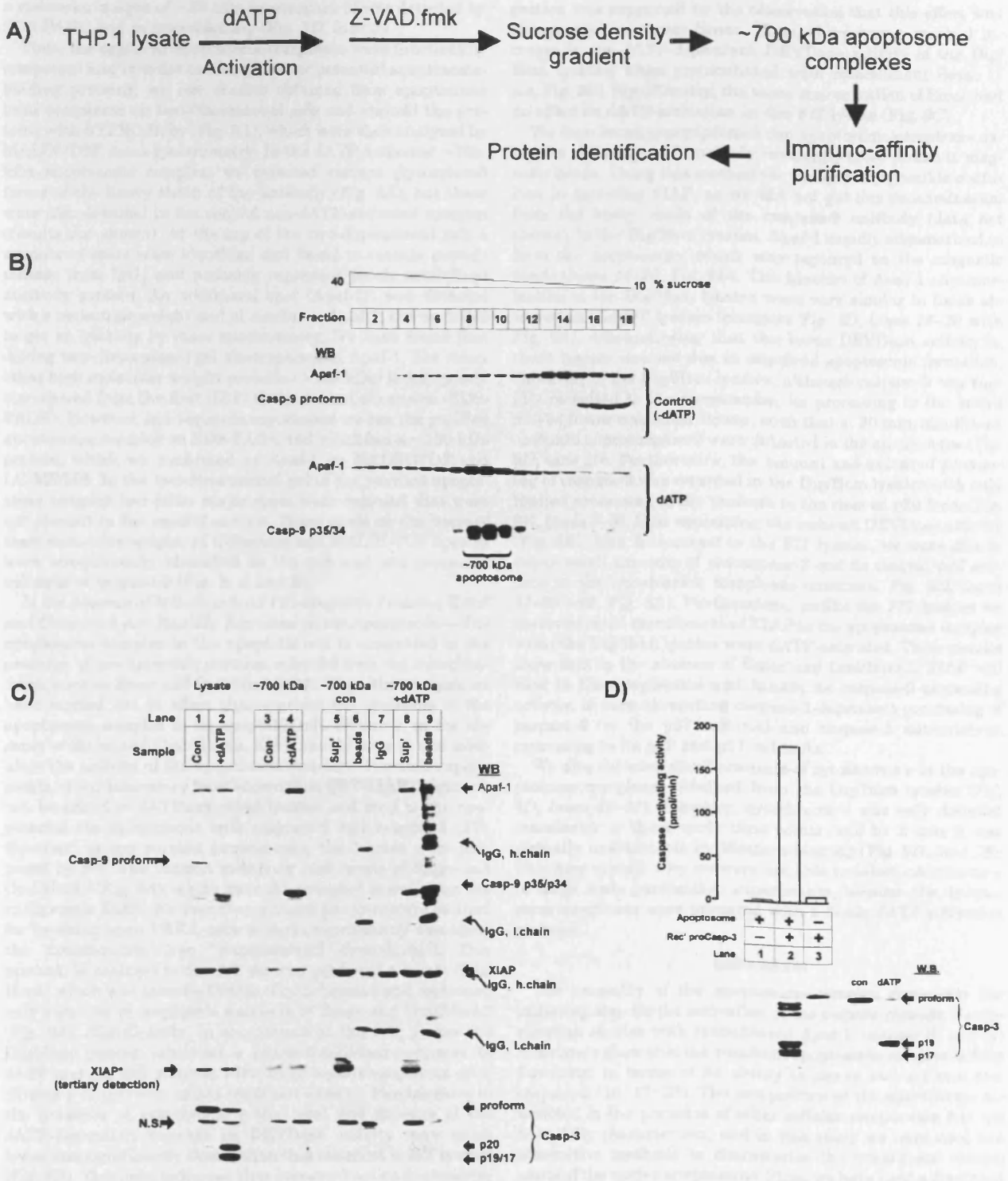

FIG. 7. **Large scale purification of the ~700-kDa apoptosome complex.** *A*, scheme summarizes the strategy used for preparing the purified apoptosome complex. Precleared THP.1 lysate (75 mg) was activated at a concentration of 15 mg/ml with dATP and cytochrome *c* for 5 min at 37 °C as described under "Experimental Procedures." The reaction was terminated by cooling to 4 °C and adding 200 μM Z-VAD.fmk, before layering the lysate onto two 10–40% sucrose gradients, which were centrifuged at 25,000 rpm for 17 h. Equivalent amounts of control nonactivated precleared lysates were also separated in the same manner. The fractionated gradients were analyzed for LLVYase activity (data not shown) and immunoblotted for Apaf-1, and caspase-9. A representative gradient for each treatment is shown which illustrates the distribution of Apaf-1 and caspase-9 (*B*). Fractions 8–10 of each gradient were pooled and concentrated before immunopurifying with anti-caspase-9 antibody and protein G Dyna beads. The concentrated ~700-kDa complexes before and after immunoaffinity purification were analyzed by SDS-PAGE/Western blotting for Apaf-1, caspase-9, caspase-3, and XIAP (*C*). *Lanes 1* and *2* show the inputs from control and dATP-activated lysates. The concentrated ~700-kDa complexes isolated from the control and dATP-activated lysates are shown in *lanes 3* and *4*, respectively. The results of the immunopurification (*i.e.* supernatants and beads) for the control and dATP-activated complexes are shown in *5* and *6*, and *8* and *9*, respectively.

a molecular weight of ~33 kDa (procaspase-3) was detected by SDS-PAGE and immunoblotting (Fig. 7*D*, *lane 3*).

Thus, the captured apoptosome complexes were functionally competent and in order to identify other potential apoptosome-binding proteins, we ran eluates obtained from apoptosome bead complexes on two-dimensional gels and stained the proteins with SYPRO Ruby (Fig. 8*A*), which were then analyzed by MALDI-TOF mass spectrometry. In the dATP-activated ~700-kDa apoptosome complex, we detected various glycosylated forms of the heavy chain of the antibody (Fig. 8*A*), but these were also detected in the control non-dATP-activated complex (results not shown). At the top of the two-dimensional gels a number of spots were identified and found to contain peptide masses from IgG_1 and probably represent poorly solubilized antibody protein. An additional spot (Apaf-1?) was detected with a molecular weight and pI similar to Apaf-1, but we failed to get an identity by mass spectrometry. We have found that during two-dimensional gel electrophoresis, Apaf-1, like many other high molecular weight proteins (>125 kDa) is only poorly transferred from the first (IEF) to the second dimension (SDS-PAGE). However, in a separate experiment we ran the purified apoptosome complex on SDS-PAGE and identified a ~130 kDa protein, which we confirmed as Apaf-1 by MALDI-TOF and LC-MS/MS. In the two-dimensional gel of the purified apoptosome complex two other major spots were detected that were not present in the control sample. These spots on the basis of their molecular weight, pI difference and MALDI-TOF spectra were unequivocally identified as the p35 and p34 processed subunits of caspase-9 (Fig. 8, *A* and *B*).

In the Absence of Mitochondrial Pro-apoptotic Proteins, XIAP and Caspase-3 Are Rapidly Recruited to the Apoptosome—The apoptosome complex in the apoptotic cell is assembled in the presence of pro-apoptotic proteins released from the mitochondrion, such as Smac and Omi/HtrA2 (36). Thus, the analysis we have carried out in effect characterizes the proteome of the apoptosome complex in an apoptotic cell. However, in the absence of Smac and Omi/HtrA2, XIAP should bind to and modulate the activity of the apoptosome complex. Previous experiments in our laboratory have shown that GST-XIAP constructs can be added to dATP-activated lysates and bind to the apoptosome via interactions with caspase-9 and caspase-3 (27). However, in our current experiments, the lysates were prepared by F/T, and contain relatively high levels of Smac and Omi/HtrA2 (Fig. 9*A*), which have the potential to sequester the endogenous XIAP. We therefore devised an alternative method for breaking open THP.1 cells without significantly damaging the mitochondria (see "Experimental Procedures"). This method, in contrast to the F/T method produced a lysate (Dig/Hom), which was essentially free of cytochrome *c* and contained only very low or negligible amounts of Smac and Omi/HtrA2 (Fig. 9*A*). Significantly, in comparison to the F/T lysates the Dig/Hom lysates exhibited a much-diminished response to dATP and did not activate with dATP unless exogenous cytochrome *c* (7 μM) was added (data not shown). Furthermore in the presence of cytochrome *c* the level and kinetics of the dATP-dependent increase in DEVDase activity were much lower and significantly slower than that observed in F/T lysates (Fig. 9*B*). This data indicated that caspase-3 activation/activity was inhibited probably by the presence of XIAP and this suggestion was supported by the observation that this effect was antagonized by excess Smac. Thus, there was a marked increase in the dATP-dependent DEVDase activity of the Dig/Hom lysates, when preincubated with recombinant Smac (1 μM, Fig. 9*C*). Significantly, the same concentration of Smac had no effect on dATP activation in the F/T lysate (Fig. 9*C*).

We then immunoprecipitated the apoptosome complexes using the anti-caspase-9 antibody covalently cross-linked to magnetic beads. Using this method we avoided any possible confusion in detecting XIAP, as we did not get any contamination from the heavy chain of the caspase-9 antibody (data not shown). In the Dig/Hom lysates, Apaf-1 rapidly oligomerized to form the apoptosome, which was captured on the magnetic beads (*lanes 15–20*, Fig. 9*D*). The kinetics of Apaf-1 oligomerization in the Dig/Hom lysates were very similar to those observed in the F/T lysates (compare Fig. 9*D*, *lanes 15–20* with Fig. 6*A*), demonstrating that the lower DEVDase activity in these lysates was not due to impaired apoptosome formation. However, in the Dig/Hom lysates, although caspase-9 was rapidly recruited to the apoptosome, its processing to the active p35/34 forms was much slower, such that at 30 min, significant amounts of procaspase-9 were detected in the apoptosome (Fig. 9*D*, *lane 20*). Furthermore, the amount and extent of processing of caspase-3 was retarded in the Dig/Hom lysates with only limited processing of the proform to the cleaved p20 form (Fig. 9*D*, *lanes 3–8*), thus explaining the reduced DEVDase activity (Fig. 9*B*). Also, in contrast to the F/T lysates, we were able to detect small amounts of procaspase-3 and its cleaved p20 subunit in the apoptosome complexes (compare, Fig. 9*D*, *lanes 17–20* with Fig. 6*A*). Furthermore, unlike the F/T lysates we observed rapid recruitment of XIAP to the apoptosome complex when the Dig/Hom lysates were dATP-activated. These results show that in the absence of Smac and Omi/HtrA2, XIAP will bind to the apoptosome and inhibit its caspase-9 processing activity, in turn abrogating caspase-3-dependent processing of caspase-9 (to the p37 subunit) and caspase-3 autocatalytic processing to its p19 and p17 subunits.

We also detected small amounts of cytochrome *c* in the apoptosome complexes obtained from the Dig/Hom lysates (Fig. 9*D*, *lanes 15–17*). However, cytochrome *c* was only detected transiently at these early time points, and by 5 min it was virtually undetectable by Western blotting (Fig. 9*D*, *lane 18*). This may explain why we were not able to detect cytochrome *c* in large scale purification experiments, because the apoptosome complexes were prepared with a 5-min dATP activation protocol.

DISCUSSION

The assembly of the apoptosome complex represents the initiating step for the activation of the caspase cascade. Reconstitution studies with recombinant Apaf-1, caspase-9, and cytochrome *c* show that the resultant apoptosome complex is fully functional in terms of its ability to cleave and activate procaspase-3 (16, 17, 23). The composition of the apoptosome assembled in the presence of other cellular components has not been fully characterized, and in this study we have used two alternative methods to characterize the constituent components of the native apoptosome. First, we have used a dominant negative inhibitor of the apoptosome complex, namely GST-

Lane 7 is the anti-caspase 9 antibody that was run as a control for XIAP immunoblotting, which was detected conventionally, and also with the triple sandwich (tertiary) detection method as described under "Experimental Procedures." A nonspecific immunoreactive band (*N.S.*) was detected in the caspase blots. *D*, in a parallel experiment the apoptosome complex was purified in the absence of Z-VAD.FMK and the caspase-activating activity of the immunoprecipitated apoptosome complex assessed by incubating with recombinant procaspase-3 (200 nM) for 1 h at 37 °C as described under "Experimental Procedures." The beads plus apoptosome complexes were then removed, and caspase-3 processing and DEVDase activity in the supernatant were analyzed by Western blotting and fluorimetry (*lanes 1–3*). Note that the proform of the recombinant caspase-3 (*lanes 2* and *3*) contain a C-terminal His_6 tag and is therefore slightly larger than the endogenous procaspase-3 (*lane 4*) detected in the control lysate.

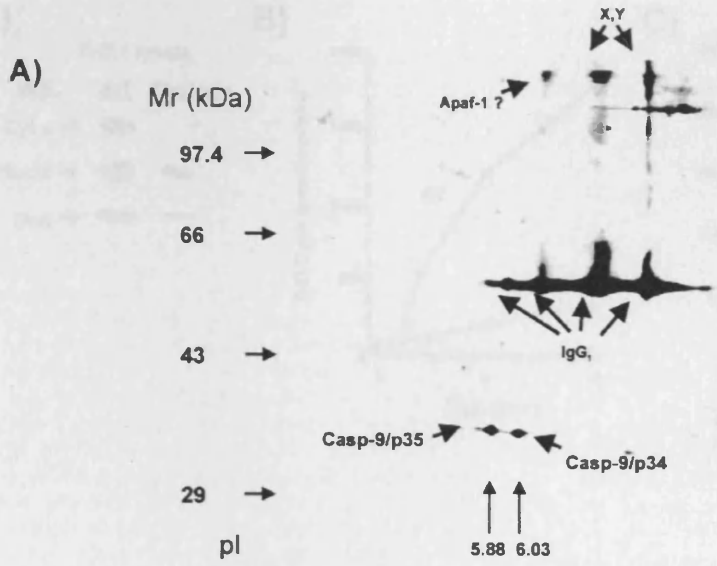

B) Casp-9/p35

```
1    MDEADRRLLR RCRLRLVEEL QVDQLWDALL SRELFRPHMI EDIQRAGSGS
51   RRDQARQLII DLETRGSQAL PLFISCLEDT GQDMLASFLR TNRQAGKLSK
101  PTLENLTPVV LRPEIRKPEV LRPETPRPVD IGSGGFGDVG ALESLRGNAD
151  LAYILSMEPC GHCLIINNVN FCRESGLRTR TGSNIDCEKL RRRFSSLHFM
201  VEVKGDLTAK KMVLALLELA RQDHGALDCC VVVILSHGCQ ASHLQFPGAV
251  YGTDGCPVSV EKIVNIFNGT SCPSLGGKPK LFFIQACGGE QKDHGFEVAS
301  TSPEDESPGS NPEPD
```

C) Casp-9/p34

```
1    MDEADRRLLR RCRLRLVEEL QVDQLWDVLL SRELFRPHMI EDIQRAGSGS
51   RRDQARQLII DLETRGSQAL PLFISCLEDT GQDMLASFLR TNRQAAKLSK
101  PTLENLTPVV LRPEIRKPEV LRPETPRPVD IGSGGFGDVG ALESLRGNAD
151  LAYILSMEPC GHCLIINNVN FCRESGLRTR TGSNIDCEKL RRRFSSLHFM
201  VEVKGDLTAK KMVLALLELA QQDHGALDCC VVVILSHGCQ ASHLQFPGAV
251  YGTDGCPVSV EKIVNIFNGT SCPSLGGKPK LFFIQACGGE QKDHGFEVAS
301  TSPEDE
```

FIG. 8. **Identification of the p35 and p34 forms of caspase-9 in the ~700-kDa apoptosome complex.** Apoptosome complexes captured on protein G Dyna beads (as described in the legend to Fig. 7) were eluted with IEF rehydration buffer and 50 μl applied to 17-cm IPG strips (pH 5–8) and isoelectrofocused as described under "Experimental Procedures." The strips were then run on 7.5% SDS-PAGE gels and stained with SYPRO Ruby. After imaging (*A*), the indicated spots were cut and analyzed by tryptic digestion and MALDI-TOF mass spectrometry. The p35 (*B*) and p34 (*C*) spots were identified by MALDI-TOF to be caspase-9. The migration in the SDS gel and the predicted pI values are compatible with them being the p35 and p34 subunits derived from cleavage of caspase-9 at Asp^{315} and Glu^{306} respectively. The two-dimensional gels after spot cutting were restained with a more sensitive silver-staining method, but no other additional proteins were detected (data not shown).

$casp9^{1-130}$, which only binds to Apaf-1 when it is oligomerized to the ~700- kDa and a ~1.4-MDa apoptosome complexes. This construct blocks caspase activation by binding to the exposed CARD domain of Apaf-1 when activated by dATP. We have prepared large quantities of the ~700-kDa apoptosome complex, using a sucrose density gradient, followed by affinity purification on GSH-Sepharose beads. The purified apoptosome complex was analyzed by SDS-PAGE/Western blotting and MALDI-TOF mass spectrometry and found to contain only Apaf-1 and the GST-$casp9^{1-130}$ proteins. We therefore conclude that the WD40 domains and other regions of the Apaf-1 apoptosome complex do not bind any other cytosolic proteins.

Second, we purified the ~700-kDa apoptosome complex with intact full-length caspase-9, using 75 mg of lysate and an initial sucrose density purification. The conditions we used in this experiment were designed to ensure maximum assembly of the complex and minimum degradation due to caspase-3 cleavage of Apaf-1. We therefore carried out a detailed time course of apoptosome assembly in F/T lysates and confirmed that oligomerization of Apaf-1 is a very rapid process being virtually complete within 5 min of initiating apoptosome assembly with

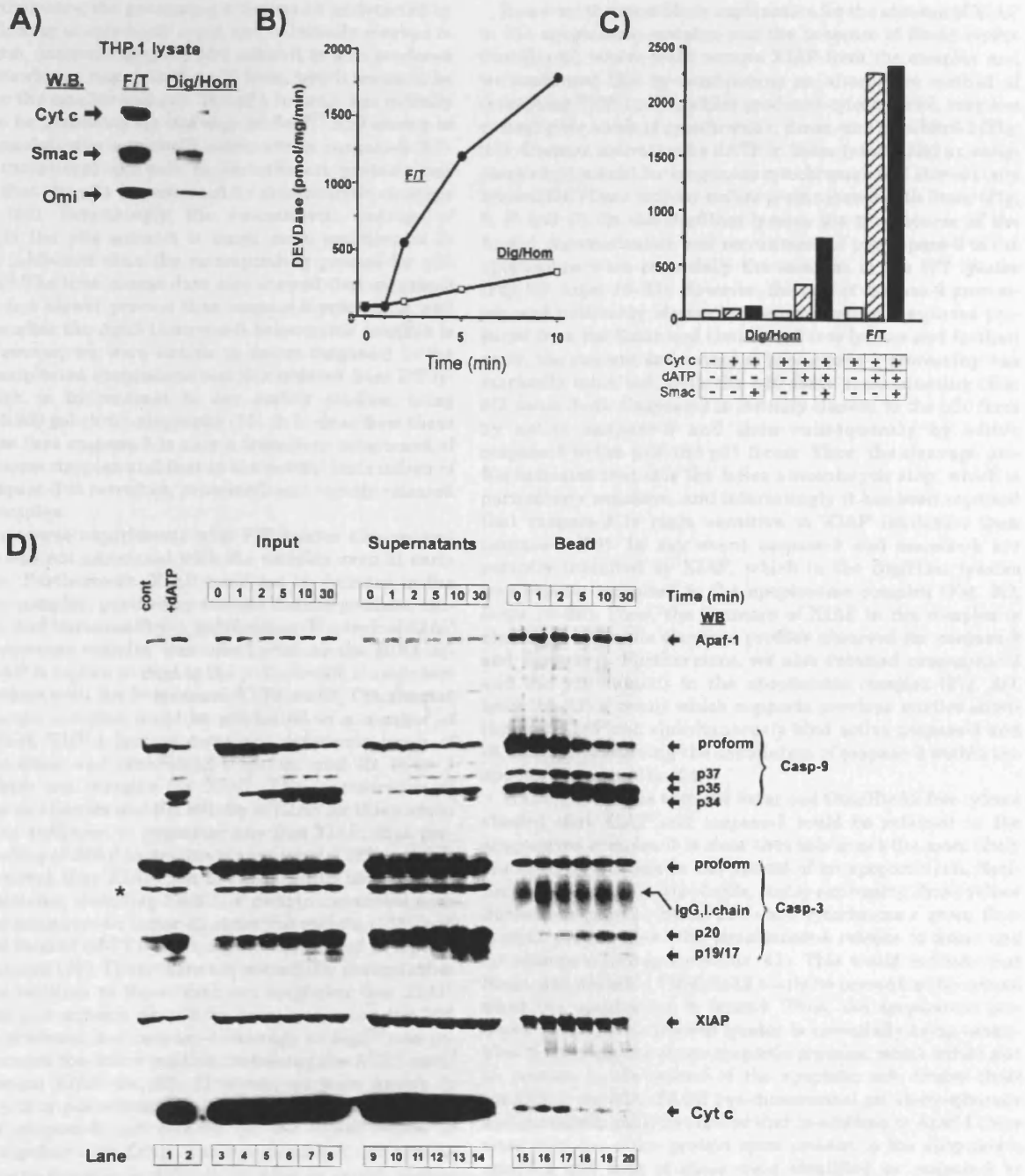

FIG. 9. **In THP.1 lysates with very low levels of Smac and Omi/HtrA2, the apoptosome rapidly recruits XIAP and caspase-3.** THP.1 lysates (Dig/Hom) were prepared in isotonic buffer using a combination of digitonin permeabilization and homogenization as detailed under "Experimental Procedures." Lysates were dATP activated as described in Fig. 6 and at the indicated times, aliquots of lysates were analyzed for DEVDase activity while the remaining sample was treated with Z-VAD.fmk (200 μM), and aliquots taken (*Input*) for SDS-PAGE/Western blotting. Apoptosome complexes were then isolated from the remaining lysate by incubating overnight at 4 °C with anti-caspase-9 antibody cross-linked to protein G Dyna Beads®. The beads were removed from the supernatants and washed before eluting with SDS-sample buffer (*bead*). The input, supernatants, and bead samples were separated by SDS-PAGE and immunoblotted for Apaf-1, caspase-9, caspase-3, XIAP, and cytochrome *c* as described under "Experimental Procedures." *A*, SDS-PAGE/Western blotting was used to compare the cytochrome *c*, Smac, and Omi/HtrA2 content of naïve Dig/Hom lysates with the normal lysate (F/T) as prepared by the freeze/thawing method. The time course of dATP activation of the DEVDase activity (before the addition of 200 μM Z-VAD.FMK) in the Dig/Hom lysate is shown in *B* and compared with an equivalent F/T lysate. *C*, Dig/Hom and F/T lysates were preincubated at 4 °C with 1 μM recombinant SmacΔ55 before measuring the DEVDase activity after dATP activation (15 min). Note that the DEVDase activity of the Dig/Hom lysate (in contrast to the F/T lysate) could not be activated by dATP without the addition of exogenous cytochrome *c* (7 μM). *D*, the apoptosome complexes isolated from the time course experiment with the Dig/Hom lysate were analyzed by SDS-PAGE/Western blotting. A control and dATP (30 min)-activated lysate were added as reference lanes (*1* and *2*) for the indicated proteins. With the anti-caspase-9 antibody covalently linked to the beads only the light chain of the IgG_1 is carried over into the SDS eluate. For Apaf-1 and caspase-9, 5% of the total inputs (*lanes 3–8*), supernatants (*lanes 9–14*), and bead samples (*lanes 15–20*) were loaded onto the gel. In the case of caspase-3, XIAP and cytochrome *c* to aid visualization, the total bead sample was increased to 20% of the input. The caspase-3 antibody also detects a nonspecific band at 25 kDa and is indicated (*).

dATP. Furthermore, the processing of caspase-9 as detected by Western blotting is extremely rapid and is initially cleaved to the p35 form. Interestingly, the p34 subunit is also produced but at a rate slower rate than the p35 form, which seems to be degraded to the smaller subunit. The p34 subunit was initially reported to be generated by cleavage at Ser^{307} and shown to require a catalytically competent active site in caspase-9 (37). However, mutational analysis in recombinant proteins has suggested that the p34 is generated by autocatalytic cleavage at Glu^{306} (28). Surprisingly, the autocatalytic cleavage of caspase-9 to the p34 subunit is much more sensitive to Z-VAD.FMK inhibition than the corresponding process for p35 generation.[3] The time course data also showed that caspase-3 processing is a slower process than caspase-9 processing, and only occurs after the Apaf-1/caspase-9 holoenzyme complex is formed. However, we were unable to detect caspase-3 in the immunoprecipitated apoptosome complex isolated from F/T lysates, which is in contrast to our earlier studies, using Sephacryl S300 gel chromatography (15). It is clear from these experiments that caspase-3 is only a transitory component of the apoptosome complex and that in the normal ionic milieu of the cell caspase-3 is recruited, processed, and rapidly released from the complex.

The time course experiments with F/T lysates also showed that XIAP was not associated with the complex even at early time points. Furthermore, XIAP could not be detected in the apoptosome complex, purified by sucrose density gradient centrifugation, and immunoaffinity purification. The lack of XIAP in the apoptosome complex was unexpected as the BIR3 domain of XIAP is known to bind to the p12 subunit of caspase-9 via interactions with the N-terminal ATPF motif. The absence of XIAP in the complex could be attributed to a number of reasons: First, THP.1 lysates contained detectable levels of endogenous Smac and Omi/HtrA2 (Figs. 6*C* and 9*D*, *lanes 1* and *2*), which can complex the XIAP. The concentration of Smac in the cell lysates and the affinity of XIAP for this protein are probably sufficient to sequester any free XIAP, thus preventing binding of XIAP to the newly generated ATPF motif. It should be noted that XIAP has been shown to bind several different proteins, including TAB 1, a protein associated with the transforming growth factor-β1 signaling pathway (38), and a processed form of GSPT1/eRF3, a protein involved in G_1 to S phase transition (39). Thus, there are potentially several other proteins in addition to Smac that can sequester free XIAP. Second, the p12 subunit should be generated when the p35 subunit is produced, but caspase-3 cleavage at Asp^{330} can potentially remove the linker peptide containing the ATPF motif and any bound XIAP (24, 27). However, we were unable to detect the p12 or p10 subunits so we cannot exclude the possibility that caspase-3 had cleaved off the linker region of caspase-9 together with XIAP. The significance of this process on apoptosome function is difficult to judge as recent studies with recombinant proteins have shown that the p10 subunit of caspase-9, which has an AISS motif can also bind XIAP, resulting in the inhibition of caspase-processing (40). Moreover, even at the very earliest time points we did not detect the p37 subunit of caspase-9, which is also generated by caspase-3 cleavage. Although, previous studies have indicated that XIAP is associated with oligomerized Apaf-1 and/or processed caspase-9 (27) it should be stressed that these experiments were done with apoptosome complexes isolated by Sephacryl S300 gel filtration using salt-free buffers. It may be that under these assay conditions it is possible to detect weak and transitory interactions between XIAP and caspase-9 in the apoptosome.

[3] K. Cain and C. Langlais, unpublished results.

However, the most likely explanation for the absence of XIAP in the apoptosome complex was the presence of Smac and/or Omi/HtrA2, which could remove XIAP from the complex and we confirmed this by establishing an alternative method of disrupting THP.1 cells, which produced cytosols with very low or negligible levels of cytochrome *c*, Smac, and Omi/HtrA2 (Fig. 9*A*). Caspase activation by dATP in these lysates had an obligatory requirement for exogenous cytochrome *c* and showed only limited DEVDase activity unless preincubated with Smac (Fig. 9, *B* and *C*). In the Dig/Hom lysates the time course of the Apaf-1 oligomerization and recruitment of procaspase-9 to the apoptosome were essentially the same as in the F/T lysates (Fig. 9*D*, *lanes 15–20*). However, the rate of caspase-9 processing was noticeably slower in the apoptosome complexes prepared from the Smac and Omi/HtrA2-free lysates and furthermore, the amount and extent of procaspase-3 processing was markedly inhibited, with the p20 form predominating (Fig. 9*D*, *lanes 3–8*). Caspase-3 is initially cleaved to the p20 form by active caspase-9 and then subsequently by active caspase-3 to the p19 and p17 forms. Thus, the cleavage profile indicates that it is the latter autocatalytic step, which is particularly sensitive, and interestingly it has been reported that caspase-3 is more sensitive to XIAP inhibition than caspase-9 (36). In any event caspase-3 and caspase-9 are potently inhibited by XIAP, which in the Dig/Hom lysates was rapidly recruited to the apoptosome complex (Fig. 9*D*, *lanes 15–20*). Thus, the presence of XIAP in the complex is consistent with the cleavage profiles observed for caspase-9 and caspase-3. Furthermore, we also detected procaspase-3 and the p20 subunit in the apoptosome complex (Fig. 9*D*, *lanes 15–20*) a result which supports previous studies showing that XIAP can simultaneously bind active caspase-3 and -9, thereby preserving the association of caspase-3 within the apoptosome complex (24).

While, the studies with the Smac and Omi/HtrA2 free cytosol showed that XIAP and caspase-3 could be retained in the apoptosome complex it is clear that this is not the most likely situation that occurs in the cytosol of an apoptotic cell. Real-time single cell analysis of cells, stably expressing Smac-yellow fluorescent protein (Smac-YFP) and cytochrome *c* green fluorescent protein show the simultaneous release of Smac and cytochrome *c* during apoptosis (41). This would indicate that Smac, and probably Omi/HtrA2 would be present in the cytosol when the apoptosome is formed. Thus, the apoptosome produced in the freeze/thawed lysates is essentially being assembled in the presence of pro-apoptotic proteins, which would also be present in the cytosol of the apoptotic cell. Under these conditions the SDS-PAGE two-dimensional gel electrophoresis and proteomic analysis showed that in addition to Apaf-1 there were only two other protein spots present in the apoptosome complex and both of these were identified as caspase-9 by MALDI-TOF. The molecular weight and pI positions of the proteins are consistent with these being the p35 and p34 large subunits of caspase-9. It was possible that that these two forms represent differentially phosphorylated forms of the same cleaved (p35) subunit, and a recent study has shown that caspase-9 processing is inhibited by phosphorylation of Thr^{125} by ERK MAPK (42). However, the two caspase-9 subunits were separated by ~1 kDa on both SDS and two-dimensional gels. This mass difference would require phosphorylation of most of the serines and threonines of the p35 subunit, which would result in a very large acidic shift in the pI value. This is clearly not the case and we conclude that during dATP activation of THP.1 lysates, caspase-9 is cleaved to give both the p35 and p34 subunits, which are tightly bound to the apoptosome.

The two-dimensional gel analysis of the F/T lysates did not identify significant amounts of any other proteins that co-purified with the apoptosome. However the apoptosome complex was clearly functional because it cleaved and activated recombinant caspase-3 (Fig. 7*D*). The lack of other proteins associated with the apoptosome complex was an unexpected finding, considering the size and possible structure of the apoptosome complex. Several studies have suggested that other proteins such as Aven, NAC, Hsp70, and Hsp-90 (43–47) are associated with the apoptosome, but we failed to detect any of these proteins in the immunoaffinity-purified apoptosome complex. Recent studies have also identified the tumor suppressor PHAP and the oncoprotein prothymosin α (ProT) as modulators of apoptosome formation and function (18). ProT apparently inhibits apoptosome formation and is antagonized by high levels of dATP whereas PHAP promotes apoptosome formation and caspase-9 activation. Interestingly, there is no evidence to suggest a direct association of ProT and PHAP with the apoptosome and significantly the effect of these proteins could not be demonstrated in reconstitution experiments with purified proteins, suggesting the involvement of additional as yet unknown or unidentified regulatory proteins. It is also possible that initial protein-protein interactions are important to trigger conformational changes leading to apoptosome formation, but are not required once Apaf-1 has unfolded and oligomerized. But once the complex is formed these interacting proteins may bind less tightly and be lost during purification. It is significant that cytochrome *c* which is essential for formation appears to be only associated with the complex for a brief period of time (Fig. 9*D*, *lanes 15–17*). We have also failed to identify cytochrome *c* in apoptosomes purified by Superose-6 gel filtration.[4] Interestingly, other studies have also reported that the apoptosome holoenzyme complex purified by sucrose density gradient purification does not contain cytochrome *c* (25). It is possible that cytochrome *c* induces conformational changes in Apaf-1, which then oligomerizes and in doing so destabilizes and weakens the Apaf-1-cytochrome *c* binding interactions. The task of identifying these transient interactions is extremely difficult and we have treated dATP-activated lysates with various cross-linking reagents[5] to try and trap other proteins in the apoptosome complex. However, these experiments produced a large array of cross-linked filamentous proteins and other large complexes, which proved impossible to analyze and separate.

While it is possible that various proteins are interacting transiently with the apoptosome complex it should be realized that *in vitro*, the formation of the ~700-kDa apoptosome complex is easily disrupted by the ionic strength of the incubating media (23). This effect can be overcome by increasing the cytochrome *c* concentration and appears to be due to disruption by K^+ of the strong electrostatic interactions between cytochrome *c* and Apaf-1 (49). The formation of the ~1.4-MDa complex is not affected by the ionic strength of the media. In this respect we have recently found that commercial preparations of purified Hsp70 will abrogate formation of the ~700-kDa apoptosome but not the ~1.4-MDa complex.[5] However, commercial preparations of Hsp70 and other heat shock proteins invariably contain 100–150 mM NaCl and under our assay conditions it is difficult to ascertain the precise contribution of the ionic environment to the observed inhibitory effects of Hsp 70 and other heat shock proteins. These considerations highlight that *in vitro* formation and protein-protein interactions of the ~700-kDa complex apoptosome are markedly affected by ionic strength and purported interactions between supraphysiological concentrations of proteins and the apoptosome complex may not necessarily occur *in vivo*.

So far no one has succeeded in producing crystals of the apoptosome and the only structural evidence available comes from a recent low resolution (27 Å) electron microscopy study using recombinant proteins (48). The apoptosome complex appears to be a wheel-like structure containing 7 Apaf-1 molecules arranged radially with the CARD and part of the CED-4 domains packing together to form a central hub. The WD40 domains appear in a Y-shaped configuration of two lobes of unequal size (7- and 6-bladed propellers), which may in the nonactivated monomeric Apaf-1 bind and occlude the hub domain. It is envisaged that cytochrome *c*, displaces the hub domain allowing binding and conformational changes, which allow oligomerization to form the apoptosome complex. Previous studies with recombinant Apaf-1 and caspase-9 had indicated a 1:1 stoichiometry (17) but in the electron microscopy (EM)-derived structures there does not seem to be enough room on the hub to accommodate 7 caspase-9 molecules. Furthermore when the apoptosome is formed in the presence of a non-cleavable mutant of caspase-9 it can apparently dimerize via the hub structures to form an even larger apoptosome structure composed of two wheels bound though their respective hubs (48). The EM structural model of the recombinant apoptosome offers intriguing insights into its formation and function, but there is as yet no evidence as to the actual structure of the native apoptosome when it is assembled in cell lysates or cells undergoing apoptotic cell death. In this respect, our data clearly show that in cell lysates in the presence of Smac and Omi/HtrA2, apoptosome assembly only involves Apaf-1 and caspase-9, which constitute the core components of the apoptosome. However, the possibility remains that in the intact cell, other proteins released from cellular organelles such as the mitochondrion could transiently bind to the apoptosome and modulate its function.

Acknowledgments—We thank Dr. Michelle Hughes and Dr. Mike Butterworth for technical advice on preparation of recombinant proteins and constructs. Thanks are also due to Dr. Shawn Bratton for helpful discussions on the article.

REFERENCES

1. Cohen, G. M. (1997) *Biochem. J.* **326,** 1–16
2. Hengartner, M. (1998) *Science* **281,** 1298–1299
3. Earnshaw, W. C., Martins, L. M., and Kaufmann, S. H. (1999) *Annu. Rev. Biochem.* **68,** 383–424
4. Conradt, B., and Horvitz, H. R. (1998) *Cell* **93,** 519–529
5. Chen, F. L., Hersh, B. M., Conradt, B., Zhou, Z., Riemer, D., Gruenbaum, Y., and Horvitz, H. R. (2000) *Science* **287,** 1485–1489
6. Bratton, S. B., MacFarlane, M., Cain, K., and Cohen, G. M. (2000) *Exp. Cell Res.* **256,** 27–33
7. Adrain, C., and Martin, S. J. (2001) *Trends Biochem. Sci.* **26,** 390–397
8. Cain, K., Bratton, S. B., and Cohen, G. M. (2002) *Biochimie (Paris)* **84,** 203–214
9. Liu, X., Kim, C. N., Yang, J., Jemmerson, R., and Wang, X. (1996) *Cell* **86,** 147–157
10. Zou, H., Henzel, W. J., Liu, X. S., Lutschg, A., and Wang, X. D. (1997) *Cell* **90,** 405–413
11. Li, P., Nijhawan, D., Budihardjo, I., Srinivasula, S. M., Ahmad, M., Alnemri, E. S., and Wang, X. (1997) *Cell* **91,** 479–489
12. Walker, J. E., Saraste, M., Runswick, M. J., and Gay, N. J. (1982) *EMBO J.* **1,** 945–951
13. Benedict, M. A., Hu, Y., Inohara, N., and Nunez, G. (2000) *J. Biol. Chem.* **275,** 8461–8468
14. Cain, K., Brown, D. G., Langlais, C., and Cohen, G. M. (1999) *J. Biol. Chem.* **274,** 22686–22692
15. Cain, K., Bratton, S. B., Langlais, C., Walker, G., Brown, D. G., Sun, X. M., and Cohen, G. M. (2000) *J. Biol. Chem.* **275,** 6067–6070
16. Saleh, A., Srinivasula, S. M., Acharya, S., Fishel, R., and Alnemri, E. S. (1999) *J. Biol. Chem.* **274,** 17941–17945
17. Zou, H., Li, Y., Liu, X., and Wang, X. (1999) *J. Biol. Chem.* **274,** 11549–11556
18. Jiang, X., Kim, H. E., Shu, H., Zhao, Y., Zhang, H., Kofron, J., Donnelly, J., Burns, D., Ng, S. c., Rosenberg, S., and Wang, X. (2003) *Science* **299,** 223–226
19. Almond, J., Snowden, R. T., Dinsdale, D., Hunter, A., Cain, K., and Cohen, G. M. (2001) *Leukemia* **15,** 1388–1397
20. Rothwarf, D. M., Zandi, E., Natoli, G., and Karin, M. (1998) *Nature* **395,** 297–300

[4] K. Cain, D. Brown, and C. Langlais, unpublished data.
[5] K. Cain and D. Brown, unpublished data.

21. Horiuchi, H., Lippe, R., McBride, H. M., Rubino, M., Woodman, P., Stenmark, H., Rybin, V., Wilm, M., Ashman, K., Mann, M., and Zerial, M. (1997) *Cell* **90,** 1149–1159
22. MacFarlane, M., Merrison, W., Bratton, S. B., and Cohen, G. M. (2002) *J. Biol. Chem.* **277,** 36611–36616
23. Cain, K., Langlais, C., Sun, X. M., Brown, D. G., and Cohen, G. M. (2001) *J. Biol. Chem.* **276,** 41985–41990
24. Bratton, S. B., Lewis, J., Butterworth, M., Duckett, C., and Cohen, G. M. (2002) *Cell Death Differ.* **9,** 881–892
25. Rodriguez, J., and Lazebnik, Y. (1999) *Genes Dev.* **13,** 3179–3184
26. Qin, H. X., Srinivasula, S. M., Wu, G., Fernandes-Alnemri, T., Alnemri, E. S., and Shi, Y. G. (1999) *Nature* **399,** 549–557
27. Bratton, S. B., Walker, G., Srinivasula, S. M., Sun, X. M., Butterworth, M., Alnemri, E. S., and Cohen, G. M. (2001) *EMBO J.* **20,** 998–1009
28. Srinivasula, S. M., Hegde, R., Saleh, A., Datta, P., Shiozaki, E., Chai, J., Lee, R. A., Robbins, P. D., Fernandes-Alnemri, T., Shi, Y., and Alnemri, E. S. (2001) *Nature* **410,** 112–116
29. Shiozaki, E. N., Chai, J., Rigotti, D. J., Riedl, S. J., Li, P., Srinivasula, S. M., Alnemri, E. S., Fairman, R., and Shi, Y. (2003) *Mol. Cell* **11,** 519–527
30. Riedl, S. J., Renatus, M., Schwarzenbacher, R., Zhou, Q., Sun, C. H., Fesik, S. W., Liddington, R. C., and Salvesen, G. S. (2001) *Cell* **104,** 791–800
31. Chai, J. J., Shiozaki, E., Srinivasula, S. M., Wu, Q., Dataa, P., Alnemri, E. S., and Shi, Y. G. (2001) *Cell* **104,** 769–780
32. Bratton, S. B., Walker, G., Roberts, D. L., Cain, K., and Cohen, G. M. (2001) *Cell Death. Differ.* **8,** 425–433
33. Deveraux, Q. L., Leo, E., Stennicke, H. R., Welsh, K., Salvesen, G. S., and Reed, J. C. (1999) *EMBO J.* **18,** 5242–5251
34. Du, C., Fang, M., Li, Y., Li, L., and Wang, X. (2000) *Cell* **102,** 33–42
35. Roberts, D. L., Merrison, W., MacFarlane, M., and Cohen, G. M. (2001) *J. Cell Biol.* **153,** 221–227
36. Salvesen, G. S., and Duckett, C. S. (2002) *Nat. Rev. Mol. Cell Biol.* **3,** 401–410
37. Stennicke, H. R., Deveraux, Q. L., Humke, E. W., Reed, J. C., Dixit, V. M., and Salvesen, G. S. (1999) *J. Biol. Chem.* **274,** 8359–8362
38. Yamaguchi, K., Nagai, S., Ninomiya-Tsuji, J., Nishita, M., Tamai, K., Irie, K., Ueno, N., Nishida, E., Shibuya, H., and Matsumoto, K. (1999) *EMBO J.* **18,** 179–187
39. Hegde, R., Srinivasula, S. M., Datta, P., Madesh, M., Wassell, R., Zhang, Z., Cheong, N., Nejmeh, J., Fernandes-Alnemri, T., Hoshino, S., and Alnemri, E. S. (2003) *J. Biol. Chem.* **278,** 38699–38706
40. Zou, H., Yang, R., Hao, J., Wang, J., Sun, C., Fesik, S. W., Wu, J. C., Tomaselli, K. J., and Armstrong, R. C. (2003) *J. Biol. Chem.* **278,** 8091–8098
41. Rehm, M., Dussmann, H., and Prehn, J. H. (2003) *J. Cell Biol.* **162,** 1031–1043
42. Allan, L. A., Morrice, N., Brady, S., Magee, G., Pathak, S., and Clarke, P. R. (2003) *Nat. Cell Biol.* **5,** 647–654
43. Chau, B. N., Cheng, E. H., Kerr, D. A., and Hardwick, J. M. (2000) *Mol. Cell* **6,** 31–40
44. Chu, Z. L., Pio, F., Xie, Z., Welsh, K., Krajewska, M., Krajewski, S., Godzik, A., and Reed, J. C. (2001) *J. Biol. Chem.* **276,** 9239–9245
45. Beere, H. M., Wolf, B. B., Cain, K., Mosser, D. D., Mahboubi, A., Kuwana, T., Tailor, P., Morimoto, R. I., Cohen, G. M., and Green, D. R. (2000) *Nat. Cell Biol.* **2,** 469–475
46. Saleh, A., Srinivasula, S. M., Balkir, L., Robbins, P. D., and Alnemri, E. S. (2000) *Nat. Cell Biol.* **2,** 476–483
47. Pandey, P., Saleh, A., Nakazawa, A., Kumar, S., Srinivasula, S. M., Kumar, V., Weichselbaum, R., Nalin, C., Alnemri, E. S., Kufe, D., and Kharbanda, S. (2000) *EMBO J.* **19,** 4310–4322
48. Acehan, D., Jiang, X., Morgan, D. G., Heuser, J. E., Wang, X., and Akey, C. W. (2002) *Mol. Cell* **9,** 423–432
49. Purring-Koch, C., and McLendon, G. (2000) *Proc. Natl. Acad. Sci. U. S. A.* **97,** 11928–11931

THE JOURNAL OF BIOLOGICAL CHEMISTRY VOL. 281, NO. ??, pp. 1–xxx, ???? ??, 2006

Caspase-7 Is Directly Activated by the ~700-kDa Apoptosome Complex and Is Released as a Stable XIAP-Caspase-7 ~200-kDa Complex*[S]

Received for publication, July 8, 2005, and in revised form, November 17, 2005 Published, JBC Papers in Press, December 13, 2005, DOI 10.1074/jbc.M507393200

Davina Twiddy, Gerald M. Cohen, Marion MacFarlane, and Kelvin Cain[1]

From the Medical Research Council Toxicology Unit, Hodgkin Building, Lancaster Rd., University of Leicester, Leicester, LE1 9HN, United Kingdom

MCF-7 cells lack caspase-3 but undergo mitochondrial-dependent apoptosis via caspase-7 activation. It is assumed that the Apaf-1-caspase-9 apoptosome processes caspase-7 in an analogous manner to that described for caspase-3. However, this has not been validated experimentally, and we have now characterized the caspase-7 activating apoptosome complex in MCF-7 cell lysates activated with dATP/cytochrome *c*. Apaf-1 oligomerizes to produce ~1.4-MDa and ~700-kDa apoptosome complexes, and the latter complex directly cleaves/activates procaspase-7. This ~700-kDa apoptosome complex, which is also formed in apoptotic MCF-7 cells, is assembled by rapid oligomerization of Apaf-1 and followed by a slower process of procaspase-9 recruitment and cleavage to form the p35/34 forms. However, procaspase-9 recruitment and processing are accelerated in lysates supplemented with caspase-3. In lysates containing very low levels of Smac and Omi/HtrA2, XIAP binds tightly to caspase-9 in the apoptosome complex, and as a result caspase-7 processing is abrogated. In contrast, in MCF-7 lysates containing Smac and Omi/HtrA2, active caspase-7 is released from the apoptosome and forms a stable ~200-kDa XIAP-caspase-7 complex, which apparently does not contain cIAP1 or cIAP2. Thus, in comparison to caspase-3-containing cells, XIAP appears to have a more significant anti-apoptotic role in MCF-7 cells because it directly inhibits caspase-7 activation by the apoptosome and also forms a stable ~200-kDa complex with active caspase-7.

The MCF-7 cell line was derived from a patient with metastatic breast cancer and is an often-used model system for studying estrogen receptor-positive breast cancer (for review, see Ref. 1). Because many of the problems associated with breast cancer treatment involve the development of chemo-resistance to apoptosis-inducing anti-cancer agents, there is extensive interest in using MCF-7 cells as a model for investigating the mechanisms of apoptosis in breast epithelial cells. Caspase activation is a key event in triggering the morphological and biochemical changes associated with cell death (2–4). There are two primary caspase activation pathways involving either stimulation of cell surface death receptors (the extrinsic pathway) or perturbation of mitochondria (the intrinsic pathway) (5). Many anti-cancer drugs induce apoptosis by activating the intrinsic cell death pathway, which involves the release of cytochrome *c* and the activation of the apoptosome-catalyzed caspase cascade (6–8). In apoptotic cells inactive procaspases are activated via this cascade mechanism in which an initiator caspase is activated and subsequently cleaves/activates an effector caspase, which then cleaves and activates the next caspase and so on.

Caspase-3 is the most active effector caspase in both the intrinsic and extrinsic pathways, where it is processed and activated by caspase-9 and caspase-8, respectively. However, MCF-7 cells do not possess caspase-3 due to a 47-base pair deletion in the caspase-3 gene (9, 10). Consequently, apoptotic cell death in MCF-7 cells must be independent of caspase-3 activation, although several studies have shown that apoptotic cell death in MCF-7 cells is accompanied by caspase activation. For example, in staurosporine-treated MCF-7 cells, recognized caspase death substrates including poly(ADP-ribose) polymerase, Rb, PAK2, DNA-PKcs, gelsolin and DFF-45 are cleaved (11). In TRAIL (tumor necrosis factor-related apoptosis-inducing ligand)-induced apoptosis, caspase-8 is activated, which cleaves Bid to release tBid, which in turn induces cytochrome *c* release and caspase-9 and caspase-7 processing (12). Other studies have also shown that caspases 9, 6, 2, and 7 are cleaved/processed to their active forms (13). Thus, in the absence of caspase-3, MCF-7 cells can still activate a caspase cascade irrespective of whether the apoptosis is initiated via the intrinsic or extrinsic pathway. The intrinsic pathway, which is activated by many chemicals, including anti-cancer drugs, involves formation of the Apaf-1 apoptosome, a large caspase-processing complex (for review, see Refs. 6 and 7) that typically activates caspase-3. Apoptosome formation can be modeled *in vitro* in cell-free lysates by the addition of dATP or ATP and requires at least three apoptotic protease-activating factors (Apaf-1–3) (14–16). The CARD (caspase recruitment) domain of Apaf-1 binds to a similar domain on procaspase-9, whereas the central CED-4 domain (98–412) is involved in Apaf-1 oligomerization. In the presence of cytochrome *c* and dATP, Apaf-1 undergoes conformational changes, allowing it to oligomerize to form a very large apoptosome complex. Using gel filtration chromatography, we have isolated from both dATP-activated THP.1 and B chronic lymphocytic leukemia cell lysates two apoptosome complexes with apparent molecular masses of ~700 kDa and ~1.4 MDa (17–19). Furthermore, we have shown in apoptotic cells that the ~700-kDa complex predominates and is the most active complex in processing exogenous procaspase-3 (18, 19). More recently, we have used a proteomic approach to characterize the composition of this ~700-kDa apoptosome complex and have shown that it contains solely Apaf-1 and caspase-9 as its core functional proteins (20).

Several studies have reported that caspase-7 is cleaved and activated in dATP stimulated lysates (17, 21, 22), and immuno-depletion studies indicate that caspase-9 is required for the processing of both caspase-3 and -7 (21). By implication, it has been assumed that the Apaf-1-caspase-9 apoptosome complex directly processes procaspase-7 in an analogous manner to that described for procaspase-3. However, there is

* The costs of publication of this article were defrayed in part by the payment of page charges. This article must therefore be hereby marked "*advertisement*" in accordance with 18 U.S.C. Section 1734 solely to indicate this fact.

[S] The on-line version of this article (available at http://www.jbc.org) contains supplemental Fig. 1.

[1] To whom correspondence should be addressed. Tel.: 44-116-252-5547; Fax; 44-116-252-5616; E-mail: kc5@le.ac.uk.

no direct evidence for this, and to address this, we have characterized the role of the apoptosome in caspase-7 activation in MCF-7 cells. Our studies show that the ~700-kDa apoptosome complex is also formed in dATP-activated MCF-7 cell lysates and apoptotic MCF-7 cells and directly cleaves and activates procaspase-7. However, although the kinetics of Apaf-1 oligomerization is normal, the recruitment and processing of caspase-9 in the holoenzyme complex is much slower than in caspase-3-containing cell lysates. We also show that caspase-7, after activation by the apoptosome complex, forms a XIAP-caspase-7 complex that is not disrupted even in the presence of Smac and Omi/HtrA2. These data suggest that the absence of caspase-3 enables XIAP to have an enhanced inhibitory effect on effector caspase activation and activity and, hence, a more significant anti-apoptotic role in MCF-7 cells.

EXPERIMENTAL PROCEDURES

Cell Culture, Apoptosis Assays, and Preparation of Control and Caspase-activated Cell Lysates—MCF-7- and MCF-7-transfected cells were cultured in RPMI 1640 supplemented with 10% fetal bovine serum and 2 mM Glutamax™ as described previously (12). For apoptosis assays, cells were harvested by mild tryptic digestion, and the percentage of apoptotic cells with exposed phosphatidylserine was determined by annexin V-fluorescein isothiocyanate binding (Bender Medsystems, Vienna, Austria) and fluorescence-activated cell sorter essentially as previously described (12). Loss of mitochondrial membrane potential ($\Delta\Psi$m) was measured with the lipophilic cationic fluorescent probe tetramethylrhodamine ethyl ester and fluorescence-activated cell sorter scan analysis (23). For assaying cytochrome *c* release, cells were resuspended in cold phosphate-buffered saline and permeabilized with 0.025% digitonin, the cell cytosol and membrane fractions were prepared by centrifugation, and the cytochrome *c* content of the various fractions was then determined by SDS-PAGE and Western blotting (24). Cell lysates (100,000 × *g* supernatants) from cells were prepared by freeze/thawing (F/T)[2] (7, 18). In some experiments, to minimize mitochondrial breakage and release of pro-apoptotic proteins, MCF-7 cell lysates (digitonin and homogenization (Dig/Hom)) were prepared in an isotonic buffer (MSH), containing 210 mM mannitol, 70 mM sucrose, 5 mM Hepes, 1 mM EGTA, 1 mg/ml Pefabloc SCD, 1 tablet/10 ml protease inhibitor mixture (Roche Diagnostics), pH 7.4, using a modified digitonin/homogenization technique (20). Caspase activation in lysates (10–15 mg/ml) was induced by incubation at 37 °C for various times with 2 mM dATP/$MgCl_2$ plus or minus 2.0 μM cytochrome *c*.

Preparation of Recombinant Procapases 3 and 7—BL21 (DE3) cells were transformed with a pET-21b (Novagen) plasmid expression vector containing procaspase-3 or -7 cDNA with a C-terminal His_6 purification tag and grown at 37 °C in terrific broth, 1% glucose, and ampicillin (100 μg/ml) essentially as described previously (20).

Fluorimetric Assays of Caspase and Caspase-activating Activity—DEVDase activity (*i.e.* primarily caspase-3 and -7) of lysates or column fractions was measured fluorimetrically with 200 μl of assay buffer (20 μM Ac-DEVD.AFC, 0.1% CHAPS, 10 mM dithiothreitol, 100 mM HEPES, and 10% sucrose, pH 7.0) using a Wallac Victor[2] 1420 Multilabel counter (18). In some experiments the Ac-DEVD.AFC substrate concentration was increased to 100 μM. The caspase processing/activating activity of soluble apoptosome complexes was assayed using purified recombinant procaspase-3 or procaspase-7 (20). Briefly, the method assays the DEVDase activity of the sample, which is a direct measure of how much procaspase-3/-7 has been processed and activated by the apoptosome. In addition, aliquots of the DEVD assay mixtures were diluted 1:1 with 2× SDS loading buffer and analyzed for caspase-3/-7 processing by SDS-PAGE and Western blotting.

Fractionation of Cell Lysates by Gel Filtration—Lysates were fractionated by size-exclusion chromatography on either Superose-6 or Sephacryl S300 columns using an fast protein liquid chromatography (HR 10/30 column) protein purification system (Amersham Biosciences). Columns were eluted at 4 °C with 5% (w/v) sucrose, 0.1% (w/v) CHAPS, 20 mM HEPES/NaOH, 5 mM dithiothreitol, and 50 mM NaCl, pH 7.0, calibrated with protein standards as previously described (18). Column fractions (0.5–2 ml) were analyzed for DEVDase activity and caspase-3 or -7 processing activity as described above. Aliquots of the column fractions were also analyzed by SDS-PAGE and Western blotting for Apaf-1, caspases 9, 7, and 3 and XIAP. For the Western blot analysis, column fractions 5–17 and 18–30 were run on separate gels, and immunoblotting procedures were carried out in parallel. To ensure uniformity in signal response, the two blots from each column run were exposed simultaneously to Kodak X-Omar film. Appropriate fractions were pooled and concentrated with Vivaspin concentrators (Vivascience AG, Hannover, Germany) before immunoprecipitation experiments with the indicated antibodies.

Affinity Purification of Caspase-7 Complexes—Immunopurification of caspase-7 complexes was carried out using either an anti-active caspase-7 (Cell Signaling, NEB UK Ltd., Herts, UK) or anti-XIAP (clone 48, BD Biosciences Pharmingen) antibody covalently bound, respectively, to protein A and G Dyna Beads® (20). Immunopurification of caspase complexes was carried out from MCF-7 cell lysates (~30 mg/ml) that had first been precleared by incubating (1 h at 4 °C) with 400 μl of Sepharose protein A-coated beads/ml of lysate. The precleared lysates were then diluted to 15 mg/ml with assay buffer and dATP-activated for 2 h at 37 °C before fractionation by gel filtration. Appropriate fractions containing active caspase-7 complexes were pooled and concentrated before adding antibody-tagged beads and roller mixing at 4 °C for 4 h. Affinity purified proteins were eluted from the beads with SDS-PAGE sample loading buffer and separated by one-dimensional SDS-PAGE. In some experiments apoptosome complexes were affinity-purified using an anti-caspase-9 antibody covalently attached to protein G Dyna Beads® (20). Apoptosome complexes were captured by adding 20 μl of cross-linked beads to 90–100 μl of dATP-activated MCF-7 cell lysate and roller mixing overnight at 4 °C. Proteins were eluted from the beads as described above.

Reagents and Western Blot Analysis—Cell culture media and materials were as previously described (12, 25). Most other reagents and cells, unless indicated otherwise, were obtained from published sources (20). MCF-7 cells stably transfected with caspase-3 (MCF-7/casp-3) or pcDNA3 vector only (MCF-7/vector) cells were a gift from Dr. Alan Porter, (National University of Singapore) and originally characterized elsewhere (9). Column, cell lysates, and immunopurified samples were analyzed for various proteins by SDS-PAGE and Western blotting as previously described (20). An antibody to procaspase-7 was obtained from BD Biosciences Pharmingen. Antibodies to active caspase-3 and -7 were sourced from Cell Signaling.

RESULTS

Caspase Activation in dATP/Cytochrome c-treated MCF-7 Cell-free Lysates Does Not Require Caspase-3—In this study we wished to investigate apoptosome formation and function in MCF-7 cells. It was, therefore, important to characterize cytochrome c and dATP-dependent caspase activation in the cell lysates. This *in vitro* model has been used

[2] The abbreviations used are: F/T, freeze/thawing; AFC, 7-amino-4-trifluoromethylcoumarin; CHAPS, 3-([3-cholamidoopropyl]-dimethylammonio)-1-propanesulfonate); IAP, inhibitor of apoptosis; IBM, IAP binding motif; Dig/Hom, digitonin and homogenization; casp, caspase; WT, wild type; fmk, fluoromethyl ketone.

balt3/zbc-bc/zbc-bc/zbc00906/zbc3971-06a saylora S=6 4/1/06 11:12 Comments: ARTNO: M507393200

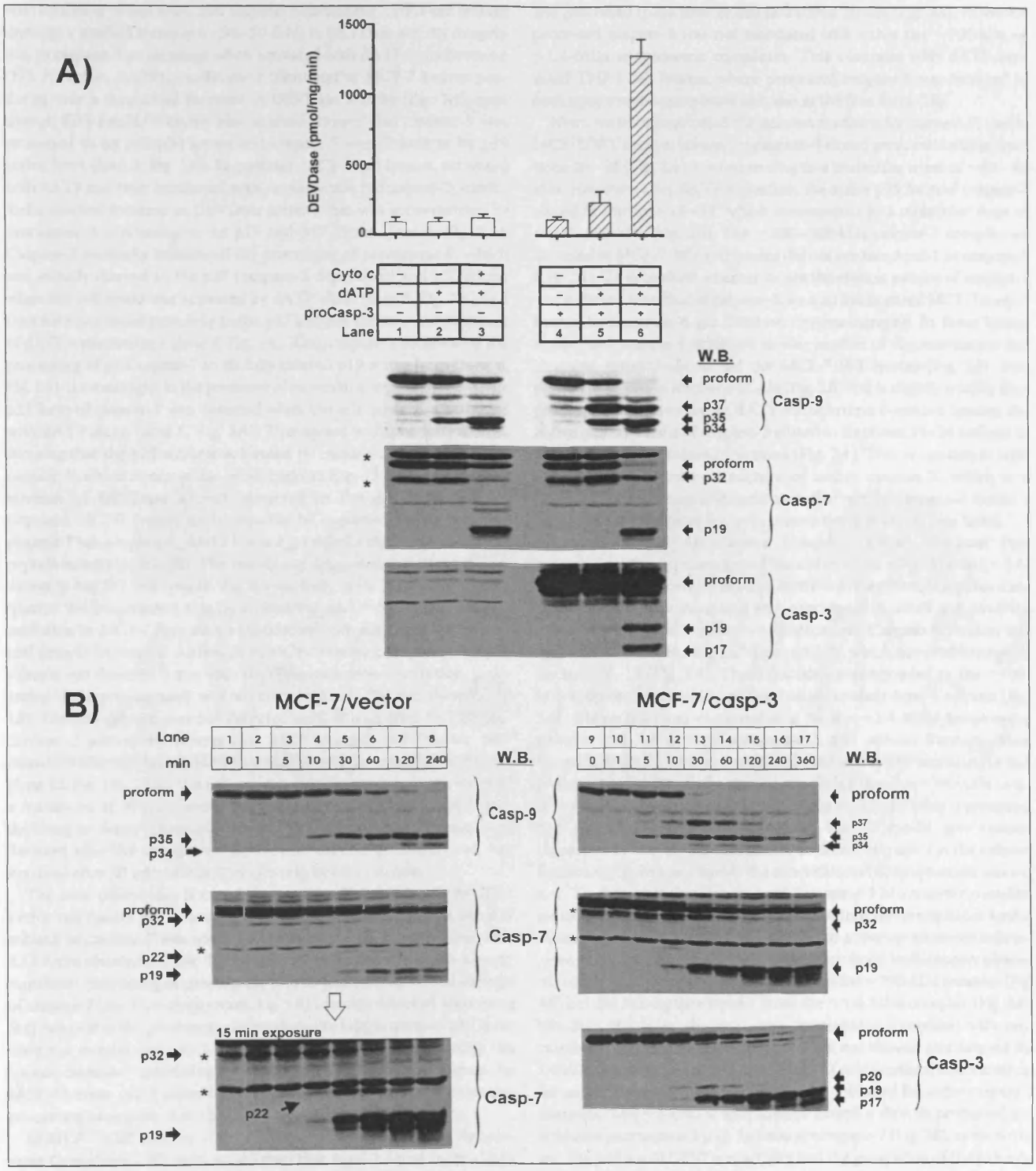

FIGURE 1. **dATP and cytochrome *c*-dependent caspase activation in MCF-7 cell lysates.** In *A*, MCF-7 cell lysates (10 mg/ml) were activated with 2 mM dATP/$MgCl_2$ with or without cytochrome *c* (*cyto c*; 2 μM) and incubated at 37 °C for 30 min. The DEVDase activity of cell lysate aliquots (100 μg) was then assayed with Ac.DEVD.AFC as described under "Experimental Procedures" (*open bars*). The caspase cleaving activity of the lysates was assayed by incubating activated cell lysates with recombinant procaspase-3 (200 nM) for 1 h and followed by assaying for caspase-3 (DEVDase) activity (*hatched bars*). Data are shown as the mean plus S.E. (n = 3). Aliquots were also taken at the end of the incubations, diluted with 2× SDS-PAGE loading buffer, and analyzed by SDS-PAGE/Western blotting (*W.B.*) for caspase-9 and -7 (20 μg/lane) and caspase-3 (7.5 μg/lane). In *B*, the time course of caspase-9, -3, and -7 processing was studied in cell lysates (10 mg/ml) prepared from MCF7/pcDNA3 vector and MCF7/casp-3-transfected cells. The cell lysates were incubated with dATP/$MgCl_2$ and cytochrome *c* as described above, and at the indicated times, 10-μl aliquots were removed, mixed with 90 μl of SDS-PAGE loading buffer, and analyzed by SDS-PAGE/Western blotting. Note in *panel B* that a longer exposure (15 min) was used to highlight the appearance of the p22 subunit of caspase-7. **, *, and † indicate protein bands non-specifically reacting with the antibody.

with a number of cell lines, and caspase-3-containing THP.1 cell lysates undergo a marked increase (~30–50-fold) in DEVDase activity (largely due to caspase-3 processing) when activated with dATP/cytochrome *c* (17). However, dATP/cytochrome *c* treatment of MCF-7 lysates produced only a very small increase in DEVDase activity (Fig. 1*A*) even though SDS-PAGE/Western blot analysis showed that caspase-9 was processed to its p35/p34 forms and caspase-7 was cleaved to its p19 active form (*lane 3*, Fig. 1*A*). In contrast, MCF-7 cell lysates, activated with dATP and then incubated with recombinant procaspase-3, exhibited a marked increase in DEVDase activity that was accompanied by procaspase-3 processing to its p19 and p17 forms (*lane 6*, Fig. 1*A*). Caspase-3 markedly influenced the processing of procaspase-9, which was initially cleaved to the p37 (caspase-3 dependent) and p35 forms when the cell lysate was activated by dATP alone (*lane 5*, Fig. 1*A*) and then fully processed primarily to the p37 and p35 forms in the presence of dATP/cytochrome *c* (*lane 6*, Fig. 1*A*). Also, caspase-3 accelerated the processing of procaspase-7 to its fully cleaved p19 active form (*lane 6*, Fig. 1*A*). Interestingly, in the presence of recombinant procaspase-3, the p32 form of caspase-7 was detected when the cell lysate was activated with dATP alone (*lane 5*, Fig. 1*A*). This agrees with previous studies showing that the p32 subunit is formed by caspase-3 cleavage of procaspase-7, which removes the prodomain at Asp-23 (26). The modest increase in DEVDase activity observed in the dATP/cytochrome *c*-treated MCF-7 lysates could possibly be explained by the fact that caspase-7 has a higher K_m and a lower k_{cat} value for the DEVD synthetic peptide substrate (26–28). The results also suggested that caspase activation in MCF-7 cell lysates was slower than in caspase-3-containing lysates. We investigated this by comparing dATP-dependent caspase activation in MCF-7 cells stably transfected with either pcDNA3 (vector) or pcDNA-casp-3. Although in MCF-7/vector cell lysates the p35 subunit was detected 5 min after dATP/cytochrome *c* activation, processing of the procaspase-9 was not complete until 120 min (*lane 7*, Fig. 1*B*). The p34 subunit was not detected until 60 min after dATP/cytochrome *c* activation, whereas in MCF-7/casp-3 cell lysates, procaspase-9 cleavage was accelerated and almost complete after 10 min (*lane 12*, Fig. 1*B*). Thus, the p35 subunit was detected at 5 min, reached a maximum at 30 min, and remained constant until 120 min before declining to barely detectable levels by 360 min. The p37 subunit was detected after the appearance of the p35 subunit at 10 min and was maximal after 30 min before disappearing by 60–120 min.

The time course also showed that caspase-7 activation in MCF-7/vector cell lysates was subsequent to caspase-9 processing, as the p19 subunit of caspase-7 was not detected until 30 min after treating with dATP/cytochrome *c* (*lane 5*, Fig. 1*B*). By this time there was already significant processing of procaspase-9 to its p35 form. The p22 subunit of caspase-7 (see *15-min exposure*, Fig. 1*B*) was also detected, indicating that removal of the prodomain to produce the fully processed p19 form does not require caspase-3. In contrast, in caspase-3-containing cell lysates, caspase-7 processing was faster and more extensive than in the MCF-7/vector cell lysates and was paralleled by rapid and extensive processing of caspase-3 to the p20, p19, and p17 forms.

In MCF-7 Cell Lysates, Apaf-1 Oligomerizes to Form Two Apoptosome Complexes—We next established that Apaf-1 could form a fully functional apoptosome complex in MCF-7 cell lysates. Gel-filtration chromatography of control lysates showed that Apaf-1 eluted as an ~130-kDa monomer (fraction 18–21, Fig. 2*A*). After dATP/cytochrome *c* activation, most of the Apaf-1 eluted either as ~700-kDa (fraction 9–14, Fig. 2*A*) or ~1.4-MDa (fraction 5–8, Fig. 2*A*) apoptosome complexes. In control cell lysates procaspase-9 (~46-kDa) eluted in fraction 20–24 (Fig. 2*A*). After dATP activation, both the proform and processed (p35) form eluted in fraction 20–24 (Fig. 2*A*). However, processed caspase-9 was not associated with either the ~700-kDa or ~1.4-MDa apoptosome complexes. This contrasts with dATP-activated THP.1 cell lysates, where processed caspase-9 was detected in both apoptosome complexes and also as the free form (18).

Next, we immunoblotted the column fractions for caspase-7, and in MCF-7/WT control lysates procaspase-7 eluted predominantly in fractions 20–24 (Fig. 2*A*), corresponding to a molecular mass of ~60–80 kDa. However, after dATP activation, the active p19 form of caspase-7 eluted in fractions 18–21, which corresponds to a molecular mass of ~200–300 kDa (Fig. 2*A*). The ~200–300-kDa caspase-7 complex we detected in MCF-7/WT cell lysates did not contain Apaf-1 or caspase-9 (Fig. 2*A*). To determine whether or not the elution pattern of caspase-7 was different from that of caspase-3, we also fractionated MCF-7/casp-3 lysates by Superose-6 gel filtration chromatography. In these lysates Apaf-1 and caspase-9 exhibited similar profiles of oligomerization and cleavage, respectively, as did the MCF-7/WT lysates (Fig. 2*B*). Procaspase-3 eluted in fractions 21–24 (Fig. 2*B*) and is slightly smaller than procaspase-7. However, in dATP/cytochrome *c*-treated lysates, the active p19/17 forms of caspase-3 eluted in fractions 22–26 and not in the caspase-7-containing fractions (Fig. 2*A*). This is consistent with the known quaternary structure of active caspase-3, which is a 58–60-kDa tetramer and indicated that active caspase-7 forms a larger ~200-kDa complex with one or more proteins (see later).

The ~700-kDa Apoptosome Complex Directly Processes Procaspase-7—We next investigated the ability of the ~700-kDa and ~1.4-MDa apoptosome complexes to directly activate effector caspases. Column fractions were incubated with procaspase-3, which is cleaved/activated by the Apaf-1-caspase-9 apoptosome. Caspase activation was determined by measuring DEVDase activity, which was predominant in fractions 9–14 (Fig. 3*A*). These fractions corresponded to the ~700-kDa apoptosome complex, as determined by their Apaf-1 content (Fig. 3*A*). Those fractions corresponding to the ~1.4-MDa apoptosome complex did not activate procaspase-3, and column fractions taken from fractionated non-activated cell lysates also did not activate this procaspase (Fig. 3*A*). From this we concluded that the ~700-kDa complex was the only active apoptosome complex. The fact that it processed and activated procaspase-3 indicated that it should also contain caspase-9. However, we were unable to detect caspase-9 in the column fractions (Fig. 2*A*), as possibly the concentration of apoptosome was too low. To show that this was an Apaf-1-caspase-9 holoenzyme complex, we used an antibody to caspase-9 that only immunoprecipitates Apaf-1 when caspase-9 is a constituent part of an active apoptosome holoenzyme complex (20). The anti-caspase-9 antibody immunoprecipitated the p35 form of caspase-9 and Apaf-1 from the ~700-kDa complex (Fig. 3*B*) but did not capture Apaf-1 from the ~1.4-MDa complex (Fig. 3*B*). We then incubated the respective apoptosome complexes with procaspase-7 (Fig. 3*C*) or procaspase-3 (data not shown) and assayed for DEVDase activity using 100 μM Ac.DEVD.AFC (optimal concentration for assaying caspase-7 activity) and immunoblotted for active caspase-7 subunits. The ~700-kDa apoptosome complex directly processed and activated procaspase-3 (Fig. 3*A*) and procaspase-7 (Fig. 3*B*), as shown by the stimulation of DEVDase activity and the generation of the p19 subunit (Fig. 3*C*). The ~1.4-MDa complex had little or no caspase-processing activity with either procaspase-3 or -7. Thus, the ~ 700-kDa apoptosome complex directly processes and activates procaspase-7. Interestingly, without caspase-3 it was still possible to generate the p19 subunit of caspase-7 (*lane 4*, Fig. 3*C*). Cleavage of the pro-domain or *N*-peptide of procaspase-7 at Asp-23 is believed to catalyzed by caspase-3. However, in caspase-3 null MCF-7/WT cells the ~700-kDa

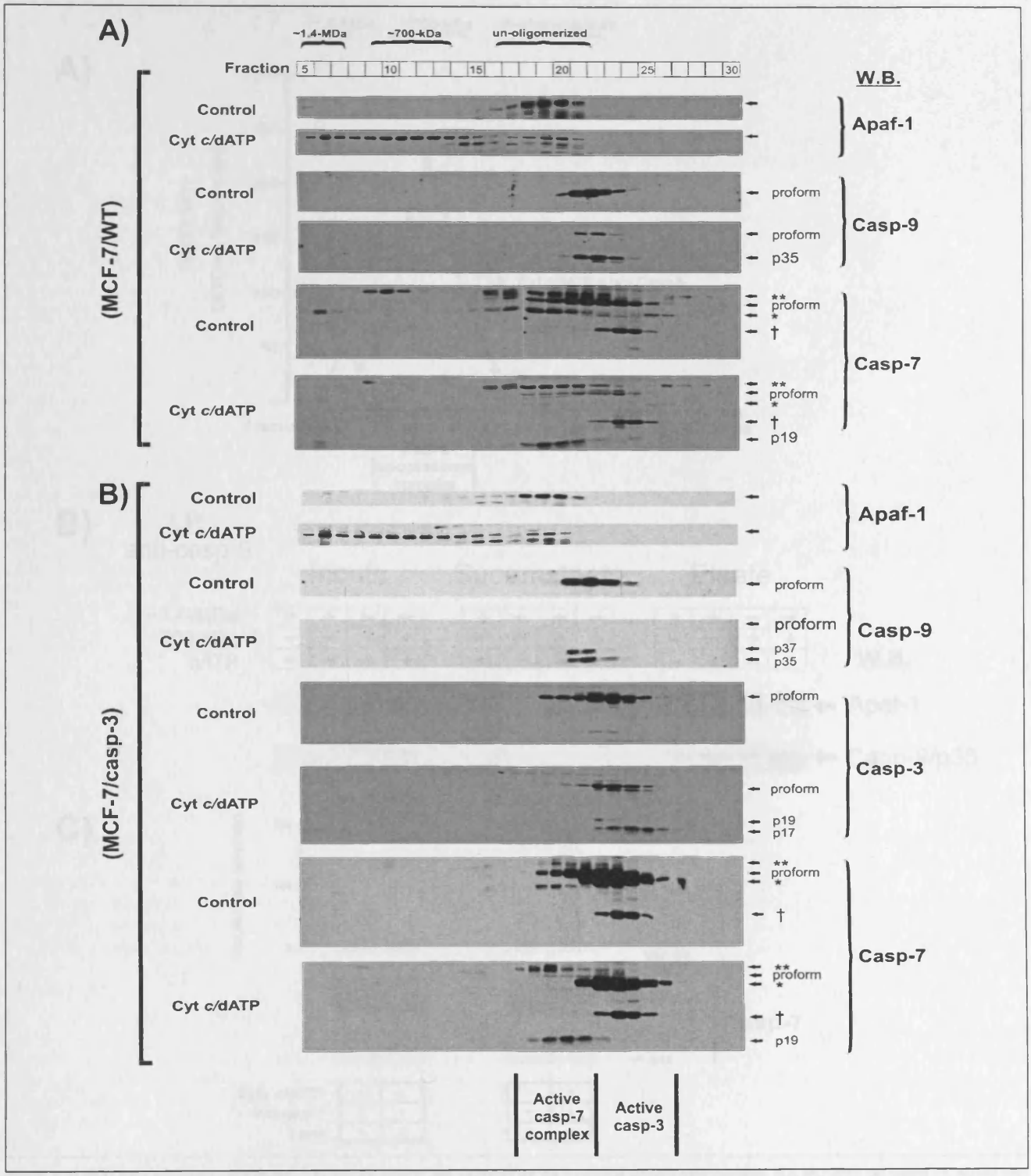

FIGURE 2. **Apoptosome formation in MCF-7 cell lysates is accompanied by the formation of an ~200-kDa active caspase-7 complex.** MCF-7/WT and MCF-7/casp-3 cell lysates (15 mg/ml) were activated with 2 mM dATP/$MgCl_2$ and cytochrome *c* (*Cyt c*, 2 μM) for 30 min at 37 °C. The lysates were then separated by Superose-6 gel-filtration chromatography, and the column fractions were assayed for DEVDase activity and for Apaf-1 and caspase-9, -3, and -7 by SDS-PAGE and Western blotting (*W.B.*) as described under "Experimental Procedures." *Panel A* shows in MCF-7/WT cell lysates oligomerization of Apaf-1 (un-oligomerized) to form ~1.4-MDa and ~700-kDa apoptosome complexes, with the attendant caspase-9 and -7 processing. The same analysis was carried out for cell lysates prepared from MCF-7 cells, stably transfected with caspase-3. Essentially similar elution profiles to the MCF-7/lysate were obtained for Apaf-1, caspase-9, and caspase-7. However, in MCF-7/casp-3 lysates, active caspase-3 was detected and eluted later than active caspase-7, demonstrating that active caspase-3 has a lower molecular mass than active caspase-7, which appears to be complexed to one or more other proteins (active caspase-7 complex, see text). As in Fig. 1, **, *, and † indicate protein bands non-specifically reacting with antibody.

AQ: N

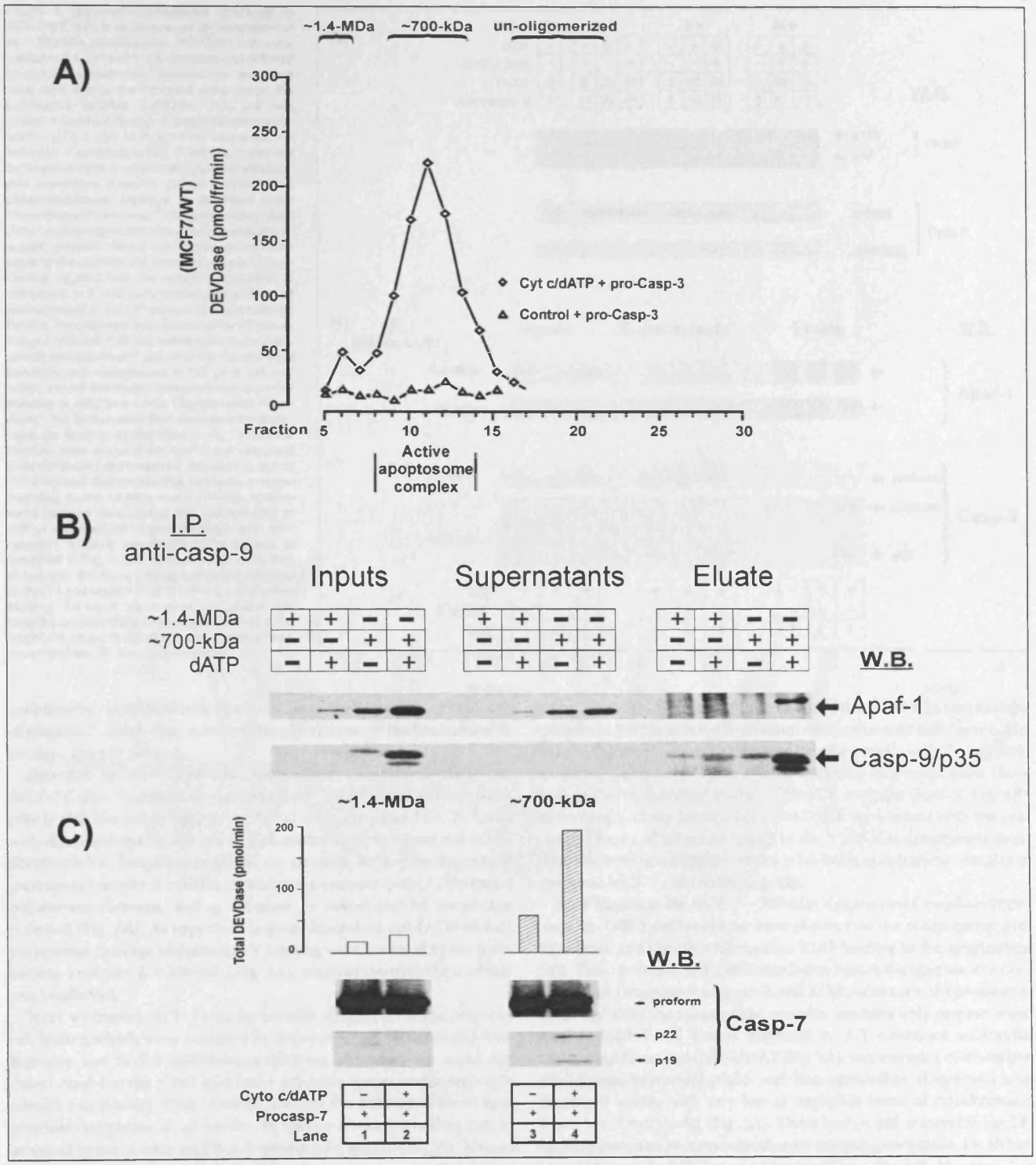

FIGURE 3. **In MCF-7/WT cell lysates procaspase-7 is directly cleaved and activated by the ~700-kDa apoptosome complex.** In *A*, MCF-7/WT cell lysates (15 mg/ml) were activated with 2 mM dATP/$MgCl_2$ and cytochrome *c* (*Cyt c*, 2 μM for 30 min), and 3 mg of lysate was separated on a Superose-6 gel filtration column. Aliquots (50 μl) of each fraction were incubated with 200 nM procaspase-3 for 1 h at 37 °C, then analyzed for DEVDase activity. In *B*, fractions 5–7 and 10–15, corresponding, respectively, to the ~1.4-MDa and ~700-kDa apoptosome complexes, were pooled and concentrated to 100 μl. The concentrated complexes were then incubated overnight with an anti-caspase-9 antibody cross-linked to Dyna beads as described under "Experimental Procedures." The beads were washed 4 times and then eluted in 50 μl of 2× SDS-PAGE loading buffer before being analyzed by SDS-PAGE/Western blotting (*W.B.*). *I.P.*, immunoprecipitate. The input, supernatant, and elution volumes loaded onto the gel were equivalent to 6.2, 7.5, and 36%, respectively, of the original concentrated fractions. In *C*, the pooled 1.4-MDa and ~700-kDa fractions were concentrated to 250 μl, and 50 μl of each fraction was incubated with procaspase-7 for 1 h at 37 °C. Ac-DEVD.AFC was then added to a final volume of 200 μl to give a final substrate concentration of 100 μM for caspase-7. At the end of the assay, 50 μl of the reaction mixture was diluted 1:1 with 2× SDS-PAGE loading buffer and analyzed by SDS-PAGE/Western blotting.

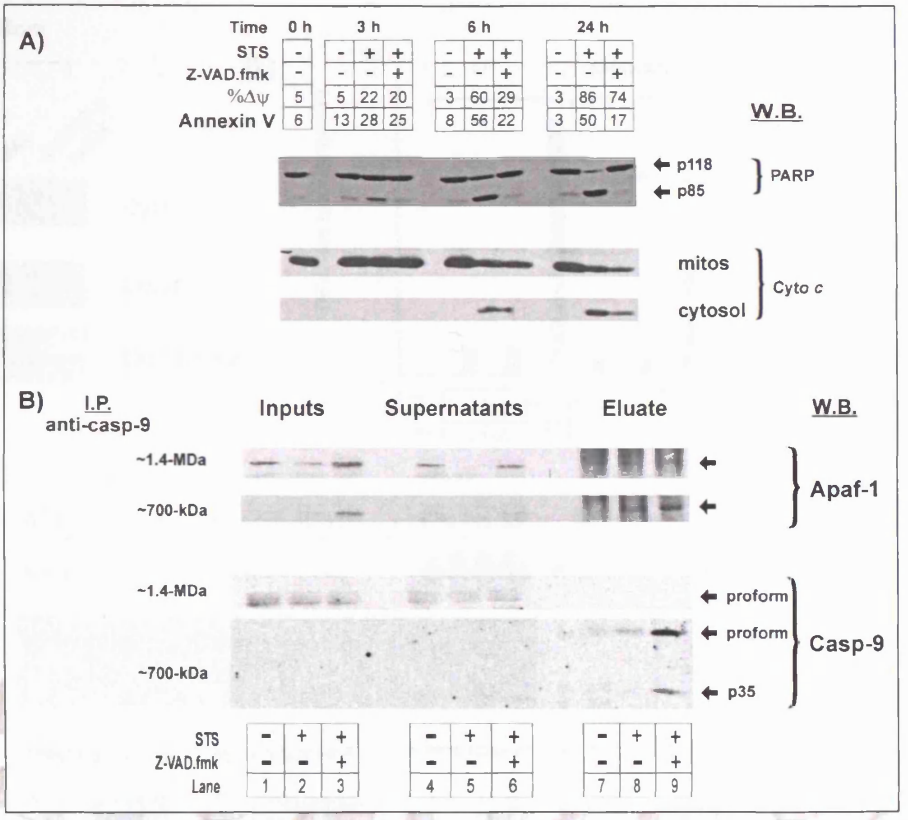

FIGURE 4. **Staurosporine-induced apoptosis in MCF-7/WT cells is accompanied by formation of an ~700-kDa apoptosome.** MCF-7/WT cells were seeded at 2×10^5/well in a 6-well plate and cultured for 18 h before treatment. Three wells per treatment were used, and in the indicated experiments the polycaspase inhibitor Z-VAD.fmk (100 μM) was added 1 h before induction of apoptosis with staurosporine (*STS*, 1 μM). In *A*, the time course for the induction of apoptosis in MCF-7 cells was measured by the percentage of cells showing loss of mitochondrial membrane potential ($\Delta\Psi$m) and increased phosphatidylserine exposure as described under "Experimental Procedures." The Western blots (W.B.) show caspase-dependent cleavage of the apoptotic specific poly(ADP-ribose) polymerase protein substrate to the cleaved p85 form and release of cytochrome *c* (*Cyto c*) from the mitochondria (*mitos*) to the cytosol. In *B*, cells were seeded in large flasks (3 per treatment) at 5×10^6 cells per flask and cultured for 18 h. The cells were then incubated for 1 h plus or minus Z-VAD.fmk (100 μM) before inducing apoptosis with staurosporine (1 μM). After 6 h the cells were harvested and resuspended in 150 μl of cell lysis buffer, and cell-free lysates were produced by freeze/thawing as described under "Experimental Procedures." The lysates were then separated by Superose-6 gel filtration as described in Fig. 3, and the fractions were analyzed for Apaf-1 and caspase-9 (data not shown) and caspase-7 (see also Fig. 6*D*) by SDS-PAGE and Western blotting. The fractions corresponding to the 1.4-MDa and ~700-kDa apoptosome fractions were pooled and concentrated to 110 μl and then incubated overnight with anti-caspase-9 antibody cross-linked to Dyna beads as described in Fig. 3. The washed beads were then eluted with SDS-PAGE loading buffer and analyzed for Apaf-1 and caspase-9 by SDS-PAGE and Western blotting. The input, supernatant, and elution volumes loaded onto the gel were equivalent to 6.0, 6.0, and 66.0%, respectively, of the pooled and concentrated fractions. *I.P.*, immunoprecipitate.

apoptosome complex clearly catalyzes the formation of the p22 subunit of caspase-7, which then autocatalytically cleaves off the prodomain to produce the p19 subunit.

Detection of the ~700-kDa Apoptosome Complex in Apoptotic MCF-7 Cells—To determine whether the ~700-kDa apoptosome complex is also formed in apoptotic MCF-7 cells, we treated MCF-7 cells with staurosporine, which is a well characterized inducer of cell death. Staurosporine induced apoptosis, as assessed by a time-dependent increase in annexin V binding, cytochrome *c* release, poly(ADP-ribose) polymerase cleavage, and a decrease in mitochondrial membrane potential (Fig. 4*A*). As expected, caspase-dependent poly(ADP-ribose) polymerase cleavage and annexin V binding were inhibited by the polycaspase inhibitor Z-VAD.fmk (Fig. 4*A*), whereas cytochrome *c* release was unaffected.

Next, we treated MCF-7 cells for 6 h with staurosporine and prepared cell lysates, which were analyzed by Superose-6 gel filtration chromatography and SDS-PAGE/immunoblotting. However, we could not detect Apaf-1 in the ~700-kDa and ~1.4-MDa apoptosome complexes (results not shown). This could be because the concentration of apoptosome complexes in apoptotic cell lysates is much less than can be achieved in the *in vitro* dATP-activated model system (17, 19). Also, *in vitro* studies have shown that Apaf-1 and the apoptosome are cleaved and degraded by effector caspases (29). Thus, lysates obtained from apoptotic cells will contain a mixture of newly formed and partially degraded apoptosome complexes and, consequently, at any one time the concentration of the apoptosome in the lysate is likely to be low. Therefore, we pooled and concentrated the column fractions containing the apoptosome complexes and used an anti-caspase-9 antibody to immunoprecipitate the Apaf-1-caspase-9 apoptosome complexes. Using this technique, we were able to detect the ~700-kDa apoptosome complex in lysates isolated from staurosporine-treated cells (*lane 8*, Fig. 4*B*). Furthermore, when we inhibited caspase activity with Z-VAD.fmk, increased amounts of Apaf-1 were immunoprecipitated from those fractions corresponding to the ~700-kDa complex (*lane 9*, Fig. 4*B*). Interestingly, in the presence of Z-VAD.fmk we detected both the pro- and p35 forms of caspase-9 bound to the ~700-kDa apoptosome complex. We were unable to detect the ~1.4-MDa apoptosome complex in apoptotic MCF-7 cell lysates (Fig. 4*B*).

XIAP Regulates the MCF-7 ~700-kDa Apoptosome Complex—Previously, in THP.1 cell lysates we have shown that the proapoptotic proteins Smac and Omi/HtrA2 regulate XIAP binding to the apoptosome (20). Thus, in Smac- and Omi/HtrA2-free lysates the apoptosome contains Apaf-1, caspase-9, caspase-3, and XIAP, whereas in the presence of Smac and Omi the apoptosome complex contains only caspase-9 and Apaf-1. MCF-7 cell lysates prepared by F/T contained substantial amounts of Smac and Omi/HtrA2 (Fig. 5*A*). In contrast, a combination of digitonin permeabilization and homogenization (Dig/Hom) produces cell lysates with very low or negligible levels of cytochrome *c*, Smac, and Omi/HtrA2 (Fig. 5*A*). These lysates still respond to dATP/cytochrome *c* and process/activate recombinant procaspase-3 as shown by the increase in DEVDase activity (*sixth lane*, Fig. 5*B*). However, F/T lysates exhibited a ~2-fold greater increase in procaspase-3 activating activity (*third lane*, Fig. 5*B*), indicating that the caspase activating activity of the Dig/Hom lysates was inhibited. We, therefore, used the anti-caspase-9 immunoprecipitation method to assess apoptosome composition in the two types of lysate. In the F/T lysates, apoptosome formation as determined by the ability of the anti-caspase-9 antibody to capture Apaf-1 was essentially maximal at 5 min and was accompanied

MCF-7 Apoptosome Complex

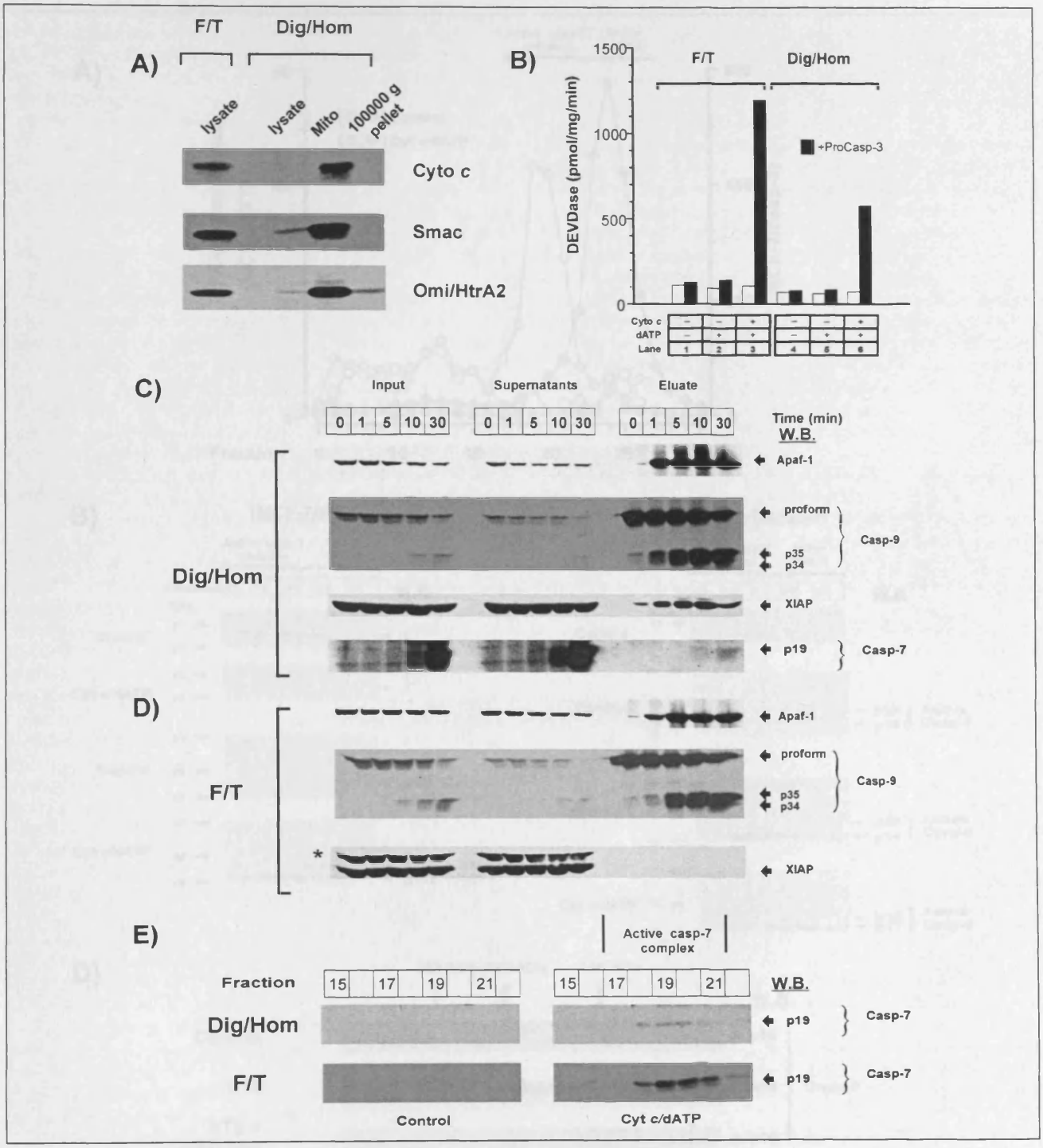

FIGURE 5. **In Smac- and Omi-free lysates, XIAP binds to the MCF-7 apoptosome.** Lysates were prepared by either F/T or Dig/Hom as described under "Experimental Procedures." In *A*, the respective lysates and cellular fractions were analyzed for cytochrome *c* (*Cyto c*) Smac, and Omi/HtrA2. In *B*, F/T and Dig/Hom lysates (10 mg/ml) were activated with 2 mM dATP/$MgCl_2$ and cytochrome *c* (2 μM) for 30 min at 37 °C. An aliquot was taken for the DEVDase activity assay (*open boxes*), and the remaining lysate was incubated with procaspase-3 (200 nM) for 1 h and before analyzing again for the DEVDase activity. In *C* and *D*, lysates (15 mg/ml) were precleared with Sepharose protein G beads and then activated with 2 mM dATP/$MgCl_2$ and cytochrome *c* (2 μM) from 10 to 30 min at 37 °C. At the indicated time caspase activation was terminated with Z-VAD.fmk (20 μM) and an aliquot (20 μg) was taken for the input sample; the remaining lysate (~100 μl) was incubated overnight at 4 °C with 20 μl of anti-caspase-9 complexed to Dyna beads. The supernatants were removed, and the beads were washed 4 times before eluting in 30 μl of SDS-PAGE loading buffer, which was analyzed by immunoblotting for Apaf-1, caspase-9, and XIAP. The input, supernatant, and elution volumes loaded onto the SDS-PAGE gels were 1, 2, and 66%, respectively, of the pooled and concentrated fractions. In *C*, an additional immunoblot is shown for caspase-7, which was only detected in the eluate fractions from the Dig/Hom lysates and only when the blot (*W.B.*) was overexposed. The *asterisk* refers to a nonspecific band, which is mitochondrial Hsp60 (D. Twiddy, . G. M. Cohen, M. MacFarlane, and K. Cain, unpublished data) and is detected in the F/T but not the Dig/Hom lysates. In *E*, F/T and Dig/Hom lysates were fractionated as described in Fig. 2, and the fractions (15–22), which should contain the active caspase-7 complex, were analyzed for the p19 form of caspase-7.

AQ: O
AQ: Q

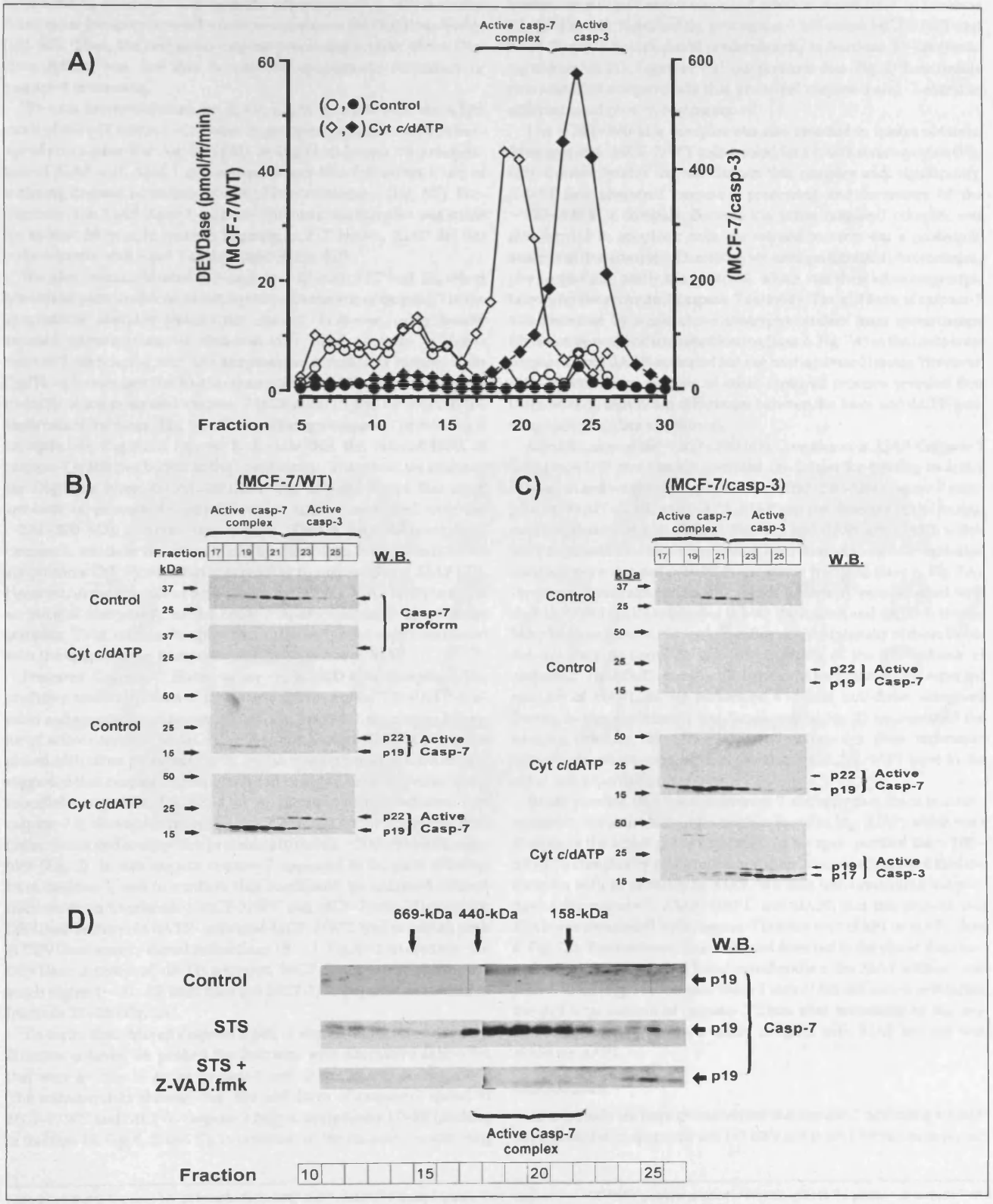

FIGURE 6. **Active caspase-7 forms an ~200–300-kDa complex that is distinct from active caspase-3.** As described in Fig. 2, MCF-7/WT and MCF-7/casp-3 cell lysates (15 mg/ml) were activated with 2 mM dATP/$MgCl_2$ and cytochrome *c* (2 μM) for 30 min at 37 °C. The lysates were separated by Superose-6 gel-filtration chromatography, and column fractions were assayed for DEVDase activity. In *A*, the DEVDase activity for the MCF-7/WT and MCF-7/casp-3 fractions is shown as *open* and *solid symbols*, respectively. Unactivated (*Control*) and cytochrome *c*/dATP-activated (*Cyt c/dATP*) lysates are shown as ○ and ● and as ◇ and ◆, respectively. Note the different *y* axis scales, respectively, for the MCF/WT and MCF/casp-3

by processing of caspase-9 to form the p35 subunit (Fig. 5*D*). A similar time course for apoptosome formation was seen in the Dig/Hom lysates (Fig. 5*C*). Thus, the decreased caspase-processing activity of the Dig/Hom lysates was not due to reduced apoptosome formation or caspase-9 processing.

We next immunoblotted for XIAP, which interacts with the ATPF motif of the p12 subunit of caspase-9, generated by autocatalytic cleavage of procaspase-9 at Asp-315 (30). In Dig/Hom lysates, co-precipitation of XIAP with Apaf-1 and caspase-9 was detected within 1 min of initiating caspase activation with dATP/cytochrome *c* (Fig. 5*C*). Furthermore, the XIAP-Apaf-1-caspase-9 holoenzyme complex was stable for at least 30 min. In marked contrast, in F/T lysates, XIAP did not co-precipitate with Apaf-1 and caspase-9 (Fig. 5*D*).

We also immunoblotted for caspase-7 in both F/T and Dig/Hom lysates and were unable to detect significant amounts of caspase-7 in the apoptosome complex (results not shown). However, using heavily exposed immunoblots, we detected very small amounts of active caspase-7 associating with the apoptosome complex as isolated from Dig/Hom lysates (see the 30-min time point, Fig. 5*C*). Furthermore, the majority of the processed caspase-7 (p19 subunit) was detected in the supernatant fractions (Fig. 5*C*). Thus, although caspase-7 processing is abrogated in Dig/Hom lysates, it is clear that the cleaved form of caspase-7 is still not bound to the apoptosome. Therefore, we analyzed the Dig/Hom lysate by gel filtration (Fig. 5*E*) and found that small amounts of processed caspase-7 were instead associated with the ~200–300 kDa complex (see Fig. 2). This is very different from caspase-3, which in the absence of Smac and Omi/HtrA2 binds to the apoptosome (20) by simultaneous binding to caspase-9 and XIAP (22). However, in the absence of Smac and Omi/HtrA2, XIAP binds to and is an integral component of the MCF-7 Apaf-1-caspase-9 apoptosome complex. Thus, our results show that caspase-7 is not stably associated with the apoptosome, irrespective of the presence of XIAP.

Processed Caspase-7 Elutes as an ~200–300-kDa Complex—The predicted molecular mass of tetrameric active caspase-7 in dATP-activated and apoptotic cell lysates is ~60 kDa. However, the elution behavior of active caspase-7 in MCF-7 cell lysates indicated that it was complexed with other proteins (Fig. 2). In this respect previous studies have suggested that caspase-7 after activation can bind to other proteins and subcellular organelles (31, 32). Our gel filtration results indicated that caspase-7 is cleaved/activated by the ~700-kDa apoptosome and then redistributes and binds with a protein(s) to form a ~200–300-kDa complex (Fig. 2). In this respect caspase-7 appeared to be quite different from caspase-3, and to confirm this conclusion we analyzed column fractions from fractionated MCF-7/WT and MCF-7/casp-3 lysates for DEVDase activity. In dATP- activated MCF-7/WT lysates a small peak of DEVDase activity eluted in fractions 18–21 (Fig. 6*A*). In contrast, the DEVDase activity of dATP-activated MCF-7/caspase-3 lysates was much higher (~10–15-fold) than the MCF-7/WT lysates and eluted in fractions 22–26 (Fig. 6*A*).

To verify that cleaved caspase-3 and -7 eluted differently on the gel filtration column, we probed the fractions with alternative antibodies that were specific to active caspase-7 and -3 and also to procaspase-7. The immunoblots showed that the p19 form of caspase-7 eluted in MCF-7/WT and MCF-7/caspase-3 lysates in fractions 17–22 (peaking in fraction 19, Fig. 6, *B* and *C*). In contrast, in the caspase-3-containing lysates, the p19/p17 active caspase-3 subunits eluted later, in fractions 22–26 (Fig. 6*C*). Significantly, procaspase-7 in control MCF-7/WT and MCF-7/casp-3 lysates eluted predominantly in fractions 20–24 (peaking in fraction 21). Together with our previous data (Fig. 2) these results demonstrated unequivocally that processed caspase-3 and -7 eluted as different sized protein complexes.

The ~200–300-kDa complex was also detected in lysates obtained from apoptotic MCF-7/WT cells treated for 6 h with staurosporine (Fig. 6*D*). Control lysates did not contain this complex and, significantly, Z-VAD.fmk abolished caspase-7 processing and formation of the ~200–300-kDa complex. Because the active caspase-7 complex was also formed in apoptotic cells, we wanted to carry out a proteomic analysis of this complex. Therefore, we used gel filtration chromatography to partially purify the complex, which was then immunoprecipitated with the active anti-caspase-7 antibody. The p19 form of caspase-7 was identified by liquid chromatography-tandem mass spectroscopy (data not shown) and immunoblotting (*lane 6*, Fig. 7*A*) in the complexes prepared from dATP-activated but not heat-activated lysates. However, mass spectrometry analysis of other captured proteins revealed that there were no significant differences between the heat- and dATP-activated samples (data not shown).

Identification of the ~200–300-kDa Complex as a XIAP-Caspase-7 Complex—IAP proteins are potential candidates for binding to active caspase-7, and we therefore probed the ~200–300-kDa caspase-7 complex for XIAP, cIAP1, and cIAP2. XIAP was not detected in the immunoprecipitated complex (*lane 6*, Fig. 7*A*), and cIAP1 and cIAP2, which were detected in the input fractions of both control and dATP-activated samples, were also not present in the eluate fractions (*lane 6*, Fig. 7*A*). However, some faint nonspecific bands (*asterisks*) were detected with the cIAP1 and cIAP2 antibodies in both the control and dATP-activated samples (*lane 5* and *6*, Fig. 7*A*). Significantly, the intensity of these bands did not vary or correlate with the intensity of the p19 subunit of caspase-7. The cIAP1-nonspecific band runs very close to the expected position of cIAP1, so we performed a second pull-down using cell lysates. In this experiment (see Supplemental Fig. 1) we extended the running time on the SDS-PAGE and achieved a clear separation between the nonspecific band in the eluate and the cIAP1 band in the input and supernatant fractions.

It was possible that the anti-caspase-7 antibody that binds to a neoepitope in the active site could displace proteins (*e.g.* XIAP) which were binding to the active site of caspase-7. So we again purified the ~200–300-kDa complex by gel filtration and then immunoaffinity-purified the complex with an antibody to XIAP. We then immunoblotted the pull-downs for caspase-7, XIAP, cIAP1, and cIAP2, and this showed that XIAP was complexed with caspase-7 but not with cIAP1 or cIAP2 (*lane 6*, Fig. 7*B*). Furthermore, Smac was not detected in the eluted fractions, and in the absence of dATP and cytochrome *c*, the XIAP antibody still pulled XIAP (Fig. 7*B*, compare *lanes 5* with *6*) but did not co-precipitate the p19 large subunit of caspase-7. Thus, after processing by the apoptosome, caspase-7 forms a stable complex with XIAP but not with cIAP1 or cIAP2.

DISCUSSION

In this study we have characterized the caspase-7-activating apoptosome complex in apoptotic MCF-7 cells and in dATP/cytochrome *c*-ac-

lysates. In *B* and *C*, fractions 17–26 from both the MCF-7/WT and MCF-7/casp-3 lysates were separated on SDS-PAGE gels and probed with antibodies to the proform of caspase-7 and the active forms of caspase-7 and caspase-3. The p19 and p22 subunits of caspase-7 and the p19/17 forms of caspase-3 are as indicated; molecular mass markers (kDa) are also shown. *W.B.*, Western blot. *D*, MCF-7/WT cells as described in Fig. 4*B* were incubated for 1 h plus or minus Z-VAD.fmk (100 μM) before inducing apoptosis with staurosporine (*STS*, 1 μM). After 6 h, cell-free lysates were produced by freeze/thawing and separated by Superose-6 gel filtration as described in Fig. 4, and the fractions were analyzed for caspase-7 by SDS-PAGE and Western blotting.

balt3/zbc-bc/zbc-bc/zbc00906/zbc3971-06a saylora S=6 4/1/06 11:12 Comments: ARTNO: M507393200

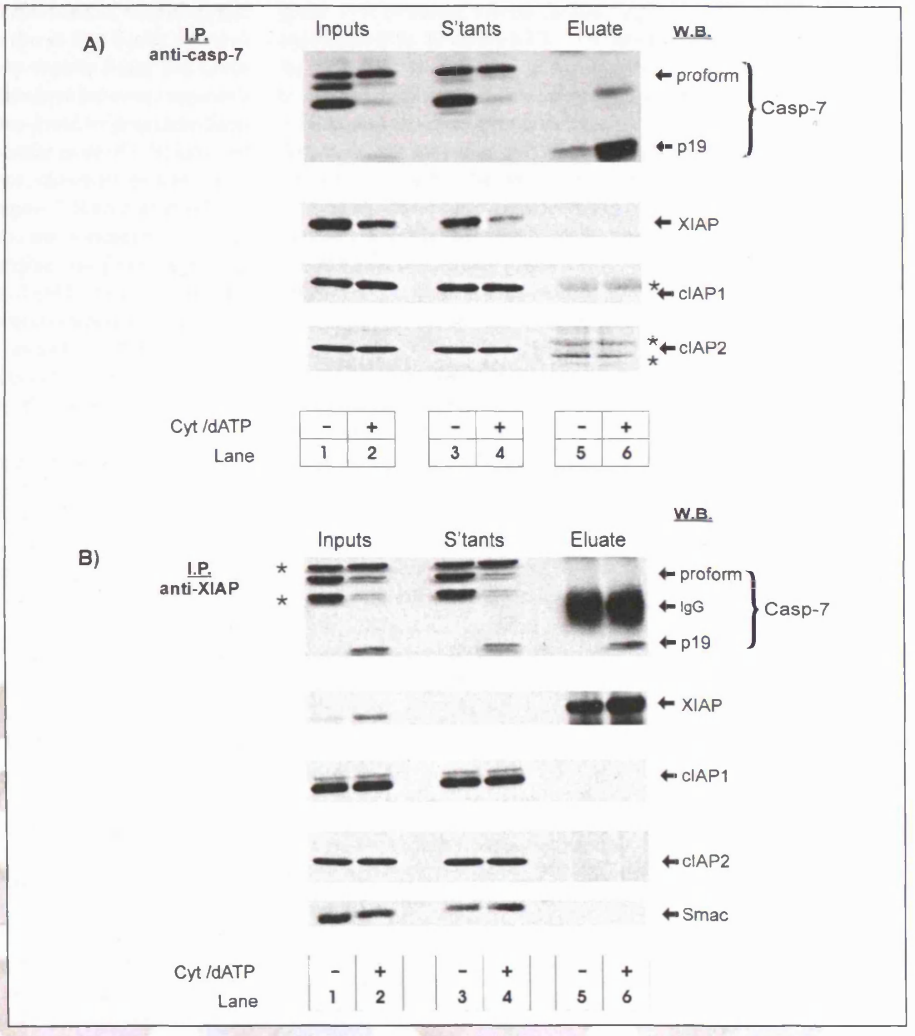

FIGURE 7. **Caspase-7 in the ~200-kDa active caspase-7 complex binds to XIAP but not cIAP1 or cIAP2.** In *A*, MCF-7/WT cell lysate (15 mg/ml) was activated with 2 mM dATP/$MgCl_2$ and cytochrome (*Cyt*) *c* (2 μM) for 2 h at 37 °C, and 3 mg of lysates were fractionated on a Superose 6 gel filtration column. The fractions corresponding to the ~200–300-kDa active caspase-7 complex were pooled and concentrated to 100 μl, and then 90 μl were incubated overnight at 4 °C with 20 μl of anti-active caspase-7 antibody complexed to Dyna beads. The beads were washed 4 times and eluted in 50 μl 2× SDS-PAGE loading buffer. The inputs, supernatants (*S'tants*), and elutions corresponding to 6, 7, and 36% of the original pooled samples were then separated on SDS-PAGE and immunoblotted (*W.B.*) for caspase-7, XIAP, cIAP1, and cIAP2. *I.P.*, immunoprecipitate. Similarly, in *B*, Sephacryl S300 gel filtration was used to partially purify the ~200-kDa active caspase-7 complex from 10 mg of activated lysates. Pooled fractions corresponding to the active caspase-7 complex were concentrated to 500 μl and incubated for 4 h at 4 °C with 150 μl of Dyna beads complexed with an anti-XIAP antibody. The beads were washed 6 times and eluted with 75 μl of SDS-PAGE loading buffer and analyzed for caspase-7, XIAP, cIAP1,cIAP2, and Smac. The input, supernatant, and elution volumes loaded onto the SDS-PAGE gels were 1, 1, and 13%, respectively, of the pooled and concentrated fractions. In *A*, proteins interacting non-specifically with the immunoblotting antibodies are indicated (*asterisk*).

tivated MCF-7 cell lysates. The rate of Apaf-1 oligomerization to form the ~700-kDa apoptosome complex is identical to that observed in caspase-3 containing THP.1 and Jurkat cell lysates (18, 20, 33). To form a fully active caspase-processing holoenzyme complex, caspase-9 must bind to the apoptosome. However, in MCF-7 cell lysates we had to immunoprecipitate caspase-9 from column fractions before we were able to detect caspase-9 in the apoptosome fractions (Fig. 3*B* and 4*B*). This apparent absence of caspase-9 in the ~700-kDa apoptosome complex may simply be a detection problem due to relatively low levels of apoptosome complex in the MCF-7 cells. Alternatively it may imply that that the apoptosome complexes are heterogeneous, containing varying amounts of caspase-9. In this respect the structure of caspase-9 in the apoptosome complex is still poorly understood (for review, see Refs. 7, 8, and 34). Procaspase-9, unlike effector caspases, has an unusually long flexible linker peptide which allows active site formation that gives the zymogen low but significant cleavage activity. This is markedly enhanced when caspase-9 is bound to the apoptosome in dATP/cytochrome *c*-activated cell lysates (18, 35, 36). Interestingly, non-cleavable caspase-9 mutants will also process procaspase-3 when incubated with dATP/cytochrome *c*-activated cytosol (22, 35). This observation can be explained by the "induced-proximity model," which proposes that monomeric procaspase-9 dimerizes at high concentrations, forcing an allosteric rearrangement of one of the monomers in the dimer to produce a catalytically active site (37, 38). It is suggested that Apaf-1 recruitment of caspase-9 facilitates caspase-9 dimerization/activation and that caspase-9 cleavage stabilizes the dimer (39). However, caspase-9 recruitment to the apoptosome is accompanied by simultaneous processing of the proform, as the p35 subunit was detected within 1–5 min of dATP/cytochrome *c* activation of MCF-7 cell lysates (Fig. 1*B* and Fig 5, *C* and *D*)). Significantly, caspase-7 processing was not detected until 30 min post-dATP activation and always lagged behind that of caspase-9 irrespective of the presence of caspase-3. Interestingly, in lysates isolated from apoptotic cells, Z-VAD.fmk seemed to freeze or stabilize procaspase-9 in the apoptosome. This suggests that caspase-9 processing destabilizes its binding to the apoptosome, resulting in the release of free caspase-9′.

In the current study we provide new insights to the processing and structure of caspase-7 in cell lysates. Crystallographic studies on recombinant caspases 1, 3, and 7 have shown that the catalytically active enzymes are heterotetramers (40–42) and at physiological concentrations form stable inactive homodimers (17, 18, 43, 44). Cleavage of the linker peptide loop produces the large and small subunits of the heterotetramer, inducing conformational changes that form the functional active site. Although recombinant caspase-7 and caspase-3 elute on gel

filtration columns with the predicted molecular mass of ~60 kDa (Ref. 17 and data not shown), our current study shows that a very different picture exists in cellular lysates (even if they contain Smac and Omi/HtrA2). Furthermore, there are marked differences between caspases 3 and 7. First, the elution pattern of procaspase-3 and its processed form (Fig. 2*B* and Fig. 6) is consistent with a molecular mass of ~60 kDa and agrees with studies on recombinant proteins. However, processing of procaspase-7 to produce the p19 form of caspase-7 is accompanied by a marked shift in the size of the cleaved protein, which elutes as an ~200-kDa complex (Fig. 2*A* and Fig. 6). This complex was detected in both MCF-7/WT (casp-3 null) and MCF-7/casp-3 cells using two separate antibodies to caspase-7. Furthermore, immuno-affinity purification established that the ~200-kDa complex contained XIAP bound to the active form of caspase-7 (Fig. 7). The stability of this interaction seems to be very high as it was not disrupted by the presence of Smac or Omi/HtrA2 in the lysates.

The role of XIAP in mammalian apoptotic cell death is still controversial even though there is evidence that some apical and effector caspases are regulated by IAPs (45). In *Drosophila*, caspase inhibition by DIAP1 is essential for survival (46). However, the loss of XIAP in mammalian cells does not result in a significant phenotype (47), although overexpression of XIAP suppresses apoptosis induced by various stimuli (48). XIAP inhibits caspases 9, 3, and 7 via interactions between processed caspases and the BIR2 and BIR3 domains, and some IAPs can regulate effector caspases by binding to the catalytically active site. However, recent studies show that XIAP inhibits caspase-7 activity by multiple interactions between the N-terminal linker region of the BIR2 domain and the active site of caspase-7 and by binding to Ala-Asn-Pro, an IAP binding motif (IBM) that is revealed by cleavage at Asp-206 (49). In *Drosophila*, DIAP1 binds to an IBM located at the N terminus of the large subunit of drICE (50), whereas cIAP1 can also bind to caspase-7 via an N-terminal Ala-Lys-Pro (AKP) IBM generated by cleavage of procaspase-7 at Asp-23. Thus, XIAP can potentially bind to the active site of caspase-7 and two separate IBM motifs. Removal of the prodomain at Asp-23 to reveal the AKP motif can be catalyzed by caspase-3 before Asp-198 cleavage by an apical caspase or granzyme B (51). However, we and others have found that active caspase-7 *in vitro* can also remove its own prodomain in dATP-activated MCF-7 lysates after cleavage at Asp-198 (Fig. 1 (26)). Furthermore, recombinant procaspase-7 is processed by the ~700-kDa apoptosome complex to yield both the p19 and p22 forms of caspase-7 (Fig. 3*C*). Interestingly, the p22 form of caspase-7 was not found in the ~200–300-kDa complex and instead eluted as a smaller-sized complex, indicating that it was probably not complexed with other proteins (*lanes 22–24*, Fig. 6*B*). This suggests that removal of the prodomain is required for forming the 200–300-kDa complex. Thus, in the absence of caspase-3, apoptosome-dependent activation of caspase-7 involves cleavage at Asp-198 followed by autocatalytic cleavage at Asp-23. The exposed AKP (IBM) sequence could in theory bind cIAP1, but we could not detect this IAP in the immunoaffinity-purified ~200-kDa complex (Fig. 7*A*). Indeed, XIAP was the only IAP bound to caspase-7, and furthermore, an antibody that was raised to the active site of caspase-7 displaced XIAP in the immunoprecipitation experiments (Fig. 7*A*), demonstrating that XIAP interacts with active site of caspase-7. Although this confirms the presence of an active caspase-7/XIAP complex, it does not exclude the possibility that cIAP1/cIAP2 could also form separate complexes by binding to the active site of caspase-7.

The absence of caspase-3 in MCF-7 cells inevitably means that the response of these cells to apoptotic stimuli is markedly altered, as they now rely on caspase-7 to be the primary executioner caspase. In a recent study, 75% of breast tumors lacked caspase-3 transcript and protein expression (52). Thus, the MCF-7 cell line seems to be a good cell model for this particular disease, and significantly, reconstitution of caspase-3 in this cell line augments the apoptotic response of these cells to doxorubicin and other apoptotic stimuli (52, 53). In this context we have delineated the activation and fate of caspase-7 during apoptosome-dependent cell death in caspase-3 null MCF-7 cells. In these cells, the rapid process of Apaf-1 oligomerization to form the ~700-kDa apoptosome complex is similar to caspase-3-containing cells. After binding to the apoptosome, procaspase-9 is cleaved to yield the processed p35 form of caspase-9. This process is slower in MCF-7/WT cells when compared with MCF-7/casp-3 cells. Similarly, in the absence of caspase-3, although the ~700-kDa Apaf-1-caspase-9 apoptosome complex catalyzes the processing of procaspase-7 to its active p19 form, it does so relatively slowly. Significantly, after processing, active caspase-7 does not associate with the apoptosome because, even in Smac/Omi-containing cells, it has such a high affinity for XIAP that it forms a relatively stable ~200-kDa XIAP-caspase-7 complex. This suggests that XIAP has a more pronounced anti-apoptotic effect in MCF-7 cells than it does in caspase-3-containing cells. The combination of slow processing/activation of caspase-7 and its strong binding to XIAP may explain in part why MCF-7 cells are relatively insensitive to apoptotic stimuli.

Acknowledgments—We thank Robert Boyd and Rebekah Jukes of the Medical Research Council Toxicology Unit Proteomics Facility for expert help in this study.

REFERENCES

1. Simstein, R., Burow, M., Parker, A., Weldon, C., and Beckman, B. (2003) *Exp. Biol. Med.* **228,** 995–1003
2. Cohen, G. M. (1997) *Biochem. J.* **326,** 1–16
3. Hengartner, M. (1998) *Science* **281,** 1298–1299
4. Earnshaw, W. C., Martins, L. M., and Kaufmann, S. H. (1999) *Annu. Rev. Biochem.* **68,** 383–424
5. Bratton, S. B., MacFarlane, M., Cain, K., and Cohen, G. M. (2000) *Exp. Cell Res.* **256,** 27–33
6. Adrain, C., and Martin, S. J. (2001) *Trends Biochem. Sci.* **26,** 390–397
7. Cain, K., Bratton, S. B., and Cohen, G. M. (2002) *Biochimie (Paris)* **84,** 203–214
8. Cain, K. (2003) *Drug Metab. Rev.* **35,** 337–363
9. Janicke, R. U., Sprengart, M. L., Wati, M. R., and Porter, A. G. (1998) *J. Biol. Chem.* **273,** 9357–9360
10. Kurokawa, H., Nishio, K., Fukumoto, H., Tomonari, A., Suzuki, T., and Saijo, N. (1999) *Oncol. Rep.* **6,** 33–37
11. Janicke, R. U., Ng, P., Sprengart, M. L., and Porter, A. G. (1998) *J. Biol. Chem.* **273,** 15540–15545
12. MacFarlane, M., Merrison, W., Dinsdale, D., and Cohen, G. M. (2000) *J. Cell Biol.* **148,** 1239–1254
13. Tang, D., Lahti, J. M., and Kidd, V. J. (2000) *J. Biol. Chem.* **275,** 9303–9307
14. Zou, H., Henzel, W. J., Liu, X. S., Lutschg, A., and Wang, X. D. (1997) *Cell* **90,** 405–413
15. Liu, X., Kim, C. N., Yang, J., Jemmerson, R., and Wang, X. (1996) *Cell* **86,** 147–157
16. Li, P., Nijhawan, D., Budihardjo, I., Srinivasula, S. M., Ahmad, M., Alnemri, E. S., and Wang, X. (1997) *Cell* **91,** 479–489
17. Cain, K., Brown, D. G., Langlais, C., and Cohen, G. M. (1999) *J. Biol. Chem.* **274,** 22686–22692
18. Cain, K., Bratton, S. B., Langlais, C., Walker, G., Brown, D. G., Sun, X. M., and Cohen, G. M. (2000) *J. Biol. Chem.* **275,** 6067–6070
19. Almond, J., Snowden, R. T., Dinsdale, D., Hunter, A., Cain, K., and Cohen, G. M. (2001) *Leukemia* **15,** 1388–1397
20. Twiddy, D., Brown, D. G., Adrain, C., Jukes, R., Martin, S. J., Cohen, G. M., MacFarlane, M. M., and Cain, K. (2004) *J. Biol. Chem.* **279,** 19665–19682
21. Slee, E. A., Harte, M. T., Kluck, R. M., Wolf, B. B., Casiano, C. A., Newmeyer, D. D., Wang, H. G., Reed, J. C., Nicholson, D. W., Alnemri, E. S., Green, D. R., and Martin, S. J. (1999) *J. Cell Biol.* **144,** 281–292
22. Bratton, S. B., Walker, G., Srinivasula, S. M., Sun, X. M., Butterworth, M., Alnemri, E. S., and Cohen, G. M. (2001) *EMBO J.* **20,** 998–1009
23. Dewson, G., Snowden, R. T., Almond, J. B., Dyer, M. J., and Cohen, G. M. (2003) *Oncogene* **22,** 2643–2654

24. Sun, X. M., MacFarlane, M., Zhuang, J. G., Wolf, B. B., Green, D. R., and Cohen, G. M. (1999) *J. Biol. Chem.* **274,** 5053–5060
25. Sun, X. M., Butterworth, M., MacFarlane, M., Dubiel, W., Ciechanover, A., and Cohen, G. M. (2004) *Mol. Cell* **14,** 81–93
26. Denault, J. B., and Salvesen, G. S. (2003) *J. Biol. Chem.* **278,** 34042–34050
27. MacFarlane, M., Cain, K., Sun, X. M., Alnemri, E. S., and Cohen, G. M. (1997) *J. Cell Biol.* **137,** 469–479
28. GarciaCalvo, M., Peterson, E. P., Rasper, D. M., Vaillancourt, J. P., Zamboni, R., Nicholson, D. W., and Thornberry, N. A. (1999) *Cell Death Differ.* **6,** 362–369
29. Bratton, S. B., Walker, G., Roberts, D. L., Cain, K., and Cohen, G. M. (2001) *Cell Death Differ.* **8,** 425–433
30. Srinivasula, S. M., Hegde, R., Saleh, A., Datta, P., Shiozaki, E., Chai, J., Lee, R. A., Robbins, P. D., Fernandes-Alnemri, T., Shi, Y., and Alnemri, E. S. (2001) *Nature* **410,** 112–116
31. Chandler, J. M., Cohen, G. M., and MacFarlane, M. (1998) *J. Biol. Chem.* **273,** 10815–10818
32. Zhivotovsky, B., Samali, A., Gahm, A., and Orrenius, S. (1999) *Cell Death Differ.* **6,** 644–651
33. Hill, M. M., Adrain, C., Duriez, P. J., Creagh, E. M., and Martin, S. J. (2004) *EMBO J.* **23,** 2134–2145
34. Fuentes-Prior, P., and Salvesen, G. S. (2004) *Biochem. J.* **384,** 201–232
35. Stennicke, H. R., Deveraux, Q. L., Humke, E. W., Reed, J. C., Dixit, V. M., and Salvesen, G. S. (1999) *J. Biol. Chem.* **274,** 8359–8362
36. Rodriguez, J., and Lazebnik, Y. (1999) *Genes Dev.* **13,** 3179–3184
37. Salvesen, G. S., and Dixit, V. M. (1999) *Proc. Natl. Acad. Sci. U. S. A.* **96,** 10964–10967
38. Renatus, M., Stennicke, H. R., Scott, F. L., Liddington, R. C., and Salvesen, G. S. (2001) *Proc. Natl. Acad. Sci. U. S. A.* **98,** 14250–14255
39. Boatright, K. M., Renatus, M., Scott, F. L., Sperandio, S., Shin, H., Pedersen, I. M., Ricci, J. E., Edris, W. A., Sutherlin, D. P., Green, D. R., and Salvesen, G. S. (2003) *Mol. Cell* **11,** 529–541
40. Wilson, K. P., Black, J. A. F., Thomson, J. A., Kim, E. E., Griffith, J. P., Navia, M. A., Murcko, M. A., Chambers, S. P., Aldape, R. A., Raybuck, S. A., and Livingston, D. J. (1994) *Nature* **370,** 270–275
41. Rotonda, J., Nicholson, D. W., Fazil, K. M., Gallant, M., Gareau, Y., Labelle, M., Peterson, E. P., Rasper, D. M., Ruel, R., Vaillancourt, J. P., Thornberry, N. A., and Becker, J. W. (1996) *Nat. Struct. Biol.* **3,** 619–625
42. Wei, Y., Fox, T., Chambers, S. P., Sintchak, J., Coll, J. T., Golec, J. M., Swenson, L., Wilson, K. P., and Charifson, P. S. (2000) *Chem. Biol.* **7,** 423–432
43. Chai, J., Wu, Q., Shiozaki, E., Srinivasula, S. M., Alnemri, E. S., and Shi, Y. (2001) *Cell* **107,** 399–407
44. Riedl, S. J., Fuentes-Prior, P., Renatus, M., Kairies, N., Krapp, S., Huber, R, Salvesen, G. S., and Bode, W. (2001) *Proc. Natl. Acad. Sci. U. S. A.* **98,** 14790–14795
45. Salvesen, G. S., and Abrams, J. M. (2004) *Oncogene* **23,** 2774–2784
46. Goyal, L., McCall, K., Agapite, J., Hartwieg, E., and Steller, H. (2000) *EMBO J.* **19,** 589–597
47. Harlin, H., Reffey, S. B., Duckett, C. S., Lindsten, T., and Thompson, C. B. (2001) *Mol. Cell. Biol.* **21,** 3604–3608
48. Salvesen, G. S., and Duckett, C. S. (2002) *Nat. Rev. Mol. Cell Biol.* **3,** 401–410
49. Scott, F. L., Denault, J. B., Riedl, S. J., Shin, H., Renatus, M., and Salvesen, G. S. (2005) *EMBO J.* **24,** 645–655
50. Tenev, T., Zachariou, A., Wilson, R., Ditzel, M., and Meier, P. (2005) *Nat. Cell Biol.* **7,** 70–77
51. Yang, X. H., Stennicke, H. R., Wang, B. K., Green, D. R., Janicke, R. U., Srinivasan, A., Seth, P., Salvesen, G. S., and Froelich, C. J. (1998) *J. Biol. Chem.* **273,** 34278–34283
52. Devarajan, E., Sahin, A. A., Chen, J. S., Krishnamurthy, R. R., Aggarwal, N., Brun, A. M., Sapino, A., Zhang, F., Sharma, D., Yang, X. H., Tora, A. D., and Mehta, K. (2002) *Oncogene* **21,** 8843–8851
53. Yang, X. H., Sladek, T. L., Liu, X., Butler, B. R., Froelich, C. J., and Thor, A. D. (2001) *Cancer Res.* **61,** 348–354